ESTABLISHING INCIDENCES OF DENTAL CALCULUS AND ASSOCIATED PLANT MICROFOSSILS ON SOUTH AFRICAN PLIO-PLEISTOCENE HOMININ DENTITION

By

Edward John Odes

A dissertation submitted to the Faculty of Science, University of the Witwatersrand, Johannesburg, in fulfilment of the requirements for the degree of Master of Science.

Johannesburg, 2013.

DECLARATION

I declare that this dissertation is my own, unaided work. It is being submitted for the Degree of Master of Science in the University of the Witwatersrand, Johannesburg. It has not been submitted before for any degree or examination in any other University.

Signature: ______________________________

Date: 27th May 2013

ABSTRACT

Recent studies of the dental remains from Malapa, a fossil-bearing karstic cave-site located in the Cradle of Humankind (Berger *et al*., 2010), have demonstrated the presence of dental calculus and associated plant material in the form of phytoliths, preserved on the teeth of *Australopithecus sediba* (MH1) (Henry *et al*., 2012). This discovery raised the probability that dental calculus and plant microremains may also be present on hominin material from other cave sites in southern Africa, where fossils are preserved under similar conditions. The aim of this study was to establish the presence of dental calculus and associated microfossils on the teeth of other southern African Plio-Pleistocene early hominins. The dental collection of the Plio-Pleistocene age hominin site of Sterkfontein was examined. Where fossils were observed with adherent material, several analyses were performed to determine whether this material was calculus or not. Where possible, comparisons with the texture of the sediment matrix surrounding the fossil were conducted. Small quantities of this material were removed and observed microscopically to determine if it included food particulates and microfossils. In these cases, we also looked for microfossils in the surrounding matrix as a control. Phytoliths were recovered from all tooth sample material tested. The establishment of phytoliths in the dental calculus is direct evidence that these two structures existed simultaneously, as the formation of calculus can only take place in the presence of saliva. A large number of phytolith morphotypes further indicated that *A.africanus* had an adaptable and diverse diet, and that monocotyledons and dicotyledons appear to have made up a considerable part of their diet. The results from this study will benefit future analyses, by not only providing new protocols for establishing the presence of dental calculus, but also for promoting better preservation of dental calculus in

the future. Further, future studies may be able to obtain direct evidence of consumed food that can directly be associated with individual hominins' feeding behaviours. This could result in significant clues to the diet and ecology of not only individual hominins, but populations, species and comparisons of diet and behaviour between species and genera.

TABLE OF CONTENTS

DECLARATION ii

ABSTRACT iii

TABLE OF CONTENTS v

ACKNOWLEDGEMENTS x

LIST OF FIGURES xiv

LIST OF TABLES xviii

CHAPTER 1 : INTRODUCTION 19

1.1 Aims of this research 19

1.2 Background Study 19

1.2.1 Aetiology of Dental Calculus (or tartar) 20

1.2.2 Composition and Structure of Dental Calculus 20

1.2.3 Categories of Dental Calculus 21

1.2.4 The Formation of Dental Calculus 24

1.2.5 Diet and its Influence on Calculus Formation 27

1.2.6 Non-Dietary effects on calculus preservation 32

1.3 Hominin Diets and Ecology and the Importance of Plant Foods 33

1.3.1 Introduction 33

1.3.2 Diets and Ecology of Early Hominins and Early Dietary Models 34

1.3.3 The Importance of Plant Foods 39

1.3.3.1 Hominin Diets Before Fire 41

1.3.3.2 Definition of Edible Plant material 46

1.3.3.3 Diet Related Competencies of Early Hominin Dentition 47

1.3.4 Carbon Isotope Studies 48

1.3.5 Diet and ecology of Au.sediba 49
1.3.6 Diet and ecology of Au. africanus and P. robustus 51
1.4 Diets and Plant Microremains 52
1.4.1 Utilising Plant Microfossils to Identify Dietary Patterns 52
1.4.2 The Formation and Composition of Phytoliths 54
1.4.3 The Recovery of Phytoliths from Dental Calculus and Tooth Enamel 56
CHAPTER 2 : MATERIALS AND METHODS 64
2.1 Materials 64
2.2 Methods 65
2.2.1 Examination of Hominin Dental Specimens 65
2.2.2 Protocols for Identifying Dental Calculus 68
2.2.2.1 Visibility factors: 69
2.2.2.2 Colour Variability: 69
2.2.3 Examination of inclusions in calculus: 70
2.3 Method for Extracting Dental calculus and Phytolith Analysis 70
2.3.1 Method for Contamination Control 72
CHAPTER 3 : RESULTS AND ANALYSIS 75
3.1 Specimen StW 53f, Left Maxillary Second Molar (LM^2) 78
3.1.1 Description of Probable Calculus on StW53f 78
3.1.2 Other probable calculus deposits on StW53f 79
3.1.3 Phytolith Results for StW 53f (taken from grid square V58) 81
3.1.4 Discussion (StW 53f tooth sample) 85

3.1.5 Phytolith comparison between tooth sample (StW 53f) and nearest bone associated breccia (StW 53d) ... 86

3.1.6 Phytolith results from StW 53d ... 88

3.2 Specimen StW 321*b* Left Mandibular Second Molar (LM_2) ... 97

3.2.1 Description of probable calculus on StW 321b ... 97

3.2.2 Phytolith Results from StW 321b (taken from grid square U49) ... 101

3.2.3 Phytolith comparison between tooth sample (StW 321b) and the nearest bone associated breccia sample (from grid square U52) ... 104

3.2.4 Comparison of the Phytoliths recovered from nearest bone associated breccia of tooth sample StW 321b (U52) and the nearest breccia control sample (U62 6w and U62 7w)106

3.2.5 Discussion (StW 321b tooth sample) ... 107

3.3 Specimen StW 534, Right Mandibular Second Molar (RM_2) ... 109

3.3.1 Description of probable calculus on StW 534 ... 109

3.3.1.1 Cervico-distal ... 110

3.3.1.2 Mid-buccal ... 111

3.3.1.3 Occluso-buccal ... 113

3.3.1.4 Sub-cervical ... 113

3.3.1.5 Sub cervico-mesial ... 114

3.3.1.6 Cervico-mesial ... 115

3.3.2 Phytoliths Results from StW 534 (taken from grid square W43) ... 116

3.3.3 Comparison between phytoliths recovered from StW 534 and the closest bone associated breccia samples (V50; V51; V52) ... 119

3.3.4 Comparison of the phytoliths recovered from the nearest bone associated breccia (V51) with the breccia control sample (U62 6w and U62 7w) 120

3.3.5 Discussion (StW 534 tooth sample) 122

3.4 Specimen StW 532 Left Mandibular Third Molar (LM_3) 123

3.4.1 Description of probable calculus on StW 532 123

3.4.2 Phytolith Results from StW 532 (taken from grid square W43) 124

3.4.3 Discussion (StW 532 tooth sample) 127

3.5 Specimen StW 183 Left Maxillary First Molar (LM^1) 129

3.5.1 Description of probable calculus 129

3.5.2 Phytolith Results from StW 183 (taken from grid square T49) 130

3.5.3 Comparison between phytoliths from StW 183; Associated bone breccia (grid square S63), and the breccia control sample (U62 6w and U62 7w). 131

3.5.4 Discussion (StW 183 tooth sample) 133

3.5.5 Results from Other Breccia Control Samples 134

3.5.5.7 Grid Square Q 64 (1w) 135

3.5.5.8 Grid Square Q 64 (2w) 135

3.5.5.9 Grid Square Q64 (3w) 136

3.5.5.10 Grid Square N 46 (4w) 137

3.5.5.11 Grid Square N 46 (5w) 138

CHAPTER 4 : DISCUSSION 143

4.1.1 Calculus 143

4.1.2 Phytoliths 144

4.1.3 Taphonomic Hypotheses of Malapa and Sterkfontein 146

4.1.3.1 Malapa 146

4.1.3.2 Sterkfontein 147

4.1.4 Palaeoenvironmental Hypotheses of Sterkfontein and Malapa 149

4.1.4.1 Sterkfontein 149

4.1.4.2 Malapa environmental setting 151

4.1.5 Is the calculus phenomenon unique to Malapa? 152

4.1.6 Suggested New Protocols.. 153

CHAPTER 5 CONCLUSIONS.. 157

REFERENCES: 159

APPENDIX A: 184

ACKNOWLEDGEMENTS

I would like to thank my supervisors, Professor Lee Berger, Professor Marion Bamford, and Dr Amanda Henry for their invaluable contributions to my studies, and for their continued support and guidance at all times.

A special thanks to Prof Lee Berger for affording me a very special opportunity to work on hominin dental calculus, and to Professor Lee Berger for arranging a grant from the National Research Foundation for this study, for which I am most grateful. I offer my most sincere thanks to Professor Marion Bamford for teaching and sharing your knowledge on phytoliths with me. It was immensely valuable and a privilege to work with and learn from you. Thank you for your guidance and moral support.

I offer my deepest gratitude to Dr Amanda Henry for the enormous input that you have put to my Masters. Thank you Amanda for the steadfast guidance through the process of identifying and extracting calculus from tooth material, and the exceptional and clear advice I always received from you. Thank you for checking my drafts so painstakingly and affording me so much of your valuable time and deep insight into field of phytoliths and dental calculus.

I would like to sincerely thank the University of the Witwatersrand for awarding me a Post Graduate Merit Award for my Masters studies.

My sincere thanks go to Professor Francis Thackeray, director of the Institute of Human Evolution, for your continued interest and support in my work, valued guidance, and sage advice always. Thank you for your steadfast belief in me. I would like to thank Dr. Lucinda Backwell for your assistance with the microscopy and photographic advice in the early days of this project. My gratitude and thanks go to Dr Bernard Zipfel for assisting me with access to the fossils at Wits Medical School, and for the unscheduled trips to the fossil laboratory, to relook at the fossils, I am most grateful.

I am deeply indebted to and wish to thank Dr. Bonita de Klerk for the massive input she has put into my Masters. For the invaluable advice on microscopy and photography; for helping especially with my dissertation template layout and the formatting, and the many questions and meetings to get it right. For the palaeodental advice, statistical assistance and help with things I would have never imagined possible with MS ‘word’, ‘SSPS’, and ‘Gimp.’ Thank you Bonita, without your help, I would’ve still been floundering in the starting stalls.

I would like to thank Natasha Barbolini for all her help this year with palaeobotanical, microfossil and especially microscopy advice. I am indebted and deeply grateful to Ashley Kruger for all his assistance with my photography plates and the associated software support. A saviour if ever there was one! My sincere thanks to Petrus Chakane in the technical laboratory for preparing the microscope slides for my project, and for technical advice. Nothing was too much trouble for you, and you always carried it out with a smile on your face.

And finally, my deepest thanks and gratitude go to three of the most important people in my life. Thank you, Dad for your constant encouragement, interest in my well-being, love and unending moral support throughout my studies. My inexpressible and deepest gratitude goes to Monica, *mi amor de mi vida*; *mi amor de mi alma*. Thank you *mi amor* for your unceasing love, constant support, relentless encouragement, steady guidance and a deep understanding of how important the pursuit of knowledge is for me. My indescribable gratitude goes to Kelly my daughter for her exceptional grasp of the work that I love and for her unwavering love, belief, and constant delight in what I do. Thank you my punky! Thank you for the sacrifices you have had to make during my studies. You are all the eternal and constant lights in my life.

To my father Wolf, my late mother Joyce, my love Monica and my daughter Kelly

LIST OF FIGURES

Figure 1: Dental calculus scoring method for supra-gingival calculus. (Adapted from Brothwell (1981), and Buikstra and Ubelaker (1994); 1=mild; 2=moderate; 3=severe).....66
Figure 2: Human dental calculus scoring system. Left (mild). Middle (moderate). Right (severe). Adapted from Buikstra and Ubelaker (1994). 66
Figure 3: Hominin tooth samples selected for calculus and phytolith examination a: StW 53f, LM^2 buccal; b: StW 183, LM_1 lingual; c: StW 321b, LM_2 buccal; d: StW 532 LM_3 buccal; e: StW 534 RM_2 buccal. Scale bar =1cm. 68
Figure 4: Location of Sterkfontein Members 4 and 5 (M4 and M5) and StW 53 Infill (hatched area south of M5 South). 74
Figure 5: Different phytolith morphotypes and plant types recovered from all tooth and breccia samples in this study.....76
Figure 6: Phytoliths extracted from breccia control sample (grid square U62 6w); a: epidermal assemblage trichome; b: indetermined. 77
Figure 7: phytoliths recovered from 2nd breccia control sample (grid square U62 7w); a: parallelepipedal psilate; b: scutiform. 77
Figure 8: StW53f LM^2 buccal view 81
Figure 9: Total phytoliths recovered from Stw53*f*, nearest bone associated breccia (StW 53*d*) and nearest breccia control grid square.....82
Figure 10: Phytoliths recovered from the StW 53f tooth sample. a: cylindroid psilate; b: epidermal assemblage trichome; c: indetermined; d: indetermined; e: indetermined; f: indetermined; g:indetermined; h:indetermined; i: indetermined (circled) and parallelepipid short; j: indetermined; k: indetermined; l: indetermined.....83
Figure 11: Phytoliths recovered from the StW 53f tooth sample; m: indetermined; n: indetermined; o: parallelepipedal elongate scabrate; p: parallelepipedal scabrate round ends; q: parallelepipedal thick; r: platelet; s: platelet; t: scabrate facetate trapezoid; u: tracheid vessel. 84
Figure 12: Phytoliths recovered from StW 53f tooth sample; y: trapezoid; z: trapezoid; aa: trapezoid; ab: weathered elongate scabrate; ac: possible woody platelet? 85
Figure 13: Phytoliths recovered from the StW 53*d* nearest bone associated breccia sample; a: bilobate; b: bulliform; c: cylindroid echinate; d: elongate sinuate; e: indetermined; f: epidermal assemblage trichome; g: indetermined; h: indetermined; i: indetermined; j: indetermined; k: indetermined. 90
Figure 14: Phytoliths and/ or plant parts recovered from the StW 53d bone associated breccia sample; m: indetermined; n: indetermined; o: indetermined; p: indetermined; q: indetermined; r: indetermined; s: parallelepipedal elongate scabrate with rounded ends; t: parallelepipedal scabrate (broken); u: parallelepipedal thick; v: parallelepipedal thick; w: silicified stoma. 91
Figure 15: Phytoliths and/ or plant parts recovered from StW 5*d* bone associated breccia sample; y: silicified vessel with bordered pits; z: silicified vessel with bordered pits; aa: trapezoid. 92
Figure 16: Comparison between phytoliths from StW 53f tooth sample and phytoliths from nearest bone associated breccia (StW 53d - from ear bone of the StW 53 cranium) showing morphotype overlap. 92

Figure 17: StW 53d bone associated breccia compared against U62 breccia control showing one overlap in one morphotype 93
Figure 18: StW 53d compared to breccia control and nearest bone associated breccia (StW 53d) excluding indetermined phytoliths..94
Figure 19: StW 53*f* compared to breccia control and nearest bone associated breccia (StW 53*d*) showing indetermined phytoliths..95
Figure 20: StW 53*d (*the StW *53* cranium) from where the nearest bone associated breccia to the StW 53*f* tooth sample was extracted from. 96
Figure 21: buccal surface of the left lower second molar of StW 321*b*............................100
Figure 22: buccal surface of LM_2 of StW 321*b* showing areas of probable calculus 101
Figure 23: No. of phytoliths recovered from the StW 321*b* tooth specimen, bone associated breccia and breccia control sample numbers 102
Figure 24: Phytoliths recovered from the StW 321*b* tooth sample (grid square U49); a-l: indetermined..103
Figure 25: Phytoliths recovered from StW 321*b* calculus sample (grid square U49); m: indetermined; n: long cell psilate; o: long cell psilate; p: parallelepipedal scabrate (broken) 104
Figure 26: Phytoliths extracted from grid square U52 (nearest bone associated breccia); a: parallelepipedal elongate psilate; b: trapezoid wavy. 105
Figure 27: Comparison of the morphotypes recovered in StW321b tooth sample and the nearest bone associated breccia sample (U52)..105
Figure 28: parallelepipedal elongate Figure 29: parallelepipedal elongate 106
Figure 30: Closest bone associated breccia for StW 321b (U52) compared to breccia control sample (U62)..106
Figure 31: StW 321b compared to breccia control (U62 6w & U62 7w) and nearest 109
Figure 32: StW 534 RM_2 buccal..116
Figure 33: No of phytoliths recovered from StW 534 tooth and other breccia sample numbers 117
Figure 34: Phytoliths recovered in the StW 534 tooth sample (grid square W43) 118
Figure 35: Comparison of the morphotypes recovered from the StW 534 tooth sample and the closest bone associated breccia (grid square V51)...119
Figure 36: Phytoliths from grid square V51 (closest bone associated breccia (bovid fragment); a: cylindroid elongate psilate; b: parallelepipedal elongate scabrate; c: parallelepipedal facetate thick; d: bulliform fan shape. 120
Figure 37: closest bone associated breccia for StW 534 and StW 532 (V51) compared to breccia control (U62) 121
Figure 38: phytolith morphotypes of StW 534 calculus sample compared with breccia control (U62 6w and U62 7w) and nearest associated breccia samples (V51).................121
Figure 39: buccal view of LM_3 StW 532 tooth sample 124
Figure 40: Total phytoliths recovered from StW 532 and comparative bone (closest) associated breccia samples including breccia control samples..125
Figure 41: phytoliths recovered from StW 532 tooth sample 126
Figure 42: epidermal assemblage trichome recovered from breccia 128
Figure 43: Total number of morphotypes extracted from the StW 532 tooth specimen, breccia controls (U62 6w; 7w) and the nearest bone associated breccia samples (V50; V51; V52) showing V50 and V52 were devoid of any phytoliths..129

Figure 44: StW 183 lingual LM^1 showing a probable calculus deposit (a) 130
Figure 45: Phytoliths recovered from the StW 183 tooth sample. a –d, indetermined phytoliths..131
Figure 46: Phytoliths recovered from the nearest bone associated breccia sample from grid square (S63); a: indeterminate; b: indeterminate; c: indeterminate; d: cylindroid scabrate; e: parallelepipid thick 132
Figure 47: StW 183 tooth specimen, breccia control and bone associated samples and the phytolith morphotypes recovered in each sample 133
Figure 48: Phytoliths recovered from Q64 (1) a breccia control sample. a: bulliform fan135
Figure 49: Phytoliths recovered from Q64 (2) breccia control sample.............................136
Figure 50: Phytoliths recovered from Q64 (3) breccia control sample. a: parallelepipedal facetate; b: epidermal assemblage trichome 137
Figure 51: Phytoliths recovered from N46 (4w) breccia control sample...........................138
Figure 52: Phytoliths recovered from N46 (5w) breccia control sample...........................139
Figure 53: StW 53a RM^1 disto-buccal; occluso-buccal view 185
Figure 54: StW 53a RP^4 disto-buccal 187
Figure 55 StW 53a RM^2 distolingual 188
Figure 56: StW 53a RM^2 distolingual..189
Figure 57 : StW 53a RM^2 occluso-mesial 193
Figure 58: StW 53a RM^2 occluso-mesial; linguo-mesial 194
Figure 59: StW 53a RM^2 occluso-mesial 194
Figure 60: StW 53a RM^3 lingual..197
Figure 61: StW 53a RM^3 occluso-buccal; mesio-buccal; a-c: potential adherent deposits and numbers 1-4 represent clusters of different adherent types.......................................201
Figure 62: StW 53a RP^4 lingual surface 203
Figure 63: StW 53a RP3 lingual surface (6.3 x) 205
Figure 64: StW 53a RP^3 mesial surface (6.3 x) 207
Figure 65: Stw 53h Isolated LM_3 distal surface (6.3 x mag)..210
Figure 66: Stw 53f Isolated LM_3 mesial (6.3 x mag) 211
Figure 67: Stw 53f Isolated LM_3 mesial 6.3x mag...212
Figure 68: Stw 53f Isolated LM_3 lingual (6.3 x mag)..215
Figure 69: Stw 53a LP^4 distal view (12.5 mag) 217
Figure 70: StW 53f LM3 buccal 222
Figure 71: StW 53f LM3 buccal 6.3 x mag 223
Figure 72: StW 53f LM^3 buccal 20x mag 223
Figure 73: StW 53f LM3 cervico-lingual and occluso-lingual 227
Figure 74: Stw 532 LM_3 lingual 232
Figure 75: StW 498d LM1 disto-lingual..235
Figure 76: StW 498d LM1 disto lingual 6.5 x mag 235
Figure 77: StW 498d LM1 distobuccal...238
Figure 78: StW 498d LM1 distobuccal...238
Figure 79: StW 498d LM_2 mid cervico-buccal; disto-cervicobuccal 243
Figure 80: StW 498d LM_2 disto-buccal; occluso-buccal...243
Figure 81: StW 498d LM2 mesio-lingual...245
Figure 82: StW 498d LM2 mesio-lingual enlarged with potential deposits 246
Figure 83: StW 498d LM3 disto-buccal 248

Figure 84: StW 498d LM3 distobuccal enlarged 248
Figure 85: StW 498d LM3 distolingual 251
Figure 86: StW 498d LM3 distolingual with potential deposits 251
Figure 87: StW 559 RM^3 mesial 254
Figure 88: StW 483 LM^3 buccal 255
Figure 89: StW 483 LM^3 buccal. Note areas of different colouring, coarseness, ...255
Figure 90: StW 483 LM^3 occluso-distal; cervico-distal 257
Figure 91: StW 246 LM^1 buccal 261
Figure 92: StW 246 LM^1 distal 261
Figure 93: StW 246 LM^1, buccal showing differential colours in subdeposits (a-e) 262
Figure 94: StW 246 LM^1, distal, showing different colours in sub-deposits (a-c; ba) 262
Figure 95: StW 183 LM^1, bucco-mesial 266
Figure 96: StW 183 LM^1, bucco-mesial and mid-mesial with differentiated 267
Figure 97: StW 151 Ldm^1, buccal view, distal interproximal 269
Figure 98: Stw 151 Ldm1, buccal view, distal interproximal with deposits demarcated 269
Figure 99: StW 151, left maxilla Ldm^2, cervico-mesial 276
Figure 100: StW 151, left maxilla Ldm2 with sub-deposits (a-d) 276
Figure 101: StW 131 RM_1 mesial 284
Figure 102: StW 131 RM_1 mesial with deposits 284
Figure 103: StW 127 LC^2; mesial 286
Figure 104: StW 109 RM^2 mesio-buccal 288
Figure 105: StW 109, RM^2 288
Figure 106: StW 131 RP_4, buccal, RM_1 buccal 293
Figure 107: StW 131 RP_4 buccal; RM_1 buccal 294
Figure 108: StW 61, RM_2; disto-cervical; disto-occlusal 296
Figure 109: StW 61, RM_2; disto-cervical; disto-occlusal 297
Figure 110: StW 9b, RM^1, occluso-mesial 300
Figure 111: StW 9b, RM^1, occluso-mesial 20 x mag 300
Figure 112: StW 9b, RM^1 disto-lingual 301
Figure 113 : StW 9b; RM^1 disto-lingual 20 x mag 301
Figure 114: StW 9b; RM^1 with sub-deposits (a1-5) 302
Figure 115: StW 12 LM^3, disto-lingual; occluso-lingual (illustrating sub-deposit b) 305
Figure 116: StW 12 LM^3 disto-lingual; occluso-lingual (illustrating deposit a) 305
Figure 117: StW 12 LM^3; buccal 308

LIST OF TABLES

Table 1: Characteristics of supra-gingival and sub-gingival calculus (Adapted from Roberts-Harry and Clerehugh 2000)...24
Table 2: Probability Index for ranking tooth specimens for calculus 67
Table 3: Samples selected from the Sterkfontein dental assemblage 68
Table 4: Breccia samples extracted from rocks used for contamination control testing received from Professor Ronald Clarke 73
Table 5: Breccia samples extracted from a hominin ear bone (StW 53*d*) and several bovid fragments for contamination control testing 73
Table 6: This table illustrates the tooth specimens, calculus scoring and location of the calculus deposit and whether upper or lower jaw. 78
Table 7: In this table is a comparison of the phytoliths collected from specimens StW 53f (tooth specimen) and StW 53d (associated bone breccia sample). This comparison establishes whether or not there is any shared phytoliths. All photos are taken at 20μ.......87
Table 8: In this table is a comparison of the phytolith morphotype common to both closest associated breccia sample (StW 53d) and breccia control sample (U62). Although they are similar they cannot be said to be identical 88
Table 9: Phytolith counts for tooth, bone associated breccia and breccia control samples 140
Table 10: Phytoliths recovered from tooth samples..141
Table 11: Phytoliths recovered from breccia samples 142

CHAPTER 1 : INTRODUCTION

Recent studies of the dental remains from the Malapa hominin site, a fossil-bearing karstic cave-site located approximately 15 kms north-east of Sterkfontein, South Africa, have demonstrated the presence of dental calculus and associated plant material microfossils in the form of phytoliths, on the upper dentition (Henry *et al*., 2012) of *Australopithecus sediba* (MH1). The dental calculus is dated to the Plio-Pleistocene (approximately 1.977 Ma) (Dirks *et al*., 2010). This important discovery raises the possibility that such material may be present on hominin material from other cave sites in southern Africa, where fossils may be preserved under similar conditions.

1.1 Aims of this research

Based on the recent demonstration of dental calculus found on the teeth of the Malapa specimen (MH1), the aim of this study is to establish the presence of dental calculus (or tartar) deposits attached to the tooth surfaces of other southern African Plio-Pleistocene early hominins. This study will further attempt to demonstrate whether the presence of calculus is a unique phenomenon to Malapa. This study will undertake an examination of the dental collection of the Plio-Pleistocene age hominin site of Sterkfontein, South Africa, in order to establish the presence of adhering matrix, which may be identified as dental calculus.

1.2 Background Study

1.2.1 Aetiology of Dental Calculus (or tartar)

The pathophysiological deposits found on teeth are known as dental calculus (Schroeder 1969). Dental calculus has been characterised as mineralised bacterial plaque, which is covered in life by an unmineralised dental biofilm, composed of living bacteria (Newman 1980; Hillson 1996; Mandel 1990). It is found attached to the surfaces of teeth and to other structures in the mouth cavity (Newman 1980; Hillson 1986, 1996; Lukacs 1989, Lindhe 1990). While dental calculus is not in itself a living organism, dental plaque is composed of living bacteria in an extra-cellular matrix, and new dental calculus forms as the dynamic layers of plaque mineralise.

1.2.2 Composition and Structure of Dental Calculus

Dental calculus comprises inorganic and organic components. The organic constituent comprises between 15-20% dry weight of supra-gingival calculus and consists of glycoproteins, lipids, proteins, amino acids, micro-organisms from the flora of the mouth and carbohydrates (Mandel 1990; Hillson 1996). The organic constituent proportion may be a lesser amount in sub-gingival calculus (Roberts and Clerehugh 2000). The inorganic constituents are predominantly calcium and phosphorous, as well as fluoride, sodium, carbonate, and magnesium (Theilade and Schroeder 1966), and appear to be similar to enamel, dentine, cementum and bone, including the deposit's crystal arrangement (Hodge and Leung 1950; Gressly 1963; Mandel 1990). Henry *et al.* (2010) found however, that on archaeological samples, dental calculus behaves more like enamel than dentine, as it is less inclined towards mineral replacement than dentine with the increasing age of calculus.

Dental calculus is diffused with several different calcium phosphate crystals (Schroeder 1969). Four types of calcium phosphate crystal have been observed, in varying percentages in supra-gingival and supra-gingival calculus, by means of both an electron microscope and through X-ray diffraction studies (Schroeder 1969; Tan *et al*., 2004):

1. HAP, hydroxyapatite, more or less [Ca_{10} $(PO_4)_6(OH)_2$], which is the principal crystal matrix structure.
2. DCPD, brushite or dicalcium phosphate dihydrate, [$CaHPO_4 \cdot 2H_2O$]
3. OCP, octacalcium phosphate, [$Ca_8H_2(PO_4)_6 \cdot 5H_2O$]
4. WHT, magnesium containing whitlockite, beta-tricalcium phosphate, [$Ca_{10}(HPO_4)(PO_4)_6$]

1.2.3 Categories of Dental Calculus

Dental calculus is broadly grouped into two categories, supra-gingival and sub-gingival. Their structure and composition are different because of their different locations in the mouth cavity relative to the marginal gingivae. They also differ in appearance, consistency, attachment, composition and structure (Forsberg *et al*., 1960).

Supra-gingival calculus is found on the tooth enamel, coronal or slightly above the gingival margin, and commonly has a strip or 'band' denoting the position of the gingival margin (Newman 1980; Friskopp 1983; Hillson 1986; 1996) It is most commonly found on the lingual surfaces of the mandibular incisors and the buccal surfaces of the first maxillary molars (Parfitt 1959), adjacent to the openings of the salivary glands (Gressly 1963; Friskopp 1983).

Sub-gingival calculus is located in the gingival pocket on the root surface as the gum tissues regress (Newman 1980; Friskopp 1983; Hillson 1996). The location of sub-gingival calculus has no association to the salivary glands (Roberts-Harry *et al*., 2000). Corbett and Dawes (1998) reported that the levels of sub-gingival calculus are markedly higher on the lingual than on the buccal surfaces. On the lingual surfaces, the lower first molars typically have the most sub-gingival calculus. On the buccal surfaces, the mandibular anterior teeth and maxillary molars are typically seen to have the largest amounts of sub-gingival calculus. Sub-gingival calculus appears to be site-specific; however it is much less apparent than supra-gingival calculus (Corbett and Dawes 1998).

There is a basic resemblance in the formation and macroscopic appearance of supra-gingival and sub-gingival calculus (Oshrain *et al*., 1971), but marked differences in their inorganic components and microstructure (Lundberg *et al*., 1966).

Supra-gingival calculus exhibits a more consistent distribution of iron and manganese than sub-gingival calculus (Roberts-Harry and Clerehugh 2000), and typically comprises more hydroxyapatite crystals and brushite than sub-gingival calculus (Driessens and Verbeeck 1989). Sub-gingival calculus is more heavily mineralised than supra-gingival calculus (Hillson 1996), and contains higher concentrations of magnesium, calcium, fluoride, strontium and sodium (Lundberg *et al*., 1966; Gron *et al*., 1967; Mandel 1990).

Supra-gingival is more heterogeneous with more areas of non-calcification, variations in shape and size of crystals, and micro-organisms (Friskopp 1983; Hillson 1996). Supra-gingival calculus is covered by a layer of micro-organisms composed of mainly filaments positioned perpendicular to the underlying calculus and in contact with it.

Sub-gingival calculus in contrast, is covered by a layer of rods, filaments and cocci with no particular pattern of organisation (Friskopp and Hammarström 1980). Supra-gingival calculus is dominated by calcified and uncalcified micro-organisms in a predominantly OCP, HAP, and DCPD matrix (Roberts-Harry and Clerehugh 2000). Sub-gingival is characterised by a more homogenous calcification with mainly uncalcified micro-organisms in a WHT matrix (Roberts-Harry and Clerehugh 2000).

Supra-gingival calculus can be linked to diseased or healthy teeth (Friskopp and Hammarström 1980; Friskopp 1983), whereas sub-gingival calculus is synonymous with periodontally diseased teeth (Friskopp and Hammarstrőm 1980; Friskopp 1983).

Plaque mineralisation transpires in a number of individual foci (Mandel *et al*., 1957; Friskopp 1983). Mineral deposits of dental calculus are present both in, and between micro-organisms conditional upon the maturity of the deposit (Donald 1997), meaning, that mineral deposits in the plaque matrix, and some plaque micro-organisms will calcify first as the calculus increases in age (Jin and Yip 2002). The differences in fluid environments and varied microbial flora may be responsible for the compositional and structural differences of supra-gingival and sub-gingival calculus (Friskopp and Hammarström 1980; Friskopp 1983; Jin and Yip 2002).

Table 1: Characteristics of supra-gingival and sub-gingival calculus (Adapted from Roberts-Harry and Clerehugh 2000)

	SUPRAGINGIVAL	SUBGINGIVAL
Location	Coronal to gingival margin	Apical to gingival margin
Colour	Yellow/white/cream/ light brown	Brown/black/grey
Distribution	Adjacent to salivary duct openings	Randomly around the mouth
Composition	Concentration of Ca, Mg, F Sr and Zn lower and of carbonate Ad Mn higher than sub-gingival calculus. More regular distribution of F	Concentration of Ca, Mg and F higher and of carbonate lower than supra-gingival calculus. More irregular distribution of F
Mineral content	Averages 37% from saliva by volume	Averages 58% from crevicular fluid by volume
Crystal type and size	Mostly OCP and HAP, some DHPD. Small needle-like and ribbon-like	Mostly WHT, no DHPD. Small crystals
Formation	Heterogeneous nucleation and crystal growth. More variable (heterogeneous) calcification	Heterogeneous nucleation growth. More uniform (homogeneous) variation
Microorganisms	Dominated by microorganisms, some non-calcified areas. More filamentous organisms; faster growth	Few non-calcified microorganisms. Less filamentous organisms; slower growth
Morphology	Indistinguishable	Several types: spiny, crusty, nodular; ledge/ring; individual islands; smooth veneers; finger/ fern-like; supra on sub-gingival
Pathogenic potential	Slight evidence	Allied to periodontal disease

1.2.4 The Formation of Dental Calculus

The formation process of dental calculus is not completely understood (Lieverse 1999). Subsequent to tooth eruption or prophylaxis, the process starts with salivary proteins rapidly adsorbing onto the tooth enamel surface, forming an acquired enamel pellicle, which is characterised as an organic layer covering tooth surfaces (Newman 1980; Mandel 1990; Hillson 1996). The pellicle is soon dominated by microorganisms, mainly bacteria, gaining their nutrients from the amino acids, peptides, glycoproteins and proteins from the oral fluids, and not from the foods that pass through the mouth cavity (Mandel 1990; Hillson 1996). Gram-positive coccoidal microorganisms are the first to attach to the formed enamel pellicle, and then filamentous bacteria follow, gradually dominating the plaque biofilm within a period of approximately 36 hours (Koparal and Tütüncu 2000).

According to Schroeder (1969), the calcium and phosphate occurring in the oral fluid must be present in ion form. This together with the idea of simple precipitation in a state of supersaturation has proven to be erroneous (Schroeder 1969). The mineralisation process is now thought to be more complex. Silicon appears to be important in calculus composition and formation; however the mechanisms involving formation are not known (Damen and ten Cate 1989).

It is now thought that the calculus mineralisation process is similar to other ectopic calcifications, such as gallstones and urinary stones (Gressly 1963; Kido *et al.*, 1995). Calcium and phosphate concentrations in the oral environment are not high enough to result in spontaneous calcification, which is necessary for the viability of the 'Booster Mechanism' – a mineralisation theory described by Mandel (1990) which relies on the supersaturation of calcium and phosphate ions in the oral fluids. It maintains that mineralisation will occur when the local pH and calcium phosphate concentrations are high enough to allow the precipitation of the mineral salts out of the oral fluids (Gressly 1963; Schroeder 1969; Mandel 1990).

The concentrations are high enough to support the growth of calcium phosphate crystals once a nucleus or seed has formed (Mandel 1990). Mineralisation therefore involves two concepts: the nucleation of crystal 'seeds' and growth of calcium phosphate crystals (Schroeder 1969).

Nucleation is thought to occur only when an organic matrix composed of oral microorganisms, and the inter-microbial substance is available for crystallisation to occur in a precise structural form (Mandel 1990). This inter-microbial mix according to Zander *et al*. (1960) infers that its composition plays a significant role in the mineralisation process.

Bacterial involvement in the mineralisation process has been supposed for over fifty years (Hodge and Leung 1950) and supported my many researchers (Zander *et al*., 1960; Sidaway 1980). It is now thought numerous microorganisms play a nucleating role in the mineralisation process of dental calculus (Sidaway 1980; Scheie 1989; Moorer *et al*., 1993).

Another mineralisation theory posited by Mandel (1990) supports the idea that hydroxyapatite crystals are not formed necessarily when mineralisation starts (Mandel

1990). Crystal deposition varies with the maturation of calculus. Brushite (DCPD) forms first, and then octacalcium phosphate, while whitlockite (WHT) and hydroxyapatite (HAP) are likely to use the first two as precursor crystals for their formation (Driessens and Verbeeck 1989). DCPD crystals are the most prevalent in immature calculus of up to three months, while HAP crystals are the most dominant in mature calculus, six months or older (Koparal and Tütüncu 2000).

According to Zander *et al*., (1960) mineralisation follows a three stage pattern. Crystals are first formed alongside the bacteria, then on the bacterial surface (extracellular), and then inside the bacteria (intracellular) (Koparal and Tütüncu 1998).

Several research studies have examined dental calculus formation (Mandel, Levy & Wasserman 1957; Turesky, Renstrup, & Glickman 1961; Theilade 1964; Schroeder, Lenz and Muhlemann 1964). These investigations demonstrate that plaque formation always precedes dental calculus formation, and that plaque accumulations exist as the organic matrix for the successive deposit mineralisation. Dental plaque absorbs calcium and phosphate from the saliva to form supra-gingival calculus and from crevicular fluid to form sub-gingival calculus (Willet *et al*., 1991; Bernimoulin 2003).

1.2.5 Diet and its Influence on Calculus Formation

Although there is adequate non-anthropological literature on dental calculus, the influence of diet on dental calculus formation has been poorly studied, and anthropologists have tended to oversimplify the concept of calculus and its formation Lieverse (1999). Many factors affect dental calculus formation in living individuals, of which dietary patterns are one of them, but they are not the central influence (Lieverse 1999). Although little study on the effects of diet on calculus formation in humans has been done, considerable studies have been done on dogs and rats (Schroeder 1969). Kakehashi *et al*., (1962) showed that diets high in calcium and phosphate did not affect calculus deposition in rats, while diets high in bicarbonate did. Smith *et al*., (1963) found that diets high in fats and carbohydrates had similar effects on calculus formation in rats. They further found that high amounts of water consumption resulted in reductions in calculus formation. Plumbo *et al*., (1963) found that a high carbohydrate diet in rats increased calculus formation. Kakehashi *et al*., (1963) demonstrated that the food found in the oral environment of rats did not appear to be the principal source of the elements of dental calculus. Baer and White (1966) showed that rats with a diet high in fats resulted in increased dental calculus formation, in comparison to a diet high in carbohydrates. This was in contrast to Smith *et al*., (1963). Baer and White (1966) further demonstrated that diets with high protein contents yielded more calculus than those with high in fat or carbohydrate contents. Tanzer *et al*. (1989) experimented with pathogen-free Osborne-Mendel rats, subjected to a diet containing sucrose and high in calcium and phosphorous, which is conducive to calculus formation. The results induced calculus and caries simultaneously.

Although these findings appear to be inconsistent with experimental findings in humans (Schroeder 1969), they are comparable to the present understanding of the effects of diet on human calculus (Lieverse 1999).

It is widely accepted that mineral precipitation and calculus formation are enhanced by an alkaline environment, and that oral micro-organisms play a significant part in facilitating this alkalinity through the production of ammonia (Scheie 1989; Mandel 1990). There is also broad consensus that increased calculus production will result from diets rich in protein (Hillson 1979). Protein consumption results in higher blood urea levels, which are metabolised by oral bacteria, producing ammonia which results in higher alkaline levels and plaque mineralisation (Dawes 1970). Thus protein rich diets can expedite calculus formation by increasing alkaline levels in the oral environment (Lieverse 1999).

Large amounts of water consumption can reduce calculus formation, by lowering the concentration of oral mineral salts and the probabilities of mineralisation (Smith *et al*., 1963). The degree of mineral content of drinking water may have an effect on calculus formation by introducing greater amounts of minerals into the mouth cavity (Gaare *et al*., 1989). Dawes (1970) observed further, that hyperhydration leads to in increased saliva flow and dehydration leads to a lower salivary flow. Therefore the level of hydration may affect the formation of calculus. These effects were interpreted by Dawes (1970) to be linked to diet.

Calculus formation can also be heightened by the degree of silicon present in surrounding oral fluids (Lieverse 1999). Connective tissue, enamel, hair and nails of humans contain high amounts of silicon (Rølla *et al.*, 1989). Silicon is also present in the structural parts of plants and drinking water, and is present in differing degrees in numerous foods eaten by humans. The effect of different amounts of silicon on the rate of calculus formation has not been addressed (Lieverse 1999).

Chewing can also promote calculus deposition by increasing salivary flow rates, and therefore salivary protein and calcium, as well as alkalinity (Dawes 1970). Conversely chewing abrasive materials may have the effect of removing adherent calculus deposits (Gaare *et al.*, 1989).

Volpe Kupczak and King (1967) observed that no information on the rate of calculus deposit formation was discernible from the studies of Muhler and Ennever (1962). The epidemiological data comparing two different periods of calculus formation did not state a deposit formation rate with regard to surface area and time (Volpe Kupczak and King 1967). Examples of quantitative data on time and its association with dental calculus formation were reported in Schroeder and Bambauer (1966).

According to Schroeder and Bambauer (1966), there have been several studies describing the components of old or unspecified supra-gingival or sub-gingival calculus. Rowles (1964a, b) studied calculus deposits aged 3-6 months or less and one not older than 14 days (Vahl *et al.*, 1964). Most of these studies do not differentiate between supra-gingival calculus and sub-gingival, upper or lower, or older or younger types (Schroeder and Bambauer 1966). The results therefore cannot be interpreted in any conclusive way. There is consensus that dental calculus deposits on teeth comprise 4 different calcium phospates (Rowles 1964a). Apatite was reported mainly for old as well as young calculus (Rowles 1964a, b; Vahl *et al*., 1964). Rowles (1964a) observed that whitlockite was less common and abundant in younger specimens in contrast to brushite, which was relatively abundant and commonly found in younger calculus, and less in older calculus.

Younger lingual supra-gingival calculus forming on a uniform surface area of lower anterior teeth appears to grow in a linear configuration during the first two weeks of development (Muhlemann and Schroeder 1964). The rate of deposit formation reported in Schroeder and Bambauer (1966) for mandibular central and lateral incisors is not considered generally representative. This study claims that it is important to get a quantifiable idea of how rapidly an individual is likely to form calculus. Earlier experiments involving the recalculation of deposit weight data (Schroeder 1963) have found that the deposit formation rate for mandibular incisors to be 0.086 mg per day, and accords with 0.83 mg per day found in the studies of Schroeder and Bambauer (1966). The average deposit formation rate in slow to rapid deposit formers is 0.08 mg per day for central, and 0.06 mg per day for lateral incisors. Dental calculus formation time is mostly not more than 12 to 14 days (Schroeder 1969).

Data on the prevalence and intensity from epidemiological field studies reviews chronologically the average data obtained for various populations groups predominantly in Asia, North- and South America, and in Australia using the OHI

(Oral Hygiene Index) developed by Greene and Vermillion (1964) and the Ramjford Index (1959), which is similar to the OHI (see Schroeder 1969).

The data of most researchers, according to Schroeder (1969) indicate that the intensity of dental calculus increases with rising age. The findings with the OHI and those obtained with the Ramjford Index were the same (Schroeder 1969). The increase seems to be the result of the continuation of the accumulation time rather than to an improved ability to form calculus (Volpe Kupczak and King 1967).

There appear to be no major differences between sexes. It is not possible to deduce from these studies whether the dissimilarities in the intensity of deposits between various groups of populations but within the same age group, are due to differences in oral hygiene, variations in climate or different living habits, or different dietary influences (Schroeder 1969).

1.2.6 Non-Dietary effects on calculus preservation

Taphonomic agents, excavation methods and weak curation practices are factors that affect the presence and degree of dental calculus on fossil specimens (Buikstra and Ubelaker 1994). Natural taphonomic agents, for example water, soil type, temperature, oxygen, flora and fauna (Henderson 1987) may negatively affect the preservation of human skeletal remains, but also that of dental calculus (Buikstra and Ubelaker 1994; Ortner and Putschar 1995). Activities such as negligent excavation and overzealous cleaning can also result in the destruction of dental calculus deposits (Buikstra and

Ubelaker 1994). Scientists eager for accurate morphological measurements, can also inadvertently damage calculus with measuring instruments.

1.3 Hominin Diets and Ecology and the Importance of Plant Foods

1.3.1 Introduction

The significance of understanding hominin diets is widely acknowledged, primarily because the search for food and its consumption impacts considerably on the behavioural and ecological variability of primates and humans (Ungar 1998; Fleagle 1999). Diet is therefore considered to be a crucial factor underscoring a variety of adaptations and evolutionary pathways of early hominins (Robinson 1963). Several large primates spend a considerable amount of their time eating and digesting food (Altmann and Altmann 1970; Teleki 1981; Goodall 1986; Whiten *et al*., 1991), and diet is largely at the base of ecological niche divisions.

Dietary information can be used to investigate the diets of extinct genera and species; however some conventional sources of information such as stone tools, bones from animals, and spatial contexts about past human diet and subsistence may provide limited data (Lee-Thorp and Sponheimer 2006).

There are however, limitations to the early fossil record where the stratified archaeological evidence is rare (Lee-Thorp and Sponheimer 2006). Numerous Plio-Pleistocene sites suffer from interpretative problems, where sites are considered 'palimpsests' and assemblages have accumulated over hundreds and thousands of years. The purpose of stone tools for instance is poorly understood, and their makers are in often doubt as to whether they are australopith or early *Homo* or even unrecognised genera (Brain 1981).

While the presence of bones and stone tools in the palaeorecord places an emphasis on animal foods, plant foods constitute the greater part of most primate foods (Milton 2002), and are likely to have been just as significant for early hominins (Lee-Thorp and Sponheimer 2006).

1.3.2 Diets and Ecology of Early Hominins and Early Dietary Models

There appears to be no consensus with the change of diets that accompanied the evolutionary shift from hominoid to hominin during the Miocene. Several models have arisen from the evolutionary studies of diets of hominins of the Plio-Pleistocene. They have emanated mainly from nutritional studies and direct analogy, or from evidence from archaeological or palaeoenvironmental indicators. The problem with these models is that they are unsuccessful at illustrating what these hominins were eating (Ungar *et al*., 2006).

Numerous researchers have emphasized the probability of increasing animal flesh consumption as the growth in the savanna habitat spread across eastern and southern Africa. Others have suggested that early *Homo* included more xeric plants in their diet, and that gathering appeared to be a ‘motile’ influence in the evolution of the human species (Linton 1971, Coursey 1973, Wolpoff 1973).

Because they are utilised to process food resources, numerous scholars have relied on dental morphologies as a means to infer dietary behaviour (Robinson 1956; Tobias 1967; Jolly 1970; Wolpoff 1973; Grine 1981; Ungar 1998). The dentition of early hominins is characterised by enlarged molars relative to its body size and to the incisors, and the reduction of the canines. The cheek teeth are generally broad, and cusps are blunt with thick enamel (Pilbeam 1972).

Robinson (1954, 1956) recognised that *Paranthropus robustus* had smaller incisors and larger molars than the gracile australopith, *Australopithecus africanus*. He hypothesised that *Paranthropus* had a herbivorous diet, and required grinding large amounts of tough plant foods. The dentition of *A. africanus*, he hypothesised indicated an omnivorous diet requiring more incisal preparation for meat and other food resources (Robinson 1956). But early researchers could not come to a consensus on the dietary behaviour of *A.africanus,* and by the mid-1970s it had been suggested, could have been either a herbivorous (Jolly 1970; Wolpoff 1973), omnivorous (Robinson 1954), or carnivorous (Szalay 1975) hominin.

Using morphologies alone as a predictor of primate diets is an unreliable method, even for extant taxa. *Papio*'s bunodont molars and large incisors for example, indicate a frugivorous diet (Fleagle 1999; Ungar 1998), yet observation of numerous extant baboon populations shows they eat high percentages of grasses (Harding 1976; Strum 1987). *Papio* it appears is therefore dependent on a food source for which it is not well provided. Dental morphology therefore will reflect an organism's adaptations to diet and offer clues to its phylogeny, which might however not accord with its actual eating behaviour (Lee-Thorp *et al*., 2003).

Attempts to solve these problems have included both occlusal tooth microwear studies, and stable light isotope studies of fossilised teeth and bone. Understanding of early hominin diets has also been enhanced through the unearthing of new fossils, better quality palaeo-environmental reconstructions (Ungar and Sponheimer 2011), and that studies on fossil and extant species of primates have demonstrated that microwear studies can distinguish between consumers of hard and soft fruits, and distinguish frugivorous from folivorous primates (Grine and Kay 1988; Teaford 1992; Ungar 1998). In applying these studies to South African australopithecines, it has been suggested that *A. africanus* ate soft fruits and leaves, while the megadont *A. robustus* ate harder more fibrous foods (Grine 1981; Grine and Kay 1988). Little is known about the microwear of early australopiths. There appears to be no tooth microwear research available for *Ar. ramidus* and *Au. anamensis*. Some research is available on *Au.afarensis* and *Au.africanus*. *Au. afarensis* studies suggest that they were starting to exploit the savannah resources (Puech and Albertini 1984). *Au.afarensis* had a combination of 'mosaic and gorilla-like' wear striae and pits like that of baboons (Ryan and Johanson 1989), indicating that incisors may have been used to remove roots, rhizomes and seeds. *Au. africanus* studies have concentrated on the comparison with *Paranthropus robustus*. *Au. africanus* had a lower amount of pitting than Paranthropus robustus, and exhibited longer and narrower scratches, and the arrangement of wear was more homogeneous, according to Grine (1986). Grine (1986) postulated that *Au. africanus* ate more soft food resources, such as fruit and leaves. Research done on

Au.africanus by Ungar and Grine (1991) concluded that *Au. africanus* exhibits higher tooth microwear feature densities than *P. robustus*, suggesting that *Au.africanus* used its anterior teeth to process a large variety of food resources including more abrasive kinds than did *P. robustus*. Tooth microwear therefore seems to suggest that the diets of the hominoids by the end of the Miocene had an extensive range. *Au. afarensis* perhaps focused on soft food resources like fruit but was beginning to add abrasive resources that required incisal preparation. *Au. africanus* it is suggested by Teaford and Ungar (2000) probably still focused on soft fruit resources, requiring a moderate anterior tooth preparation. The drawback with tooth microwear studies is, that it includes the 'last supper effect', showing only a short term dietary signal, and the inability to discern certain food resources in the fossil record, for example grubs, insects and animal meat, as well as the consistency of food resources (Lee-Thorp *et al.,* 2003) in the tooth microwear record. Teaford and Ungar (2000) pose the question: 'Can we speak of a diagnostic australopithecine dietary pattern?' To some extent this may have been the case, but although australopiths had characteristics in common, there were also differences, leading to a changing diet through time. These morphological changes manifested as a mosaic over time (Teaford and Ungar 2000), and may have affected the consistency of food resources in the tooth microwear record over time.

It has been hypothesised that some of the earlier hominins may have had thinly enamelled and smaller molars in comparison to the later hominins, and were more likely to be closer to extant chimpanzees and bonobos, indicating a possible diet of fruit and leaves (Wood and Lonergan 2008; Ungar and Sponheimer 2011). Species of later *Australopithecus* reflect a shift from diets characterised by soft forest fruits to brittle and hard nuts or seeds, or underground plant storage organs (USOs) that were becoming more easily accessible in Plio-Pleistocene settings (Teaford and Ungar 2000). Changes in diet have been recognised as significant markers in the spectrum of evolution (Ungar 2011). The dietary competencies of early hominins underwent far-reaching changes between 4.4 Ma to 2.3 Ma.

The only direct source of data of early *hominins* is the fossil record itself. Researchers have developed a number of tools for extracting aspects of diet from these fossils. Mainly the evidence has come from biological factors such as: tooth shape and size, jaw morphologies, enamel structure and dental microwear and mineralised tissue chemistry (Ungar 1998, 2002). This evidence appears to indicate a shift in the diets of australopithecines to a more flexible dietary regime as a result of changes in climate. Diet related changes for the early hominins also indicate that hard coarse food resources, potentially became critical items in their diet, and therefore increasingly significant throughout the Pliocene (Teaford and Ungar 2000). Although applications of these approaches to early *Homo* have been limited, there has been some work done on australopiths (Ungar, Grine and Teaford 2006; Henry *et al*., 2012) which were examined for evidence of diet.

Research on the diets of early hominins has historically focused on archaeological and morphological elements. Dietary evidence can suffer from inherent drawbacks. Not much can be ascertained from excavated bones or stone tools about the types of plant foods consumed by early hominins (Ungar and Sponheimer 2011). Although the osteology of teeth and jaws present significant indications of the stresses of the jaw apparatus to which hominins may have been adapted, they can only infer what their diet must have been, and not what was actually eaten by an individual hominin. Thus direct evidence of the diets of fossil hominins requires evidence such as dental microwear, stable isotope analysis (Ungar and Sponheimer 2011) and forms of direct evidence such as phytoliths from dental calculus studies (Henry and Piperno 2008; Henry *et al*., 2010, 2012).

Numerous dietary models such as graminivory (Jolly 1970); herbivory (Wolpoff 1973); frugivory (Walker 1979); nuts (Kay 1981); roots and tubers (Coursey 1973); carrion and carnivory (Szalay 1975); game (Leopold and Audrey 1972); sedges and grasses (Cerling *et al*., 2011) have been suggested as the major constituents of the proto-hominin and hominin diets (Kurland and Beckerman 1985). The evidence according to Gregory (1922), Pilbeam (1972), and Simons (1972) is highly supportive of an omnivorous diet. Kay (1975) has argued that the large postcanines of the australopithecines suggest a fibre rich diet, which includes considerable amounts of grit. According to Dunbar (1976), likenesses in tooth morphology don't necessarily mean precise dietary correspondences, but that those diets require similar pre-processing before the foods are consumed.

1.3.3 The Importance of Plant Foods

The role that plant food played in contrast to meat in early hominin diets has long been debated amongst scholars (Stahl *et al*., 1984). Dietary patterns are crucial to the development of hominin ecological models and evolution, because they have a direct bearing on subsistence behavioural patterns, trophic adaptations and various inter-specific relationships (Boaz 1977; Peters 1979). Early scholars emphasised the significance of carnivory and meat (Dart 1953; Ardrey 1961, 1976; Laughlin 1968, Lee 1968; Washburn, Sherwood and Lancaster 1968; Szalay 1975; Isaac 1976), however, much less attention has been paid to the role of plant foods (Lee 1968; Woodburn 1968; Jolly 1970; Zihlman and Tanner 1978; Peters and O'Brien 1981). While higher primates are omnivorous (Gaulin and Konner 1977), the bulk of their diet emanates from plants.

Previous studies of extant hunter-gatherers have demonstrated that their diet includes less meat and more vegetable foods, and this pattern can be inferred back to the Plio-Pleistocene (Stahl *et al*., 1984) Preservational bias seems to cause the apparent incapacity to evaluate the role that vegetable foods play in the early hominin diet.

The dentition of the early hominins, both 'protohominin' and australopithecine, according to Kurland and Beckerman (1985) and Wolpoff (1980), suggest a highly eclectic diet, which includes a wide range of plant and animal prey types, derived from a temperate and mixed habitat (Wolpoff 1980). According to Kay (1981) and Isaac and Crader (1981) there is significant doubt surrounding the amount of animal prey contained in the diets of Pliocene hominins. Despite the variety of opinions on early hominid diets, a high quality diet where the food is dispersed appears to be commonly associated with these models (Kurland and Beckerman 1985). Early hominins appear to have developed a variation similar to primate 'opportunistic omnivory' (Gaulin and Konner 1977; Rose 1978).

1.3.3.1 Hominin Diets Before Fire

A key variance between modern hunter-gatherers and Plio-Pleistocene hominins potentially may lie with the control of fire and its function in the preparation of food resources (Stahl *et al*., 1984). Leopold and Ardrey (1972) argued that without fire to prepare food resources, this would have prevented the consumption of plant foods with chemical limitations, which could have only been surmounted with cooking. They do not discuss 'toxins' of various plant foods and their effect on the physiology of humans, their distribution in the plant kingdom, or how cooking might affect them. Stahl *et al*. (1984) argue that these issues need addressing, in order to measure the impact of plant toxins on plant selection by hominins. Stahl *et al*. (1984) study plant foods that would potentially be inedible without the processing of fire, to attempt to gain insight into the possible limitations of dietary choices made by hominins without the capability of fire.

Stahl *et al*. (1984) developed a list of food resources most likely to have been consumed by hominins prior to the use of fire, and this acted mainly as a heuristic mechanism. The dietary patterns of a distinct group of hominins would have been conditioned by the specific abundance, distribution and procurement costs of their available resources (Milton 1981). Two factors significant in determining the utilisation of plant parts by hominins: their digestibility and their 'toxin' component (Stahl *et al*., 1984).

According to Stahl *et al*. (1984) cellulose and starch are not easily digested when raw. Given that nutrient intake is limited by processing time, plant parts high in carbohydrates (leaves, stems, smaller roots) (Lamb and Harden 1973), are less likely to be sources of food than plant parts with low levels of starches and cellulose. Smaller amounts of cellulose are found in immature plant parts (shoots, buds, and young leaves), flowers, fruits, and seeds (Lamb and Harden 1973). Bulbous underground storage organs (tubers, bulbs, corms and storage roots) lack extreme amounts of cellulose; however a high proportion of the stored food reserves come in the form of starch (Stahl *et al*., 1984). Carbohydrates for instance, occur mainly in the form of starches in the tubers of yams (*Dioscorea* spp.) (Purseglove 1972), while in onion bulbs of *Allium cepa* food reserves are stored as sugars and are more digestible form of energy (Purseglove 1972). Therefore discrimination between the varieties of underground plant storage organs is important, in determining the potential plant food sources of early hominins (Stahl *et al*., 1984). Another source of stored starch is the seed. Starch content is considerably elevated in the seeds of monocotyledonous plants (Bondi 1958), where the main focus of storage is the endosperm. Storage in dicotyledonous plants occurs more often in the cotyledons and starch content is lower (Stahl *et al*., 1984). The location of toxins in particular parts of plants is a factor that potentially may have played a significant role in the dietary choices of early hominins, as toxins are frequently located in areas of stored food reserves (Stahl *et al*., 1984).

There is evidence that humans have developed mechanisms to assist them in digesting starch, including increased amylase manufacture (Perry *et al*., 2007). According to Perry *et al*. (2007), starch intake is a significant constituent in the diets of some agricultural (Zohary and Hopf 2000) and hunter-gatherer societies in dry regions, and is much lower in rain forest and arctic hunter-gatherer environments. According to Perry *et al*. (2007), this variation raises the probability that a diversity of selective pressures may have had an effect on amylase, the enzyme responsible for hydrolysis (Lebenthal 1987). Therefore evolutionary studies of amylase in humans and their near primate relatives may well provide clues to their ecological past (Perry *et al*., 2007).

The studies of Peters and O'Brien (1981) used modern analogues to model potential early hominin plant foods, by demonstrating the difference between the 'fundamental' versus 'realised' plant food niche of early hominins. Their model specified wild plants eaten today by humans, chimpanzees and baboons in eastern and southern Africa that may have also been eaten by early hominins. The final list contained those genera exploited by all three primates. Six genera were recognised in the palaeobotanical record: *Acacia* (pods), *Albizia* (flowers and leaves), *Cordia* (fruits), *Diospyros* (fruit), *Ficus* (fruits), and *Ziziphus* (fruits). Their analysis demonstrates that fruit and/or leaves to be the most common food types exploited by early hominins (Peters and O'Brien 1981). Underground plant storage organs and seeds/pods are the second most important group resulting from these studies. This supports the conclusion of Dunbar (1976) on the basis of limited data, that these types of foods would constitute staples for the early hominins. Peters and O'Brien's (1981) research shows that the food niche is characterised by more variety than has been commonly recognised.

Early hominins are relatively large in comparison to other primates (White 1980; Wolpoff 1980). The shifting from a forest to a savanna environment, causes habitat productivity decreases, food abundance decreases, and quality foraging areas become more widely dispersed (Gaulin 1979). Thus from the perspective of a relatively large forager, the distribution of potential food types becomes more coarse grained in the open savannah habitat. Therefore the larger body size favours a diet of widely available, but poor quality items (Bell 1971). Thus high-quality, rare animal prey could become a significant part of the early hominin diet only with the assistance of tools or social foraging (Gaulin 1979). The increase in the hominin body size and the allometrically large expansion of the posterior dentition (Wolpoff 1980) suggests that the diet included low-quality food items requiring considerable chewing. Optimal foraging thus suggests that 'omnivory was the dominant dietary adaptation' (Gaulin 1979).

While Szalay (1975) believed that the functions of incisors were adapted to a meat diet, Hatley and Kappelman (1980) have argued that the cutting and ripping functions of incisors are also suited to the breaking down of tough plant rhizomes into parts that can be processed by the cheek dentition. They further conclude that molars and premolars which have thickened enamel and heavy jaw musculature appear to be pre-adapted for processing this kind of food.

Jolly's (1970) findings, which were considered controversial, found that australopithecines were provided with relatively small anterior teeth (incisors) in comparison to posterior teeth (molars), and postulated that by analogy with the modern gelada, the large molar teeth and small incisors of *Paranthropus* were interpreted as adaptations to consume small tough seeds (Jolly 1970). Jolly's (1970) hypothesis further concluded that *Australopithecus* and *H. habilis*, shifted from consuming grass seeds to meat and plant food material, on the basis that the trend to the 'dominance' of back teeth was 'partially reversed' (Jolly 1970). According to Dunbar (1976), a specialisation of grass seeds is considered uncertain. Microwear data also appears to discount gelada-like graminivory, since the pitted molars of the australopiths (Grine 1986; Grine and Kay 1988) are not similar those of the modern geladas, whose molar microwear is characterised by striations (Teaford 1993).

The fruit and nut dietary model is strongly associated with an arboreal rain forest feeding niche, as opposed to a terrestrial ecotone environment (Kurland and Beckerman 1985). The thickly enamelled 'early hominoid' dentition is indicative of a hard textured diet, as in nuts. In contrast to the Miocene hominoids which had dental patterns similar to those of living apes (Kay 1977, 1981), the australopithecine dentition appeared to have a 'megadont' adaptation of a large, thickly enamelled cheek teeth pattern and massive chewing musculature relative to their body plan (Walker 1981). These types of dental patterns are suited to diets that require large-scale mastication, and include foods requiring major crushing or extensive chewing (Grine 1981; McHenry 1984). The australopithecines that appeared later, *A. robustus*, developed these characters to an extreme, and was characterised by relatively small anterior teeth, but huge molars and premolars with thickly enamelled crowns, frequently worn flat. Young juvenile robust australopithecines also demonstrate heavy wear on their milk molars (Grine 1981). Many scholars have postulated the study of the wild plant foods eaten by terrestrial monkeys, apes and humans could provide insights into early hominin diets (Peters and O'Brien 1981). Dunbar (1976) suggested that the diet of australopithecines might have resembled that of terrestrial baboons which were dependent on fruits, seeds and roots. Clark (1975) emphasised the possibility that the plant foods exploited by chimpanzees in east Africa (Miombo Woodlands) could provide an indication of the dietary scheme that could be expected from early hominins.

Despite the evidence of plant feeding being problematic to obtain, hominin dentition and ecology as well as contemporary human nutritional requirements, imply a considerable reliance on plants (Gaulin and Konner 1977; Gaulin 1979; Mann 1981).

1.3.3.2 Definition of Edible Plant material

Savanna chimpanzees are used as reference models for early hominins, to assist in developing hypotheses of hominin foraging behaviour, constructed on suggested similarities between chimpanzee and early hominin environments (Moore 1996). Copeland (2009) studied the food accessibility of early hominins in African savannas, which function as possible analogues for some early hominin palaeoenvironments, and compares that with food available at modern savanna chimpanzee sites. Copeland examines the potential differences in ecology between chimpanzees and early hominins. This information would then have been used to posit what early hominins may have eaten, and indicate how similar or dissimilar potential early hominin diets may have been from modern savanna chimpanzees (Copeland 2009).

Since hominin digestive competencies are not known, and may have also varied between species, Copeland (2009) provides a wide definition for potentially edible plant material. Plant species that are known to be eaten in the wild by baboons, chimpanzees, or humans are considered edible for early hominins (Peters and O'Brien 1981; Peters *et al*., 1992). It is possible that some plants eaten by chimpanzees may not have been edible by early hominins. Early hominins for instance may have had difficulty digesting fibre in the quantities that chimpanzees normally consume (Conklin-Brittain *et al*., 2002).

Conclusions drawn by Copeland (2009) show that the semi-arid savannas of east Africa are dominated by *Acacia* and grass plant food resources, have fewer fleshy fruits, and have wetland environments with copious edible below-ground parts of marsh plants. According to these modern analogues, early hominins that inhabited the partly dry savannas of east Africa were probably not as frugivorous as chimpanzees and thus potentially had a dissimilar ecological emphasis (Copeland 2009). Copeland's (2009) study does not determine what early hominins ate, but infers a more direct means is needed to determine what hominins consumed.

1.3.3.3 Diet Related Competencies of Early Hominin Dentition

Au. africanus has been found to exhibit more occlusal relief than that of *Paranthropus robustus*, indicating a differentiated diet (Grine 1981). Early stage shearing quotient studies confirm that australopithecines did not have the shearing crests observed in some extant hominoids, but had more or less flat, blunted molar teeth (Kay 1985).

According to Teaford and Ungar (2000), this indicates that early hominins may have found it problematic to break down tough and malleable foods, like soft seed coverings and leaf stems, but may have found it easier to process young foliage and new growth (Teaford and Ungar 2000). Lucas and Peters (2000) have noted that australopithecines, may have found it problematic to process meat, which is also characterised as a tough, flexible food resource. Therefore it appears that early hominins were not adapted to eat meat, as they were not fortified with sharp 'reciprocally concave' shearing surfaces for processing this particular food resource (Teaford and Ungar 2000). Their blunted, flat teeth it appears were better suited for processing tough and brittle food resources. The question of fruits as a food resource depended on whether they were tough or not. If they were tough, they would've had to be retained between the teeth and sheared. Early hominins according to Teaford and Ungar (2000) would have been highly inefficient at processing this tough type of material.

1.3.4 Carbon Isotope Studies

Carbon isotopes offer a clear indication of hominin diets from the Plio-Pleistocene. According to Lee-Thorp *et al*. (2003) none of the South African hominins had a diet similar to modern chimpanzee (*Pan*) or gorilla (*Gorilla gorilla*), which consumed mostly C_3 foods; however australopithecines and early *Homo* probably did eat substantial amounts of fruits and leaves. Their results show that they included large amounts of tropical grasses and sedges, and animals that ate C_4 plants (including insects and vertebrates) (Lee-Thorp *et al*., 2003). The results of their studies (Lee-Thorp *et al*., 2003) further indicate that South African australopithecines broadened their resource base to include foods not generally consumed by extant great apes. This appears to be a probable significant step in the development of the hominin lineage, compelled by the drying pattern taking place during the Pliocene where forests were being replaced by grasslands and woodlands (Brain 1981; Vrba 1985; Feibel 1997). Studies of fossil hominin sites have implied that hominins fed in open habitats and ate a wide range of C_4 foods, which made up around 35% of the diet of *Au. africanus* and approximately 100% of the foods consumed by the east African species *P. boisei* (Sponheimer *et al*., 2005). This dominant C_4 signal led certain researchers to suggest that the intake of C_4 foods was a basic hominin characteristic (Sponheimer *et al*., 2005).

1.3.5 Diet and ecology of Au.sediba

Henry *et al*.'s (2012) study of *Au.sediba* suggests that its feeding ecology differed from the diet of other australopiths and later hominins. Carbon isotope evidence suggests that the diet of *Australopithecus*, *Paranthropus* and early *Homo* involved more C_4 foods than that of extant chimpanzees, indicating that they potentially used their environments in dissimilar ways than did extant apes (Lee-Thorp *et al*., 2000; Van der Merwe *et al*., 2003, 2008). The two individuals (MH1 and MH2) examined in Henry *et al*.'s (2012) study consumed mostly a C_3 diet which potentially included foods with a harder texture, and both monocotyledons, including grasses and sedges and dicotyledons, such as fruit, the leaves of trees, wood and bark. The diet of *Au. sediba* which appears similar to *Ardipithecus ramidus* (around 4.4Ma) and extant savanna chimpanzees seemed to favour C_3 foods in contrast to the widely accessible C_4

food resources. The apparent consumption of C_3 monocotyledons and bark increases the range of early hominin foods (Henry *et al*., 2012).

Henry *et al*., (2012) recovered phytoliths (silica bodies), which are markers for specific plant taxa (Piperno 2006) in the dental calculus of juvenile australopith individual *Au. sediba* (MH1), a South African Plio-Pleistocene hominin from Malapa, South Africa. The types of phytoliths recovered include monocotyledon and dicotyledon morphotypes, and potentially offer direct evidence of early hominin dietary patterns. The monocotyledon morphotypes appear to suggest the ingesting of C_3 grasses and sedges by these specimens. The evidence of leaf, wood, bark and fruit phytoliths suggest that they were potentially all part of the food resource complex consumed by these australopiths (Henry *et al*., 2012). The bark and woody tissue was unforeseen as an element of the australopiths' diet, although these food items are eaten by numerous primates and are composed of protein and various sugars (Lambert *et al*., 2004; Rogers *et al*., 1994). The variability of phytoliths thus appears to indicate the diversity of the dietary repertoire of these early hominins (Henry *et al*., 2012).

The general evidence suggests that the two *Au. sediba* individuals (MH1 and MH2) had some unpredicted elements in their dietary spectrum, in comparison to other African hominins of similar temporal periods. Dental microwear evidence suggests a diet which includes some hard food resources, to an extent not seen before in the majority of *Australopithecus* spp. or *in P.boisei*, and perhaps more similar to *H.erectus* or *P.robustus*. The carbon isotope results suggest that these hominin individuals were almost totally C_3 feeders and similar to savanna chimpanzees (Henry *et al*., 2012).

Henry *et al*., (2012) suggests that *Au. sediba* made use of settings where C_3 monocotyledons and dicotyledons thrived together with C_4 grass resources, much like a gallery forest environment. *Au. sediba* individuals (MH1 and MH2) showed a preference for C_3 food resources, as opposed to the amply available C_4 food resources on the landscape, and maybe included in their diet seasonally accessible bark and other fracture-resilient food resources.

1.3.6 Diet and ecology of Au. africanus and P. robustus

The microwear of early australopiths is poorly studied (Teaford and Ungar 2000). Some microwear analysis has been done on *Au. afarensis* and *Au. africanus*. The studies completed on *Au. afarensis* suggest that these hominins were starting to exploit resources of the open savanna (Puech and Albertini 1984). Research on *Au. africanus* has focused on comparing this species to *Paranthropus robustus* rather than to extant hominoids (Teaford and Ungar 2000). Studies done by Grine (1986) showed less pitting in *Au.africanus* molars than seen in *Paranthropus*. *Au. africanus* shows longer and thinner striations and more 'homogeneity in orientation'. Grine suggested *Au. africanus* ate more soft fruits and leaves compared with the 'robust' hominin types. Research on *Au.africanus* incisors has demonstrated that this species has greater microwear feature surface densities than does *Paranthropus* (Ungar and Grine 1991). This proposes that *Au. africanus* processed a larger variety of food resources with its anterior teeth, including larger more abrasive foods than did *Paranthropus* (Teaford and Ungar 2000).

During the 1990s it was broadly accepted that the diet of *Au. africanus* consisted mainly of soft fruits and leaves, similar to the extant chimpanzee. *P. robustus* in contrast consumed harder, small foods such as nuts (Grine 1981; Grine and Kay 1988; Ungar and Grine 1991). Since these are all C_3 foods, it could be hypothesised that *Au. africanus* and *Paranthropus robustus* should have the same $\delta^{13}C$ values as C_3 browsers and frugivores (Lee-Thorp and Sponheimer 2006). This was not the outcome. The data showed that $\delta^{13}C$ of both australopiths is quite different from that of C_3 eating coevals. It found further that *Au. africanus* could not be distinguished from *P. robustus* (Sponheimer and Lee-Thorp 1999a; Lee-Thorp *et al*., 1994, 2000; van der Merwe *et al*., 2003; Sponheimer *et al*., 2005b). According to Lee-Thorp and Sponheimer (2006), they argued that both *Australopithecus* and *Paranthropus* obtained approximately 30% or more of their carbon from C_4 resources. Therefore both species were consuming large quantities of C_4 foods, and these resources most probably comprised sedges, grasses, or animals that ingested these plant material.

1.4 Diets and Plant Microremains

1.4.1 Utilising Plant Microfossils to Identify Dietary Patterns

Previous studies have used microremains, such as phytoliths to recover direct evidence of diet (Armitage 1975; Dobney and Brothwell 1987; Gobetz and Bozarth 1990; Ciochon *et al*., 1990; Hardy *et al*., 2009; Henry and Piperno 2008; Wesolowski *et al*., 2010; Henry *et al*., 2010, 2011, 2012). Microfossils are commonly utilised to extract significant data from the archaeobotanical (Piperno 2006; Weiner 2010) and palaeobotanical record (Henry and Piperno 2008; Henry *et al*., 2010; 2012).

Early microscopic studies of phytoliths in the beginning of the 19^{th} century demonstrated their diversity. In the 1970s and 1980s scholars began to use microremains to explore diets of human groups for which no data was available. These studies focused on the domestication of particular plant groups (Ugent *et al*., 1982; 1986). Microremains are being researched currently to record archaeological plant use, in many temporal periods and geographical locations worldwide (Piperno and Becker 1996; Perry *et al*., 2007; Li *et al*., 2010; Henry *et al*., 2011).

Several researchers have demonstrated that they can be used effectively to provide evidence of the diets of non-human species (Ciochon *et al*., 1990; Gobetz and Bozarth 2001; Mercader *et al*., 2007; Middleton and Rovner 1994). Phytoliths can be recovered from a variety of different sources, for example dental calculus (Lalueza Fox *et al*., 1994; Henry *et al*., 2011, 2012), soil sediments (Rovner 1971), coprolites and tools (Mercader *et al*., 2007).

The study of phytoliths in soils and archaeological material has also been valuable in establishing vegetation types, as an indicator of ancient animal diets, and also in the reconstruction of palaeoenvironments (Prychid *et al*., 2003; Piperno 2006). Many studies have extracted residual material, for example phytoliths and starch grains from the edges of flaked stone tools, the pits in grinding or milling stones, from the surfaces of pots, and from sediments in archaeological sites (Hardy *et al*., 2009; Iriarte *et al*., 2004; Perry *et al.*, 2006; Piperno *et al.*, 2000, 2004; Van Peer *et al.*, 2003). This presumed however, a particular function for specific tools, for instance, grinding tools have been assumed to be used for the preparation of foods. Baysal and Wright (2006) however, showed that grinding tools may have also been utilised for other reasons besides food preparation. Likewise, while some stone tools have been used for acquiring and processing of food, they were used for example, to prepare raw materials (Hardy and Sillitoe 2003). Thus biases may sometimes exist in dietary related information, from stone tools or sediments rendering them inadequate. An example may be the utilisation of plants that were not consumed, but may have been recorded, or food resources having being left out, that needed no preparation prior to being eaten, for instance fruits (Henry and Piperno 2008).

1.4.2 The Formation and Composition of Phytoliths

After oxygen, silicon is the second most universal element on the planet (Hodson and Evans 1995). Phytoliths generally refer to any mineral accumulation within a plant; however within an archaeological context the term indicates opal or stuctureless silica phytoliths (Rovner 1971). It is also referred to as "plant opal" or "biogenic" silica, and assumes a variety of shapes and sizes depending on the tissue of the plant (Piperno 1988, 2006). Other forms include 'hat shaped' (also called 'truncated-conical'), trough shaped, and a haphazard fragmentary-type (silica sand). Silica phytoliths are mainly composed of SiO_2 with 5-15% H_2O as well as trace elements, for instance Ca, Mg, Al, Fe, and K and organic carbon (Rovner 1983).

The word “phytolith” originates from the Greek (*phyto* = plant, *lithos* = stone) meaning “plant rock”. They are rigid, small, isotropic and symmetrical mineral particles of silica (Prychid *et al*., 2003), also known as microremains.

Phytoliths are formed when hydrated silica dissolves in groundwater, is absorbed through the roots of plants, and carried through its vascular system and deposited either into a solid form within their cell walls, or in the lumina, or in intercellular spaces of any plant organ (Piperno 1988; Piperno 2006). The relative location of silica bodies in plant tissue is variable, and is generally found in the epidermis or in sheath cells of vascular bundles (Prychid *et al*., 2003). Phytoliths offer researchers the potential to classify plant taxa, and sometimes the plant organ that manufactured them (Henry 2011). Phytoliths can provide valuable information on the identity and potential concentration of source plant species, and may be useful indicators of diet in ancient animals (Prychid *et al*., 2003; Piperno 2006).

Phytoliths are formed principally in organs that are traditionally located above the ground such as leaves, bark, fruits, husks, of plants, however some taxa do accumulate them in underground structures (for instance, corms, tubers, rhizomes and roots) (Henry 2011). The deposition of silica is irregular, with different species depositing silica in a variety of places, while some species do not manufacture silica, thus often making it unlikely to identify which family or species of plant that the phytolith originated from (Piperno 1988; Piperno 2006). In some cases they are often only identifiable to the level of morphotype, especially in the palaeoanthropological environment (Bamford *pers. comm*). Phytoliths are one of the preferred types of microremains for the reconstructions of diets, because they appear in the fruit and leaves, which are the plant organs most frequently eaten (Henry 2011). A number of ecological factors affect the scale of phytolith development, such as the taxonomic affinity of the plant, age of the plant material, climatic environment, types of soil, and the accessibility of moisture, by adjusting the amounts of silica available to plants (Piperno 1988).

Phytoliths or silicified plant cells and cell walls are recognisable at all taxonomic levels and can distinguish woody and herbaceous dicots, grasses and conifers long after plant remains have degenerated (Piperno 1988). These microscopic cells can become trapped in the bacterial mass, in the dental calculus of herbivores (Gobetz and Bozarth 2001) and early hominins (Henry *et al*., 2012).

Much of what is known about phytolith morphologies comes from grasses (Twiss *et al*., 1969; Twiss 1992; Rosen 1992). There is little known about phytoliths in bark and wood, and according to Piperno (1988), have not produced substantial amounts of phytoliths (Piperno 1988). Bark phytoliths were recovered however, from the dental calculus of an early juvenile australopith (*Au. sediba*) hominin individual (MH1), from the South African site of Malapa, South Africa (Henry *et al*., 2012).

1.4.3 The Recovery of Phytoliths from Dental Calculus and Tooth Enamel

Direct evidence of diet may potentially be achieved from the recovery of preserved microfossils, in the form of phytoliths from dental calculus of fossil animals, early humans and early hominins (Armitage 1975; Puech *et al*., 1983; Lalueza Fox *et al*., 1996; Cummings and Magennis 1997; Juan-Tresserras *et al*., 1997; Gügel *et al*., 2001; Acuna-Mesen and Garcia Diaz 1998; Ciochon *et al*., 1990; Gobetz and Bozarth 2001; Henry and Piperno 2008; Henry *et al*., 2010, 2012). Dental calculus has the potential for revealing the genera and species of dietary plants (Hardy *et al*., 2009; Reinhard *et al*., 2001; Henry and Piperno 2008; Wesolowski 2010), and the presence of plant microfossils from dental calculus can potentially provide a direct means to assess the dietary patterns of early hominins.

Although the occurrence of fragmentary food debris in dental calculus has long been recognised (Cummings and Magennis 1997; Dobney and Brothwell 1987; Lieverse 1999), it has not been extensively investigated using archaeological (Hardy *et al*., 2009) or older material (Henry and Piperno 2008; Henry *et al*., 2010, 2012).

Phytoliths function as a structural reinforcement for plant tissues, and also operate as a protection against herbivory, as they can abrade the tooth enamel of animals that chew plant material containing large amounts of phytoliths (Baker *et al*., 1959; Massey and Hartley 2006). Sanson *et al*. (2007) however, hold an opposing view, observing that silica phytoliths are softer than tooth enamel, and have suggested that they (silica phytoliths) be re-assessed as a significant source of dental microwear. They further suggest that external dust and grit appears to be a more plausible cause (Sanson *et al*., 2007). Gügel *et al*. (2001) demonstrated with a chewing apparatus, that phytoliths can become embedded in tooth enamel with simple mastication, and remain lodged in the tooth enamel despite several cleaning attempts.

Phytoliths are not processed when plants are eaten, and pass directly through the digestive tract, as they are impervious to most acids, and dissolvable only in the presence of high pH levels (Piperno 2006), or they become entombed within the dental calculus matrix.

Armitage (1975) was the first to report the extraction of phytoliths from herbivore calculus, and proposed a method for the extraction of phytoliths. He also identified specific phytoliths and silicified cells from the dental calculus of extinct herbivores from several historical sites in Britain. He was further able to show dietary changes over time. Armitage's (1975) first method was a simple one. It involved washing the teeth with running water, scraping the calculus deposit, and dissolving it in a solution of hydrogen peroxide and chromic acid. This method may be competent, but does not provide any regulation for *post-mortem* contamination, and may also cause damage to the enamel surfaces of teeth.

There are few studies that have utilised microfossils to carry out dietary pattern reconstruction in human calculus. Dobney and Brothwell (1987) were one of the first set of researchers of dental calculus to realise the lack of appropriate methods, for the comprehensive recording of the severity of calculus from archaeological specimens. They established improved methods for the recording of dental calculus, which enabled them to demonstrate the relative position of a calculus deposit, and also offer accurate recording of the fluctuating profile of dental calculus deposits (Dobney and Brothwell 1987).

Middleton (1990) reported the recovery of phytoliths from grasses, beans, herbs, fungal spores and pollen from teeth, maxillae and mandibles of cows, pigs and sheep from the colonial site of Hampton, Virginia, North America, and was able to also demonstrate dietary variation in different time periods. Middleton (1990) subsequently enhanced Armitage's (1975) methods by adding phases to control *post-mortem* contamination and lessen enamel surface damage. The thrust of Middleton and Rovner's (1994) study highlights the importance of controlling and assessing potential contamination, during the preparation phase of sampling.

Ciochon *et al.*'s (1990) studies offer a different approach. Instead of examining the dental calculus matrix layers, their studies involved the examination of enamel surfaces of isolated teeth of *Gigantopithecus blacki*, for attaching phytoliths and wear striations. It appears that the striations were made by the embedded phytoliths observed at the end of scratches on the teeth. The phytoliths recovered were from bamboo and dicotyledonous fruits, suggesting a broad diet of different grasses and fruits. Their method is in contrast to Middleton (1990), and provides no direct control of contamination by the matrix; however, an assumption is made that as the phytoliths were found on the surface of the tooth, they may be constituents of the diet (Middleton and Rovner 1994).

Henry (2011) described a method known as 'plant microremains analysis', which is used to complement research on extant and extinct primate diets. Plant microremains are often characteristic of distinct plant taxa and plant parts, for instance, a fruit or leaf, and offer valuable information on the identity of types of foods eaten. Information can also be acsertained on the variation in intake of food resources for different seasons, or between individuals, or the dietary regime of a particular individual or group of individuals (Henry 2011). Plant microfossil analysis offers the potential opportunity to study the diets of extinct species. Phytoliths are often preserved in dental calculus, which is mostly found attached to the enamel surface of teeth of some extinct animals and hominins, and is comparatively easy to recover from skeletal material (Henry 2011; Henry *et al*., 2012).

A study to isolate phytoliths from the enamel surfaces of human teeth was carried out by Lalueza Fox *et al*. (1994). The study was an attempt to establish a standard method for studying phytoliths in human teeth, from archaeological remains, and also an attempt to determine diets in past human groups, particularly in the location of the Mediterranean.

Later studies by Lalueza Fox *et al*., (1996) compared phytoliths recovered from tooth enamel surfaces to phytoliths recovered from calculus and burial soils, from a late Roman necropolis in Tarragona (Spain) dated to 300-550 BP. Their method included a comparison of untreated calculus, with calculus treated with hydrochloric acid. The acid treatment resulted in removing most of the organic contents of the dental calculus matrix, except for the phytoliths. Phytoliths in the untreated deposits were embedded in the calculus matrix and covered mostly by carbonates (Lalueza Fox *et al*., 1996). As mineralisation of dental plaque takes place in the presence of saliva only (MacPhee and Cowley 1975), the presence of phytoliths and/or silica fragments embedded in the dental calculus matrix demonstrates evidence of both structures simultaneously, and therefore not as a result of '*post-mortem* remodeling' of dental calculus (Middleton and Rovner 1994; Lalueza Fox *et al*., 1996). Phytoliths were however, confirmed by X-ray analysis, due to their silica presence (Lalueza Fox *et al*., 1996).

In a study done by Hershkovitz *et al*. (1997) dental calculus was recovered and identified from the Miocene ape *Sivapithecus*. This primate is recognised from middle to late Miocene sediments of South Asia, and dated to approximately 12.5- 8.5 Mya (Pilbeam *et al*., 1977). This indicates that this method makes it probable to access microremains from deep geologic time (Gobetz and Bozarth 2001). It appears that no examination for phytoliths was performed on the specimens in this study, as no results have been reported (Odes *pers. observation*). The studies of Gobetz and Bozarth (2001) concentrated mainly on phytoliths and associated dental calculus, and their relationship to diets and palaeoenvironmental reconstruction of extinct herbivores.

Wesolowski *et al*. (2010) improved on the previous methods of Boyadjian *et al*. (1997) and Reinhard *et al*. (2001) which involved the extracting of microremains from extremely small calculus deposits. These authors found a relatively high concentration of microfossils (phytoliths and starches) in Brazilian archaeological shell mounds or 'sambaquis', and also noted that mineral fragments and charcoal might be contaminants.

Henry and Piperno (2008) studied five isolated human teeth from a Syrian middle Holocene site. The method used demonstrated that no damage took place on the enamel surface. Inspection of the microfossils showed that adequate material was available for research. The removal of dental calculus using a dental pick, and further processing, illustrated not only is the method an effective one to recover microfossils, but also that no damage was caused to the teeth (Henry & Piperno 2008). Other studies have endeavoured to recover phytoliths (Boyadjian *et al*., 1997; Lalueza Fox & Perez-Perez 1994; Lalueza Fox *et al*., 1996; Juan Tresseras *et al*., 1997; Cummings and Magennis 1997).

More recently, Henry *et al*. (2010) reported direct evidence of plant food consumption by Neanderthals from Shanidar III, Iraq, and Spy Cave in Belgium, from phytoliths and other microremains extracted from Neanderthal dental calculus. A significant aim of their research was to better explore Neanderthal use of plant foods, thus plant microfossils (starch grains and phytoliths) entombed in dental calculus of several Neanderthal individuals were analysed. The plants recovered from the Neanderthal dental calculus included date palms (*Phoenix* spp.), grass seeds (Triticeae), and legumes, demonstrating high levels of dietary complexity (Henry *et al*., 2010). It has been frequently shown that dental calculus is a reliable source of plant microfossils for dietary reconstruction (Boyadjian *et al*., 1997; Henry and Piperno 2008; Juan-Tresserras *et al*., 1997; Lalueza Fox and Pérez-Pérez 1994; Cummings and Magennis 1997; Piperno and Dillehay 2008).

Recently, Henry *et al*. (2012) reported for the first time the recovery of plant phytoliths, from the dental calculus of a South African early hominin juvenile individual, *Au sediba* (MH1). Their diet potentially included harder foods, dicotyledons and monocotyledons. The phytoliths that were recovered from the dental calculus of MH1 indicate, that C_3 dicotyledons and monocotyledons were probably large constituents of their diet, and that the diversity of phytolith morphotypes suggests that the early hominin individual (MH1) ate a wide variety of food resources. Unexpected consumption of bark or wood, and C_3 monocotyledons in the early hominin diet enlarged the known diversity of the early hominin food resource repertoire. The research further shows that the diet of the two australopith individuals (MH1 and MH2) examined, appears to be different from the acknowledged data for early hominins in the region, as well as other locations (Henry *et al*., 2012).

CHAPTER 2 : MATERIALS AND METHODS

2.1 Materials

In order to establish the presence of dental calculus and associated microfossils (phytoliths) in South African Plio-Pleistocene hominin individuals, I examined the Sterkfontein hominin dental assemblage housed in the Phillip Tobias Hominin Laboratory, School of Anatomical Sciences, at the University of Witwatersrand. Specifically, my goal was to establish and inventory which specimens exhibited dental calculus or adherent materials which might be preserved in the calculus. Sterkfontein was the only site chosen for this study because it provides a good comparison to the assemblage from Malapa, a nearby site from which phytoliths have been successfully recovered from calculus from an australopith individual. Sterkfontein is roughly the same age as Malapa, and has a substantial collection of *Australopithecus africanus* specimens, a species likely closely related to the *Au. sediba* individuals found at Malapa. I hoped to show from the Sterkfontein study that dental calculus may be more ubiquitous than previously thought.

The dental assemblage consists of approximately 260 specimens out of a total assemblage of approximately 765 specimens. From the Sterkfontein hominin dental assemblage, five (5) samples with a high probability of calculus were finally selected for further testing. Four of the five samples are isolated teeth, the fifth (StW 53*f*) is a left maxillary jaw fragment.

2.2 Methods

2.2.1 Examination of Hominin Dental Specimens

The Sterkfontein hominin dental collection was examined in several stages to ascertain whether any specimens exhibited any adherent material that followed the physical morphological characteristics of dental calculus, as outlined in Henry (2011), the Brothwell (1981) calculus severity scoring method, and Buikstra and Ubelaker (1994). This material was noted, described, photographed and compared to existing collections of known calculus.

I observed dental calculus as a mineralised, coarsely textured material, which attaches to the teeth, either above or below the gingivae, and ranges in colour from light brown to darkish brown. I further scored the calculus using Brothwell's (1981) calculus scoring index which has four levels: (0) absent, (1) mild, less than a third of the crown surface; (2) moderate, 1/3 to 2/3 of the crown surface, and (3) severe, over 2/3rds of the crown surface (Figure 1). I noted the location of dental calculus for all the samples as buccal (B), lingual (l), and also recorded whether the tooth was mandibular (M^n) or maxillary (M_n), right (R), or left (L).

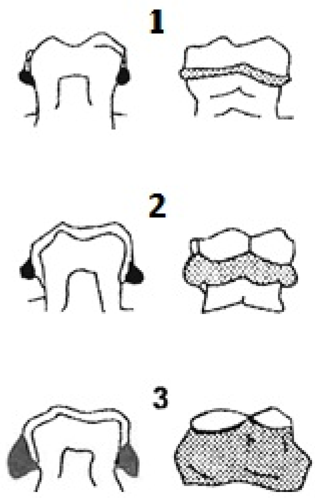

Figure 1: Dental calculus scoring method for supra-gingival calculus. (Adapted from Brothwell (1981), and Buikstra and Ubelaker (1994); 1=mild; 2=moderate; 3=severe)

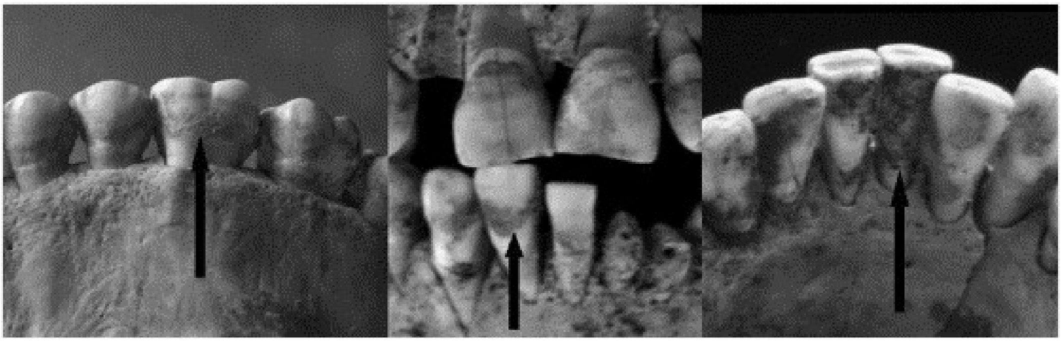

Figure 2: Human dental calculus scoring system. Left (mild). Middle (moderate). Right (severe). Adapted from Buikstra and Ubelaker (1994).

I carried out several physical assessments of the Sterkfontein hominin collection. The initial assessment of the hominin dental collection resulted in a list of 71 specimens with probable dental calculus. For the second assessment, I then examined all dental specimens using an Olympus microscope, model: SZX16 zoom ratio 16.4: 1, and zoom range 7 – 115x, with trinocular head, and camera adapter: TV0.5X. The microscope is fitted with Olympus Analysis GeTIT software (Freeware software). Each tooth was examined at three magnification levels. Based on this second examination, I concluded that 20 specimens had a stronger probability of exhibiting dental calculus than the rest. These 20 specimens with probable dental calculus were photographed, and fully described (see Appendix A). In collaboration with Dr. Amanda Henry, I then ranked these 20 specimens according to either a high, medium or low probability of dental calculus (seeTable 3). The specimens with the highest probability ranking (5) were then selected as samples in this study (Table 3 and Figure 3).

Table 2: Probability Index for ranking tooth specimens for calculus

Probability Calculus Testing (Final observation - 3rd)				
Tooth Specimen		**HIGH**	**MEDIUM**	**LOW**
Stw 53a RM1			x	
RP4 buccal				x
RM2 distolingual				x
Stw RM3 lingual				x
StW 53a RP4 lingual surface			x	
RP3 lingual /mesial				x
Stw 53h			x	
Stw 53a LP4			x	
StW 53f LM2 buccal		x		
StW 53f LM3 buccal				x
Stw 532 LM3		x		
Stw 534 RM2 buccal		x		
Stw 321b LM2		x		
StW 246 LM1			x	
StW 498d				x
StW 498 (a)				x
StW 559 RM3				x
Stw 483 LM3				x
Stw 183 LM1		x		
StW 151				x
Stw 131				x
Stw 127 LC			x	
StW 109				x
StW 61				x
StW 9b				x
Stw 12				x
Stw 313a				x
Stw 313b,c				x
StW 313				x
Stw 327; 327a,b				x
Stw 332				x
Totals	**31**	**5**	**6**	**20**
Total specimens dental collection	**260**			
% high probability	**1.90%**			
% medium probability	2.30%			

Table 3: Samples selected from the Sterkfontein dental assemblage

No	Sample No.	Species	Tooth	View	Grid	Depth	Member
1	StW 53*f*	*Au.africanus**	LM^2	buccal	V/58	11'2"-12'0"	StW 53Infill
2	StW 321*b*	*Au.africanus*	LM_2	buccal	U/49	24'0"-25'0"	4
3	StW 534	*Au.africanus*	RM_2	buccal	W/43	23'10"-24'10"	4
4	StW 532	*Au.africanus*	LM_3	buccal	W/43	21'10"-22'10"	4
5	Stw 183	*Au.africanus*	LM_1	lingual	T/49	14'8"-15'8"	4

* late *Australopithecus* (Clarke 1995); *H.habilis* (Hughes and Tobias 1977)

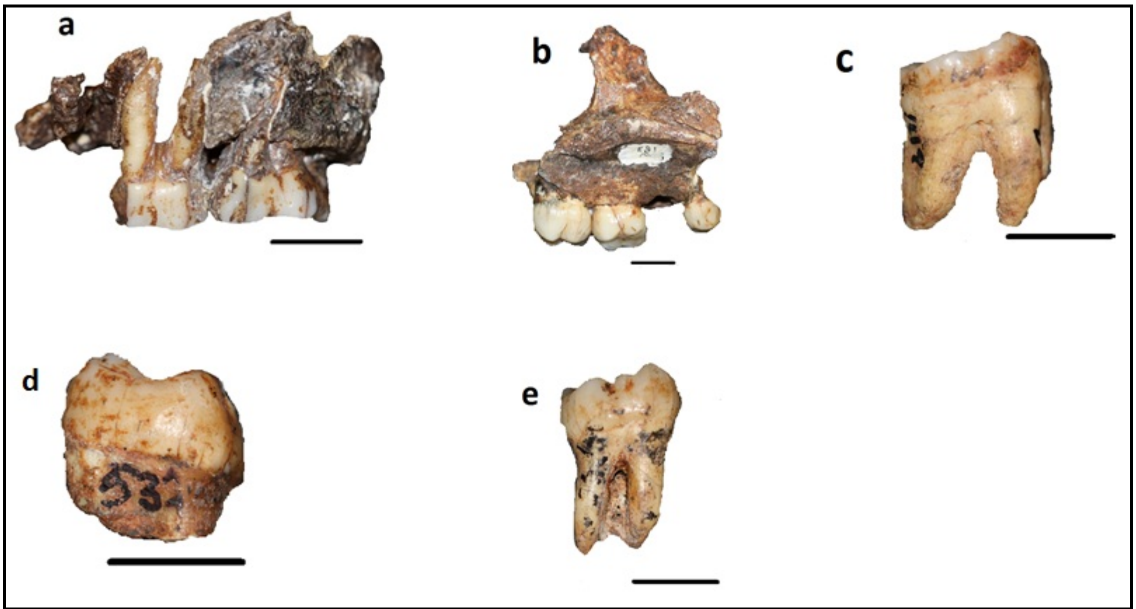

Figure 3: Hominin tooth samples selected for calculus and phytolith examination a: StW 53f, LM^2 buccal; b: StW 183, LM_1 lingual; c: StW 321b, LM_2 buccal; d: StW 532 LM_3 buccal; e: StW 534 RM_2 buccal. Scale bar =1cm.

2.2.2 Protocols for Identifying Dental Calculus

In addition to the guidelines established by Henry (2011), Brothwell (1981), and Buikstra and Ubelaker (1994), I established additional protocols for recognising calculus that took the following into account:

2.2.2.1 Visibility factors:

a. A description of texture, whether rough or smooth, and the level of textural coarseness, for instance (1) low, (2) medium and (3) high (Odes, *pers. observation*).
b. the description of what the calculus looks like: its shape, for instance, 'band'-like, or amorphous with no shape; patch-shape or round shape;
c. the type of calculus: supra-gingival or sub-gingival;
d. the location of attachment (buccal, lingual or mesial);
e. the amount of supra-gingival buccal calculus was scored using the levels established by Dobney and Brothwell (1987), Brothwell (1981), and Buikstra and Ubelaker (1994) including: mild (1), moderate (2) and severe (3); scoring of lingual supra-gingival calculus may be evaluated on a similar basis to buccal calculus (it is not described by Dobney and Brothwell (1987) or Brothwell (1981);
f. Observation of the topography of calculus thickness distributions, for instance to determine whether the calculus has an equal or uneven thickness distribution throughout the deposit.

2.2.2.2 Colour Variability:

The colour of adherent material is often a significant factor in determining whether it is calculus. I coded the colour according to Munsell color charts. Although different categories of calculus have a distinguishing colour ranges for hominins, colour in and of itself is a weak determinant of dental calculus identification, and thus, must be evaluated jointly with textural factors (Odes *pers. observation*). The colour coding of calculus may have a benefit when identifying the genus of a tooth fragment; and where colour of calculus may become a significant diagnostic tool, is in the absence of any other identifying factor (Odes, *pers. observation*).

2.2.3 Examination of inclusions in calculus:

An exploratory study was undertaken to determine whether dietary markers were preserved in the dental calculus. Samples were selected and analysed for plant microfossils, such as phytoliths, and compared to existing comparative collections (Henry *et al*., 2012).

2.3 Method for Extracting Dental calculus and Phytolith Analysis

I followed a method for extracting the calculus from the protocols used in Henry and Piperno (2008). We made several efforts to reduce the chance of contamination. The particular environment to extract the dental calculus was made as 'clean' as possible to avoid the movement of air. Windows and doors were kept closed, and air conditioners were switched off to avoid airborne phytoliths as far as possible. In this study Dr Henry and I both wore unpowdered nitrile gloves when working with the samples. We used new picks and toothbrushes for each sample.

Following Henry and Piperno (2008) and Gordon (1988), the protocol used in this study limited the extraction to the thickest part of the dental calculus. The surface of each tooth sample was first gently cleaned with a toothbrush to remove any surface contamination. Each tooth sample was held over a piece of weighing paper, as a receptacle area. The calculus was then carefully picked off using a sterile dental pick. The calculus from each sample was then transferred to a microcentrifuge tube. Photographic images were then taken of the sampling location on each tooth, before and after extracting the calculus. These images provide the basis to assess if there was any damage done to the teeth.

The microcentrifuge tubes were carefully opened and using a pipette the tube was filled with distilled water, and vortexed to dislodge material that might be attached to the sides of the tube. The tube was inserted into the centrifuge at 3000 rpm for 5 minutes. Some water was pipetted off leaving the material at the bottom of the centrifuge tube. The calculus samples were dissolved in a 10% solution of HCl for 30 minutes and deflocculated to ease diffusion. The samples were then subsequently centrifuged again at 3000 rpm for 5 minutes, and some of the HCl (supernatant) was pipetted off. Distilled H_20 was added again for a final rinse, centrifuged again at 3000 rpm for 5 minutes, and further H_20 was pipetted off. The remaining material was then wet mounted onto microscope slides. The samples were then examined under a transmitted light microscope at 400x magnification using a Zeiss Axioskop petrographic microscope. Phytoliths based on comparisons with phytolith reference collections of modern South African plant material were counted, photographed, and identified to morphotype and plant association where possible.

2.3.1 Method for Contamination Control

A total of 13 breccia samples were tested and used as a contamination control in this study. A small amount of breccia was extracted from the ear bone of the cranial material of StW 53*d* (by AH). I also extracted five small (5) samples of breccia from several bovid bones associated with Member 4 grid squares V50 (depth: 9’7”- 10’0”); V51 (depth: 4’9”- 5’9”); V52 (depth: 10’1”- 11’1”); S63 (depth: 9’1”- 10’1”) and U52 (depth 10’11”-11’11”) from Member 4 Sterkfontein. I further removed a further 7 breccia samples (see Table 4) from rocks specimens supplied by Professor Ronald Clarke and Steven Motsumi from the Sterkfontein cave complex. The rock specimens associated with grid squares Q64 (3 samples); N46 (2 samples) and U62 (2 samples) were collected by Mr Steven Motsumi.

The method used to extract phytoliths from the breccia from rock and bone samples was similar to the method used to extract phytoliths from the calculus samples. The samples were dissolved in 10% HCl for approximately 30 minutes, and stirred regularly. They were subsequently washed using distilled H_20, and centrifuged three times at 3000 rpm for 5 minutes each. The breccia samples were wet mounted onto microscope slides, and I then analysed the slides for the presence or absence of phytoliths.

Professor Ronald Clarke a co- permit holder of the Sterkfontein caves complex and Professor Kathleen Kuman, both of the University of the Witwatersrand, confirmed to me that no separate breccia material was retained at all during the excavations of

Tobias and Hughes in the 1970s, and more specifically that no breccia material was saved from the grid squares and associated depths for the tooth samples in this study (Clarke and Kuman, *pers.comm*).

Table 4: Breccia samples extracted from rocks used for contamination control testing received from Professor Ronald Clarke

Grid square	Depth	Sample weight (Dry (g)	Member *
Q64	18”2’	0.05	5
Q64	18”2’	0.16	5
Q64	18”2’	0.22	5
N46	29”7’	0.07	4
N46	29”7’	0.11	4
U62 6w	16”3	0.08	Adjacent to 4 and 5 and StW53 infill
U62 7w	16”3’	0.01	Adjacent to 4 and 5 and StW53 infill

*Kuman and Clarke (2000); U62 6w and U62 7w were selected for breccia controls
To test contamination

Table 5: Breccia samples extracted from a hominin ear bone (StW 53*d*) and several bovid fragments for contamination control testing

Grid Square	Depth	Weight (Dry)(g)	Member	Bone element
V50	9’7”-10’0”	0.06	4	humerus & metacarpal fragments
V51	4’9”-5’9”	0.04	4	bovid rib
V52	10’1”-11’1”	0.07	4	1st phalanx Class III bovid
S63	9’1”-10’1”	0.001**	4	thoracic vertebra Class III bovid
U52	10’11”-11’11”	0.03	4	humerus shaft- juvenile bovid
V60	12’8”	***	StW 53 Infill	ear bone/ StW 53*d* cranium

**** rounded up from 0.000**
***** no weight for sample**

Figure 4: Location of Sterkfontein Members 4 and 5 (M4 and M5) and StW 53 Infill (hatched area south of M5 South). Member 5 is shaded in black. M5 East (lines 49–58), M5 West (lines 59–65), and M5 South (southern lines 58–61). (After Kuman and Clarke 2000)

CHAPTER 3 : RESULTS AND ANALYSIS

Establishing the Presence of Dental Calculus

In this chapter a brief description of each specimen containing probable calculus is given, highlighting the distribution of calculus or other adherent deposits on the tooth specimens. All additional teeth described are included in the Appendix A. All phytolith results will also be reported in this chapter.

The presence of sub-gingival calculus was not found on any of the Sterkfontein tooth specimens selected for this study. A high probability exists that supra-gingival calculus is present on at least 4 out of the 5 tooth specimens selected for this study, and hence only probable supra-gingival calculus is described. Phytoliths were recovered from all the tooth samples tested, and indetermined phytoliths made up a large percentage. A few broken phytoliths and different plant types were also observed in this study.

Establishing the presence of Phytoliths

This study recovered 187 phytoliths and plant types from all tooth and breccia samples selected. 107 phytoliths were recovered from the tooth samples, and 80 phytoliths and plant types from breccia samples. In this study 19 different morphotypes and/or plant types were identified, and are presented in Figure 6.

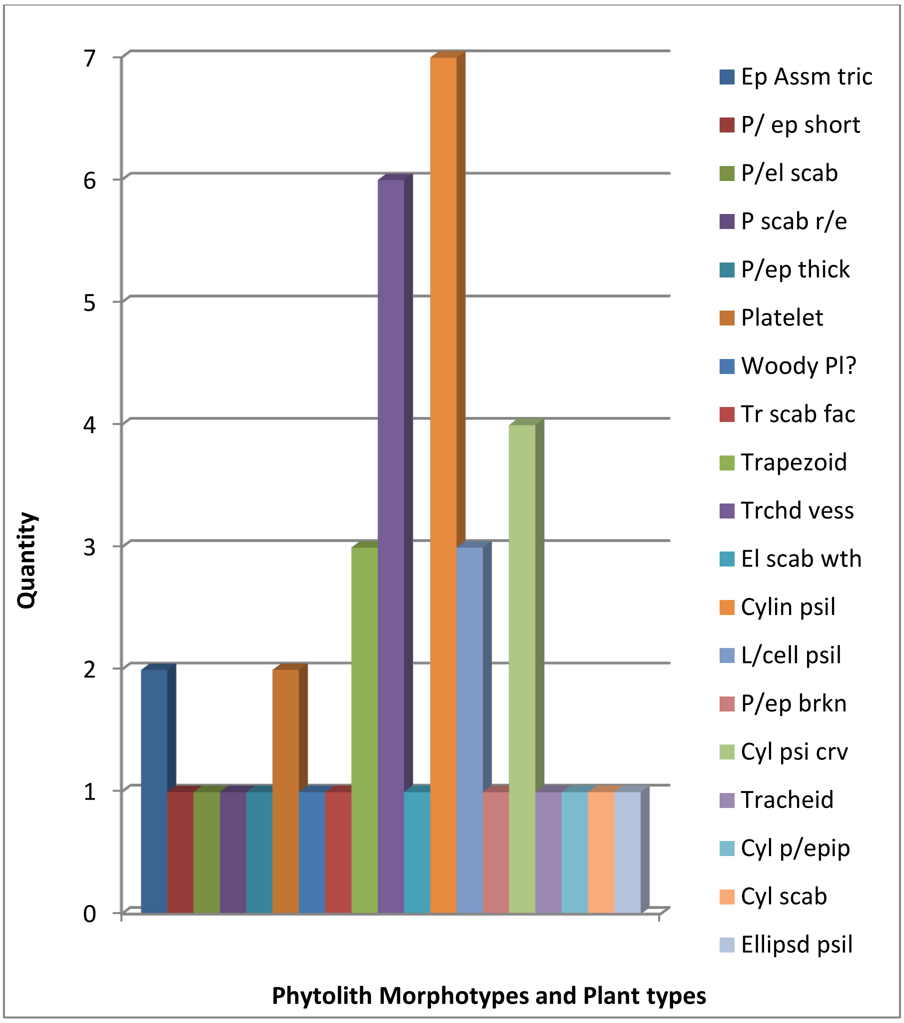

Figure 5: Different phytolith morphotypes and plant types recovered from all tooth and breccia samples in this study

<u>Phytolith Breccia Control Samples used in this study (U62 6w and U62 7w)</u>

Three sets of breccia controls samples were included in this study to test for contamination, but only one was used for all tooth samples. The breccia control samples (from grid squares U62 6w and 7w) were used for all five tooth samples (StW 53*f*; StW 321*b*; StW 534, StW 532 and StW 183). The grid squares for the breccia control samples were chosen for their proximity to the where the tooth specimens were originally excavated from.

The breccia control samples used in this study from grid squares U62 (6w) and U62 (7w) yielded 4 phytoliths. One was classified as indetermined. Three different morphotypes were identified:

- epidermal assemblage trichome
- parallelepipedal elongate psilate and;
- scutiform.

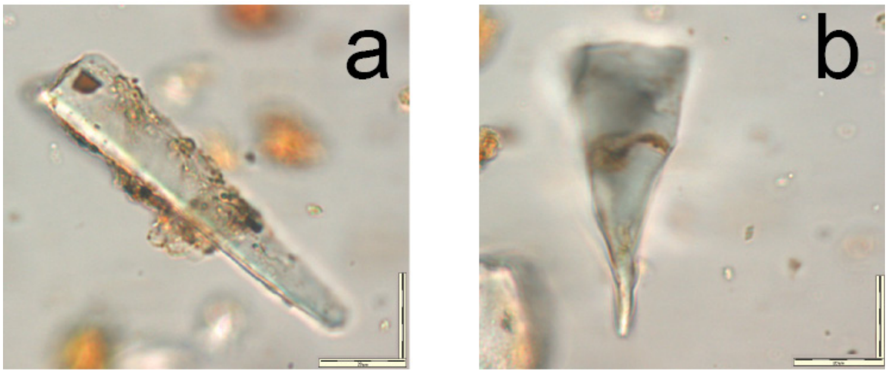

Figure 6: Phytoliths extracted from breccia control sample (grid square U62 6w); a: epidermal assemblage trichome; b: indetermined.

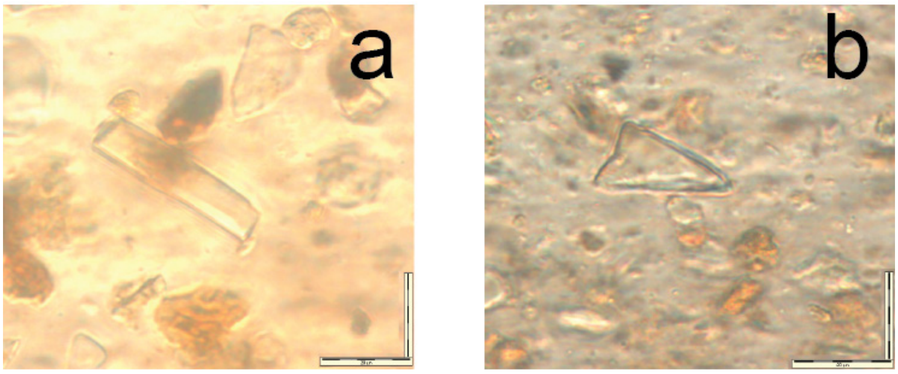

Figure 7: phytoliths recovered from 2nd breccia control sample (grid square U62 7w); a: parallelepipedal psilate; b: scutiform.

Table 6: This table illustrates the tooth specimens, calculus scoring and location of the calculus deposit and whether upper or lower jaw.

Sample No	Specimen No	Site	Tooth	Score	Location	M_n/M^n
1	StW 53*f*	Sterkfontein	LM^2	1	B	M^n
2	StW 321b	Sterkfontein	LM_2	2	B	M_n
3	StW 534	Sterkfontein	RM_2	1	B	M_n
4	StW 532	Sterkfontein	LM_3	1	B	M_n
5	Stw 183	Sterkfontein	LM^1	1	l	M^n

M^n = mandibular; M^n = maxillary; B = Buccal; l = Lingual; L = left; R = right

3.1 Specimen StW 53f, Left Maxillary Second Molar (LM^2)

3.1.1 Description of Probable Calculus on StW53f

The buccal surface exhibits three locations of probable calculus. Two distinct sub-deposits (a) and (b) are situated mesio-buccally, and one sub-deposit (c), is located disto-buccally.

Sub-deposit (c), which is attached to the buccal surface of the left maxillary second molar of StW 53*f*, exhibited similar morphological characteristics to sub-gingival calculus. The second and more distally located of the two occluso-buccal cluster deposits (sub-deposit c) is located buccally between the middle third and the occlusal third of the tooth. Its buccal location is highly diagnostic of supra-gingival calculus (Parfitt 1959; Gressly 1963; Friskopp 1983). Its shape is broadly band-shaped mesio-distally. This deposit was scored with a calculus severity score of (1), indicating a mild severity (covering less than a third of the enamel surface), according to the Brothwell (1981) method of calculus scoring. This score indicated a high probability of supra-gingival calculus. The deposit has a moderate thickness, and its colour ranges from light to dark brown which is diagnostic of ancient dental calculus (Hillson 1996). The texture of the deposit was coarse, also diagnostic of dental calculus.

There is a superior sub-cluster deposit and an inferior sub-cluster deposit within this sub-deposit, separated with a small portion of adherent-free enamel. The inferior edge of this occluso-buccal deposit measures approximately 0.5mm from the occluso-buccal junction. The superior edge of the deposit measures approximately 2mm from the cervico-buccal junction. The texture of this sub-deposit has a compact component mesially and a small compact component inferiorly, and is coarse and uneven throughout, excepting for the highly compacted areas.

3.1.2 Other probable calculus deposits on StW53f

Sub-deposit (a) is located obliquely distal and within the cervico-buccal third of the upper left second molar, where the cervico-buccal margin is the apical limit. The vertical measurement of this deposit, which begins from the cervico-enamel junction and ranges occlusally to the inferior most point of this deposit, is approximately 2.1mm. The texture of the inferior part of the sub-deposit is grainy, condensed, irregular and lightly coarse; while the superior part of the deposit is medium coarse, uneven, and not tightly compacted. Some adherent material lies horizontally on the cemento-enamel junction. This deposit is not compacted, has a moderately thick texture, and a narrow width (approximately 0.10mm). The brown colour and buccal location is diagnostic of archaeological dental calculus (Hillson 1996; Parfitt 1959).

The first and more mesially situated of the two occluso-buccal cluster deposits (sub-deposit b) consists of three irregular shapes. The most mesial deposit has an oblique shape, barely distinguishable on the enamel surface, is light brown, and has a very fine texture. The second and more distal of the deposits is broadly rectangular, slightly more rough in texture and measures 0.9mm vertically (occluso-apically) and mesio-distally (horizontally) 0.25mm. The third deposit and the most distal of the occluso-buccal deposit, is substantially larger than the latter two occluso-buccal deposits and has a slightly mesially concave shaped longitudinal section, measuring approximately 2.1mm from the inferior (occlusal) base to the superior edge of the deposit; it is joined by a separate relatively square section divided into two rectangles, one superior and one inferior, situated on the superior end of the longitudinal section. The width of the longitudinal deposit is approximately 0.4mm at its base and approximately 0.35mm at its apical end. The inferior edge lies on the occluso-buccal margin. Sub-deposit (b) has an amorphous configuration, however may also be broadly seen as part of a larger 'band'- like sub-deposit including sub-deposit (c) (refer Figure 9). The texture of the most mesial sub-deposit of the mesio-buccal cluster deposit is extremely coarse and is dark brown, highly diagnostic of supra- gingival calculus (Parfitt 1959; Gressly 1963; Friskopp 1983; Hillson 1996).

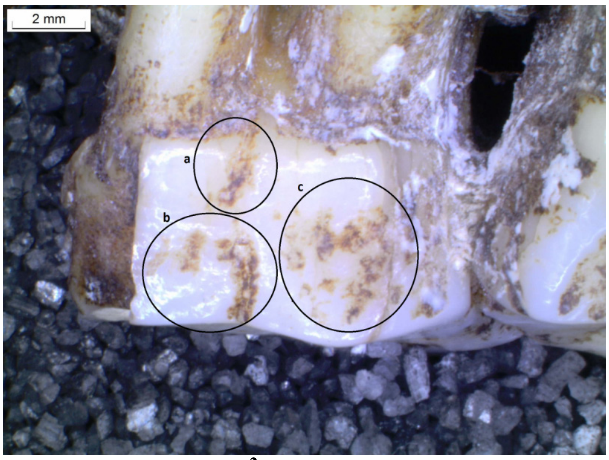

Figure 8: StW53f LM^2 buccal view

3.1.3 Phytolith Results for StW 53f (taken from grid square V58)

Forty nine phytoliths were extracted from the StW 53*f* tooth sample extracted from the buccal surface of LM2 (grid square V58). The sample produced 30 indetermined phytoliths. Some platelets, a possible woody platelet, and several tracheid vessels (Bamford *pers. comm.*) were identified. The sample identified 13 different phytolith morphotype and/or plant types from this tooth sample:

- Cylindroid psilate
- Tracheid vessel
- Trapezoid
- Trapezoid scabrate facetate
- Trapezoid wavy
- Woody platelet (?)
- Platelet
- Parallelepipedal thick
- Parallelepipedal scabrate with rounded ends

- Parallelepipedal elongate scabrate
- Parallelepipedal short
- Epidermal assemblage trichome

Of the 49 phytoliths recovered from the StW 53*f* tooth sample 31 (63%) were classified as indetermined (refer Table 9). Parallelepipids accounted for approximately 8%, trapezoids comprise approximately 6%, and tracheid vessels make up approximately 10% of the phytoliths and/or plant parts recovered from the StW 53*f* tooth sample.

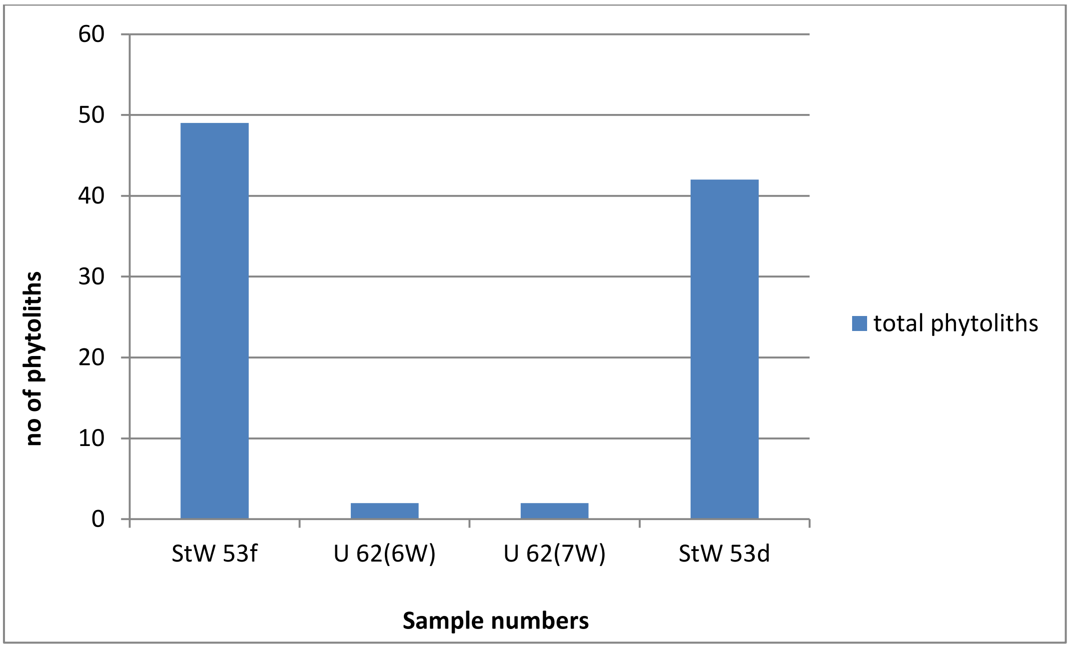

Figure 9: Total phytoliths recovered from Stw53*f*, nearest bone associated breccia (StW 53*d*) and nearest breccia control grid square.

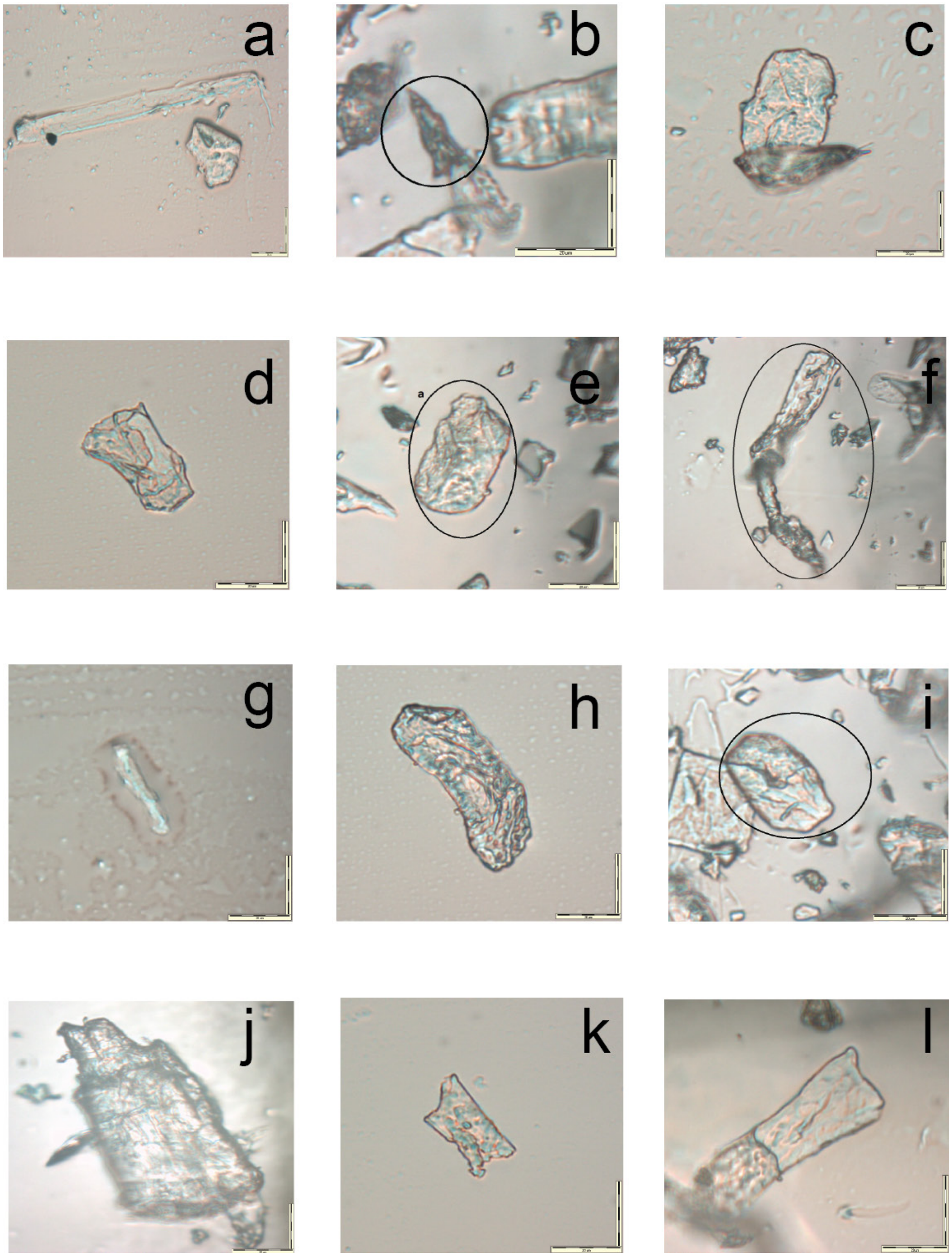

Figure 10: Phytoliths recovered from the StW 53f tooth sample. a: cylindroid psilate; b: epidermal assemblage trichome; c: indetermined; d: indetermined; e: indetermined; f: indetermined; g:indetermined; h:indetermined; i: indetermined (circled) and parallelepipid short; j: indetermined; k: indetermined; l: indetermined.

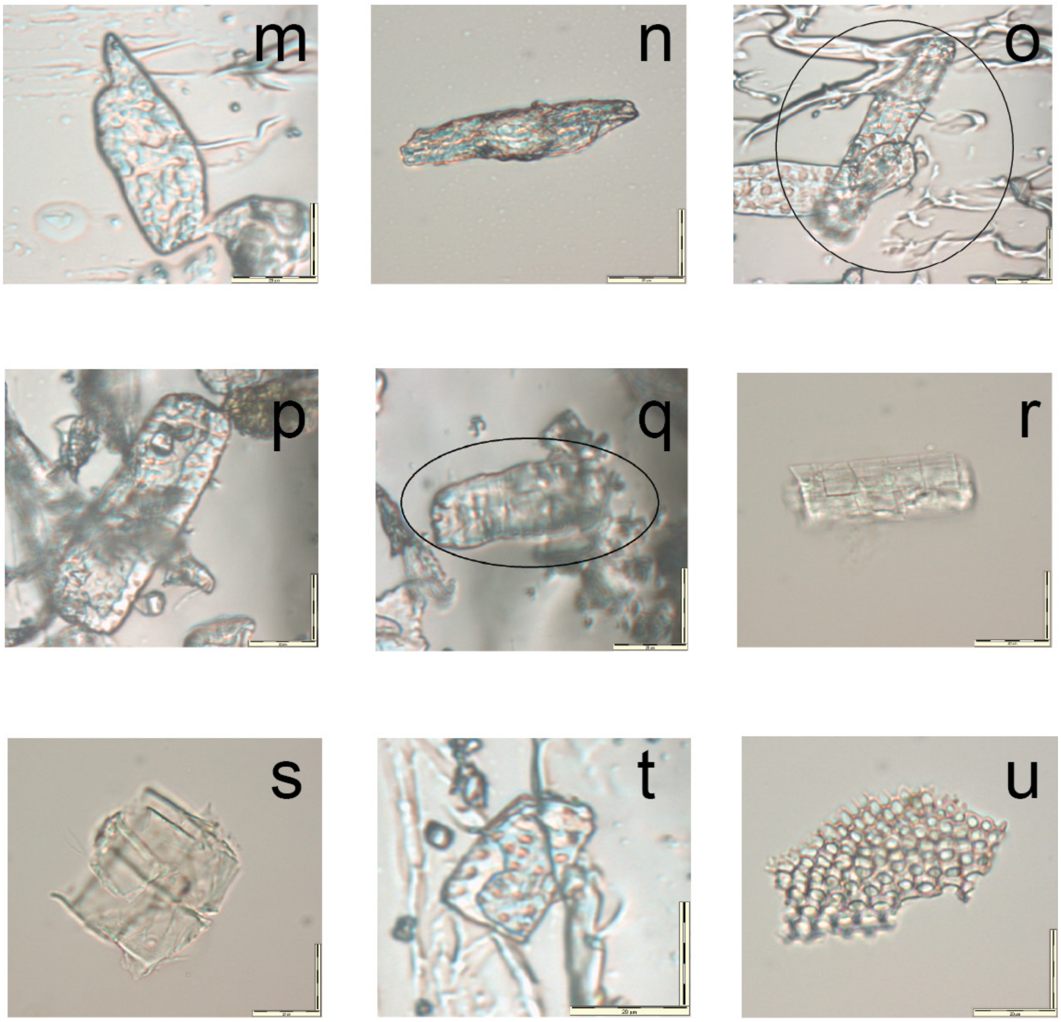

Figure 11: Phytoliths recovered from the StW 53f tooth sample; m: indetermined; n: indetermined; o: parallelepipedal elongate scabrate; p: parallelepipedal scabrate round ends; q: parallelepipedal thick; r: platelet; s: platelet; t: scabrate facetate trapezoid; u: tracheid vessel.

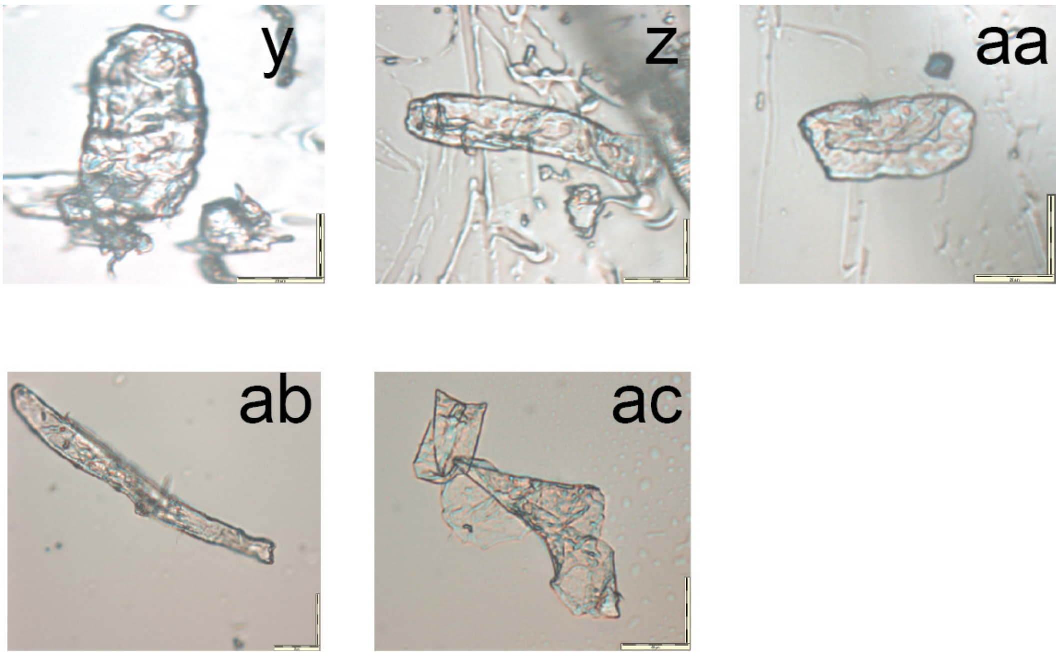

Figure 12: Phytoliths recovered from StW 53f tooth sample; y: trapezoid; z: trapezoid; aa: trapezoid; ab: weathered elongate scabrate; ac: possible woody platelet?

3.1.4 Discussion (StW 53f tooth sample)

The StW 53*f* tooth specimen shows several morphological characteristics diagnostic to dental calculus, such as the course texture of the deposit and the location of the adherent deposit to the buccal surface of LM^2 (Parfitt 1959; Gressly1963; Friskopp 1983). The light brown colour is diagnostic of ancient dental calculus (Hillson 1996). The deposit is partly amorphous and partly 'band-like' (Hillson 1996), and is located above the gum tissue, strongly diagnostic of supra-gingival calculus. These morphological characteristics in sum infer that the sample extracted from StW 53*f* tooth specimen exhibits a strong probability of being dental calculus. Out of all the tooth samples, StW 53*f* had the most amount of phytoliths (49) and the closest bone associated breccia sample to StW 53*f* (StW 53*d*- breccia from the ear bone of the StW

53 cranium) had the second highest number of phytoliths (42) of all the tooth and breccia specimens in this study.

The morphotypes that were common to both the tooth sample (StW 53*f*) and the bone associated breccia (StW 53d) were:

- epidermal assemblage trichome;
- parallelepipid thick; and
- Trapezoid

3.1.5 Phytolith comparison between tooth sample (StW 53f) and nearest bone associated breccia (StW 53d)

Comparison of the phytoliths between the tooth sample (StW 53*f*) and the phytoliths of the nearest bone associated breccia sample (StW 53*d*) showed, that despite three cases of morphotype overlap, none can be said to be identical. These differences therefore implied that the tooth sample (StW 53*f*) indicated no contamination, and that it possessed a high probability of being calculus.

Conversely however, the presence of the overlap introduces the possibility that contamination of the sample cannot be ruled out. If the sample is contaminated, an inference cannot be made that the plants associated with these phytoliths were part of this individual's (StW 53*f*) diet, but can only be inferred that the plants associated with this morphotype (epidermal assemblage trichome), were present on the landscape after the hominin died (Bamford, *pers. comm.*).

Table 7: In this table is a comparison of the phytoliths collected from specimens StW 53f (tooth specimen) and StW 53d (associated bone breccia sample). This comparison establishes whether or not there is any shared phytoliths. All photos are taken at 20µ.

morphotype	StW 53f	StW53d	Comments
Epidermal assemblage trichome		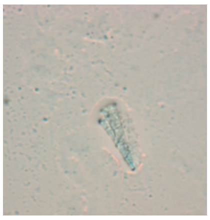	Both have triangular forms; StW53f has a flat base; StW 53d has a convex base
Parallelepipid thick		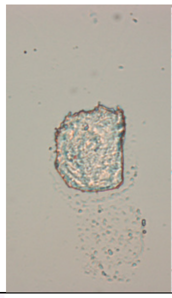 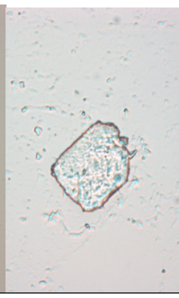	Morphotypes are identical, form varies. Two form were identified from StW53d
Trapezoid	  		

The result of the comparison however, between the bone associated breccia (StW 53*d*) and the breccia control (U62) resulted in an overlap of 1 morphotype:

- epidermal assemblage trichome (see Table 8).

Table 8: In this table is a comparison of the phytolith morphotype common to both closest associated breccia sample (StW 53d) and breccia control sample (U62). Although they are similar they cannot be said to be identical

morphotype	StW53d Bone breccia sample	U 62 breccia control sample	Comment
Epidermal assemblage trichome	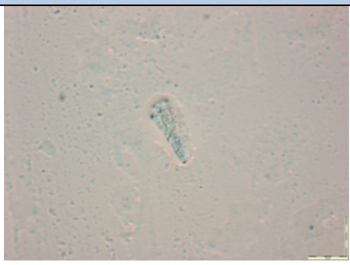		Similar forms are found in both samples, but are not identical

The two epidermal assemblage trichomes (refer Table 8) are morphologically different from each other, indicating that despite the overlap between the two samples, no contamination is present between the two samples.

3.1.6 Phytolith results from StW 53d

The StW 53*d* breccia sample (the nearest available bone associated breccia to StW 53*f,* taken from grid square V60) was extracted from the ear bone of the StW 53 cranium (grid square V60) (refer Figure 21) yielded 42 phytoliths. The sample yielded 27 indetermined phytoliths, and 14 morphotype and/or plant types were identified:

- Silicified vessels with bordered pits
- Silicified stoma
- Bilobate
- Bulliform fan shape
- Cylindroid echinate

- Elongate sinuate
- Trapezoid
- Parallelepipedal thick
- Parallelepipedal scabrate (broken)
- Parallelepipedal scabrate with rounded ends (r/e)
- Epidermal assemblage trichome

The plants associated with the phytoliths recovered from this sample were predominantly from woody dicots, however some came from sedges (monocotyledons), and a few from trees and shrubs (dicotyledons) (refer Table 10).

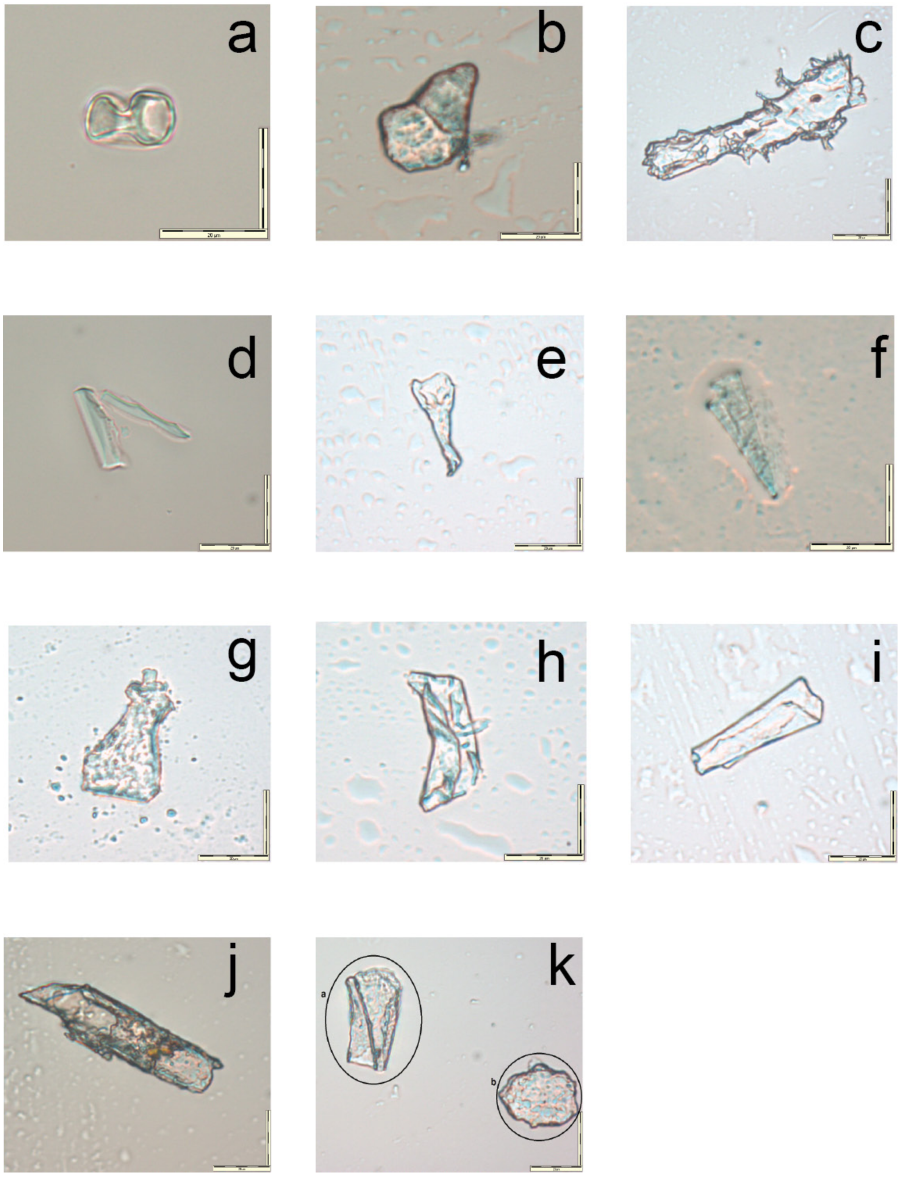

Figure 13: Phytoliths recovered from the StW 53*d* nearest bone associated breccia sample; a: bilobate; b: bulliform; c: cylindroid echinate; d: elongate sinuate; e: indetermined; f: epidermal assemblage trichome; g: indetermined; h: indetermined; i: indetermined; j: indetermined; k: indetermined.

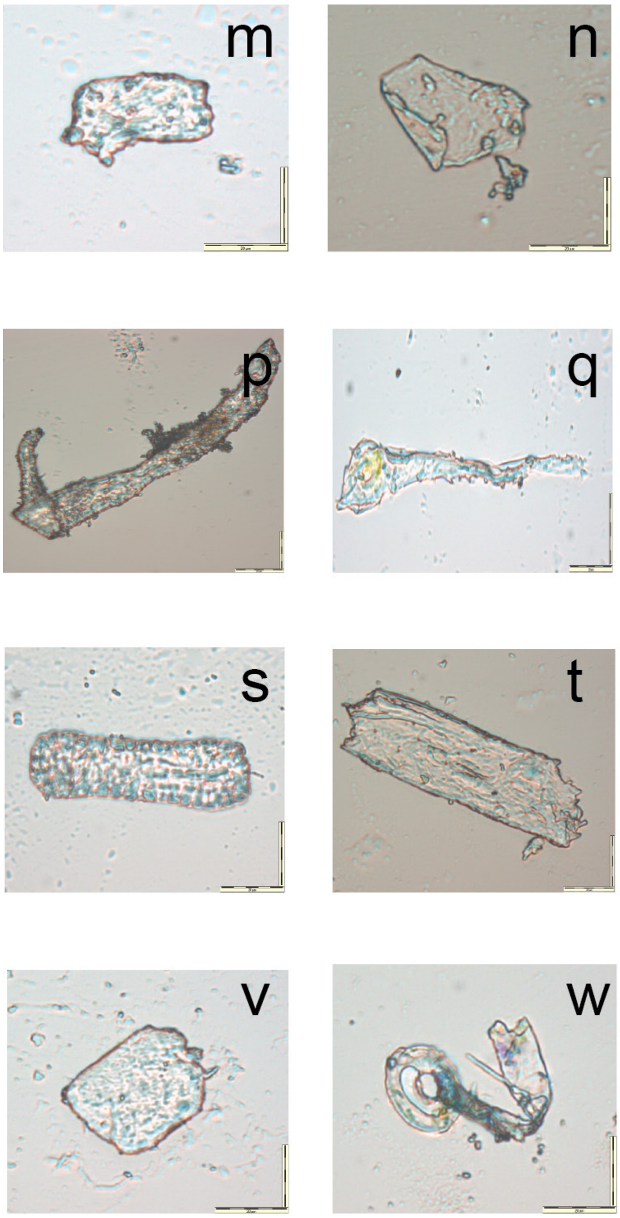

Figure 14: Phytoliths and/ or plant parts recovered from the StW 53d bone associated breccia sample; m: indetermined; n: indetermined; o: indetermined; p: indetermined; q: indetermined; r: indetermined; s: parallelepipedal elongate scabrate with rounded ends; t: parallelepipedal scabrate (broken); u: parallelepipedal thick; v: parallelepipedal thick; w: silicified stoma.

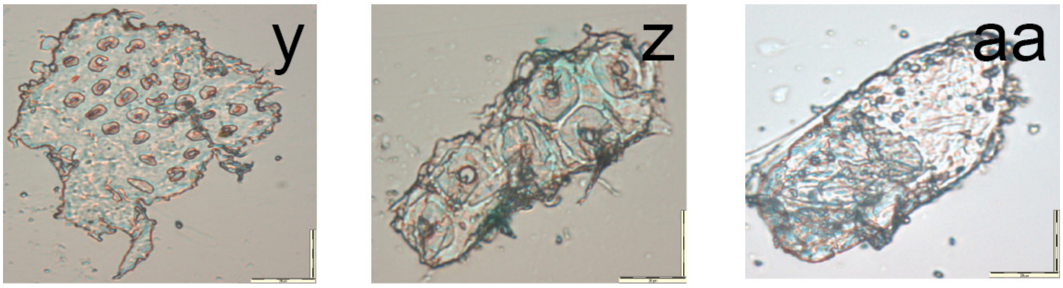

Figure 15: Phytoliths and/ or plant parts recovered from StW 53 *d* bone associated breccia sample; y: silicified vessel with bordered pits; z: silicified vessel with bordered pits; aa: trapezoid.

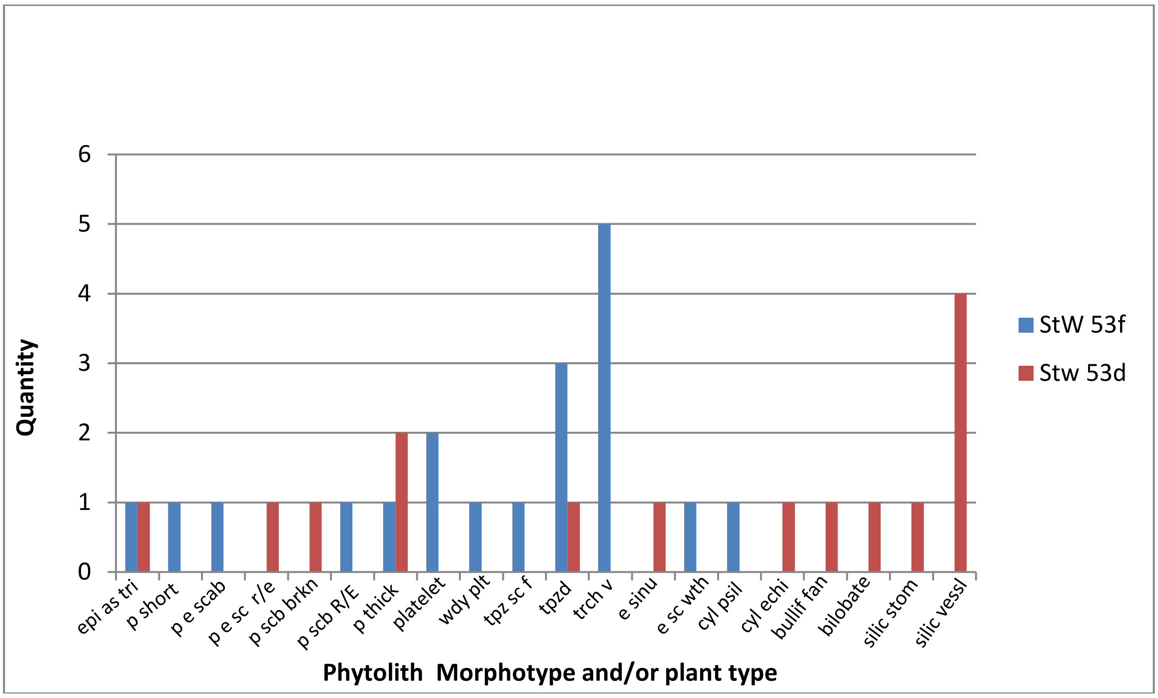

Figure 16: Comparison between phytoliths from StW 53f tooth sample and phytoliths from nearest bone associated breccia (StW 53d - from ear bone of the StW 53 cranium) showing morphotype overlap.

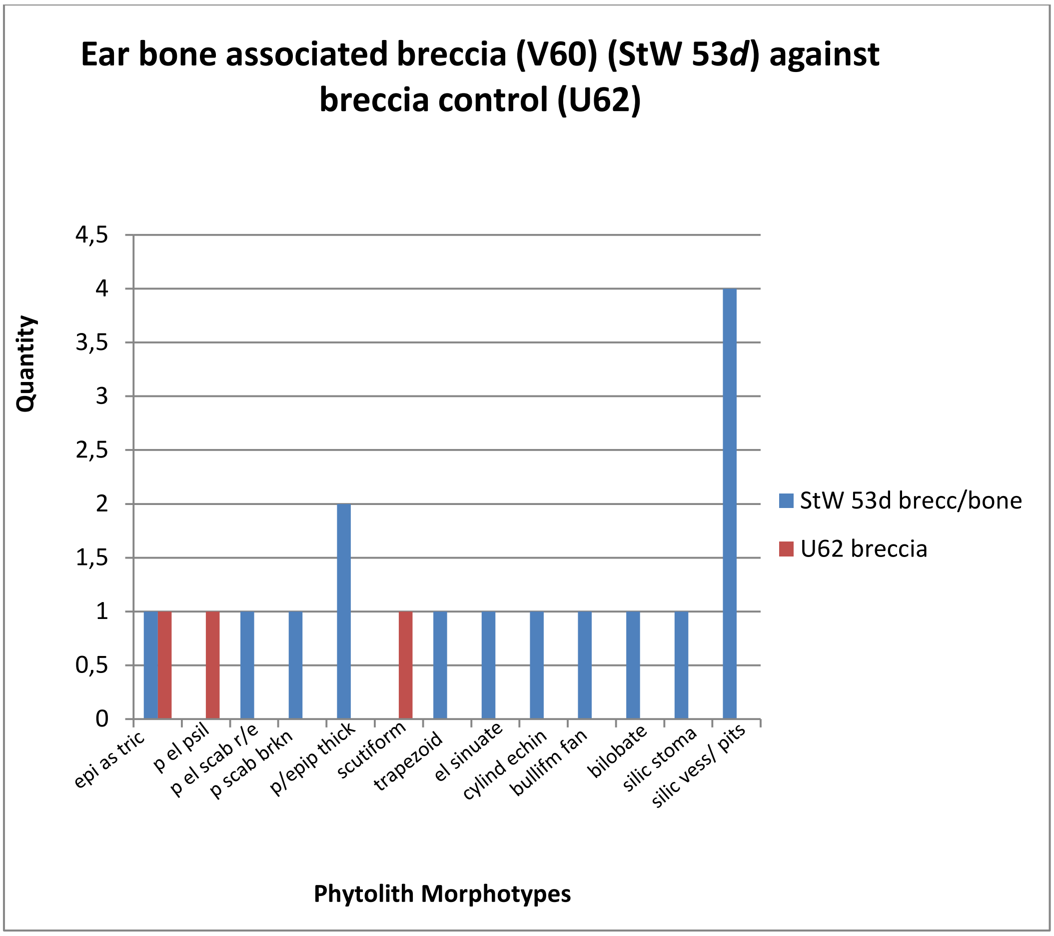

Figure 17: StW 53d bone associated breccia compared against U62 breccia control showing one overlap in one morphotype

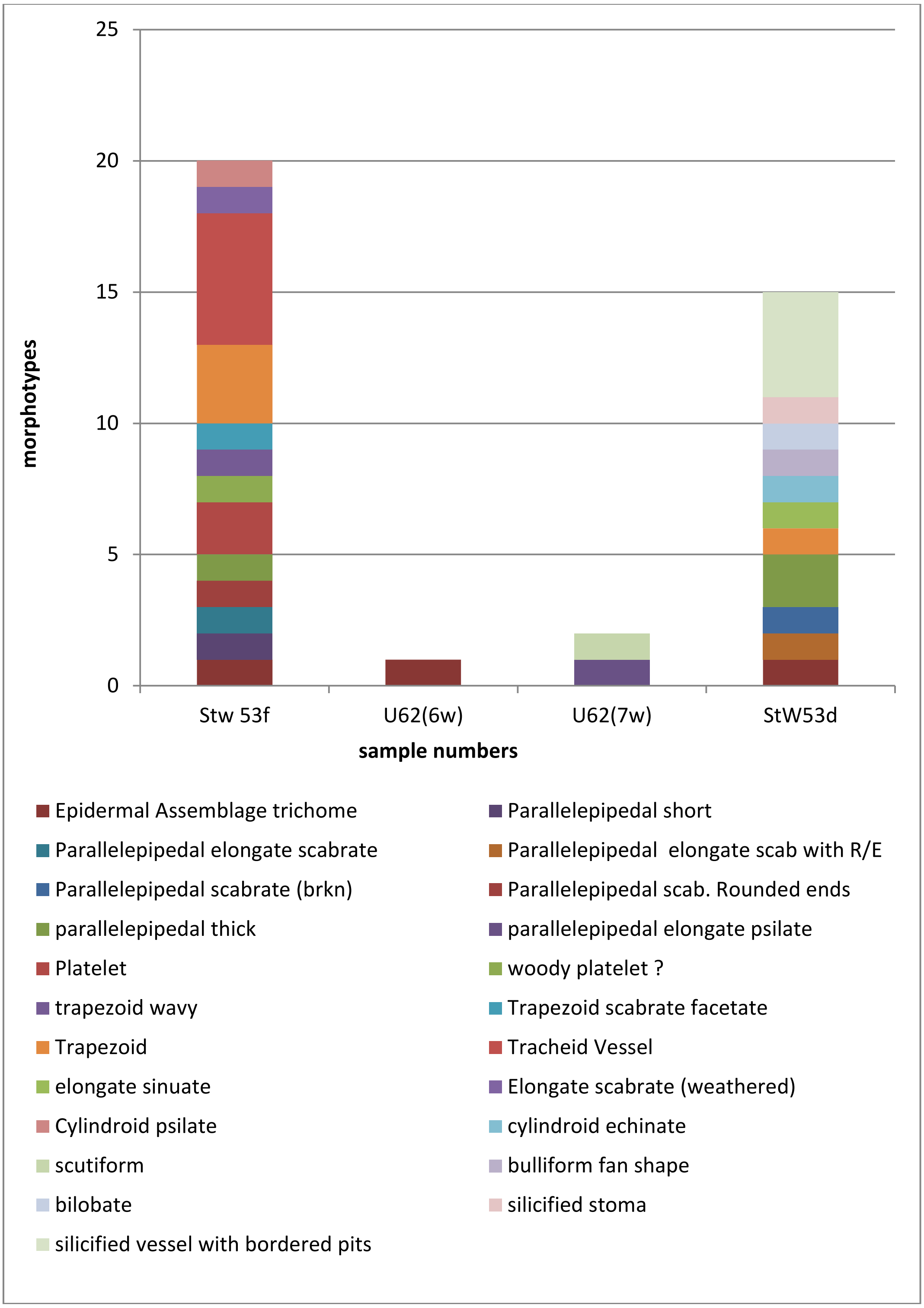

Figure 18: StW 53d compared to breccia control and nearest bone associated breccia (StW 53d) excluding indetermined phytoliths

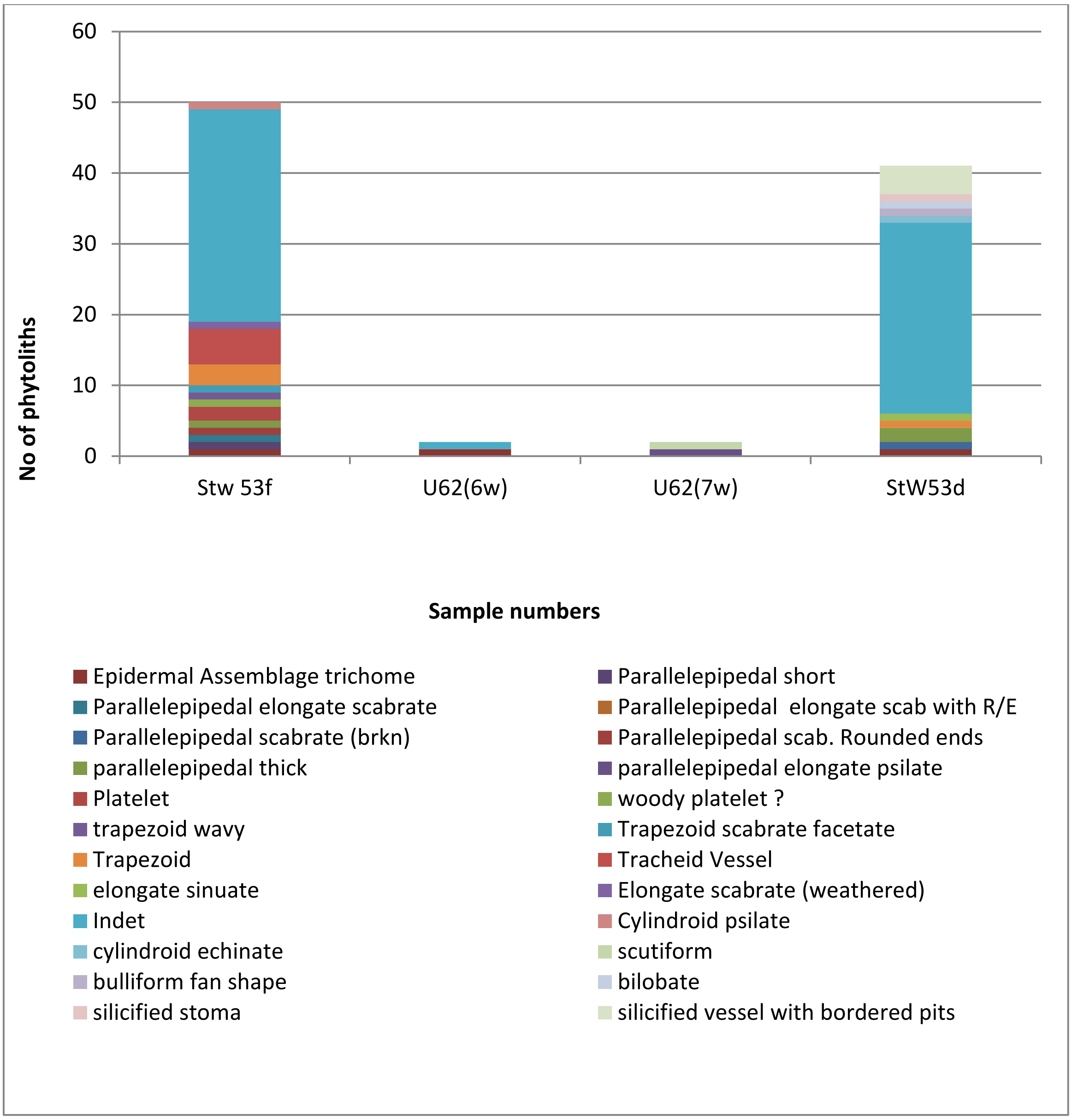

Figure 19: StW 53*f* compared to breccia control and nearest bone associated breccia (StW 53*d*) showing indetermined phytoliths

Figure 20: StW 53*d (*the StW *53* cranium) from where the nearest bone associated breccia to the StW 53*f* tooth sample was extracted from.

3.2 Specimen StW 321*b* Left Mandibular Second Molar (LM_2)

3.2.1 Description of probable calculus on StW 321b

There are several sub-deposits attached to the buccal surface of the LM_2 of StW 321*b* (refer Figure 22 & Figure 23). Sub-deposit (b) lies on the bucco-distal surface, diagnostic of supra-gingival calculus and is located within the occlusal third of the LM_2 of StW 321*b*. Dental calculus on upper molars is mostly found on buccal surfaces (Parfitt 1959, Gressly 1963; Friskopp 1983). The bucco-distal deposit (sub-deposit b) of the left mandibular molar of StW 321*b* exhibits a moderately rough and fairly thick textural material, which is equally diagnostic of dental calculus. The sub-deposit (b) demonstrates a severity score of (2) on the Brothwell Index, indicating that a deposit is moderate, covering at least a third to two thirds of the calculus surface (Brothwell 1981). Sub-deposit (b) measures 4.18mm horizontally at its maximum and 3.05mm at its vertical maximum. Sub-deposit (b) is diagonally 'band - shaped' and is one of the diagnostic shapes of supra-gingival calculus (Hillson 1996). The sub-deposit (b) is made up of several colours; however the spectrum of brown and grey-brown tones indicates that it fits into the colour spectrum that is diagnostic for supra-gingival calculus (Brothwell 1981; Hillson 1996). The morphological characteristics of sub-deposit (b) of the left lower second molar of StW 321*b* thus implies that it exhibits a high probability of dental calculus (refer Figure 22).

This sub-deposit (b) extends supero-distally from the inferior margin of the occlusal third to slightly inferior of the occlusal-distal margin. Sub-deposit (b) is made up of several colours: pinkish white (b1) (5YR 8/4), pinkish grey (b1) (5YR 7/2), pink (b2) 5YR 7/3 and 5YR 7/4), located in the supero-mesial segments of the mesio-buccal surface of LM_2; In the mid buccal area, a pinkish grey (b3), black and very dark grey (7.5 N2 and 7.5 N3) and found slightly inferior to (b3); yellowish brown (b4) (10YR 5/4); and yellowish brown (10YR 5/6) in the most supero-distal segment of the disto-buccal surface of LM2; In the most infero-distal segment (b5), a yellowish brown (10YR 5/6) and very pale brown (10 YR 7/4) colour is observed. The thickness of the deposit varies from thin in the supero-mesial segment (b1-2) to thick, in the middle buccal area (b3) to very thick (b4) in supero-distal corner of the disto-buccal surface of LM2. The thickest area of sub-deposit (b) appears to coincide with the yellowish brown area of (b4).

Sub-deposit (a) is located on the mesio-buccal surface of StW 321*b*, within the occlusal third of LM_2. The sub-deposit is placed slightly inferior to the occlusal surface. It measures 3.15mm and vertically 3.1mm. The texture is rough in the occluso-mesial segment and less coarse in the smaller occluso-distal and larger inferior portions of sub-deposit (a). This sub-deposit has no set shape pattern. Sub-deposit (a) is characterised by several colours. The colours characterising the supero-mesial (a1) segment of sub-deposit (a) are: very reddish grey (10YR 2/2), lighter red (10YR 6/6) and red (10YR 5/6) and light grey (2.5YR 7/2) and dark greyish brown 2.5YR 4/2). The colours characterising the single superior (a2) and middle segments, of sub-deposit (a) [parts of (1, 3 and 4)] are: white (2.5YR 8/2), pale yellow (2.5YR 7/4) and light grey (2.5YR 7/2). The colours characterising the infero-distal segments (a3) are: light brownish grey

(2.5YR 6/2) and greyish brown (2.5YR 5/2), and white (2.5YR 8/2). Sub-deposit (a) is amorphous in shape.

Sub-deposit (c) is located infero-mesial to sub-deposit (b), distal to sub-deposit (a) and is situated in the mid-buccal area at the cemento-enamel junction of LM_2. The sub-deposit begins slightly disto-laterally of sub-deposit (a) until the inferior midpoint of sub-deposit (b). The deposit is made up of three segments, a mesial and middle continuous segment, and a separate distal segment. There is also a small isolated deposit located in the mid-buccal section. It measures 5.20 mm. horizontally and 1.2mm vertically. The continuous segment appears to be less coarse and granular. The colours of this section of the sub-deposit (c4) and slightly superior to it, are white (2.5YR N8) and light grey (5YR 7/2) and pale yellow (5 YR 7/4). Sub-deposit (c2) appears to present with the same colours as (c4). Sub-deposit (c1) is a pinkish grey (7.5YR 6/2). Sub-deposit (c2) presents with the same colours as (c4). Sub-deposit (c3) is composed of several colours, pinkish white (7.5YR 8/2), light grey (7.5YR N7), and grey (7.5YR N5) mesially, mid- and distally buccal. Sub-deposits (c2 and c4) present as fine, sub-deposit (c1), exhibits a slightly more coarse texture, and sub-deposit (c3) has a coarse texture.

Sub-deposit (d) is located inferiorly mesial to the cemento-enamel junction and to sub-deposit (c). The texture of sub-deposit (d) is less coarse and granular than sub-deposit (a), (e), or (b). The horizontal measurement is 4.2mm, and its vertical width is 0.9mm. The colours exhibited by sub-deposit (d2) are pinkish white (7.5YR 8/2), two shades of light grey (7.5YR N7 and 7.5 YR N6), and grey (7.5YR N5). Sub-deposit (d1) presents with several colours: a reddish yellow (7.5YR 7/6), pink (7.5YR 8/4), and light grey, and two shades of grey, one lighter and one darker (7.5YR N6; border of light grey and grey) and (7.5YR N5-grey).

Sub-deposit (e) is located in the mid-buccal area, within the occlusal third of the tooth, and is situated in between sub-deposit (a) and (b). It measures 3.05mm horizontally and 1.5mm. The texture of sub-deposit (e) is coarse and granular, and exhibits a ‘pockmarked and indented shape. The colours exhibited by sub-deposit (e1 and e3) are light grey (7.5YR N7), a darker shade of grey (7.5YR N6), dark grey (7.5YR N4). Sub-deposit (e1) also exhibits an area of black (7.5YR N2) infero-mesially. Sub-deposit (e2) presents with a reddish yellow area superiorly (7.5YR 6/8), light brown in the mid- and distal sections (7.5YR 6/4). Sub-deposit (e) like sub-deposit (a) is amorphous in shape.

Figure 21: buccal surface of the left lower second molar of StW 321*b*

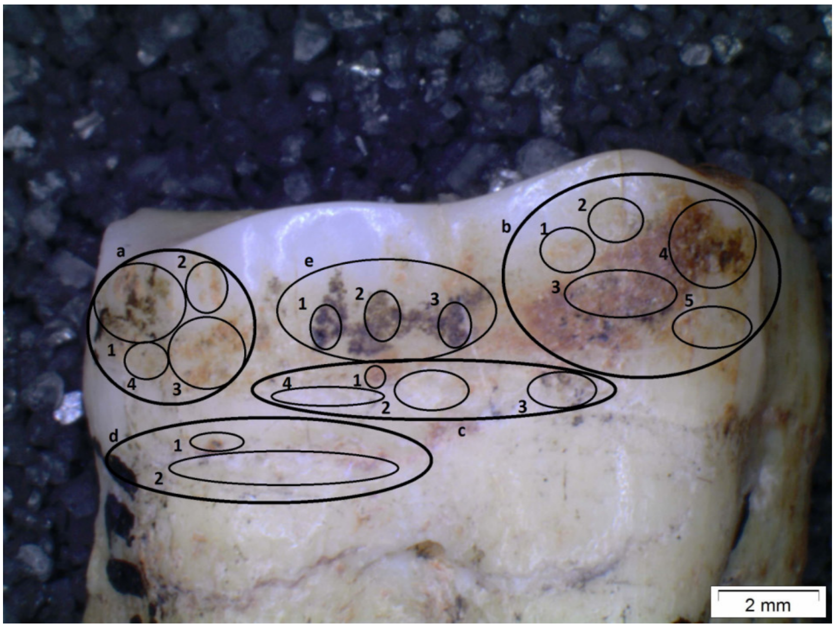

Figure 22: buccal surface of LM_2 of StW 321*b* showing areas of probable calculus

3.2.2 Phytolith Results from StW 321b (taken from grid square U49)

Twenty nine phytoliths were recovered from the StW 321*b* tooth sample. Out of this sample 26 phytoliths were classified as indetermined. From this tooth sample 2 morphotypes were identified:

- long cell psilate (2) and
- parallelepiped (1) (broken)

Long cell psilates in this sample constitute approximately 7%. Woody dicots and grasses made up the associated plants from the phytoliths in this sample. StW 321*b* presented with the second highest percentage of indetermined phytoliths of the total tooth sample (89%).

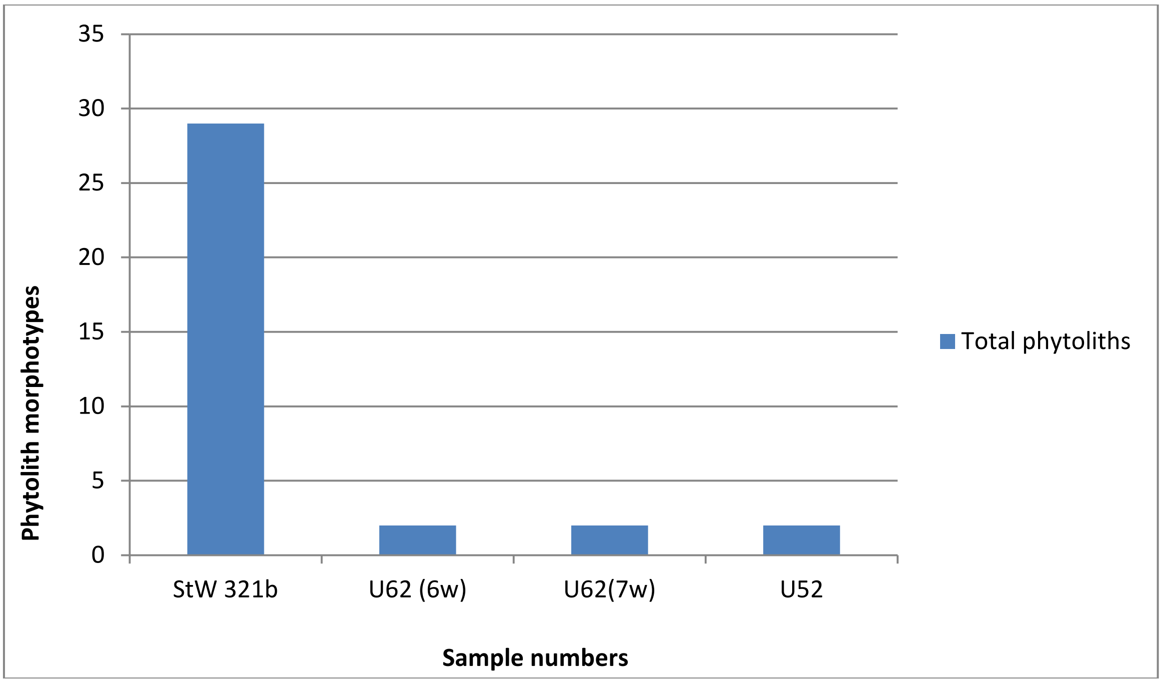

Figure 23: No. of phytoliths recovered from the StW 321*b* tooth specimen, bone associated breccia and breccia control sample numbers

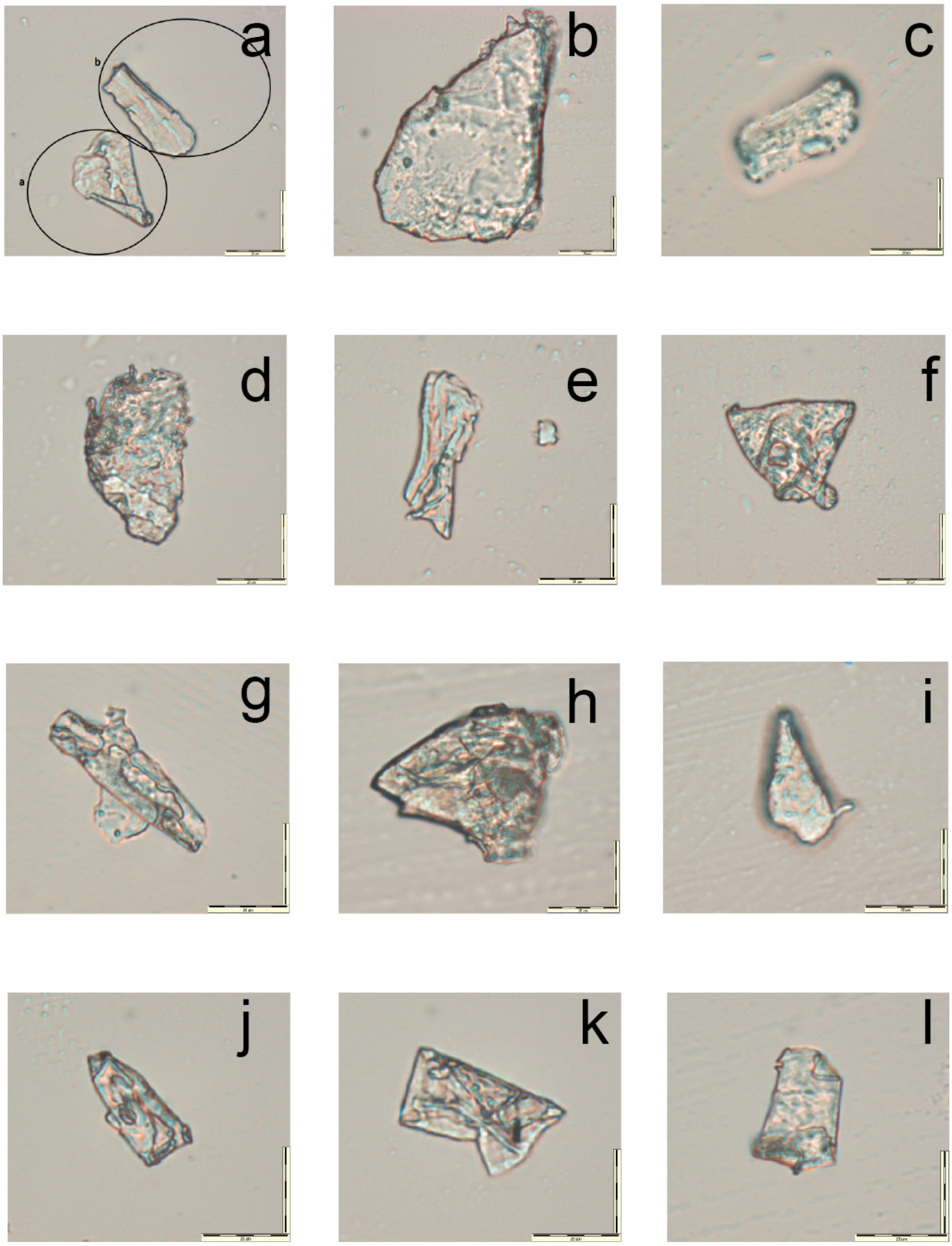

Figure 24: Phytoliths recovered from the StW 321*b* tooth sample (grid square U49); a-l: indetermined

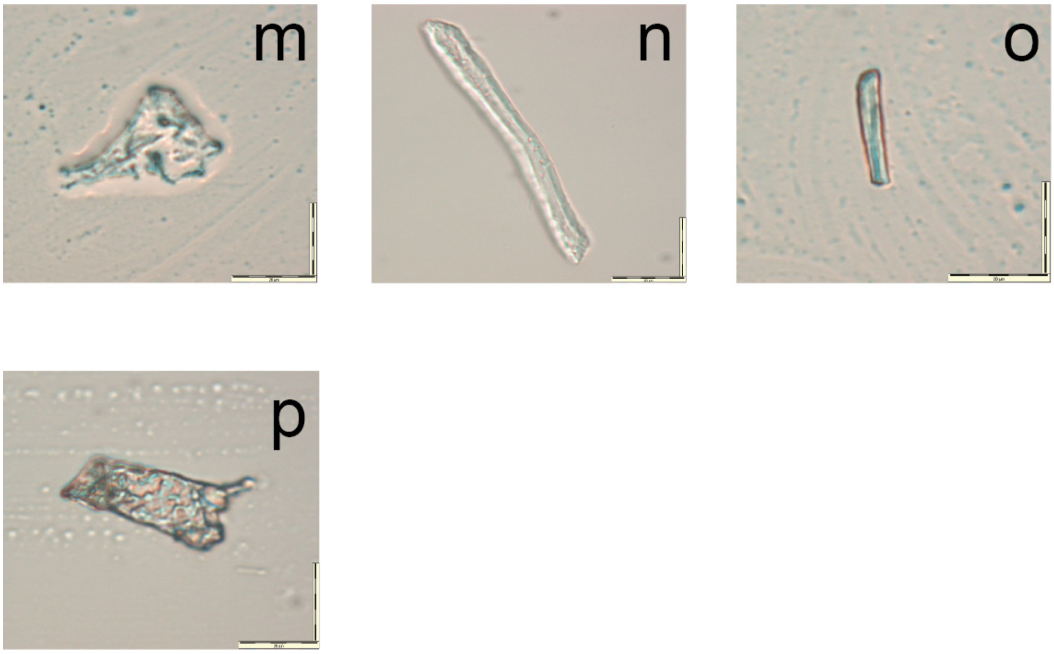

Figure 25: Phytoliths recovered from StW 321*b* calculus sample (grid square U49); m: indetermined; n: long cell psilate; o: long cell psilate; p: parallelepipedal scabrate (broken)

3.2.3 Phytolith comparison between tooth sample (StW 321b) and the nearest bone associated breccia sample (from grid square U52)

Two phytoliths were recovered from the U52 breccia sample (the closest bone associated breccia sample to the StW 321*b* (U49) tooth specimen). From this sample 2 morphotypes were identified:

- parallelepipedal elongate psilate (2) and
- trapezoid wavy (1)

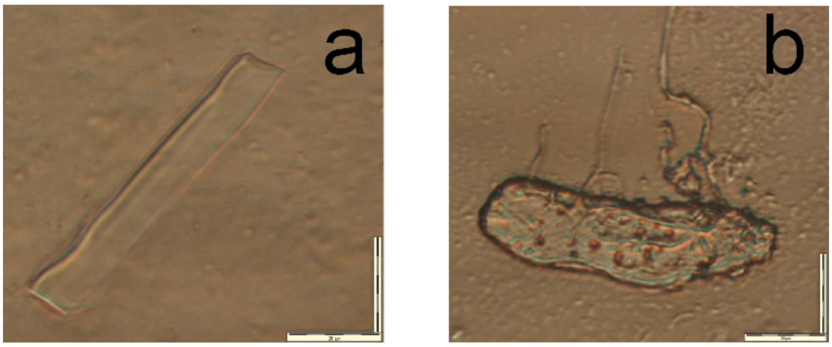

Figure 26: Phytoliths extracted from grid square U52 (nearest bone associated breccia); a: parallelepipedal elongate psilate; b: trapezoid wavy.

These morphotypes were different from those recovered in the StW 321*b* tooth sample (U49) (refer Figure 26). The phytolith comparison between the StW321*b* sample and the U52 breccia sample yielded no common phytoliths.

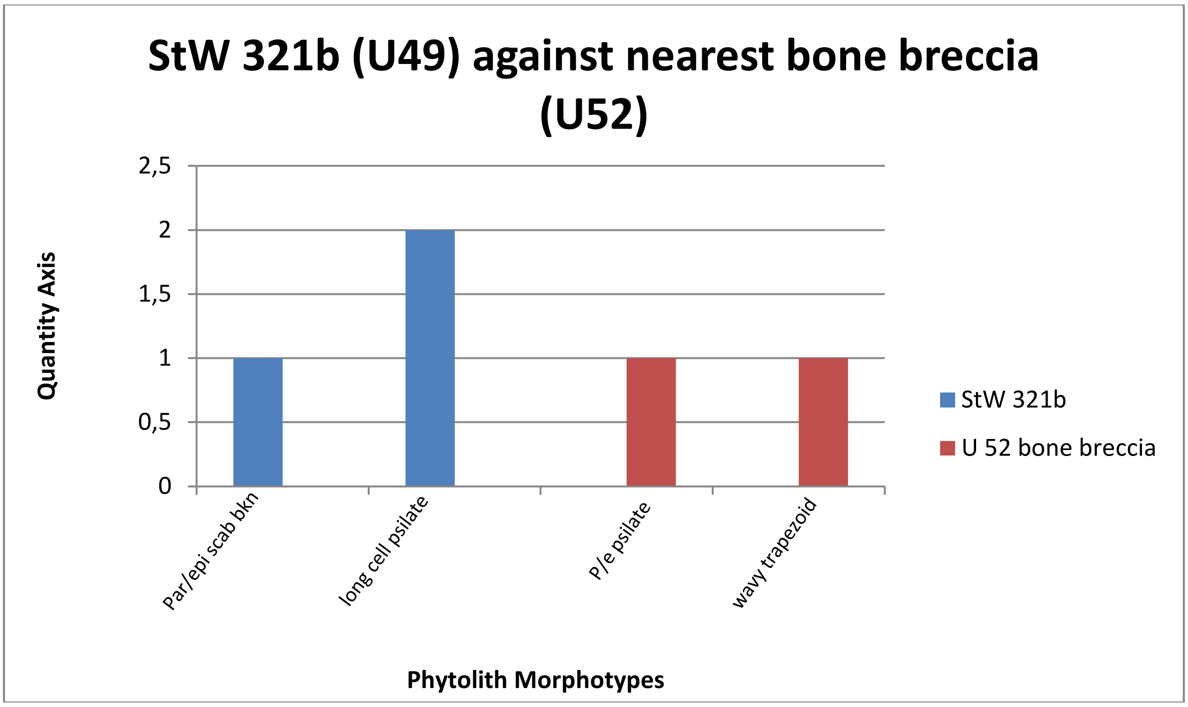

Figure 27: Comparison of the morphotypes recovered in StW321b tooth sample and the nearest bone associated breccia sample (U52)

3.2.4 Comparison of the Phytoliths recovered from nearest bone associated breccia of tooth sample StW 321b (U52) and the nearest breccia control sample (U62 6w and U62 7w)

Comparison between the phytoliths of the nearest bone associated breccia sample (U52) and the breccia control samples (U62 6w and 7w) resulted in one phytolith common to both:

- parallelepipedal elongate psilate.

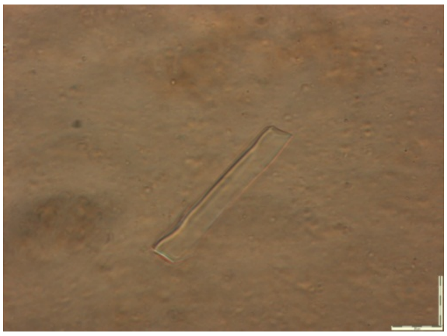

Figure 28: parallelepipedal elongate psilate (U52)

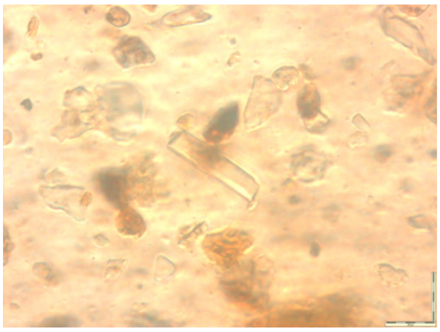

Figure 29: parallelepipedal elongate psilate (U62)

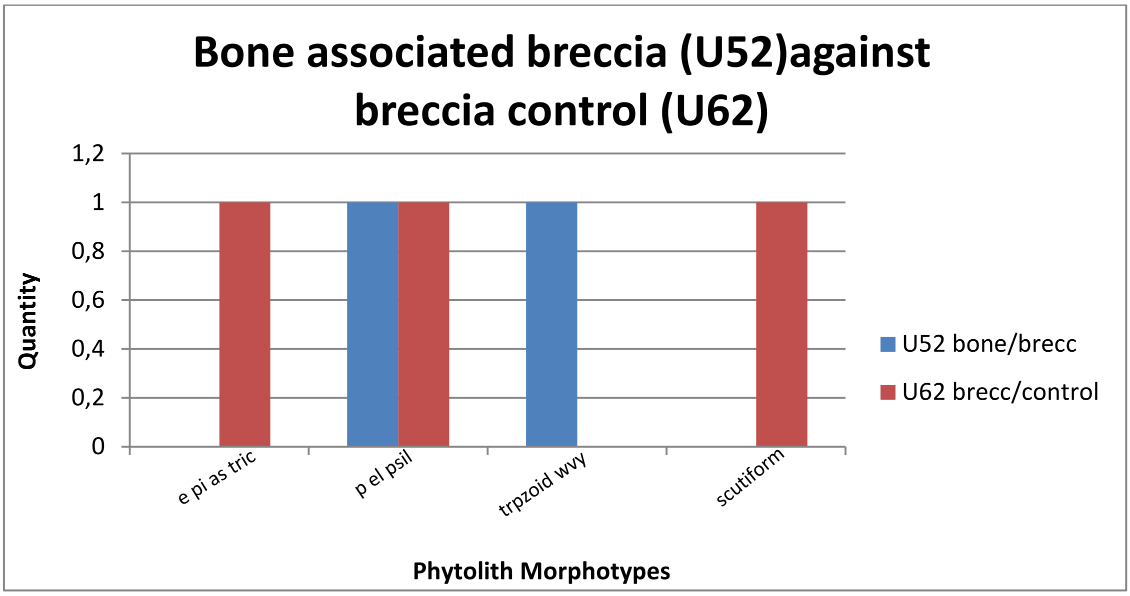

Figure 30: Closest bone associated breccia for StW 321b (U52) compared to breccia control sample (U62)

3.2.5 Discussion (StW 321b tooth sample)

The comparison between the tooth sample extracted from StW 321*b* and the nearest bone associated breccia; and between the tooth sample (StW 321b) and the breccia controls (U62 6w and U62 7w), show no common phytoliths and infer that this tooth sample is not contaminated. It further shows that these phytoliths can only have come from inside the adherent tooth deposit, confirming that calculus is only formed in the presence of saliva (MacPhee and Crowley 1975), and there is no post-mortem remodelling (Lalueza Fox *et al*., 1996). The extracted material therefore has a high probability of being dental calculus.

Comparison of the two parallelepipedal elongate psilates shows that despite their similarity, they are not identical, implying no contamination of the tooth sample. The grid square from which the control breccia originates (U62 6w and 7w) is further away however, from the grid square associated with the tooth specimen (StW 321*b*-U49) than the bone associated breccia (U52) is from the specimen sample, and thus is not as reliable a comparison as the bone associated breccia sample (U52) is with the tooth sample (StW 321*b*).

The former and more reliable comparison (U49 vs. U52), and not the latter (U52 vs. U62) also suggests that the absence of any overlap indicates that no contamination exists.

Whether this hominin actually partook of woody dicot meal from the phytoliths recovered in this tooth sample, is highly probable using the comparison of the StW 321*b* tooth sample and the bone associated breccia sample (U49 vs. U52). It is further highly probable that if the sample is as suggested not contaminated, then the material extracted from this tooth sample has a high probability of being dental calculus, and the phytoliths were therefore not surface phytoliths attached to the enamel as a result of the depositional environment.

By contrast, if the result of the comparison between the bone associated breccia sample and the breccia control sample (U52 vs. U62) is followed, then despite the morphotype overlap demonstrating similarity (but not identical), then contamination may not be ruled out. In this case, woody dicots (the plant type associated with the morphotype involved in the overlap - parallelepipedal elongate psilate), can then only be inferred as having been present on the landscape when this hominin died, and its inclusion as part this hominin's diet may not be inferred from this sample. In sum, the stronger and more reliable comparison (StW 321*b* vs. U52) which concludes that there is no contamination should be followed for reasons outlined above.

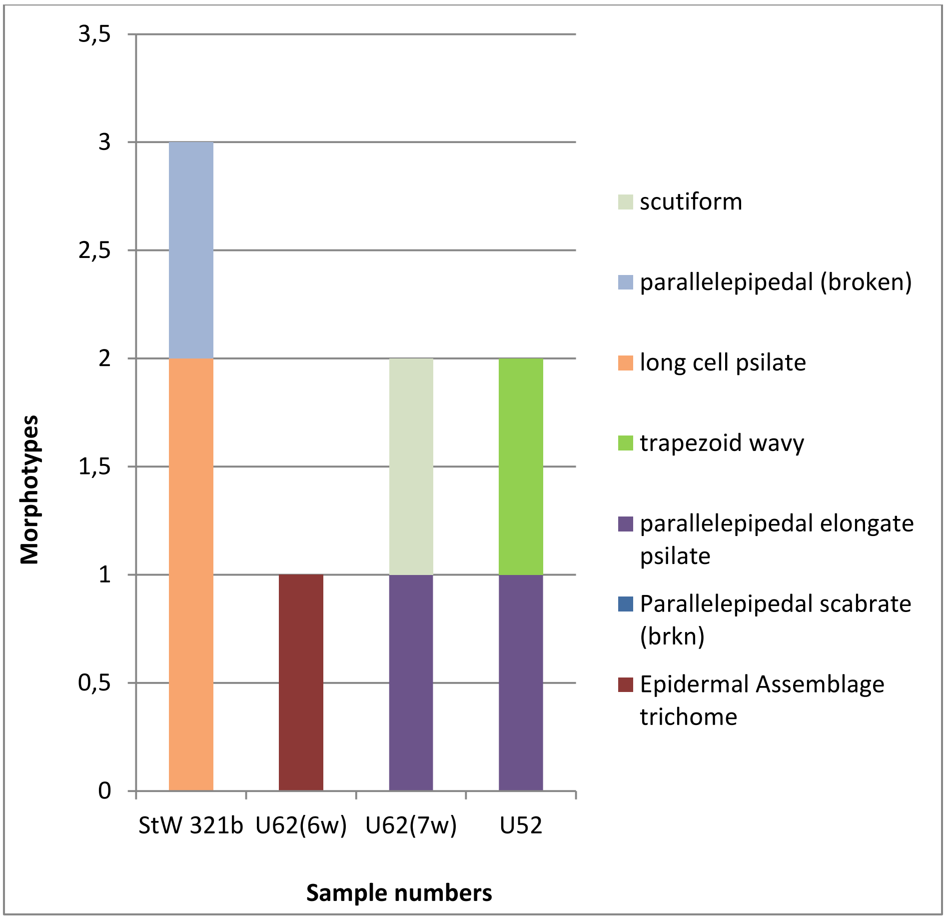

Figure 31: StW 321b compared to breccia control (U62 6w & U62 7w) and nearest bone associated breccia (U52) showing no contamination between the calculus sample and the nearest bone associated breccia sample (U52)

3.3 Specimen StW 534, Right Mandibular Second Molar (RM_2)

3.3.1 Description of probable calculus on StW 534

The buccal surface of the right lower second molar of StW 534 contains several deposits. The deposits which are firmly attached to the buccal surface and indicated within and slightly distal of sub-deposit (b), as well as including the area between sub-deposit (a) and sub-deposit (b), indicate the strongest similarity to the morphological characteristics of supra-gingival calculus (refer Figure 42). These characteristics include a granular and coarse texture. The calculus is white, yellow and brown colouring, which is diagnostic of the colour spectrum of supra-gingival calculus (Hillson 1996; Roberts-Harry and Clerehue 2000). The probable calculus deposits are located on the buccal side of the tooth, which is diagnostic for the location of upper and lower molar supra-gingival calculus (Parfitt 1959, Gressly 1963; Friskopp 1983). According to Brothwell's (1981) scoring index, the probable calculus deposit of the StW 534 tooth specimen demonstrates a score of (1) indicating mild severity, being less than a third of the crown surface (Brothwell 1981). Based on these morphological similarities with dental calculus, the RM_2 from StW 532 exhibits a high probability of being dental calculus.

3.3.1.1 Cervico-distal

Sub-deposit (a) is located disto-buccally on the cervico-buccal margin of RM_2. The deposit is attached to the enamel at the CEJ (cemento-enamel junction), and overlaps onto the cementum directly inferior to the CEJ. This sub-deposit (a) measures approximately 2.3mm horizontally and approximately 1.1mm vertically. The compacted deposit appears to extend obliquely mesial and superiorly, for another 2mm into approximately the start of the middle third of the buccal surface between the distal third and the mesial third. The distal and disto-inferior part of the deposit is white (5Y 8/1). The adjoining inferior mid-portion is a light grey colour (5Y 7/1). The most supero- mesial part of the deposit is darker than the latter to portions, and exhibits two isolated areas of grey shades of colour, below the cervico-distal margin, the more distal of which, is bordering on grey/light grey (5Y 6/1); and the more mesial of the two isolated coloured portions is grey (5Y 5/1). The texture is granular and coarse. The thickness of the adherent deposit appears to be at least 0.5mm thick at its maximum, and at a level of approximately 0.4mm below the CEJ.

3.3.1.2 Mid-buccal

Sub-deposit (b) is located in the middle portion of the tooth, between the distal and the mesial thirds on the buccal surface. Although it presents as a group of isolated small deposits, it has been grouped however, as a distinct cluster deposit with several closely associated component parts. This is demonstrated by their inclusion in the elongated circle, making up a distinct sub-deposit cluster (b). It is made up of four concretions, three of which are separate. There are two superior and two inferior deposits. The two inferiorly placed concretions are conjoined by a whitish material. The first of these concretions is located distally superior, relative to the other concretions in this sub-deposit (b) and seems to be associated with, and may be continuation of the sub-deposit (a). Of the two superiorly located deposits, the distally superior one is characterised by a compact and concentrated material. The horizontal measurement is approximately 3.75 mm; the vertical height is approximately 1.25mm. This concretion is composed of various different colours. The most distal location is light grey in colour (5Y 7/2); the middle superior middle area has an olive yellow colour (5Y 6/6); and the mesial location is a slightly lighter pale olive (5Y 6/3). The texture appears to range from slightly granular and coarse distally to heavily coarse and concentrated in the middle of the concretion and mesially. The thickness ranges from thin distally to extremely thick in the middle and mesial area of the concretion.

The second superiorly located concretion in group (b) is located mesially. It is characterised by a granular and coarse texture, exhibiting no pattern or recognisable shape. The horizontal extent measures approximately 1.98mm and the vertical width measures approximately 1.9mm. The colour of this concretion consists of four colours. The supero-distal portion is olive yellow (5Y 6/6); the middle portion which extends superiorly and inferiorly is grey 5Y (5/1) including two distinctly darker areas of very dark grey to black (5Y 3/1 to 5Y 2/1), one of which is superiorly located, and the other is more inferiorly placed, slightly superior to the inferior margin of the deposit; the outermost infero-distal area of this mesial portion of the group (b) sub-deposit is light olive grey (5Y 6/2); and the most infero-mesial portion of the mesial portion of the group (b) sub-deposit and inferiorly placed middle portion, is a shade of olive (5Y 5/3). The thickest area is in the middle portion of the concretion, which is at least 0.5mm and attached to the enamel surface.

The infero-distal concretion (the third segment) of sub-deposit (b) located on the mid buccal surface appears to be located on the cervico-enamel margin of RM_2, and is also contained within the cluster sub-deposit (b). Its horizontal extent measures approximately 1.85mm and vertically it measures approximately 1.1mm at its maximum. This concretion extends mesially and is joined by a less grainy and coarse textured material. The horizontal measurement of this middle concretion is approximately 1.7mm and its vertical width measures approximately 1.35mm. The colour of this middle concretion is white. The most distal inferior segment of the sub-deposit (b) has a light brown colour (7.5Y 6/4); the middle portion of this concretion has a white (7.5Y N8) and the most mesial portion is a shade of brown (7.5YR 5/4).

The last concretion contained in this sub-deposit (b) is situated infero-mesially on the mesio-buccal surface. The horizontal measurement is approximately 2.15mm and its vertical height measures approximately 1.2mm. The colours of this infero-mesial concretion are: the distal segment is a dark shade of brown (7.5YR 5/4); the middle segment is mostly light brown (7.5YR 6/4; and pinkish grey in the mesial segment (7.5YR 7/2).

3.3.1.3 Occluso-buccal

Sub-deposit (c) is located on the occluso-buccal surface in superiorly central position. The sub-deposit is concentrated and compact is relatively smooth, no evidence of any coarseness or granular texture. It has a horizontal measurement of approximately 1.25mm and a maximum vertical width of approximately1.8mm. This sub-deposit (c) is composed of two principal colours pink and brown (7.5YR 7/4; 7.5YR 5/4). The distally inferior and superior segments are pink (7.5YR 7/4), and central area is pink (7.5YR 7/4) and has a light grey area bordering on grey (7.5YR N7 - N6), the superiorly central area is brown (7.5YR 5/4). The deposit is thickest in the superiorly central portion, with a minimum thickness of approximately 0.5mm.

3.3.1.4 Sub-cervical

Sub-deposit (d) is located inferior to sub-deposit (b) on the cementum, and at the bifurcation of the tooth. The deposit extends along the superior margin and extends laterally on both sides inferiorly of the bifurcation. The deposit has three predominant colours, the superiorly placed portion is brown (7.5YR 5/2), the slightly inferior or middle part of the deposit, is dark brown (7.5YR 4/4) (the portion sandwiched between the superior and inferior portions), i.e. the 'second level' of the deposit; the most inferior level of the deposit is a brown colour (7.5YR 5/2); and the most mesial portion of the sub-deposit which extends inferiorly lateral to the bifurcation is a pinkish grey (7.5YR 6/2).The horizontal measurement (which is the horizontal measurement across the superior portion of the bifurcation) of the sub-deposit is approximately 2.6mm mesiodistally and the maximum vertical width (being the largest inferiorly mesio-lateral width to the most superior margin of the sub-deposit (d) i.e. superior to the bifurcation) is approximately 2.8mm. The thickness of this deposit appears to be approximately 0.7mm. The texture of the material is extremely coarse and granular.

3.3.1.5 Sub cervico-mesial

Sub-deposit (e) is situated supero-distally to sub-deposit (d) and infero-distally to the CEJ, and is located on the *cementum* of the tooth. The adherent material is granular and coarse. The supero-distal location presents with a creamy granular textured material, similar to the material in sub-deposit (a) and the material in sub-deposit (f). The deposit is situated and interspersed with a dark material (possibly manganese, or residual organic material, which has not been tested). The inferior section of the deposit is more coarse and granular than the middle or superior parts of the sub-deposit (e). The horizontal width of this deposit is approximately 4.2mm and vertically approximately 6mm. The colour of this deposit is described by three principal areas. The supero-mesial area is a white to light grey colour (7.5YR N8 – N7); the area slightly infero-distal to the supero-mesial area is predominantly a brownish shade (7.5YR 5/2); and the most inferior part of the sub-deposit ranges from pink to light brown (7.5YR 7/4-7.5YR 6/4). This grainy sub-deposit (e) is also attached and to the dark ‘manganese-type’ material which is adherent to the *cementum*. The deposit is an amorphous one and has no set form.

3.3.1.6 Cervico-mesial

Sub-deposit (f) is located directly mesial to sub-deposit (d) and supero-mesial to sub-deposit (e). This sub-deposit is made up of two main areas. An inferior portion which is spotty with a grainy texture and a superior portion made up of a thin longitudinal distally placed sub-deposit and a more mesial, but thicker group of small isolated granular globules in a longitudinal shape. This sub-deposit is made up of different forms but has no set pattern to it. The maximum vertical width of the inferior section of the sub-deposit is 1.15mm, and horizontally the maximum extent of the inferior section is 1.7mm. The maximum vertical height of the total deposit is approximately 2.2mm. The colours of this deposit are: inferior portion is light grey (7.5YR N7) with a thick isolated mesial globule which ranges from light brown to dark brown (7.5YR 6/4 – 7.5YR 4/4), and a distal globule which is very dark brown (7.5YR 3/2); the mesial longitudinal group of spotty deposits range from light brown to a slightly darker shade of brown (7.5YR 6/4 – 7.5YR 5/4), and the distal thin longitudinal ‘stick-like’ deposit is strong brown in colour (7.5YR 5/6), with a reddish yellow distal longitudinal margin (7.5YR 8/6).

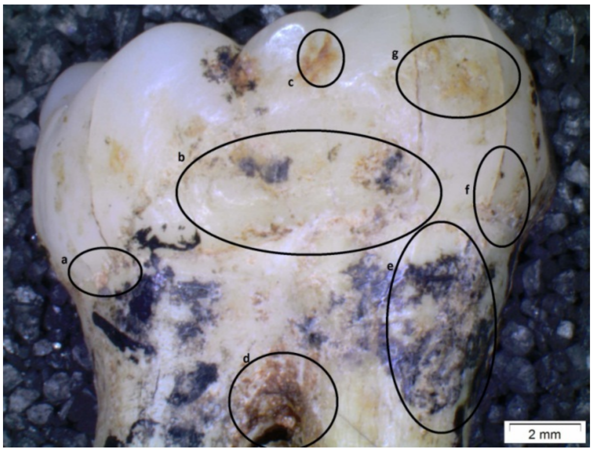

Figure 32: StW 534 RM_2 buccal

3.3.2 Phytoliths Results from StW 534 (taken from grid square W43)

Twelve phytoliths were recovered from the StW 534 calculus sample (see Table 10). Out of the phytoliths found, two morphotypes were identified:

- cylindroid psilate (5) and
- cylindroid psilate curved (3) (see Figure 35).

Four phytoliths were classified as indetermined and constituted 31% of the phytoliths recovered from this tooth sample, with cylindroids (cylindroid psilates and cylindroid psilate curved) making up approximately 7% of the phytoliths. The plant types mostly associated with the two phytolith morphotypes identified in this sample are monocotyledons (sedges) and woody dicotyledons (see Table 8).

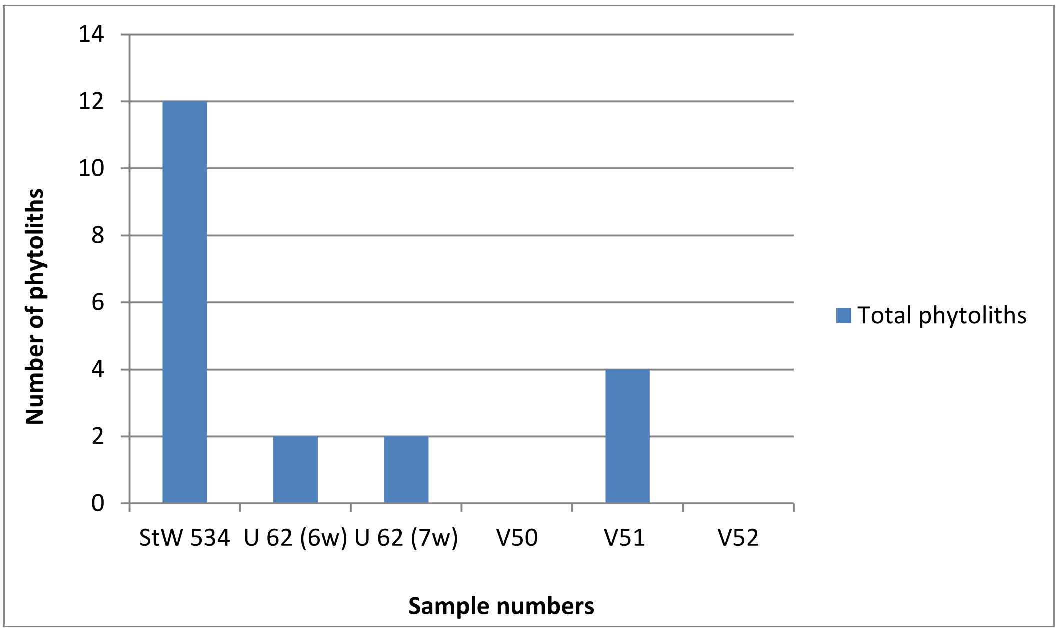

Figure 33: No of phytoliths recovered from StW 534 tooth and other breccia sample numbers

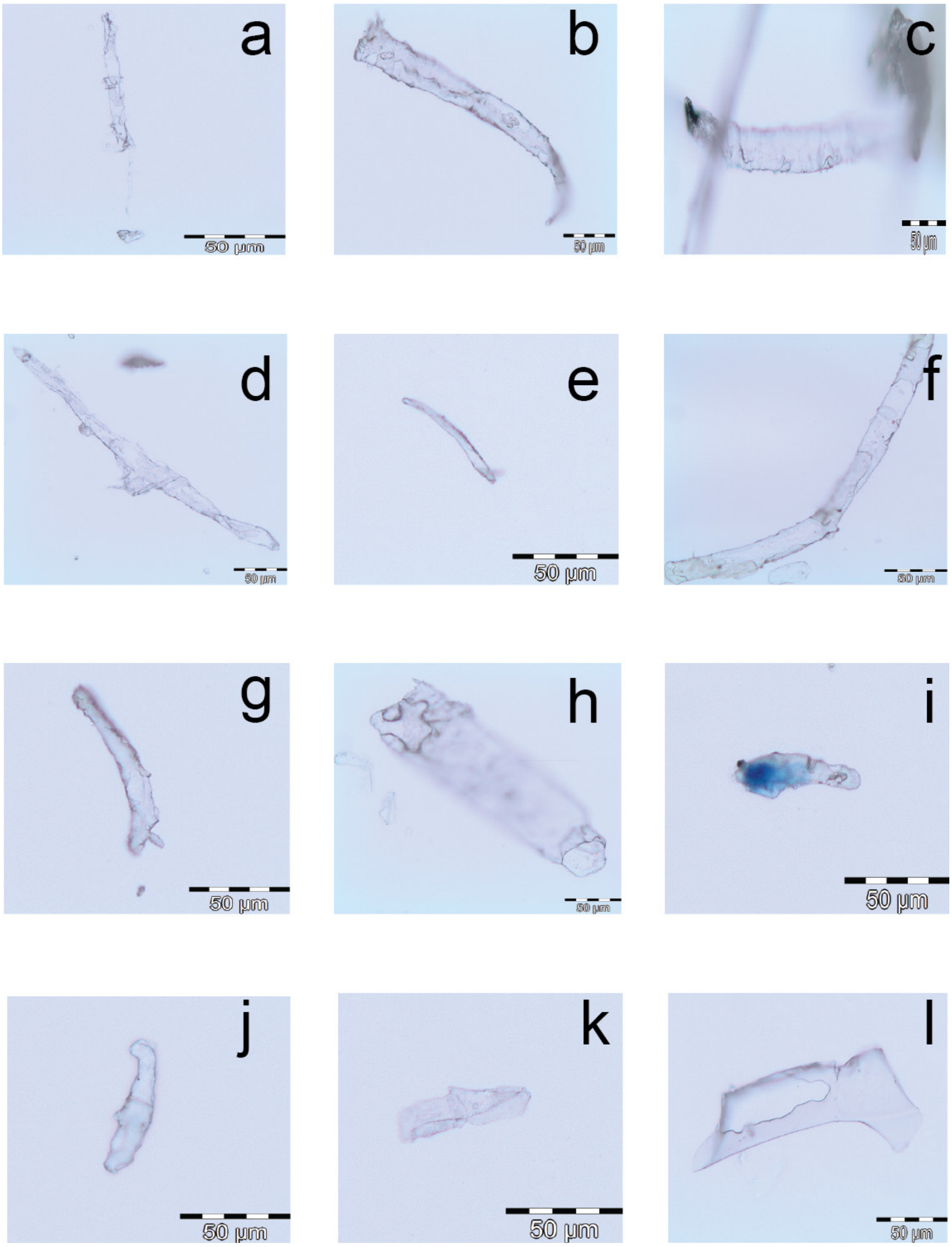

Figure 34: Phytoliths recovered in the StW 534 tooth sample (grid square W43)

3.3.3 Comparison between phytoliths recovered from StW 534 and the closest bone associated breccia samples (V50; V51; V52)

No phytoliths were found in the closest bone associated breccia samples for grid squares V50 and V52. Four (4) phytoliths were recovered from the grid square sample V51. There was no overlap found between the closest bone associated breccia (bovid) (V50, V51, and V52) and the StW 534 calculus sample. The four phytoliths recovered from the V51 grid square belong to four different morphotypes:

- parallelepipedal elongate scabrate;
- parallelepipedal facetate;
- cylindroid elongate psilate; and
- bulliform fan shape.

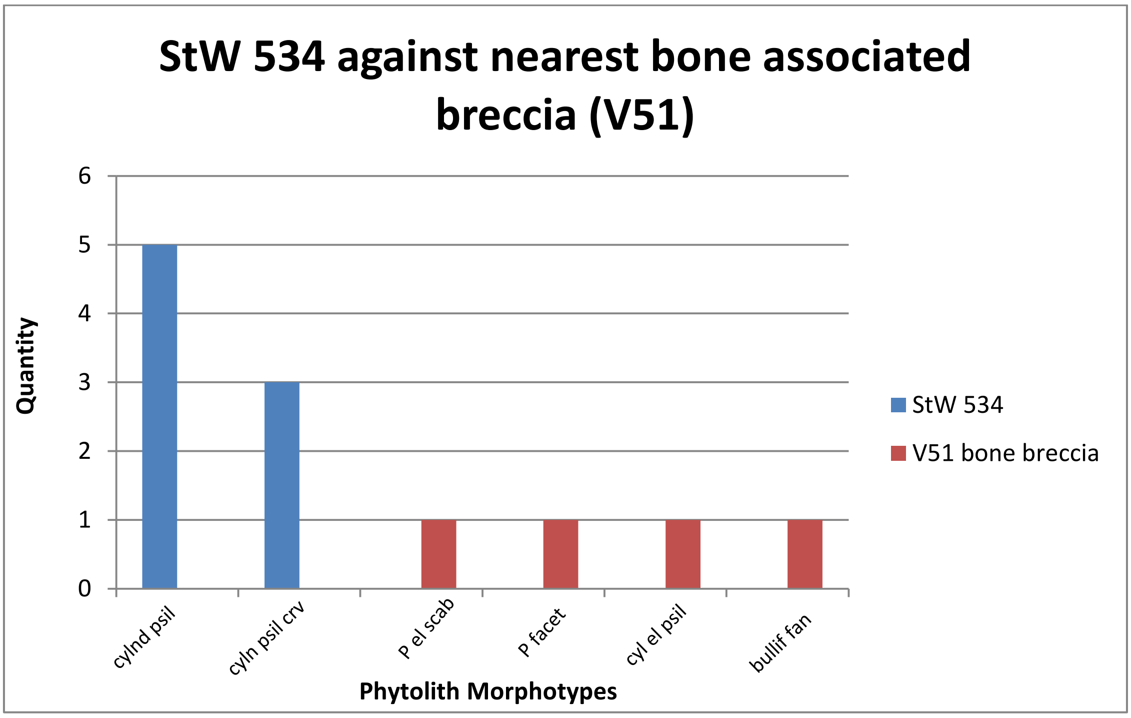

Figure 35: Comparison of the morphotypes recovered from the StW 534 tooth sample and the closest bone associated breccia (grid square V51)

There were no indetermined phytoliths recovered from this sample. The plants associated with the four phytolith morphotypes recovered are trees shrubs (dicotyledons) and sedges (monocotyledons) (refer Table 8). Parallelepipedals were the predominant morphotype found in the V51 bone associated breccia sample.

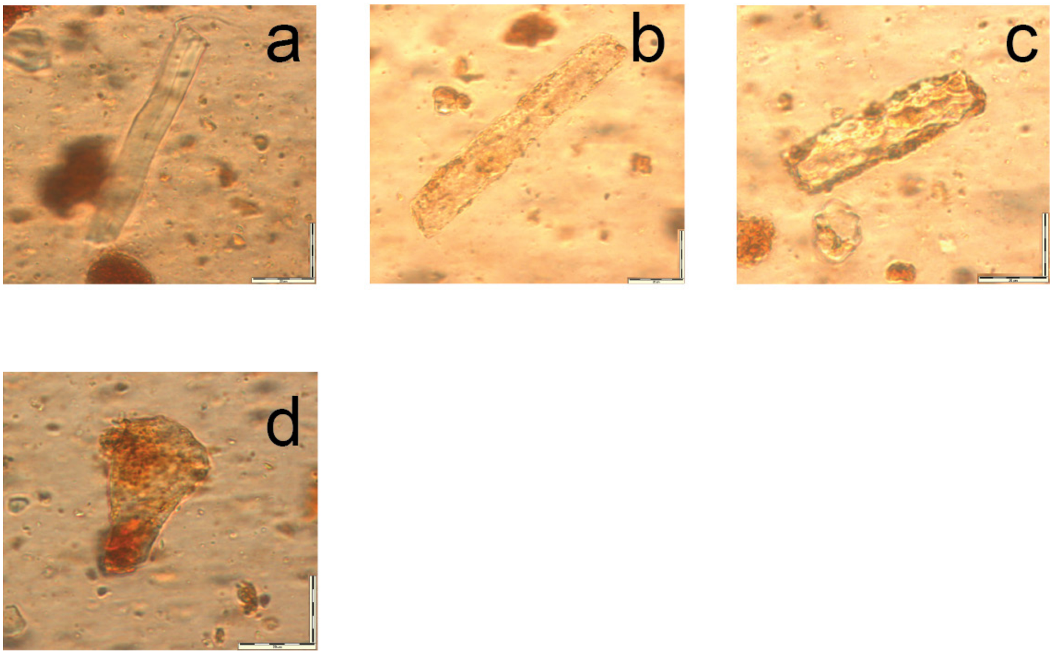

Figure 36: Phytoliths from grid square V51 (closest bone associated breccia (bovid fragment); a: cylindroid elongate psilate; b: parallelepipedal elongate scabrate; c: parallelepipedal facetate thick; d: bulliform fan shape.

3.3.4 Comparison of the phytoliths recovered from the nearest bone associated breccia (V51) with the breccia control sample (U62 6w and U62 7w)

Comparison of the nearest bone associated breccia (V51) with the breccia control (U62 6w and 7w) revealed no common morphotypes (refer Figure 47 and Figure 48).

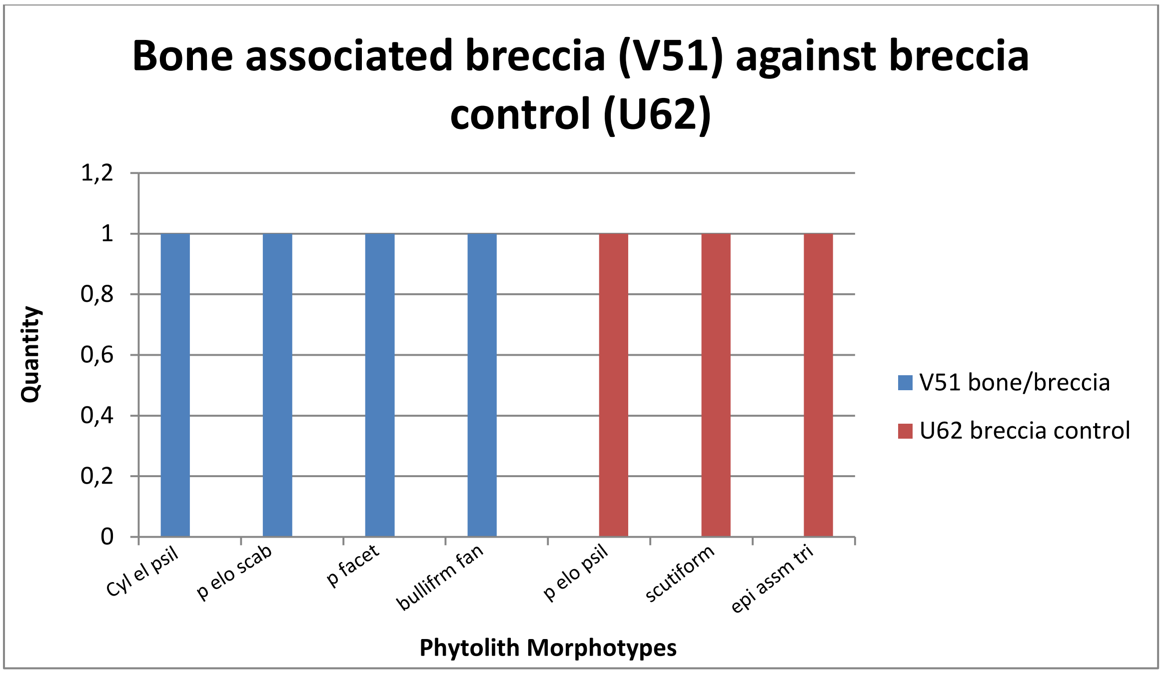

Figure 37: closest bone associated breccia for StW 534 and StW 532 (V51) compared to breccia control (U62)

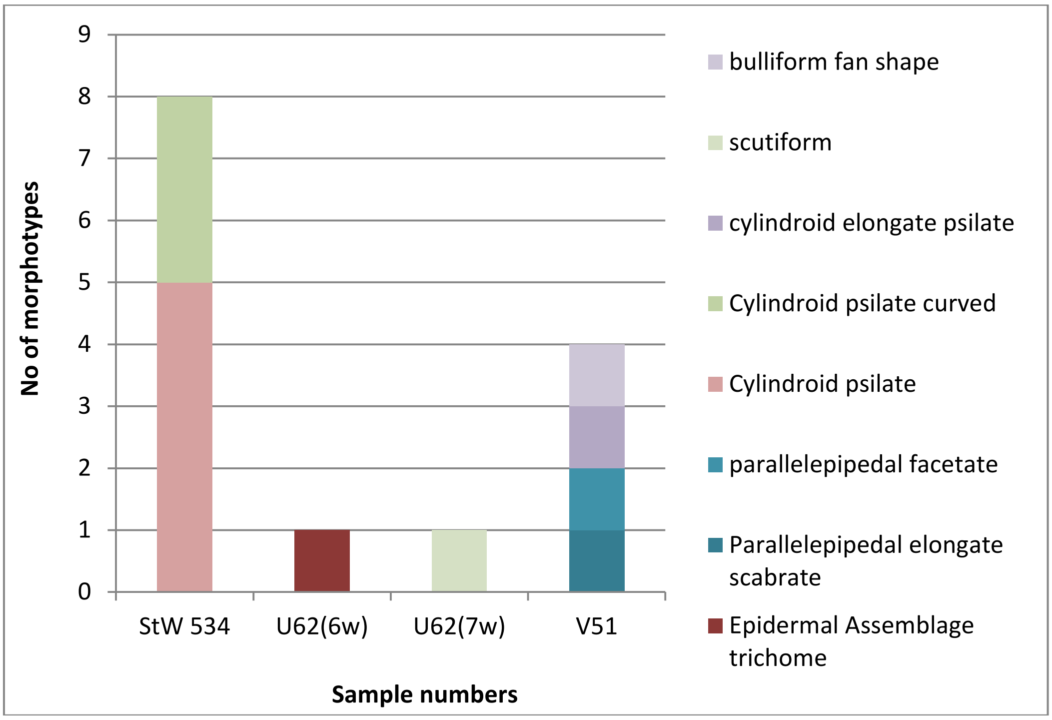

Figure 38: phytolith morphotypes of StW 534 calculus sample compared with breccia control (U62 6w and U62 7w) and nearest associated breccia samples (V51)

3.3.5 Discussion (StW 534 tooth sample)

Comparison of the phytoliths recovered from the StW 534 (grid square W43) calculus sample with those from the nearest bone associated breccia samples (grid squares V51) showed no common phytoliths, and implies that the tooth sample was not contaminated (refer Figure 48). The observation that no phytoliths were found in two of the nearest bone associated breccia samples (grid squares V50 and V52) also indicates a strong possibility that the StW534 tooth sample was not contaminated. Further, the phytoliths recovered from the bone associated breccia sample (grid square V51) are different to those recovered from the breccia control (U62 6w and U62 7w), indicating no contamination exists. The phytoliths recovered from the StW 534 tooth sample are also different to the phytoliths from the breccia control (U62 6w and U62 7w).

On the basis that there are no common phytoliths found between the tooth sample and any one of the breccia controls, not only infers a high probability that the StW 534 tooth sample is not contaminated, but also infers that the sample material extracted from the StW 534 tooth specimen has a high probability of being calculus.

3.4 Specimen StW 532 Left Mandibular Third Molar (LM_3)

3.4.1 Description of probable calculus on StW 532

The buccal surface of LM_3 exhibited distinctive areas of similarity with dental calculus morphology, for instance, the distribution of adherent material was limited to the buccal surface, which is diagnostic of molar calculus (Parfitt 1959;Gressly 1963; Friskopp 1983); the shape of the calculus was patchy. The level of textural coarseness was low. The colour spectrum reflected yellowish, dark and light brown hues which are diagnostic of ancient and modern human dental calculus (Hillson 1996; Roberts-Harry and Clerehugh 2000). This specimen was scored (1) on the Brothwell's (1981) index of scoring calculus. Four areas display a high degree of probable calculus (refer sub-deposits (a-d) Figure 49).

Sub-deposit (a) is located occluso-buccally within the mesial third of LM_3 mesio-distally. The deposit is patchy and may be part of a 'band' shaped deposit covering the whole buccal surface, which continues inferiorly from sub-deposit (a) into sub-deposit (c) and slightly supero-laterally into sub-deposit (b). It then continues infero-distally into sub-deposit (d) located in the bucco-distal segment of the specimen. The colouring of sub-deposits (a) is characterised as a range of light to medium brown hues which is diagnostic of dental calculus (Hillson 1996). The textural buccal deposits are mildly coarse (Hillson 1996). There are potential calculi deposits attached to the occlusal surface, and located adjacent to sub-deposit (a).

Sub-deposit (b) is located laterally of sub-deposit (a) and has a similar colouring to sub-deposit (a). The texture of sub-deposit (b) is mildly coarse. The shape of sub-deposit (b) is fairly 'band like' with intermittent patches. Sub-deposit (c) which is located on the cemento-enamel junction, and within the cervical third of the buccal surface occluso- apically, exhibits a fairly coarse deposit with similar brown colouring to sub-deposits (a) and (b) and (d). Sub-deposit (c) has a haphazard and patchy shape. Sub-deposit (d) is located disto-buccally, has a patchy and irregular shape, and also exhibits a brown diagnostic colouring. This sub-deposit has a mildly coarse texture.

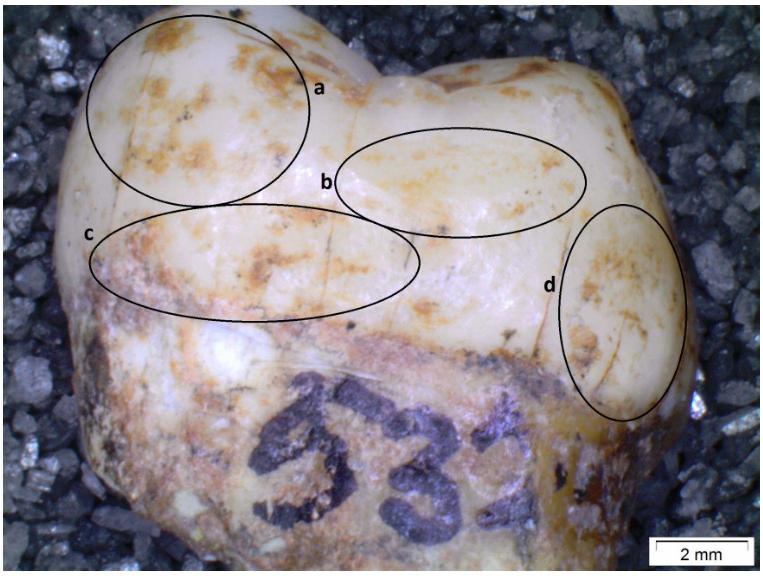

Figure 39: buccal view of LM$_3$ StW 532 tooth sample

3.4.2 Phytolith Results from StW 532 (taken from grid square W43)

Thirteen phytoliths were recovered from the StW 532 tooth sample. Nine morphotypes were identified:

- Ellipsoid psilate
- Cylindroid scabrate

- Cylindroid parallelepipedal
- Cylindroid psilate curved
- Cylindroid psilate
- Long cell psilate
- Tracheid vessel
- Epidermal assemblage trichome
- Tracheid

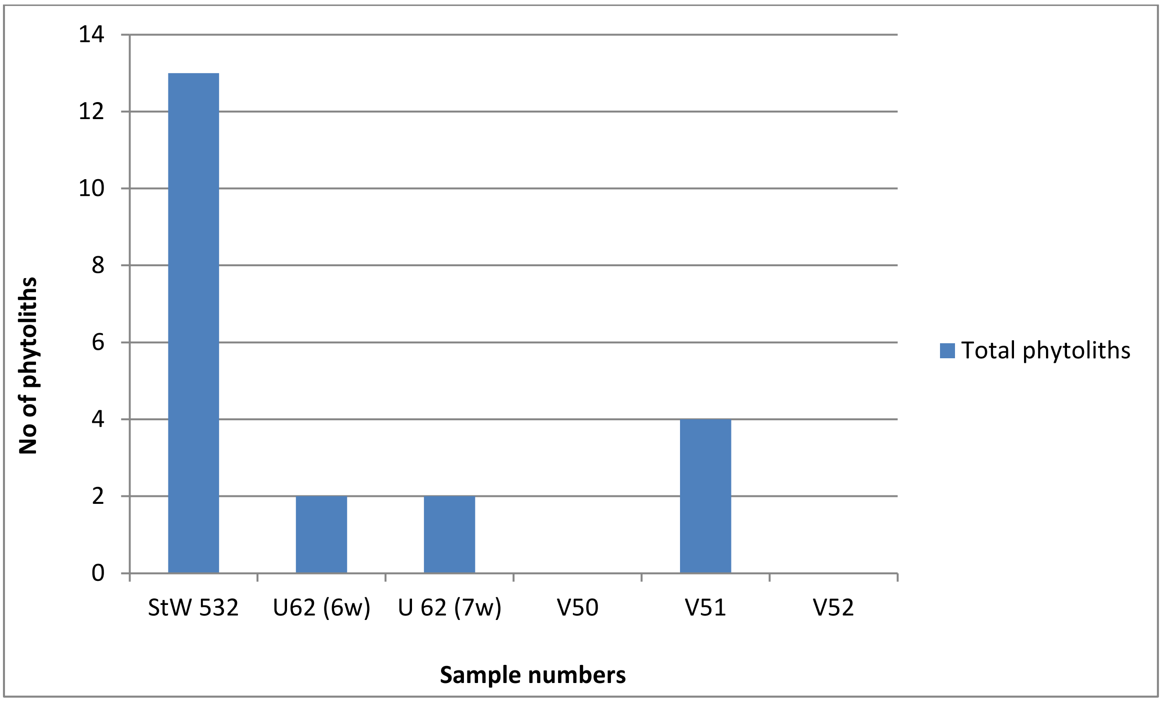

Figure 40: Total phytoliths recovered from StW 532 and comparative bone (closest) associated breccia samples including breccia control samples

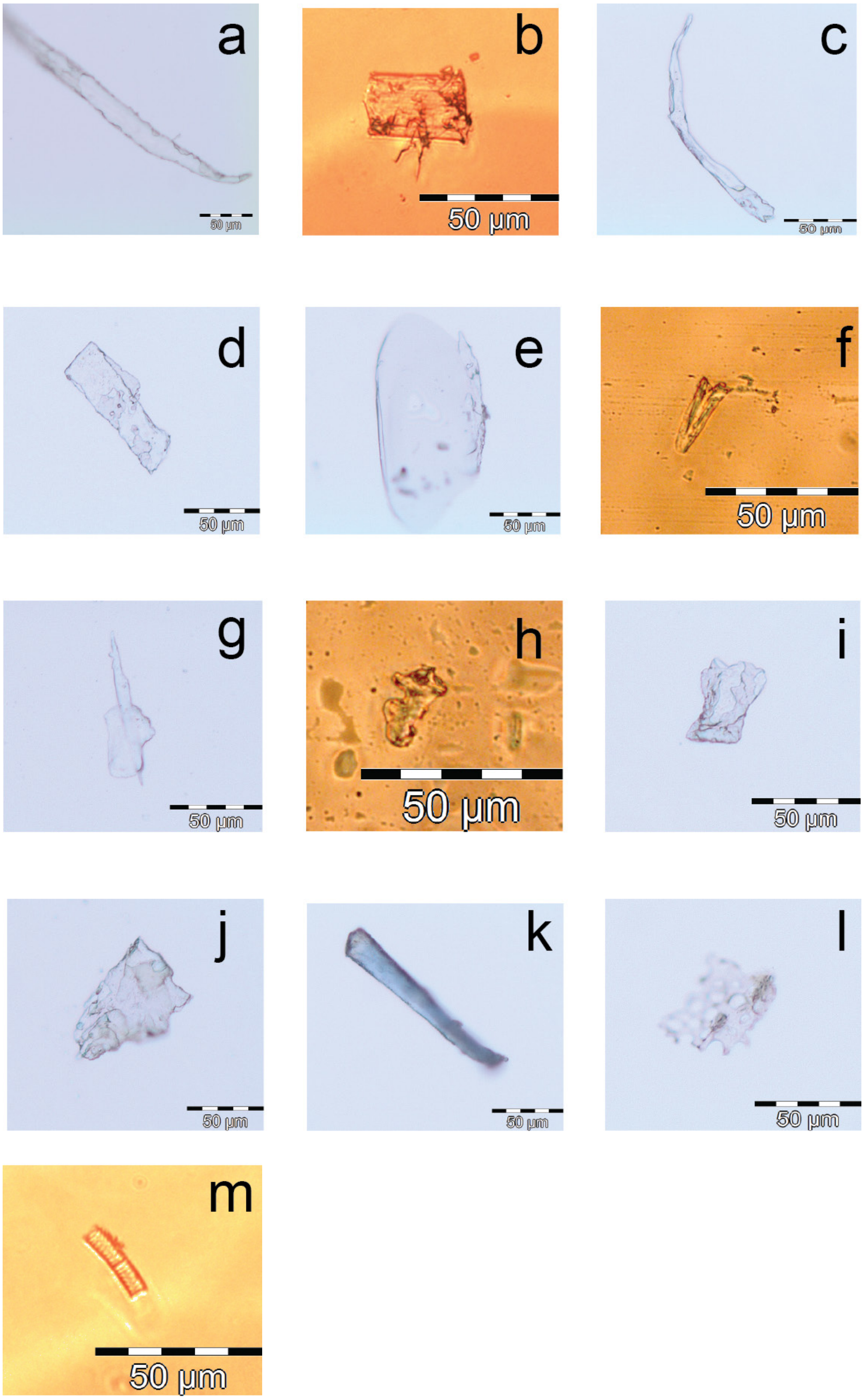

Figure 41: phytoliths recovered from StW 532 tooth sample

3.4.3 Discussion (StW 532 tooth sample)

Cylindroids constitute approximately 30% of the phytolith morphotypes found, and were the most common in this tooth sample. The StW 532 tooth sample showed the least percentage of indetermined phytoliths out of the total tooth sample (23%). A tracheid was recovered from this specimen. Plants associated with the morphotypes recovered from the StW 532 tooth sample include monocotyledons in the form of sedges and grasses, and trees and shrubs and woody dicots (refer Table 8).

No phytoliths were recovered from the V50 and V52 grid square breccia samples (refer Figure 54). This result indicates a high probability that the tooth sample was not contaminated. Comparison between the phytoliths recovered from the StW 532 tooth sample and the phytoliths found in grid square V51 (one of three of the closest bone associated breccia samples) resulted in no overlap of phytolith morphotypes either (refer Figure 54 and Figure 54), which further implies a high probability that the tooth sample (StW 532) was not contaminated. Comparison of the phytoliths between the associated bone breccia (V51) and the breccia control sample (U62 6w and U62 7w) also demonstrated that there was no overlap in phytoliths, and therefore further appears to confirm that a high probability exists that the tooth sample is not contaminated. A comparison of the morphotypes recovered from the StW 532 tooth specimen and the breccia control specimen (U62 6w) however, reveals that both display epidermal assemblage trichomes (refer Figure 41).

Direct comparison of the two phytoliths reveals that although they show some similarity, they are not identical. The bases of the triangular form show dissimilarity, their lengths are different, and their texture is dissimilar. In summary, a high probability exists that the adherent material extracted from the buccal surface of the StW 532 tooth sample is calculus.

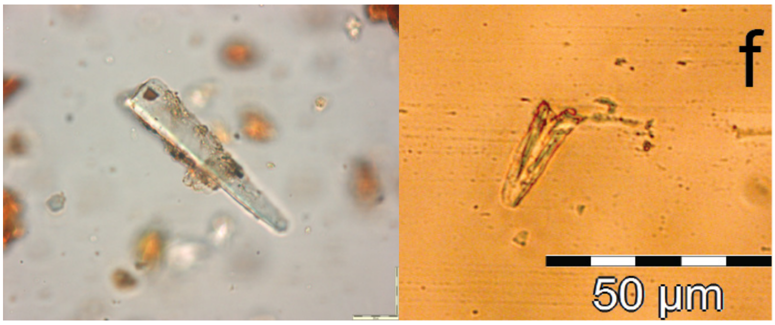

Figure 42: epidermal assemblage trichome recovered from breccia control sample (U62 6w) (left); epidermal assemblage trichome recovered from the StW 532 tooth sample (right). Left scale is 20µ. Right scale is 50 µ

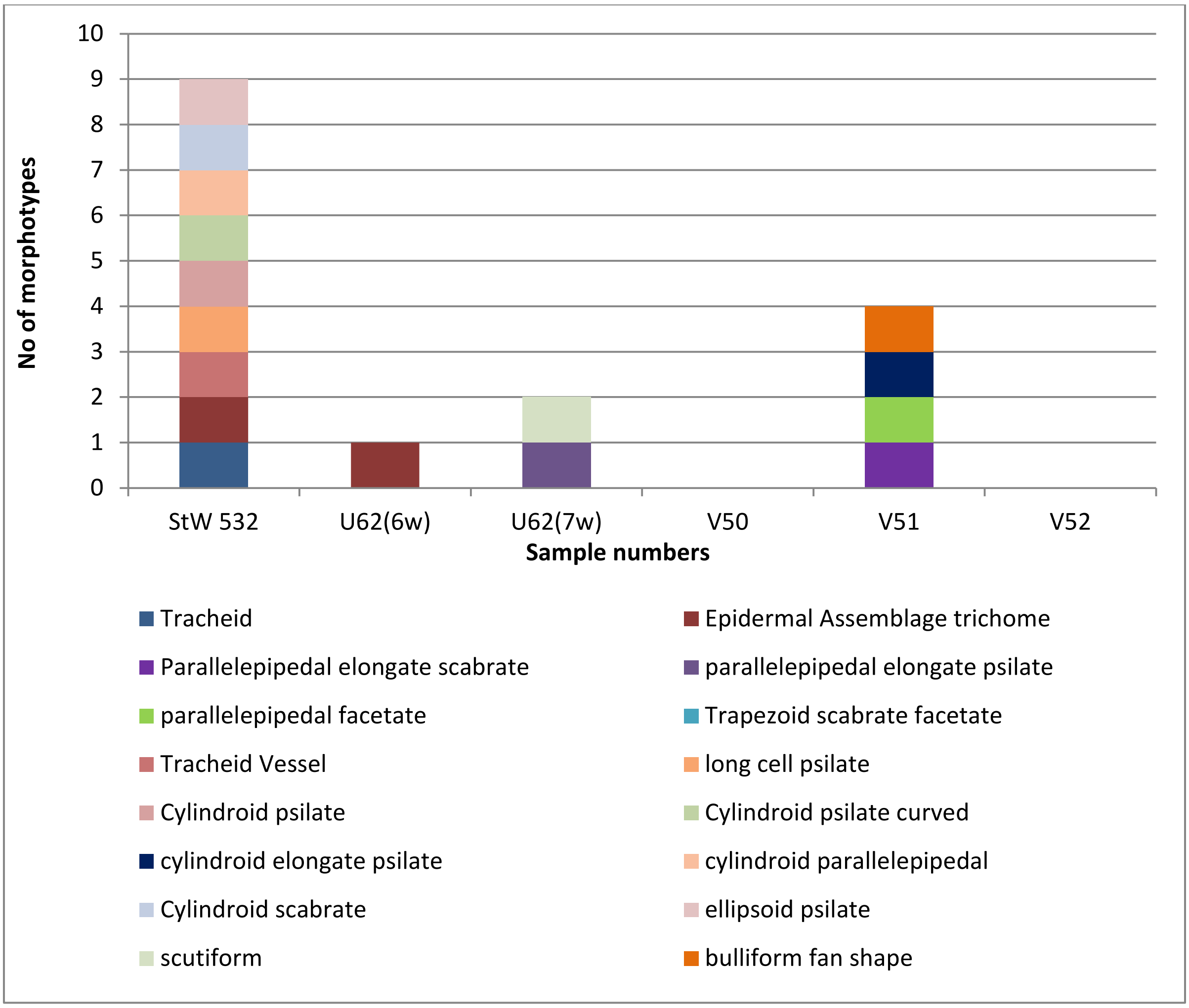

Figure 43: Total number of morphotypes extracted from the StW 532 tooth specimen, breccia controls (U62 6w; 7w) and the nearest bone associated breccia samples (V50; V51; V52) showing V50 and V52 were devoid of any phytoliths.

3.5 Specimen StW 183 Left Maxillary First Molar (LM^1)

3.5.1 Description of probable calculus

Deposit (a) is attached to the linguo-mesial surface of LM^1 and located in the cervical third (occluso-apically) of the StW 183 maxillary specimen. This deposit exhibits a moderate textural coarseness in the centre of the deposit, reducing as the deposit extends outward from the centre. The surface thickness also reduces as the deposit widens distally and supero-mesially. Probable calculus severity was scored as mild (covering less than 1/3 of the crown surface), according to the Brothwell (1981) Index. The shape of the deposit is patch shaped. Colouring of the deposit ranges from a light to medium brown, which is diagnostic of human supra-gingival calculus (Hillson 1996). Human dental calculus is mostly found on the buccal surfaces of upper and lower molars (Parfitt 1959; Gressly 1963; Friskopp 1983). This deposit was identified on the lingual surface of the LM^1 of the tooth specimen, which is generally accepted as not as common as buccal calculus.

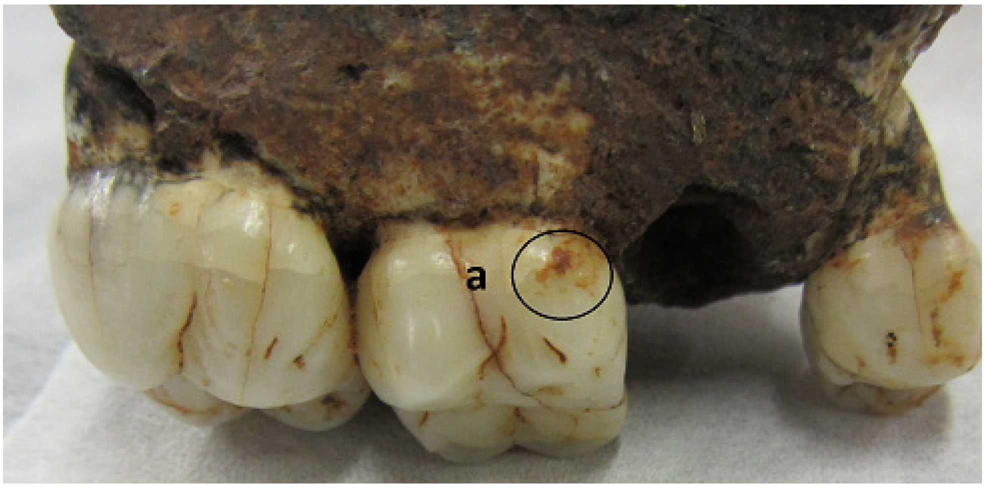

Figure 44: StW 183 lingual LM^1 showing a probable calculus deposit (a)

3.5.2 Phytolith Results from StW 183 (taken from grid square T49)

Four phytoliths were recovered from the lingual surface of the LM^1 tooth sample from the StW 183 maxillary specimen. All 4 phytoliths were classified as indetermined (refer Figure 56). No associated plants could be inferred from the tooth sample as a result.

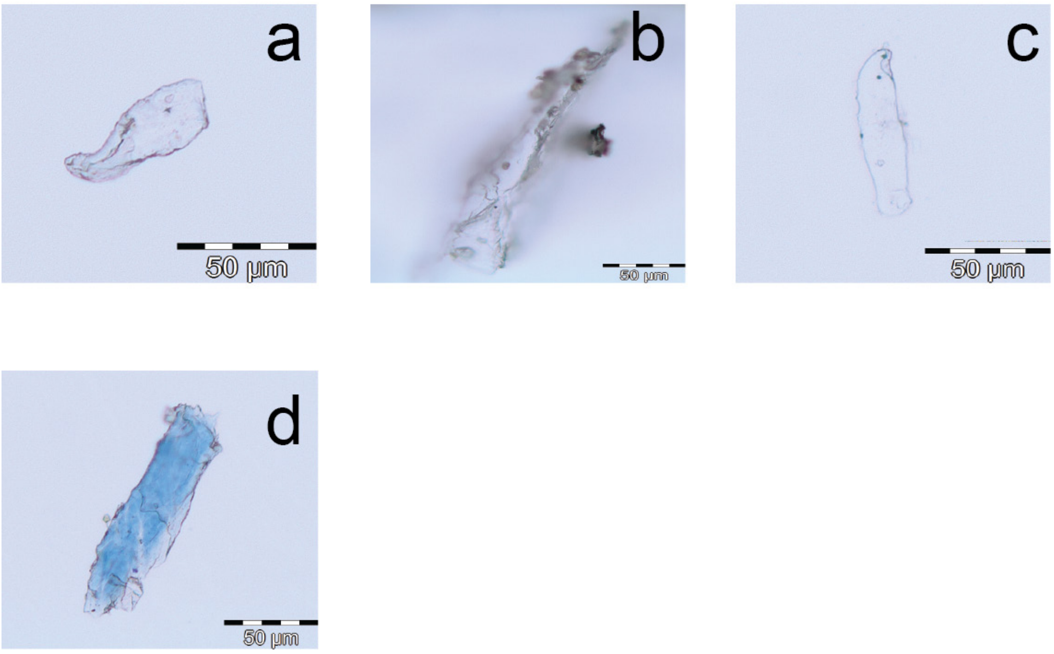

Figure 45: Phytoliths recovered from the StW 183 tooth sample. a –d, indetermined phytoliths

3.5.3 Comparison between phytoliths from StW 183; Associated bone breccia (grid square S63), and the breccia control sample (U62 6w and U62 7w).

Five (5) phytoliths were recovered from the S63 breccia sample (nearest bone associated breccia sample to the StW 183 tooth specimen). Three indetermined phytoliths and two morphotypes were recognised:

- cylindroid scabrate
- parallelepipid thick

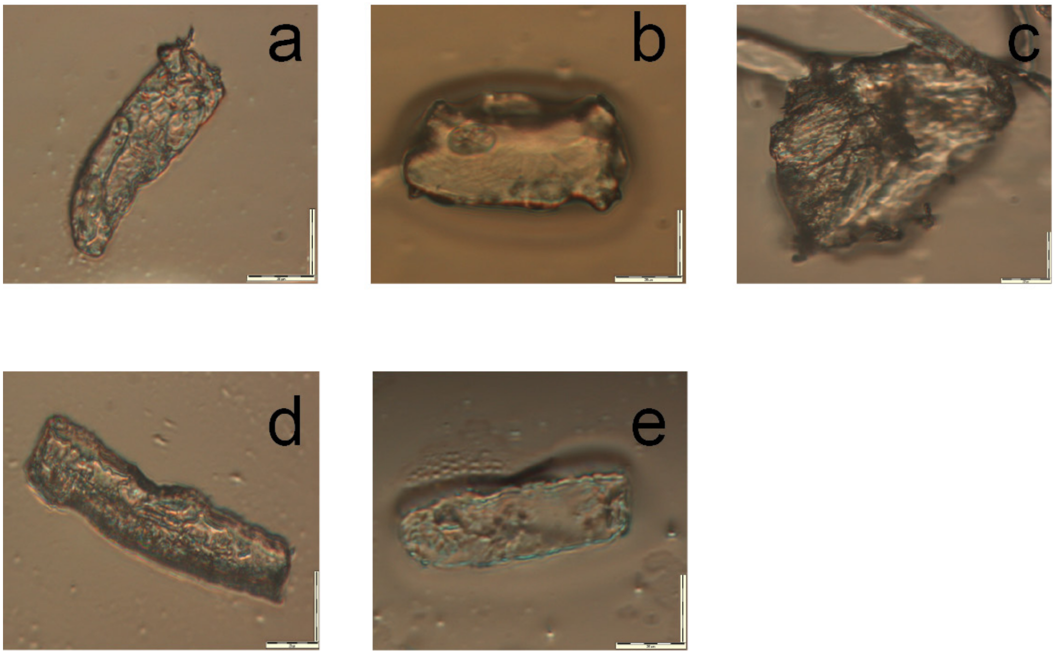

Figure 46: Phytoliths recovered from the nearest bone associated breccia sample from grid square (S63); a: indeterminate; b: indeterminate; c: indeterminate; d: cylindroid scabrate; e: parallelepipid thick

No comparison could be made between the StW 183 tooth specimen sample and any bone associated breccia, or breccia control samples, as all the phytoliths recovered from the StW 183 tooth specimen sample were classified as indetermined.

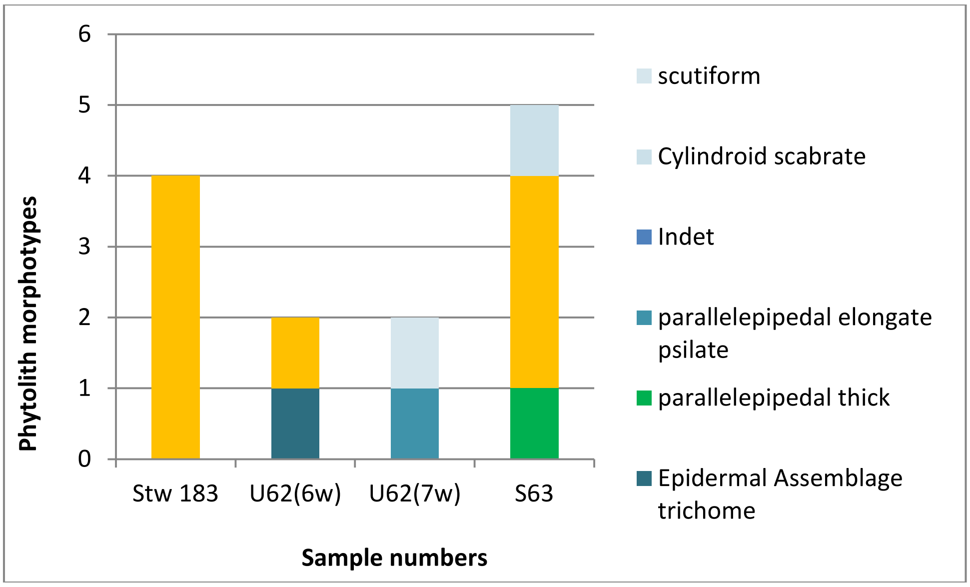

Figure 47: StW 183 tooth specimen, breccia control and bone associated samples and the phytolith morphotypes recovered in each sample

3.5.4 Discussion (StW 183 tooth sample)

StW 183 (refer Figure 44) follows diagnostic morphologies of dental calculus, for example scoring of calculus (Brothwell 1981, Dobney and Brothwell 1987), thickness, texture and colour (Hillson 1996). The colour of this probable supra-gingival deposit ranged from light brown to dark brown, diagnostic of ancient calculus (Hillson 1996). It differs from the yellow/white morphology described in Roberts-Harrry and Clerehugh (2000) for modern supra-gingival calculus. Supra-gingival calculus occurs most often on the lingual surfaces of the lower incisors and the buccal surfaces of the first and second maxillary molars (Parfitt 1959; Gressly 1963; Friskopp 1983). In this specimen, the deposit adhered to the lingual upper first molar LM^1, which is also diagnostic of dental calculus, but not as common, and is known from younger human archaeological specimens (Lalueza Fox; Juan and Albert 1996), but none has been found on any Plio-Pleistocene hominin dental specimens, excepting for the StW 183 specimen (Odes *pers. observation*.).

The comparison between the StW183 tooth sample and the nearest bone associated breccia sample (S63) demonstrates only that both samples have a high percentage of indetermined phytoliths (Figure 58). Comparisons between the tooth sample and breccia controls are not possible as the total tooth sample consists of only indetermined phytoliths.

Although phytoliths recovered from this tooth sample were all classified as indetermined, it evinces that plant material was preserved but unidentifiable, indicating a strong probability of dental calculus. It is not possible to tell however, whether this tooth sample was contaminated or not due to the level of indetermined phytoliths. This, in and of itself, does not negate the probability of calculus, but it cannot be said with certainty that this deposit is calculus.

3.5.5 Results from Other Breccia Control Samples

Breccia material from three different grid squares was received from Prof. Ronald Clarke, curator of Sterkfontein cave complex, and proposed as breccia controls for this project (U62; Q64; and N46). The breccia samples from grid squares Q, and N were not used in this project as the grid squares were found to be too far away from the grid squares where the tooth specimens were originally found. Based on this consideration, they were considered less relevant than the breccia control samples used (U62 6w and

U62 7w) for contamination testing, which were chosen for their proximity to the excavation grid of the tooth specimens used.

The breccia samples from the grid square U62 (6w and 7w) were the closest to the the grid squares from all the tooth specimens, and hence they was used for all the breccia controls. The phytolith results recovered from all the other proposed breccia control samples are set out below:

3.5.5.7 Grid Square Q 64 (1w)

Two phytoliths, belonging to two morphotypes were recovered from this breccia control sample:

- bulliform fan shape
- Trapezoid smooth psilate

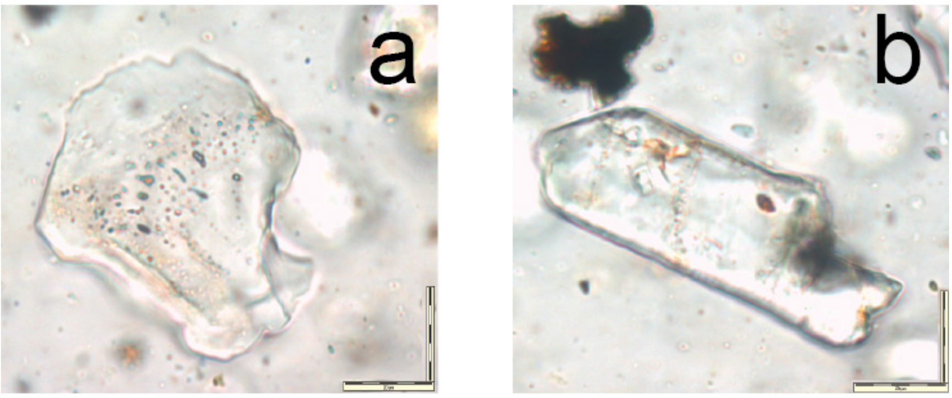

Figure 48: Phytoliths recovered from Q64 (1) a breccia control sample. a: bulliform fan shape; b: trapezoid psilate.

3.5.5.8 Grid Square Q 64 (2w)

Six phytoliths were recovered from this breccia control specimen. One indetermined phytolith and 4 morphotypes:

- Epidermal assemblage trichome
- Parallelepipedal square ends (s/e)
- Parallelepipedal psilate
- Trapezoids (2)

Monocotyledons (sedges), trees and shrubs (dicotyledons) are examples of the plants associated with the phytoliths found in this breccia control sample.

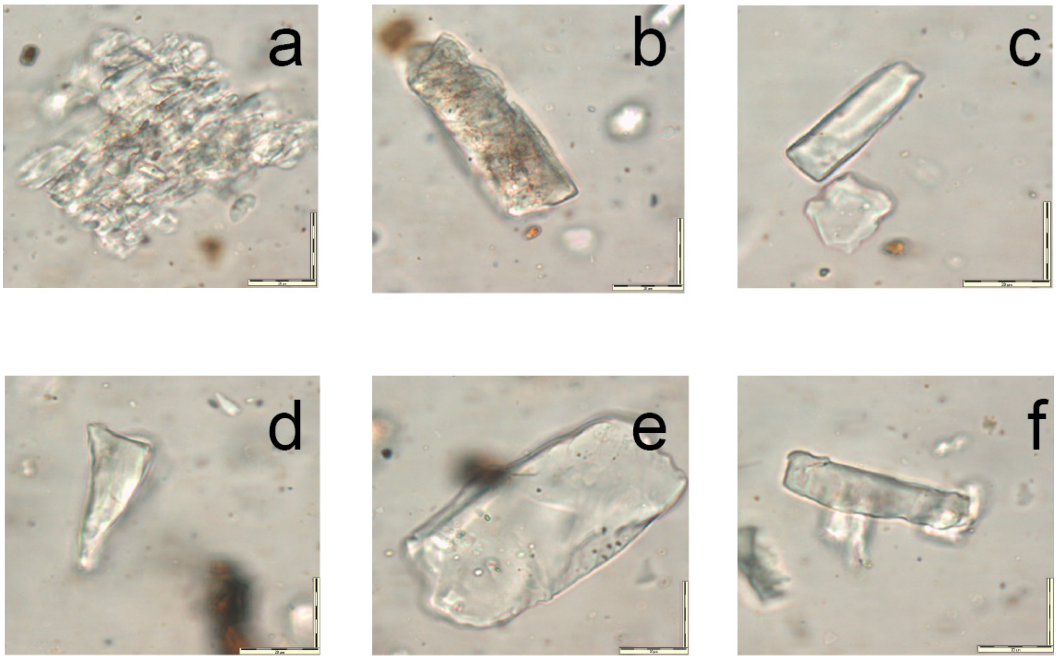

Figure 49: Phytoliths recovered from Q64 (2) breccia control sample

3.5.5.9 Grid Square Q64 (3w)

Two phytoliths were recovered from this breccia control sample and 2 morphotypes were identified:

- Epidermal assemblage trichome
- Parallelepipedal facetate

The plants associated with these phytolith types are trees, shrubs (dicots) and sedges (monocotyledons).

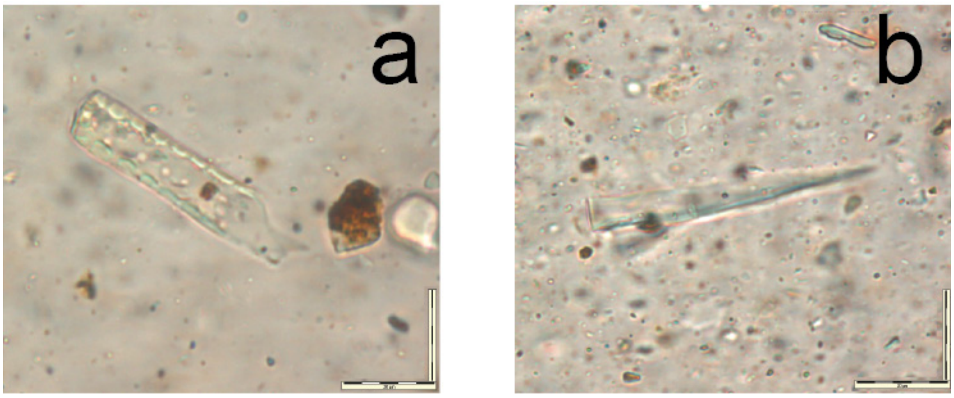

Figure 50: Phytoliths recovered from Q64 (3) breccia control sample. a: parallelepipedal facetate; b: epidermal assemblage trichome

3.5.5.10 Grid Square N 46 (4w)

Nine phytoliths were recovered from this breccia control sample. Two indetermined phytoliths and 5 morphotypes and/or plant types were identified:

- Tracheid
- Epidermal assemblage trichome
- Acicular (2) (one broken)
- Tracheary element
- Cylindroid psilate (2)

Two acicular phytoliths, one broken, were recovered from this sample. A tracheid and a tracheary element were also recovered from this breccia control. Woody dicots are possibly associated with the tracheid (Bamford, *pers.comm.*) Indetermined phytoliths accounted for 22% of the total phytoliths recovered from this sample.

Figure 51: Phytoliths recovered from N46 (4w) breccia control sample.

3.5.5.11 Grid Square N 46 (5w)

Four phytoliths were recovered from this breccia sample. No indetermined phytoliths were found and 4 morphotypes were identified:

- Strings of centric diatoms (2) (Bamford, *pers. comm.*)
- Platelet
- Cylindroid psilate

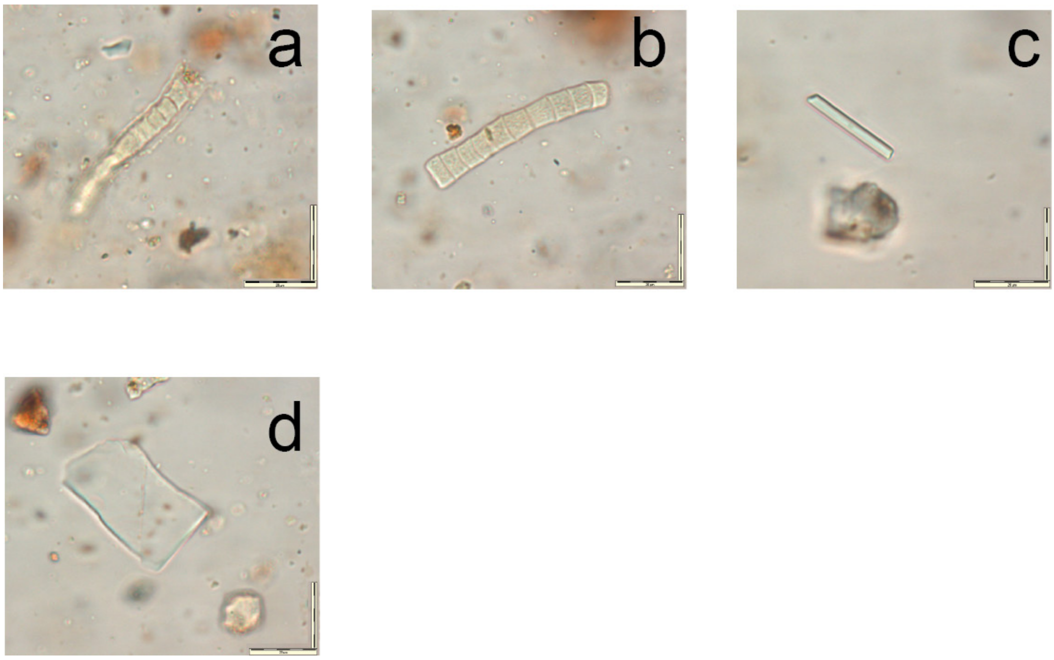

Figure 52: Phytoliths recovered from N46 (5w) breccia control sample.

Table 9: Phytolith counts for tooth, bone associated breccia and breccia control samples

Sample No	Specimen no	No of phytoliths	Indetermined	% Indet
1	Stw 53*f*	49	31	63
2	Stw 321*b*	29	26	89
3	Stw 534	12	4	31
4	Stw 532	13	3	23
5	Stw 183	4	4	100
Total phytoliths from tooth samples		**107**	**68**	**72**
6	N46 4 (w)	9	2	22
7	N46 5 (w)	4	0	0
8	Q64 (1w)	2	0	0
9	Q64 (2w)	6	1	16
10	Q64 (3w)	2	0	0
11	U62 (6w)	2	1	50
12	U62 (7w)	2	0	0
13	V50	0	0	0
14	V51	4	0	0
15	V52	0	0	0
16	S63	5	3	60
17	U52	2	0	0
18	StW53*d* (V60)	42	27	64
Total Phytoliths		**187**	**102**	

Table 10: Phytoliths recovered from tooth samples

Tooth specimens	Morphotypes	Associated Plants
StW 53f	Cylindroid psilate	Woody dicots; sedges
	Epidermal assemblage trichome	Trees, shrubs and sedges
	Indetermined (30)	
	Parallelepiped short	sedges
	Parallelepipedal elongate scabrate	Woody dicots
	Parallelepipedal scabrate Round ends	Woody dicots
	Parallelepipedal thick	Woody dicots
	Platelets (2)	Dicot leaf
	Scabrate facetate trapezoid	
	Tracheid vessel (5)	
	Trapezoid scabrate (3)	
	Weathered elongate scabrate	Woody dicots
	Woody platelet (possible)	
StW 321*b*	Indetermined (26)	
	Long cell psilate (2)	grasses
	Parallelepipedal elongate psilate	Woody dicots
StW 532	Cylindroid psilate curved	Sedges
	Cylindroid psilate	Woody dicot; sedges
	Cylindroid scabrate	
	Cylindroid parallelepipid	
	Ellipsoid psilate	Woody dicots
	Epidermal assemblage trichome	Trees; shrubs and sedges
	Indetermined (4)	
	Long cell psilate	Grasses
	Tracheid vessel	
	Tracheid	Woody dicot (possibly)?
StW 534	Cylindroid psilate curved (3)	Sedges
	Cylindroid psilate (5)	Woody dicot; sedges
	Indetermined (4)	
StW 183	Indetermined (4)	

Table 11: Phytoliths recovered from breccia samples

Breccia sample No.	Morphotypes	Associated Plants
Q64 (1)	Bulliform fan shape	Grasses
	Psilate trapezoid	Grasses
Q64 (2)	Indetermined (1)	
	Trapezoid scabrate and psilate (2)	Grasses
	Parallelepipedal psilate square ends (S/E)	Sedges
	Parallelepipedal psilate	Sedges
	Epidermal assemblage trichome	Trees; shrubs; sedges
Q64 (3)	Epidermal assemblage trichome	Trees; shrubs; sedges
	Facetate parallelepipedal	
N46 (4)	Acicular (2)	
	Epidermal assemblage trichome (1)	Trees; shrubs; sedges
	Cylindroid psilate	Woody dicot; sedges
	Tracheid	Possibly woody dicot?
	Indetermined (2)	
	Tracheary element (1)	
N46 (5)	Cylindroid psilate	Sedges; woody dicots
	Platelet	
	Diatoms (2)	
U62 (6w)	Epidermal assemblage trichome	Trees; shrubs; sedges
	Indetermined (1)	
U62 (7w)	Epidermal assemblage trichome	Trees; shrubs; sedges
	Parallelepipedal elongate psilate	Sedges
Breccia (bone associated)		
V50	No phytoliths recovered	
V51	Cylindroid elongate psilate	Sedges; woody dicots
	Parallelepipedal elongate scabrate	Woody dicots
	Parallelepipedal facetate	Dicots, sedges
	Bulliform fan shape	Monocots; grasses; sedges
V52	No phytoliths recovered	
S63	Indetermined (3)	
	Parallelepipid thick	Woody dicots
	Cylindroid scabrate	sedges

CHAPTER 4 : DISCUSSION

Based on the recent demonstration of dental calculus found on the teeth of the Malapa hominin specimen attributed to *Australopithecus sediba* (MH1), this study aimed to establish the presence of dental calculus (or tartar) on the tooth surfaces of other southern African Plio-Pleistocene hominins. This was achieved by first identifying the presence of probable calculus on teeth and then collecting the suspected calculus using an established protocol (Henry and Piperno 2008; Henry, Brooks and Piperno 2011). The author then examined and analysed phytoliths using transmitted light microscopy at 400 x magnification. This study undertook an examination of the total dental collection of the Plio-Pleistocene age hominin site of Sterkfontein, and the results of this project established the presence of dental calculus (or tartar) deposits attached to the tooth surfaces of other southern African Plio-Pleistocene early hominins, besides the Malapa specimen (MH1). This study also developed protocols that help to identify the presence of calculus, and it further demonstrated that the presence of calculus was not a phenomenon unique to the Malapa hominin site.

4.1.1 Calculus

All five of the tooth samples showed a high probability of calculus despite the inability to identify distinctive morphotypes from the StW 183 tooth material. The tooth samples preserved a varying amount of phytoliths (refer Table 9). The amounts of probable calculus recovered were extremely small. The quality of the phytoliths was generally badly preserved. A few broken and damaged phytoliths and plant types were observed. The majority of the phytoliths found within the dental calculus sample were indetermined (refer Table 9).

The inclusion of phytoliths in the dental calculus is direct evidence that these two structures existed at the same time, as the formation of calculus can only take place in the presence of saliva (MacPhee and Crowley 1975).

4.1.2 Phytoliths

A wide variety of phytolith morphotypes were recovered from the calculus samples from *Au. africanus*, which were mostly associated with dicotyledon and monocotyledon plant types, inferring that dicotyledons and monocotyledons made up a substantial part of the *Au. africanus diet*, and implied an omnivorous, adaptable diet for *Au. africanus*, despite the small sample.

Unlike *Au.sediba*, monocotyledon morphotypes were found in the *Au.africanus* calculus, which indicated a consumption of grasses and sedges. While this result confirms similar results found in Lee-Thorp and Sponheimer (2006), who argue that australopiths and *Paranthropus* consume large C_4 resources; probably sedges and grasses, this result however, partly contrasts with Grine (1981) and Grine and Kay (1988), who suggest that *Australopithecus* ate soft fruit and leaves, but make no mention of their consumption of sedges and grasses. The presence of associated plants such as woody dicots and dicot leaves, and tree and shrub associations infers that all of these plant types were probably ingested by *Au.africanus*. This work therefore confirms the findings of Ungar and Sponheimer (2011) and Henry *et al*., 2012 that *Australopithecus africanus* had a diverse and adaptable diet.

Although *Au. sediba* had a diverse diet, it avoided savanna grasses, even though they were abundant and available to them in the environment in which they lived. Their preference was concentrated however, on tree leaves, bushes, fruits, bark and wood. (Henry *et al*., 2012).

The difference between the diets of *Au. sediba* and *Au. africanus* inferred from the phytolith results of this study appears to be that *Au. africanus* from Sterkfontein had a flexible diet, and *Au. sediba* seemed to select for C_3 foods even although C_4 foods were broadly accessible on the landscape (Henry et al., 2012).

Despite the low quantity of phytoliths recovered from the tooth and the breccia samples tested, it remains to be seen whether other samples in the future deliver a similar indetermined percentage. The percentage of indetermined phytoliths for the two Malapa calculus samples (MH1) was 45% for LI^2 and 21% for LP^3. The percentages of indetermined phytoliths five samples tested in this project: StW 53(*f*) [LM^2] (63%); StW 321*b* [LM_2] (89%); StW 534 [RM_2] (31%); StW 532 [LM_3] (23%); StW 183 [LM1] (100%). Not all researchers would agree with the interpretation of indetermined phytoliths, and some might consider some not to even be phytoliths. Based on the material used in this project all been considered as phytoliths. These results from Sterkfontein and the Malapa results both indicate a very high indetermined phytolith percentage, implying that preservation of phytoliths is a problem for both cave sites, only insofar as the quality of the modern phytolith reference collection that is used.

The results further indicate that the general preservation of phytoliths from tooth calculus is lower from Sterkfontein than Malapa, however in sum the samples from both sites were badly preserved and preservational factors cannot be ruled out.

4.1.3 Taphonomic Hypotheses of Malapa and Sterkfontein

4.1.3.1 Malapa

The Malapa cave was formed in the dolomite of the late Archaean Malmani subgroup (2.64 billion-2.5 billion years ago) (McB Martin *et al*., 1998; Eriksson *et al*., 2006). The remains of two hominin individuals ascribed to *Au. sediba* recovered from Malapa (Zipfel and Berger 2010) have been dated to 1.977-1.98 million years (Pickering *et al*., 2011). These skeletal remains were recovered close to large amounts of well-preserved fauna (Dirks *et al*., 2010; Kuhn *et al*., 2011) and flora (Bamford *et al*., 2010). Some of the preservation seen in the Malapa hominin skeletal material is considered better than seen in many cases throughout the early fossil record (Berger *et al*., 2010; Carlson *et al*., 2011; Kibii *et al*., 2011; Kivell *et al*., 2011; Zipfel *et al*., 2011). Dirks *et al*., (2010) and Pickering *et al*., (2011) have posited that this well-preserved material may have deposited during a single rapid debris flow event, possibly from a high-volume inflow of water. Perhaps a storm may have carried partially articulated hominin bodies with it deeper into the cave, until they came to rest next to a body of shallow water. This event may have transpired over a few days or months. The excellent state of preservation and articulation of the hominin fossil material (Berger *et al*., 2010) implies that the remains may have been transported only for a short distance with 'laminar flow conditions' reliably associated with debris flows (Tucker 1991; Coussot and Meunier 1996). The occurrence of isopachous sparite indicates that cementation took place soon after deposition (Blatt *et al*., 2006). The swift deposition most likely caused a quick burial which produced the exceptional preservation that followed.

4.1.3.2 Sterkfontein

The Sterkfontein cave complex is a dolomite cave system in Gauteng Province, South Africa. The caves comprise a number of a series of caverns that became exposed to the environment resulting in sediment deposition during the Pliocene and Pleistocene. Although the preservation of the hominin remains has been well preserved from Member 4, the underground deposits of Sterkfontein are poorly preserved (Pickering and Kramers 2010). The cave system may have been the receptacle of debris, organic and inorganic from run-off, and flooding, or gravitation (Kuman 1994a, b; Pickering 1999). Several cave entrances may have developed and the original entrance may have become clogged up with sediment and fallen blocks from the cave roof (Partridge 1978; Brain 1981; 2004b).

The faunal elements in Member 4 point to a deposition age of between 2 and 3 million years ago (Clarke 2002). During this time a continuing infill of rocks, sediment and bones formed Member 4, as a talus cone sloping to the north reached the cave roof and to the west (Clarke 2006). Berger *et al*. (2002) however, suggests a revised date of approximately 1.5 to 2.5 Mya for Member 4.

The cave systems and their infills of South African caves are complicated (Brain 1993; Kuman and Clarke 2000). It is exacerbated by a weak understanding of the taphonomic and geochemistry of dolomitic caves and their associated fossils (Brain 1981; Backwell 2000; de Ruiter and Berger 2000). As a result of the complicated nature of dolomitic cave systems and disturbances to infills, brought about by erosion and collapsing floors, as well as lime and exposed section mining operations, only a limited indication of the stratigraphic history of the Sterfkontein infills can be provided (Clarke 2006). "Many questions remain and much research needs to be done", (Clarke 2006, pp. 117). Past research has also demonstrated that the Sterkfontein cave system was not occupied by hominids, but at times functioned as traps for australopiths and different fauna living on the landscape. Natural death traps have been recorded in Member 2 and in the Oldowan Infill deposits at Sterkfontein (Pickering, 1999; Pickering *et al*., 2004). This is a commonality between Sterkfontein and Malapa.

According to Brain's (1981) taphonomic hypothesis, the skeletons found in the Sterkfontein's Member 4 assemblage are generally not complete. Animals either went to the cave to die or they accidentally fell into a natural death trap. He further observed however, that had this been the case, and the carcasses were protected from scavenging animals in the cave, reasonably complete skeletons would have been recovered. This is not the case, and he has posited other possible reasons for state of preservation, such as carnivore involvement.

The preservational hypothesis of a single rapid debris flow event, potentially from a high volume body of water for Malapa does not appear to accord with Sterkfontein's stratigraphic history, and there is nothing in the literature which contradicts this. This may be the reason for the well preserved material from Malapa.

The low preservation of phytoliths and hence high percentage of indetermined phytoliths demonstrated in both the Malapa (Henry *et al*., 2012) and Sterkfontein samples demonstrates that despite different site formation processes, the samples from both sites resulted in poor phytolith preservation. Taphonomic effects must therefore be ruled out for both Malapa and Sterkfontein as a reason for the high indetermined phytolith count. The poor preservation of phytoliths from both sites may be attributable to other factors, including excavation techniques or curation protocols, which can reduce the presence of calculus (Lieverse 1999). Another plausible reason may be from the chewing of abrasive materials by the hominins, as it can remove or reduce calculus deposits (Gaare *et al*., 1989). As a result of the small sample sizes in the Malapa (Henry *et al*., 2012) and the Sterkfontein project, more research is needed to answer what is causing the high indetermined number of phytoliths, and why the preservation of phytoliths extracted from calculus is so poor?

4.1.4 Palaeoenvironmental Hypotheses of Sterkfontein and Malapa

4.1.4.1 Sterkfontein

A variety of flora has been suggested for Member 4 times. Open grassland and closed wooded environments has been recognised around the Blaaubank River from faunal, fossil wood, and isotopic evidence (Vrba, 1974, 1975, 1980; Reed, 1997; Luyt, 2001; Van der Merwe *et al*., 2003). Vrba uses the abundance, presence and preference of various habitats of bovid species to reconstruct the palaeoenvironment at Sterkfontein. According to Vrba (1974, 1975, 1980), in modern environments, the ratio of alcelaphines and antilopines in relation to other bovid tribes is a good indicator of open grassy plains, with the opposite also being true. Vrba thus indicated the presence of open grassland. Vrba also noted the presence of *Makapania broomi* and Hippotragines, and concluded that a wooded environment most probably existed in the cave surroundings during Member 4 times.

Reed (1997) supported this research and demonstrated that there was a high population of terrestrial animals (23%), a large portion of frugivorous animals (16%) and a small amount of arboreal animals (3%). Reed concluded open woodland mixed with thicket and bush.

These two conclusions were given a much stronger weighting with the discovery and analysis of fossil wood from this infill (Bamford 1999). The presence of a large variety of primate species and liana vines (similar to the modern species *Dichapetalum mombuttense*), *Anastrabe integerrima* and *Tricalysia* within the fossil wood sample implies a 'forest fringe' environment comparable to a modern day tropical forest of the Democratic Republic of Congo and Cameroun (Bamford 1999; Kuman and Clarke

2000). The occurrence of an extinct colobus monkey (*Cercopithecoides williamsi*) indicates the probable existence of a forest-type environment (Kuman & Clarke 2000). Partridge & Watt (1991) have suggested that a poorly calcified section of Member 4 (south west section) breccia appeared to have collapsed and displaced these deposits inferiorly by approximately 5 m. If this was the case, the importance of the fossil wood and its distribution as an inimitable marker of the Member 4 deposits, remains resolute. The work done by Avery (2001) on micromammal species accumulated by owls and other birds of prey, offers a variant palaeoenvironmental hypothesis suggesting that there were "grass with trees" alongside "the river" , "bush with grass" on the hills and "grass with trees and bushes on the open plains during Member 4 times".

Further work was done by Luyt 2001, and Luyt *et al*., 2003 on isotope analyses of fossil fauna from this infill. Luyt's reconstruction demonstrated a more closed environment, which is more aligned to Bamford's conclusion. Luyt's (2001) results showed that the woodland regions would have been heavier than originally posited by Vrba (Luyt 2001). Avery's results may be explained by owls using the open grassland regions and were returning to the cave which was located in a more forest-type environment.

4.1.4.2 Malapa environmental setting

Malapa is situated in a Grassland Biome, close to the transition to the Savanna Biome (Bamford *et al*., 2010). *Podocarpus/Afrocarpus* occurs about 30km distance in the Northern Afromontane Forest Biome and occurs in small patches in the mountain canyons. It seems likely that *Podocarpus* existed in the Pliocene and the occurrence of this vegetation at Malapa in the past implies that the cooler, moister forest vegetation was more widespread than it today (Bamford *et al*., 2010). Pollen, phytoliths and wood fragments from *Podocarpus* trees and other woody taxa recovered from a coprolite from a carnivore suggest a forest or woodland biome in the area (Bamford *et al*., 2010). The occurence of fossil grazers including *Megalotragus* and *Equus* supports the palaeoenvironmental hypothesis of plentiful amounts of grass around Malapa (Dirks *et al*., 2010). Bovid and rodent fossils from Malapa indicate isotopic composition indicating high C_4 consumption, which is common among modern rodents at the site. Therefore there appears to be a high probability that the palaeoenvironment of Sterkfontein included a wealth of grassy areas and woody flora (Henry *et al*., 2012).

4.1.5 Is the calculus phenomenon unique to Malapa?

The question posed by Berger (*pers.comm*) whether the recovery of dental calculus on hominin specimens from Malapa was a unique phenomenon was answered through this project. The recovery of phytoliths extracted from tooth material samples from Sterkfontein specimens StW 321*b*, StW 534, and StW 532, that were not contaminated, indicates a strong probability that this extracted material is dental calculus, as the mineralisation of dental plaque can only occur in the presence of saliva (McPhee and Cowley 1975), and there is a lack of *post-mortem* remodelling and contamination (Lalueza Fox *et al*., 1996). In addition, phytoliths recovered from the dental calculus matrix thus demonstrates evidence of these two structures existing at the same time. Based on this finding, the dental calculus phenomenon recovered from the Malapa cave site, cannot be considered unique.

4.1.6 Suggested New Protocols

Previous studies have indicated that the process for assessing the presence of dental calculus is a simple one, as long as the teeth are well preserved, identified acceptably to taxon, and have not been well cleaned by preparatory staff, so that all the calculus has been dispensed with (Henry 2011). The rarity of calculus on palaeoanthropological tooth specimens therefore, may be either ascribed either to the preservation of specific environments, and/or the inappropriate preparation or handling of fossil material or a process of abrasion with the dentition by hominins themselves Gaare *et al*., 1989).

The preparation and cleaning of tooth fossils it seems can be a relatively controllable function (Odes, *pers. observation*). New protocols however, are needed to obviate and control overzealous cleaning by preparatory staff of calculus from tooth material (Henry 2011). It is necessary to also to amend existing protocols used by research scientists when handling dental specimens, so as not to diminish calculus on enamel surfaces by inadvertently damaging and/or removing of calculus with measuring instruments coming into contact with the enamel deposit, in the relentless determination for exact measurements.

During this study several observations were made that may assist researchers to identify and evaluate calculus, and prevent destruction to dental calculus in the future:

1. The level of textural coarseness, for instance (1) low, (2) moderate and (3) high, needs to be scored (Odes, *pers. observation*). Thick and coarse adherent

material is diagnostic, but thin low coarse material can also be diagnostic of dental calculus. The adherent material extracted from StW 532 for instance, was not coarse or very thick. It is easy to miss very fine calculus, and mistake it for staining, when in fact it is extremely fine calculus and can only be properly seen under some magnification, for instance some sub-gingival and supra-gingival calculus can be extemely fine (Roberts-Harry and Clerehugh 2000). In this study however, examination of some specimens showed supra-gingival hominin calculus to be very fine (Odes *pers. observation*).

2. Mesially located dental calculus appears to be rare in hominin dental material, as none was found in this study.

3. Scoring of lingual supra-gingival calculus may be evaluated on a similar basis to buccal calculus [evaluation of lingual calculus is not described by Dobney and Brothwell (1987), or the Brothwell (1981) scoring method (Odes, *pers. observation*)]. This study has observed that the prevalence of upper or lower molar lingual supra-gingival calculus is low in hominin palaeodental specimens. The distribution of upper molar buccal calculus and lower incisor lingual calculus has been broadly accepted as being the most prevalent location for calculus (Parfitt 1959).
4. This study has observed that dental calculus in hominin specimens is not film-like, unlike some bovidae calculus. Although hominin dental calculus may be extremely thinly distributed and strongly attached the enamel surface (refer StW

532), it is typically accompanied by some textural coarseness (Odes, *pers. observation*).

5. Although different categories of calculus have distinguishing colour ranges for hominins, colour itself was found to be a weak determinant of dental calculus identification on its own, and must be evaluated jointly with textural factors (Odes *pers. observation*). The colour coding of calculus may have a benefit when identifying the genus of a tooth fragment. The colour of calculus may become a significant diagnostic tool in the absence of any other identifying factor.

6. Hillson (1996) observed brownish hues on archaeological specimens. The majority of the calculus observed in the hominin sampled tooth material in this project, is characterised by light and dark brown colouring, which shows a similarity with Hillson's (1996) findings, but is in contrast to supra-gingival calculus of modern human calculus colouring, which ranges from yellow to white (Roberts-Harry and Clerehigh 2000).
7. This study has observed a need for a fully comprehensive and centrally accessible South African phytolith comparative collection to evaluate phytolith specimens.
8. Evaluation of fossil teeth should be carried out first by researchers, and thereafter preparatory guidelines should be issued to technical staff before the cleaning of fossil hominin teeth begins. Micro-CT scanning may be able to provide an alternative 'window' into assessing fossil surface morphology not only for calculus specifically, but also for other adherent material, prior to

preparatory staff working on fossils with air-drills (Berger *pers. comm*.). There is no guarantee presently however, that air drills are not inadvertently removing calculus while the preparation of fossil teeth takes place (Odes, *pers. observation*). It is currently impossible with the present method of surface removal to effectively ascertain what sits on the surface of the enamel, and what is attached to the adjoining breccia material in all cases, prior to air drilling. Perhaps Micro-CT scanning would alleviate this problem considerably (Odes, *pers. observation*). It is also probable that other investigations of dentition are in fact inadvertently removing dental calculus. These studies may include studies of Microwear and other such work where taking peels of the surface of the teeth are deemed necessary. It is also possible that such classical intervention such as casting may be damaging such evidence.

As an important footnote in the study of the Sterkfontein hominins in particular, it is possible that since these fossils have been extensively handled and studied, perhaps more so than any other southern African assemblage of early hominin remains, that the actual percentages of calculus presented in the present dissertation are in fact underestimates of the original presence of calculus due to its inadvertent removal. Future specimens recovered from the site should give us a better idea of the actual percentage of the dental calculus on the Sterkfontein sample.

CHAPTER 5 CONCLUSIONS

The establishment and recovery of phytoliths from dental calculus of Plio-Pleistocene aged hominins from Sterkfontein have provided a means for researchers of palaeontological remains to reconstruct palaoediets as well as adding additional information about the past environments in which these hominins lived. . The presence of dental calculus and associated microfossils in the form of phytoliths, will assist future studies, by giving them the advantage of obtaining direct evidence of food consumed, which can be directly associated with individual hominins' feeding behaviours. This could result in significant clues to the diet and ecology of not only individual hominins but populations, species and comparisons of diet and behaviour between species and genera. The recovery of phytoliths from calculus potentially offers the advantage of direct evidence to researchers when reconstructing and interpreting the vegetation of Plio-Pleistocene palaeoenvironments in order to piece together the greater palaeoecology of hominin and other fossil environments as well as lead to a more direct understanding of those species interaction with this environment.

Much work is needed in the area of phytolith recovery from dental calculus, as very little research has been done in this area. There is, however also a need for detailed studies of diet of extant primates and how this diet is reflected in their dental calculus. Such studies would allow a greater utilisation of data such as is presented in this dissertation. The results presented here additionally identified a need for new protocols to be developed for the identification and preparation of dentition for the purpose of calculus sampling. The protocols laid out in the discussion may be applied to future studies.

REFERENCES:

Acuna-Mesen, R. & E. Garcia-Diaz. 1998. New Cuvieronius hyodon (Proboscidea: Gomphotheriidae) from the Pleistocene of Costa Rica. *Revista de Biologia Tropical*. **46**: 1167-1172.

Altmann, S., & Altmann, J. 1970. *Baboon ecology*. Chicago: University of Chicago Press.

Ardrey, R. 1976. *The hunting hypothesis*. New York: Atheneum.

Ardrey, R. 1961. *African genesis*. New York: Atheneum.

Armitage, P.L. 1975. The extraction and identification of opal phytoliths from the teeth of ungulates. *Journal of Archaeological Science*. **2**, 187-197.

Avery, D.M., 2001. The Plio-Pleistocene vegetation and climate of Sterkfontein and Swartkrans, South Africa, based on micromammals. *Journal of Human Evolution*. **41**, 113–132.

Baer, P.N., & White, C.L. 1966. Studies on experimental calculus formation in the rat. IX. Relation to diet and selected salivary constituents. *Journal of Periodontology*. **37**, 113.

Backwell L.R. 2000. *A Critical Assessment of southern African Early Hominid Bone Tools.* M.Sc. thesis. University of the Witwatersrand, Johannesburg.

Baker G, Jones L.H.P., & Wardrop I.D. 1959. Cause of wear in sheep's teeth. *Nature* **184**, 1583-1584.

Bamford M.K., Neumann F.H., Pereira L.M., Scott L., Dirks P.H., & Berger L.R. 2010. Botanical remains from a coprolite from the Pleistocene hominin site of Malapa, Sterkfontein Valley, South Africa. *Palaeontologia Africana*, **45**: 23 - 28.

Bamford, M. 1999. Pliocene woods from an early hominid cave deposit, Sterkfontein, South Africa. *South African Journal of Science*. **95**, 231–237.

Baysal, A., Wright, K., Members of the Çatalhőyűk Teams, 2006. Cooking, crafts and curation: ground-stone artefacts from Çatalhőyűk. In: Hodder, I. (Ed.), Changing *Materialities at Çatalhőyűk: Reports from the 1995–1999 Seasons. Excavations at Çatalhőyűk, vol. 5, Monographs of the McDonald Institute for Archaeological Research*, University of Cambridge, British Institute for Archaeology at Ankara, Cambridge and London, pp. 307–324.

Bell, R. H. V. 1971 A Grazing Ecosystem in the Serengeti. *Scientific American.* **225** (1):84-93.

Berger L.R., Lacruz R.S., de Ruiter D.J. 2002. Revised age estimates of *Australopithecus*-bearing deposits at Sterkfontein, South Africa. *American Journal of Physical Anthropology.* **119**: 192-197.

Berger L.R., de Ruiter, D.J., Churchill, S.E., Schmid, P, Carlson, K.J, Dirks, P.H.G.M Kibii, J.M. 2010. *Australopithecus sediba*: A new species of *Homo*-like australopith from South Africa. *Science*. **328**, 195-204.

Bernimoulin, J.P. *2003*. Recent concepts in plaque formation. *Journal of Clinical Periodontology*. **30** (5), 7-9.

Blatt H. *et al*., 2006. *Petrology: Igneous, Sedimentary and Metamorphic* (Freeman, New York, ed. 3).

Boaz, Noel T. 1977 Paleoecology of Early Hominidae in Africa. *Kroeber Anthropological Society Papers.* **50**, 36-62.

Bondi, A. 1958. *"Plant proteins," in Processed plant proteinfoodstuffs.* Edited by Aaron M. Altschul, pp. 43-66. New York: Academic Press.

Boyadjian, C.H.C., Eggers, S., Reinhard, K., 2007. Dental wash: a problematic method for extracting microfossils from teeth. *Journal of Archaeological Science.* **34**, 1622-1628.

Brain, C.K. 2004b. *A taphonomic overview of the Swartkrans fossil assemblages. In: Brain, C.K. (Ed.), Swartkrans: A Cave's Chronicle of Early Man*. Transvaal Museum Monograph, second ed., vol. 8, pp. 257–264. Pretoria.

Brain, C.K. 1993. *Swartkrans, a Cave's Chronicle of Early Man*. Pretoria: Transvaal Museum Monograph, No. 8.

Brain, C.K. 1981. *The Hunters or the Hunted?* University of Chicago Press, Chicago.

Brothwell, D.R. 1981. *Digging up Bones*. New York: Cornell University Press, 159–160.

Buikstra, J.E. and Ubelaker, D.H. 1994 *Standards for Data Collection from Human Skeletal Remains*: *Proceedings of a Seminar at the Field Museum of Natural History*, *Organized by Jonathan Haas*. Fayetteville: Arkansas Archaeological Survey, 56.

Carlson K.J., Stout D., Jashashvili T., de Ruiter D.J., Tafferou P. & Berger L.R. 2011. The Endocast of MH1, *Australopithecus sediba*. *Science*. **333**, 1402-1407.

Cerling, T.E., Mbua, E., Kirera F.M., Manthi,K.M., Grine, F.E. Meave G. Leakey, M.G. Sponheimer, M. & Uno K.T. 2011. Diet of *Paranthropus boisei* in the early Pleistocene of east Africa. *Proceedings of the National Academy of Sciences of the U.S.A*. 9337-9341.

Ciochon, R.L., Piperno, D., Thompson, R., 1990. Opal phytoliths found on the teeth of the extinct ape *Gigantopithecus blacki:* implications for paleodietary studies. *Proceedings of the National Academy of Sciences of the United States of America*. **87**, 8120-8124.

Clarke, R.J. 2002. Newly revealed information on the Sterkfontein Member 2 *Australopithecus* skeleton. *South African Journal of Science* **98**, 523-526

Clarke, R.J. 2006. A deeper understanding of the stratigraphy of Sterkfontein fossil hominid site, *Transactions of the Royal Society of South Africa*. **61**, 2, 111-120

Clarke, R. J. 1995. Mr, Mrs and Miss: conceptions in studies of human ancestry. In: *Hominids and Their Environment during the Lower and Middle Pleistocene of Eurasia: Proceedings of the International Conference of Human Palaeontology, Orce, Spain.* (J. Gibert, Ed.) pp. 327–329.

Clark, J. D. 1975. "A comparison of the Late Acheulian industries of Africa and the Middle East," In: *After the australopithecines*. Eds. by K. W. Butzer and G. Ll. Isaac, pp. 605-60. The Hague: Mouton.

Conklin-Brittain, N.L., Wrangham, R.W., Smith, C.C. 2002. A two-stage model of increased dietary quality in early hominid evolution: the role of fiber. In: Unger, P.S., Teaford, M.F. (Eds.), Human Diet: its Origin and Evolution. Bergin and Garvey, Westport, pp. 61–76.

Copeland, S. R. 2009. Potential hominin plant foods in northern Tanzania: semi-arid savannas versus savannah chimpanzee sites. *Journal of Human Evolution*. **57**, 365-378.

Corbett, T.L., & Dawes C. 1998. A comparison of the site-specificity of supragingival and subgingival calculus deposition. *Journal o*f *Periodontology.* **69**, 1-8.

Cortella, A.R., & Pochettino, M.L. 1994. Starch grain analysis as a microscopic diagnostic feature in the identification of plant material. *Economic Botany*, **48**, 171–181.

Coursey, D.G. 1973. Hominid evolution and hypogeous plant foods. *Man* **8**, 634-635.

Coussot, P., Meunier, M. *Earth Science Review*. 1996. **40**, 209.

Cummings, L.S., Magennis, A. 1997. A phytolith and starch record of food and grit in Mayan human tooth tartar. In: Pinilla, A., Juan-Tresserras, J., Machado, M.J. (Eds.), *Estado Actual de los Estudios de Fitolitos en Suelos y Plantas: The State of- the-Art of Phytoliths in Soils and Plants*, Monografı´as del Centro de Ciencias Medioambientales, CSIC, **4**, Madrid, pp. 211–218.

Damen J.J.M., & ten Cate J.M. Calcium phosphate precipitation is promoted by silicon. In: ten Cate J.M. (ed): *Recent advances in the study of dental calculus.* Oxford, England: IRL Press, 1989: 105-114.

Dart, R.A. 1953. The predatory transition from ape to man. *International Anthropological and Linguistic Review* **1**:201-18.

Dawes, C. 1970. Effects of diet on salivary secretion and composition. *Journal of Dental Research*. **49**, 1263–1272.

de Ruiter, D. J. and Berger, L. R., 2000. Leopards as taphonomic agents in dolomitic caves-implications for bone accumulations in the hominid-bearing deposits of South Africa. *Journal of Archaeological Science.* **27**: 665–684.

Dirks Paul, H. G. M., Kibii, J.M., Kuhn, B.F., Steininger, C., Churchill, S.E., Kramers, J.D., Pickering, R., Farber, D.L. Mériaux, A-S., Herries, A. I. R., King, G.C.P., & Berger, L.R. 2010. Geological setting and age of *Australopithecus sediba* from southern Africa. *Science*. **328**, 205-208.

Dobney, K., and Brothwell D. 1987. A method for evaluating the amount of dental calculus on teeth from archaeological sites. *Journal of Archaeological Science.* **14**, 343-35.

Donald J.W. 1997. Dental calculus: recent insight into occurrence, formation, prevention, removal and oral health effects of supragingival and subgingival deposits. *European Journal of Oral Science* **105**, 508-522.

Driessens, F. C. M. & Verbeeck, R. M. H. 1989. Possible pathways of mineralisation of dental plaque. In: ten Cate, J.M. (ed). *Recent Advances in the Study of Dental Calculus*. pp. 7-17. Oxford: IRL Press at Oxford University Press.

Dunbar, R. I. M. 1976.Australopithecine diet based on a baboon analogy. *Journal of Human Evolution*. **5**, 161-167.

Eriksson *et al*. 2006. In: *The Geology of South Africa*, M. R. Johnson, C. R. Anhaeusser, R. J. Thomas, Eds. (Geological Society of South Africa, Johannesburg), pp. 237–260.

Feibel CS. 1997. Debating the environmental factors in hominid evolution. *GSA Today* **7**: 1–7.

Fleagle JG. 1999. *Primate adaptation and evolution*. 2nd ed. New York: Academic Press.

Forsberg, A., Lagergren, C., & Lönnerblad, T. 1960. Dental calculus: A biophysical study. *Oral Surgery*. **13**, 1051.

Friskopp, J. and Hammarstrom, L. 1980. A comparative, scanning electron microscope study of supragingival and subgingival calculus. *Journal of Periodontology.* **51**, 553-562.

Friskopp, J. and Isacsson, G. 1983. A quantitative microradiographic study of mineral content of supragingival and subgingival dental calculus. *Scandinavian Journal of Dental Research*. 1984. **92**, 25-32.

Friskopp, J. 1983 Ultrastructure of nondecalcified supragingival and subgingival calculus. *Journal of Periodontology*. **54**, 542 – 550.

Gaare, D., Rølla, G. and van der Ouderaa, F. (1989). Comparison of the rate of formation of supragingival calculus in an Asian and European population. In: *Recent Advances in the Study of Dental Calculus* (ed.) by J.M. ten Cate). Oxford: IRL Press, 115–122.

Gobetz, K. & Bozarth, S.R. 2001.Implications for late Pleistocene mastodon diet from opal phytoliths in tooth calculus. *Quaternary Research.* **55**, 115-122.

Goodall J. 1986. *The Chimpanzees of Gombe*. Cambridge University Press: Cambridge.

Gordon, K.D., 1988. A review of methodology and quantification in dental microwear analysis. *Scanning Microscopy.* **2**, 1139-1147.

Green, J.C., and Vermillon, J.R. 1960. The oral hygiene index: a method for classifying oral hygiene status. *Journal of the American Dental Association*. **61**, 171.

Gressly, F. 1963. Experimental calculus formation. *Journal of the American Society of Periodontists*. **1**, 53 – 62.

Grine, F.E., 1981. Trophic differences between 'gracile' and 'robust' australopithecines: a scanning electron microcope analysis of occlusal events. *South African Journal of Science*. **77**, 203-230.

Grine F.E. 1986. Dental evidence for dietary differences in *Australopithecus* and *Paranthropus*. *Journal of Human Evolution* **15**, 783–822.

Grine F.E., Kay, R.F. 1988. Early hominid diets from quantitative image analysis of dental microwear. *Nature* **333**, 765–768.

Gaulin, S.J. C. 1979. A jarman bell model of primate feeding niches. *Human Ecology*. **7**, 1-20.

Gaulin, S.J., Konner, C., & M. 1977. On the Natural Diet of Primates, Including Humans. In: *nutrition and the brain, vol. 1: determinants of the availability of nutrients to the brain*. R.J. Wurtman and J.J. Wurtman, eds. pp. 1-86. New York: Raven.

Gregory, W. K. (1922). *The Origin and Evolution of the Human Dentition*. Williams and Wilkins, Baltimore.

Grine F.E., Kay R.F. 1988. Early Hominid Diets from Quantitative Image Analysis of Dental Microwear. *Nature.* **333**: 765–768.

Gron P, Van Campen GJ, Lindstrom I. 1967. Human dental calculus, inorganic chemical crystallographic composition. *Archives of Oral Biology* **12** (7): 829–37.

Gügel, I.L., Grupe G., & Kunzelmann, K.H. 2001. Simulation of dental microwear: Characteristic traces by opal phytoliths give clues to ancient human dietary behavior. *American Journal of Physical Anthropology*. **114**, 124-138.

Harding RSO. 1976. Ranging patterns of a troop of baboons (*Papio anubis*) in Kenya. *Folia Primatologia.* **25**, 143.

Hardy, K., Blakeney, T., Copeland, L., Kirkham, J., Wrangham, R., Collins, M. 2009. Starch granules, dental calculus and new perspectives on ancient diet. *Journal of Archaeological Science*. **36**, 248-255.

Hardy, K., Sillitoe, P., 2003. *Material perspectives: stone tool use and material culture among the Wola*, PNG. Internet Archaeology 14. Available from: http:// intarch.ac.uk/journal/issue14/hardy_index.html.

Hatley, T., Kappelman, J., 1980. Bears, pigs, and Plio- Pleistocene hominids: a case for the exploitation of below-ground food resources. *Human Ecology* **8**, 371-387.

Henderson, J. 1987. Factors determining the state of preservation of human remains. In: *Death*, *Decay and Reconstruction*: *Approaches to Archaeology and Forensic Science* (eds.) by A. Boddington, A.N. Garland, and R.C. Janaway). Manchester: Manchester University Press, 43–54

Henry, A.G., Piperno D.R. 2008. Using plant microfossils from dental calculus to recover human diet: a case study from Tell al-Rāqa'i, Syria. *Journal of Archaeological Science*. 1-8.

Henry, A.G., Brooks A.S, & Piperno D.R. 2010. Microfossils in calculus demonstrate consumption of plants and cooked foods in Neanderthal diets (Shanidar III, Iraq; Spy I and II, Belgium). *Proceedings of the National Academy of Sciences of the United States of America.* **108**, 486-491.

Henry, A.G., 2011. Recovering dietary information from extant and extinct primates using plant Microremains. *International Journal of Primatology*. DOI 10.1007/s10764-011-9556-1.

Henry, A.G., Ungar, P.S., Passey, B.H., Matt Sponheimer, M., Rossouw, L., Bamford, M., Sandberg, P., de Ruiter D.J. & Berger, L.R. 2012. *The diet of Australopithecus sediba*. *Nature* DOI: 10.1038/nature11185

Hershkovitz, I., Kelly, J., Latimer, B., Rothschild, B.M., Simpson, S., Polak, J., Rosenberg, M. 1997. *Journal of Human Evolution*. **33**, 507-512.

Hillson, S.W. 1979. Diet and dental disease. *World Archaeology*. **2**, 147-162.

Hillson, S.W. 1986. *Teeth*. Cambridge: Cambridge University Press, 300-303.

Hillson, S.W. 1996. *Dental Anthropology*. Cambridge: Cambridge University Press, Hodge, H.C. and Leung, S.W. 1950. Calculus formation. *Journal of Periodontology*. **21**, 211 – 221.

Hodson, M. J. & Evans, D.E. 1995. Aluminium/silicon interactions in higher plants. *Journal of Experimental Botany*. **46**, 161- 171.

Hughes, A. R. & Tobias, P. V. 1977. A fossil skull probably of the genus *Homo* from Sterkfontein, Transvaal. *Nature.* **265,** 310.

Iriarte, J., Holst, I., Marozzi, O., Listopad, C., Alonso, E., Rinderknecht, A., Montana, J., 2004. Evidence for cultivar adoption and emerging complexity during the Mid-Holocene in the La Plata Basin. *Nature.* **432**, 614–617.

Isaac, G. LI. 1976. The activities of early African hominids. In: Isaac, G. LI., and McCown, E. R. (eds.), *Human Origins. Louis Leakey and the East African Evidence*, W. A. Benjamin, Menlo Park, Calif., pp. 483-514.

Isaac, G. LI., and D. C. Crader 1981 To What Extent Were Early Hominids Carnivorous? An Archaeological Perspective. In Omnivorous Primates: *Gathering and Hunting in Human Evolution*. R. S. O. Harding and G. Teleki, eds. pp. 37-103. New York: Columbia University

Jin, Y., Yip, H., 2002. Supragingival calculus: formation and control. *Critical Reviews in Oral Biology and Medicine.* **13**, 426-441.

Jolly C.J. 1970. The seed-eaters: a new model of hominid differentiation based on a baboon Analogy. *Man.* **5**, 5-26.

Juan-Tresserras, J., Lalueza, C, Albert, R.M., Calvo, M., 1997. *Identification of phytoliths from prehistoric human dental remains from the Iberian Peninsula and the Balearic Islands. In: Pinilla, A., Juan-Tresserras, J., Machado, M.J. (Eds.), Primer encuentro Europeo sobre el estudio de fitolitos.* Gráficas Fersán, Madrid, pp. 197-203.

Kakehashi, S., Baer, P.N. and White, C. 1962. Studies on experimental calculus formation in the rat. II. Effect of calcium, phosphate, bicarbonate. *Journal of Periodontology.* **33**, 186

Kakehashi, S., Baer, P.N. and White, C., & Gluck, G. 1963. Studies on experimental calculus formation in the rat. VI. Effect of diet intubation, meal feeding and nibbling. *Journal of Periodontology.* **34**, 513.

Kay, R. F. (1985) *Annual Review of Anthropology.* **14,** 315–341.

Kay, R.F. 1981. The nut-crackers: A new theory of the adaptations of the Ramapithecinae. *American Journal of Physical Anthropology.* **55**, 141-151.

Kay R.F. 1977. The evolution of molar occlusion in the Cercopithecidae and early Catarrhines. *American Journal of Physical Anthropology*. **46**, 327–352.

Kay, R. F. 1975. Allometry and early hominids. *Science.* **189**, 63.

Kibii J.M., Churchill S.E., Schmid P., Carlson K.J., Reed N.D. de Ruiter D.J. & Berger L.R. 2011. A new partial pelvis of *Australopithecus sediba*. *Science,* **333**, 1407- 1411.

Kido J., Kasahara C., Ohishi K., Nishikawa S., Ishida H., Yamashita K., Kitamura S., Kohri K., Nagata T., Identification of osteopontin in human dental calculus matrix. *Arch Oral Biol* 1995: **40**, 967-972.

Kivell T.L., Kibii J., Churchill S.E., Schmid P. & Berger L.R. 2011. Australopithecus sediba hand demonstrates mosaic evolution of locomotor and manipulative abilities. *Science*. **333**, 1411-1417.

Klepinger, L.L., Kuhn, J.K. and Thomas, J. Jr. (1977) Prehistoric dental calculus gives evidence for coca use in early coastal Ecuador. *Nature*. **269**, 506 – 507.

Koparal, E. and Tütüncu, R.2000. Investigation of plaque formation by scanning electron microscopy. *Turkish Journal of Medical Science*. **30**, 119-124.

Kuhn B.F., Werdelin L., Hartstone-Rose A., Lacruz R.S. & Berger L.R. 2011. Fossil Carnivoran remains from the Malapa hominin site, South Africa. *Plos One*. **6**, 26940.

Kuman, K., & Clarke, R.J., 2000. Stratigraphy, artifact industries and hominid associations for Sterkfontein, Member 5. *Journal of Human Evolution*. **38**, 827–847.

Kuman, K. 1994*a*. The archaeology of Sterkfontein:preliminary findings on site formation and cultural change. *South African Journal of Science.* **90,** 215–219.

Kuman, K. (1994*b*). The archaeology of Sterkfontein-past and present. *Journal of Human Evolution.* **27,** 471–495.

Kurland, J.A. and Beckerman S.J. 1985. Optimal foraging and hominid evolution: Labour and reciprocity. *American Anthropologist*, New Series. Vol 87, 1, pp 73-93.

Lalueza Fox, C, Juan, J., Albert, R.M., 1996. Phytolith analysis on dental calculus, enamel surface, and burial soil: information about diet and paleoenvironment. *American Journal of Physical Anthropology*. **101**, 101-113.

Lalueza Fox, C and Pérez-Pérez, A. 1994. Dietary information through the examination of plant phytoliths on the enamel surface of human dentition. *Journal of Archaeological Science.* **21**, 29-34.

Lalueza C., Pérez-Pérez A., & Turbón, D. 1996. Dietary inferences through buccal microwear analysis of middle and upper Pleistocene human fossils. *American Journal of Physical Anthropology*. **100**, 367–387.

Lamb, M. W., & Harden, M.L. 1973. *The meaning of human nutrition*. New York: Pergamon Press

Lambert, J. E., Chapman, C. A., Wrangham, R. W. & Conklin-Brittain, N. L. Hardness. 2004. Of cercopithecine foods: implications for the critical function of enamel thickness in exploiting fallback foods. *American Journal of Physical Anthropology*. **125**, 363–368.

Laughlin, W.S. 1968. "Hunting: An integrating biobehavior system and its evolutionary importance," In: *Man the hunter*. (eds.) by R. B. Lee and I. DeVore, pp. 204-320. Chicago: Aldine.

Lebenthal E. 1987. Role of salivary amylase in gastric and intestinal digestion of starch. *Digestive Diseases & Sciences.* 32:1155–7. [PubMed: 2443325]

Lee, R. B. 1968. "What hunters do for a living, or How to make out on scarce resources," In: *Man the hunter*, (eds.) by R. B. Lee and I. DeVore, pp. 30-48. Chicago: Aldine.

Lee-Thorp, J., & Sponheimer, M. 2006. Contributions biogeochemistry to understanding hominin dietary ecology. *Yearbook of Physical Anthropology*. **49**, 131-148.

Lee-Thorp JA, Sponheimer M, van der Merwe NJ. 2003. What do stable isotopes tell us about hominin diets? *International Journal of Osteoarchaeology*. **13**, 104–113.

Lee-Thorp, J., Thackeray, F. & van der Merwe, N. J. 2000. The hunters and the hunted revisited. *Journal of Human Evolution*. **39**, 565–576.

Lee-Thorp J.A., van der Merwe N.J., Brain C.K. 1994. Diet of *Australopithecus robustus* at Swartkrans from stable carbon isotopic analysis. *Journal of Human Evolution*. **27**, 361–372.

Leopold, A. C., and R. Audrey 1972 Toxic Substances in Plants and Food Habits of Early Man. *Science*. **176**, 512-514.

Li, M.Q., Yang, X.Y., Wang, H., Wang, Q., Ji'a, X., & Ge, Q.S. 2010. Starch grains from dental calculus reveal ancient plant foodstuffs at Chenqimogou site, Gansu Province. *Science China Earth Sciences*. **53**, 694–699.

Lieverse, A.R., 1999. Diet and the aetiology of dental calculus. *International Journal of Osteoarchaeology.* **9**, 219-232.

Lindhe J. 1990. *Textbook of clinical periodontology, 2*. Munksgaard,

Linton, S., 1971. Woman the gatherer: male bias in anthropology. In: Jacobs, S.E. (ed.), *Woman in Cross-Cultural Perspective: A Preliminary Sourcebook*. University of Ilinois Press, Urbana, pp. 9-21.

Lucas, P. W. & Peters, C. R. (2000) in *Development, Function and Evolution of Teeth*, eds. Teaford, M. F., Smith, M. M. & Ferguson, M. W. J. (Cambridge Univ. Press, Cambridge, U.K.), pp. 282–289.

Lukacs, J.R. 1989. *Dental paleopathology: methods for constructing dietary patterns. In: Reconstruction of life from the Skeleton* (edited by M.Y. Iscan and K.A. Kennedy). New York: Alan R. Liss., 261-286.

Lundberg, G., Soremark, R. and Thilander, H. 1966. Analysis of some elements in supra- and subgingival calculus. *Journal of Periodontal Research*, **1**, 245-249.

Luyt, C.J., 2001. *Revisiting Palaeoenvironments of the Hominid-Bearing Plio-Pleistocene Sites: New Isotopic Evidence from Sterkfontein. Masters Dissertation, University of Cape Town*.

Luyt, C. J., and J. A. Lee-Thorp. 2003. Carbon isotope ratios of Sterkfontein fossils indicate a marked shift to open environments c. 1.7 Myr ago. *South African Journal of Science* 99, 271- 273.

Mann, A. E. 1981 Diet and Human Evolution. In: *Omnivorous Primates: Gathering and Hunting in Human Evolution.* R. S. O. Harding and G. Teleki, eds. pp. 10-36. New York: Columbia University.

MacPhee, T., and Cowley, G. 1975. *Essentials of Periodontology and Periodontics*. Second edition. Oxford: Blackwell Scientific Publications.

Mandel, I.D. 1990. Calculus formation and prevention: an overview. *Compendium for Continuing Education in Dentistry*, *Supplemental*, **8**, 235-241.

Mandel, I.D. *Contemporary periodontics*, Mosby: Genco, Goldman and Walter Cohen, 1990. p. 135-46, chap. 10.

Mandel, L.D., Levy, B.M., & Wasserman, B.H. 1957. Histochemistry of calculus formation. *Journal of Periodontology* **28**, 132-137.

Massey, F.P., & Hartley, S.E. 2006. Experimental demonstration of the antiherbivore effects of silica in grasses: Impacts on foliage digestibility and vole growth rates. *Proceedings of the Royal Society B: Biological Sciences*. **273**, 2299–2304.

McB. Martin, D., Clendennin, C.W., Krapez, B. & McNaughton, N.J. 1998. *Journal of the Geological Society*. London. **155**, 311.

McHenry, H. M. 1984. *American Journal of Physical Anthropology.* **64,** 297–306.

Mercader, J., Barton, H., Gillespie, J., Harris, J., Kuhn, S. L., Tyler, R., & Boesch, C. 2007. 4,300-Year old chimpanzee sites and the origins of percussive stone technology. *Proceedings of the National Academy of Sciences of the USA*. **104**, 3043–3048.

Middleton, W. 1990. An improved method for extraction of opal phytoliths from tartar residues on herbivore teeth . *Phytolitharian Newsletter.* **6** (3), 2-5.

Middleton, W., and Rovner, I. 1994. Extraction of opal phytoliths from herbivore dental calculus. *Journal of Archaeological Science*. **21**, 469-473

Milton K. 2002. Hunter–gatherer diets: Wild foods signal relief from diseases of affluence. In: Ungar PS, Teaford MF, editors. *Human diet: Its origin and evolution*. Westport: Bergin and Garvey. p 111–122.

Milton, K. 1981. Distribution patterns of tropical food plants as an evolutionary stimulus to primate mental development. *American Anthropologist.* **83**, 534-48.

Moore, J., 1996. Savanna chimpanzees, referential models and the last common ancestor. In: McGrew, W.C., Marchant, L., Nishida, T. (Eds.), *Great Ape Societies*. Cambridge University Press, Cambridge, pp. 275–292.

Moorer, W.R., ten Cate, J.M., and Buijs, J.F.1993. Calcification of cariogenic Streptococcis and of Carynebacterium (*Bacterionema matruchotii*). *Journal of Dental Research.* **72**, 1021- 1026.

Muhler, J.C., and Ennever, J. 1962. The occurrence of dental calculus through several successive periods in a selected group of subjects. *Journal of Periodontology*. **33**, 22.

Mühlemann, H.R., and Schroeder, H.E. 1964. Dynamics of supra-gingival calculus formation. *In: Advanced Oral Biology I,*175 (P.H. Staple, Ed). Academic Press, New York/London.

Newman, H.M. 1980. *Dental Plaque: The ecology of the flora on human teeth*. Springfield: Charles C. Thomas Publishers.

Ortner, D.J., and Putschar, W.G. 1995. *Identification of Pathological Conditions in Human Skeletal Remains*. Washington, DC: Smithsonian Institution Press, 442.

Oshrain, H.I., Salkind, A. and Mandel, I.D. 1971. An histologic comparison of supra- and sub-gingival plaque and calculus. *Journal of Periodontology*. **42**, 31 – 33.

Parfitt, G. 1959. A survey of the oral health of Navajo Indian children. *Archives of Oral Biology*. **1**, 193-205.

Partridge, T.C. & Watt, I.B. 1991. The stratigraphy of the Sterkfontein hominid deposit and its relationship to the underground cave system. *Palaeontologia africana.* **28,** 35–40.

Partridge, T.C. 1978. Re-appraisal of lithostratigraphy of Sterkfontein hominid site. *Nature*. **275**, 282–287.

Perry, L., Dickau, R., Zarrillo, S., Holst, I., Pearsall, D. M., Piperno, D. R., Berman, M. J., Cooke, R. G., Rademaker, K., Ranere, A. J., Raymond, J. S., Sandweiss, D. H., Scaramelli, F., Tarble, K., & Zeidler, J. A. 2007. Starch fossils and the domestication and dispersal of chili peppers (Capsicum spp. L.) in the Americas. *Science*. **315**, 986–988.

Perry, L., Sandweiss, D.H., Piperno, D.R., Rademaker, K., Malpass, M.A., Umire, A., de la Vera, P., 2006. Early maize agriculture and interzonal interaction in southern Peru. *Nature*. **440**, 76–79.

Perry, G. H., Dominy, N.J., Claw, K.G., Lee A.S., Fiegler, H., Redon, R., Werner, J., Villanea, F.A., Mountain, J.L., Misra R., Carter, N.P., Lee C., & Stone A.C. 2007. Diet and the evolution of human amylase gene copy number variation. *Nature Genetics Letters*. **39** (10): 1256–1260.

Peters, C.R., O'Brien, E.M., Drummond, R.B., 1992. *Edible Wild Plants of Sub-Saharan Africa*. Royal Botanical Gardens, Kew.

Peters, C.R. 1979. Robust vs. Gracile Early Hominid Masticatory Capabilities: The Advantages of the Megadonts. In: *The Perception of Evolution*, Essays in Honor of J. B. Birdsell. L. L. Mai, (ed). Los Angeles: Anthropology UCLA.

Peters, C.R., & O' Brien E.M., 1981. The early hominid plant food niche: Insights from an analysis of plant exploitation by *Homo*, *Pan*, and *Papio* in eastern and southern Africa. *Current Anthropology.* **22**, 127-40.

Pickering R., Dirks P.H.G.M., Jinnah Z., de Ruiter D., Chruchill S.E., Herries A.I.R., Woodhead J.D., Hellstrom J.C. & Berger L.R. 2011. *Australopithecus sediba* at 1.977 Ma and implications for the origins of the genus *Homo*. *Science.* **333**, 1421.

Pickering R. & Kramers J.D. 2010. Re-appraisal of the stratigraphy and determination of new U-Pb dates for the Sterkfontein hominin site, South Africa. *Journal of Human Evolution.* **59**, 70-86.

Pickering, T.R., Dominquez-Rodrigo, M., Egeland, C.P., & Brain, C.K. 2004 New data and ideas on the foraging behaviour of Early Stone Age hominids at Swartkrans cave, South Africa. *South Africa Journal of Science.* **100**, 1-5.

Pickering, T. R. 1999. *Taphonomic interpretations of the Sterkfontein Early Hominid site (Gauteng, South Africa) reconsidered in light of recent evidence. Ph.D. Dissertation, University of Wisconsin*.

Pilbeam, D., Barry, J., Meyer, G.E., Ibrahim Shah, S.M., Pickford, M.H.L., Bishop, W., Thomas, H. & Jacobs, L.L. 1977. Geology and paleontology of Neogene strata of Pakistan. *Nature* **270,** 684–689.

Pilbeam, D. R. 1972. *The Ascent of Man*. New York: Macmillan.

Piperno, D.R., Ranere, A.J., Holst, I., Hansell, P., 2000. Starch grains reveal early root crop horticulture in the Panamanian tropical forest. *Nature*. **407**, 894–897.

Piperno, D.R., Weiss E, Holst I., Nadel, D. 2004. Processing of wild cereal grains in the Upper Palaeolithic revealed by starch grain analysis. *Nature.* **430**, 670–673.

Piperno, D.R. 2006. *Phytoliths: A comprehensive guide for archaeologists and paleoecologists*. Lanham, MD: Alta Mira Press.

Piperno, D.R., Dillehay T.D. 2008. Starch grains on human teeth reveal early broad crop diet in northern Peru. *Proceedings of the National Academy of Science of the United States of America*. **105**, 19622–19627.

Piperno, D.R., & Becker, P. 1996. Vegetational history of a site in the central Amazon basin derived from phytolith and charcoal records from natural soils. *Quaternary Research*. **45**, 202–209.

Piperno, D. R.1988. *Phytolith analysis: An archaeological and geological perspective*. Academic Press, San Diego.

Plumbo, J., Baer, P.N., & White, C.L. Studies on experimental calculus formation in the rat. V. 1963. Effect of skim milk and cornstarch in the diet. *Periodontic*s. **1**, 34.

Prychid, C.J., Rudall, P.J. Gregory, M. 2003. Systematics and biology of silica bodies in monocotyledons. *The Botanical Review.* **69** (4), 377-440.

Puech, P.-F. & Albertini, H. 1984. *American Journal of Physical Anthropolology.* **65,** 87–91.

Puech, P.-F., C. Serratrice & F. F. Leek. 1983. Tooth wear as observed in ancient Egyptian skulls. *Journal of Human Evolution*. **12**, 617-629.

Puech, P.-F., & Albertini, H. 1984. *American Journal of Physical Anthropology.* **65,** 87–91.

Purseglove, J. W. 1972. *Tropical crops: Monocotyledons*. London: Longman

Purseglove, J. W. 1968. *Tropical crops: Dicotyledons*. London: Longman

Ramjford, S.P. 1959. Indices for prevalence and incidence of periodontal disease. *Journal of Periodontology*. **30**, 51.

Reed, K.E. 1997. Early hominid evolution and ecological change through the African Plio-Pleistocene. *Journal of Human Evolution*. **32**, 289–322.

Reinhard, K.J., Mendonça de Souza, S.F., Rodrigues, C., Kimerle, E., Dorsey-Vinton, S., 2001. Microfossils in dental calculus: a new perspective on diet and dental disease. In: Williams, E. (Ed.), *Human remains: Conservation, retrieval and analysis*. Proceedings of a conference held in Williamsburg, VA, Nov 1999. BAR International Series 934, Oxford, pp. 113–118.

Robinson J.T. 1956. *The dentition of the Australopithecinae*. Transvaal Museum Memoir 9:1–179.

Robinson, J.T. 1954. Prehominid dentition and hominid evolution. *Evolution.* **8,** 324-334.

Robinson, J.T. 1963. Adaptive radiation in the australopithecines and the origin of man. In (Howell, F.C. & Bourliere, F., Eds) *African Ecology and Human Evolution*, pp. 385–416. Chicago: Aldine.

Roberts-Harry E.V., & Clerehugh V. 2000. Subgingival calculus: where are we now? A comparative view. *Journal of Dentistry*. **28**, 93-102.

Rogers, M. E. *et al*. 1994. *Current Primatology Volume 1: Ecology and Evolution* (eds. Thierry, B., Anderson, J. R., Roeder, J. J. & Herrenschmidt, N.) 37–43 (Universite Louis Pasteur).

Rølla, G., Gaare, D., Langmyhr, F.J. and Helgeland, K. 1989. Silicon in calculus and its potential role in calculus formation. In: *Recent Advances in the Study of Dental Calculus* (edited by J.M. ten Cate). Oxford: IRL Press, 97–103.

Rose, M.D. 1978. The Roots of Primate Predatory Behavior. *Journal of Human Evolution.* **7**, 179-189.

Rosen, A. M. 1992. Preliminary identification of silica skeletons from Near Eastern archaeological sites: An anatomical approach. Pp. 129-147 In: G. Rapp & S. C. Mulholland (eds.), *Phytolith systematics: Emerging issues. Advances in Archaeological and Museum Science, 1*. Plenum Press, New York & London

Rovner, I., 1971, Potential of opal phytoliths for use in paleoecological reconstruction, *Quaternary Research*. **1**, 343-59.

Rovner, I. 1983. *Plant Opal Phytolith Analysis: Major Advances in Archaeobotanical Research. Advances in Archaeological Method and Theory, Vol. 6* .1983. pp. 225-266.

Rowles, S. L. 1964a. The inorganic composition of dental calculus. in: *Bone and Tooth. Proeedings of the First European Symposium*. (H. J. J. Blackwood. Ed.). Oxford. pp.175-183. Pergamon Press. London.

Rowles, S. L: 1964b. Biophysical studies on dental cakulusinrclation to periidontai disease. *Dental Practitioner dental Records.* **15**, 2-7.

Ryan, A. S. & Johanson, D. C. 1989. *Journal of Human. Evolution.* **18,** 235–268.

Sanson, G. D., Kerr, S. A., & Gross, K. A. 2007. Do silica phytoliths really wear mammalian teeth? *Journal of Archaeological Science*. **34**, 526–531.

Scheie, A.A., 1989. The role of plaque in dental calculus formation: a review. In: ten Cate, J.M. (Ed.), *Recent Advances in the Study of Dental Calculus*. IRL Press, Oxford, pp. 47–55.

Schroeder, H.E., & Bambauer, H.U. 1966. Stages of calcium phosphate crystallization during calculus formation. *Archives of Oral Biology,* **11**, 1-14.

Schroeder, H.E. 1969. *Formation and inhibition of dental calculus*. Verlag Hans Huber Berne, Switzerland.

Schroeder, H. E. 1963. Inorganic content and histology of early dental calculus in man. *Helvetia Odontologica Acta.* **7**, 17-30.

Schroeder H.E., Lenz H, Muhlemann HR. 1964. Microstructures and mineralization of early dental calculus. *Helvetica Odontologica Acta*. **8**, 1.
Shaw, J.C.M., 1939. Further remains of a Sterkfontein ape. *Nature.* **143**, 117.

Sidaway D.A. 1980. A microbiological study of dental calculus. IV. An electron microscope study of in vitro calcified microorganisms. *Journal of Periodontal Research*. **15**, 240-254.

Simons, E. L. (1972). *Primate Evolution*. Macmillan, New York.

Smith, L. W., Baer, P.N., King, C.T.G., & White, C.L. 1963. Studies on experimental calculus formation in the rat. III. Calculus formation as influenced by high fat, high carbohydrates, and sucrose in the drinking water. *Journal of Periodontology*. **34**, 327.

Sponheimer M., Lee-Thorp J.A., de Ruiter D., Codron D., Codron J., Baugh A., & Thackeray J.F. 2005b. Hominins, sedges and termites: New carbon isotope data for the Sterkfontein Valley. *Journal of Human Evolution*. **48**, 301–312.

Sponheimer M., de Ruiter D., Lee-Thorp J.A., & Spàth, A. 2005a. Sr/ Ca and early hominin diets revisited: New data from modern and fossil tooth enamel. *Journal of Human Evolution*. **48**, 147‑156.

Sponheimer, M., Lee-Thorp, J.A., 1999a. Isotopic evidence for the diet of an early hominid, *Australopithecus africanus*. *Science* **283**, 368-370.

Sponheimer M. 1999. *Isotopic ecology of the Makapansgat Limeworks fauna. PhD Dissertation, Rutgers University.*

Stahl, A.B., Dunbar, R.I.M., Homewood, K., Ikawa-Smith, F., Kortlandt, A., McGrew, W.C., Milton, K. Paterson, J.D., Poirier, F.E., Sugardjito, J., Tanner, N.M. & Wrangham, R.W. 1984. Hominid dietary selection before fire. *Current Anthropology*. **25**, 2, 151-168.

Strum S.C. 1987. *Almost Human: A Journey into the World of Baboons*. Random House: New York.

Szalay F.S. 1975. Hunting-scavenging protohominids: A model for hominid origins. *Man.* **10**, 420–429.

Tan B, Gillam D.G, Mordan N.J, Galgut P.N. 2004. A preliminary investigation into the ultrastructure of dental calculus and associated bacteria. *Journal of Clinical Periodontology*. **31**, 364–369.

Tanzer, J.M. 1989. On changing the cariogenic chemistry of coronal plaque. *Journal of Dental Research.* **68**, 1576-1586.

Teaford MF. 1993. Dental microwear and diet in extant and extinct *Theropithecus*: Preliminary analyses. In: Jablonski NC, editor. *Theropithecus: The life and death of a primate genus*. Cambridge: Cambridge University Press. p 331–349.

Teaford MF. 1992. Dental microwear and diet in extant and extinct *Theropithecus*: preliminary analyses. In *Theropithecus: the Rise and Fall of a Primate Genus*, Jablonski N (ed.). Cambridge University Press: Cambridge; 331–349.

Teaford, M. F., Ungar, P.S. 2000. Diet and the evolution of the earliest human ancestors. *Proceedings of the National Academy of Sciences of U.S.A*. **97**, 13506.

Teleki G. 1981. The omnivorous diet and feeding habits of chimpanzees in Gombe National Park, Tanzania.'' In: *Omnivorous Primates*, Harding RSO, Teleki G (eds), Columbia University Press: New York; 303–343.

Theilade J.1964. Electron microscopic study of calculus attachment tosmooth surfaces. *Acta Odontologica Scandinavia*. **22**, 379–87.

Theilade J, Schroeder H.E. 1966. Recent results in dental calculus research. *International Dental Journal.* **16**, 205–21.

Tobias, P. V. *Olduvai Gorge*, vol. 2, *The Cranium and Maxillary Dentition of* Australopithecus (*Zinjanthropus*) boisei (Cambridge Univ. Press, London, 1967).

Tucker. M.E. 1991. *Sedimentary Petrology*. Blackwell, Oxford, ed. 2.

Turesky S, Renstrup G, Glickman I. 1961. Histologic and histochemical observations regarding early calculus formation in children and adults. *Journal of Periodontology.* **32**, 7–14.

Twiss, P. C., Suess, E. & R. M. Smith. 1969. Morphological classification of grass phytoliths. *Proceedings of Soil Science Society of America*. **33**, 109-115.

Twiss, P.C. 1992. *Phytolith systematics*. Eds. by G. Rapp Jr, and S.C. Mulholland. Plenum Press New York.

Ugent, D., Pozorski, S., & Pozorski, T. 1986. Archaeological manioc (Manihot) from Coastal Peru. *Economic Botany*. **40**, 78–102.

Ugent, D., Pozorski, S., & Pozorski, T. 1982. Archaeological potato tuber remains from the Casma Valley of Peru. *Economic Botany*. **36**, 182–192.

Ungar, P.S., & Sponheimer, M.J. 2011. Hominin diets. In : *A companion to paleoanthropology*. D. R. Begun, ed. New York: Wiley-Blackwell.

Ungar P.S. 2002. Reconstructing diets of fossil primates. In: *Reconstructing Behavior in the Primate Fossil Record*, ed. JM Plavcan, RF Kay, W.L. Jungers, CP van Schaik, pp. 261–96. New York: Kluwer Academic.

Ungar, P. S. 1996. *Journal of Human Evolution.* **31,** 335–366.

Ungar, P.S., 1998. Dental allometry, morphology and wear as evidence for diet in fossil primates. *Evolutionary Anthropology*. **6**, 205–216.

Ungar, P.S., Grine, F. E. Teaford, M. F. 2006. *Annual Review of Anthropology*. **35**, 209.

Ungar, P. S. & Grine, F. E. 1991. *Journal of Human Evolution.* **20,** 313–340.

Vahl, J., Hohling, H.J., Gullenstern, F and Wannenmacher, E. 1964.: *Ein Betrag zur eleckronenoptishen und rontgenographischen Untersuchung supragingivaler Belage auf Zahnfolien.* Dtsche Zahnarztebl. 18, 1.

Van der Merwe, N.J., Thackeray, J.F., Lee-Thorp, J.A. & Luyt, J. 2003. The carbon isotope ecology and diet of *Australopithecus africanus* at Sterkfontein, South Africa. *Journal of Human Evolution*. **44**, 581–597.

Van der Merwe, N. J., Masao, F.T., & Bamford, M.K. 2008. Isotopic evidence for contrasting diets of early hominins *Homo habilis* and *Australopithecus boisei* of Tanzania. *South African Journal of Science*. **104**, 153-155.

Van Peer, P., Fullagar, R., Stokes, S., Bailey, R.M., Moeyersons, J., Steenhoudt, F., Geerts, A., Vanderbeken, T., De Dapper, M., Geus, F. 2003. The Early to Middle Stone Age transition and the emergence of modern human behaviour at site 8-B-11. Sai Island, Sudan. *Journal of Human Evolution*. **45**, 187–193.

Volpe A.R., Kupczak, L.J., and King, W.J. 1967. : In vivo calculus assessment: Part III. Scoring techniques, rate of calculus formation, partial mouth examinations versus full mouth examinations, and intra-examiner reproducibility. *Periodontics* **5**, 184.

Vrba E.S. 1985. Ecological and adaptive changes associated with early hominid evolution. In *Ancestors: The Hard Evidence*, Delson E (ed.). Alan R. Liss: New York; 63–71.

Vrba, E.S., 1980. The significance of bovid remains as indicators of environment and predation patterns. In: Behrensmeyer, A.K., Hill, A.P. (Eds.), *Fossils in the Making*. University of Chicago Press, Chicago, pp. 247–271.

Vrba, E. S. 1975 Some Evidence of Chronology and Paleoecology of Sterkfontein, Swartkrans, and Kromdraai from the Fossil Bovidae. *Nature.* **254**, 301-304.

Vrba, E.S., 1974. Chronological and ecological implications of the fossil Bovidae at the Sterkfontein Australopithecine site. *Nature.* **250**, 19–23.

Walker, A. 1981 *Dietary Hypotheses and Human Evolution*. Philosophical Transactions of the Royal Society of London. **292**, 57-64.

Walker, A. 1979 S.E.M. Analyses of Microwear and Its Correlation with Dietary Patterns. *American Journal of Physical Anthropology*. **50**, 489.

Washburn, S.L. Sherwoood L., & Lancaster, C.S. 1968. "The evolution of hunting," In: *Man the hunter*, (eds.) by R. B. Lee and I. DeVore. 293-303. Chicago: Aldine.

Weiner S. 2010. *Microarchaeology: beyond the visible archaeological record*. Cambridge University Press, Cambridge.

Weselowski, V., Ferraz Mendonça de Souza, S.M. Karl J. Reinhard, K.J., Ceccantini, G. 2010. *Journal of Archaeological Science (in press),* 1-13.

White, T. D. 1980. Evolutionary Implications of Pliocene Hominid Footprints. *Science.* **208**, 175-176.

Whiten A, Byrne RW, Barton RA, Warterman PG, Henzi SP. 1991. Dietary and foraging strategies of baboons. *Philosophical Transactions of the Royal Society of London B*. **334**, 187–198.

Willett, N.P., White, R.R., and Rosen, S. 1991. *Essential Dental Microbiology*. Norwalk. Appleton and Lange.

Wolpoff, M. H. 1980 *Paleoanthropology*. New York: Knopf.

Wolpoff, M.H., 1973. Posterior tooth size, body size, and diet in South African gracile australopithecines. *American Journal of Physical Anthropology*. **39**, 375-393.

Wolpoff, M. H. 1980. *Paleoanthropology*. New York

Wood, B., & Lonergan, N. 2008. *Journal of Anatomy*. **212**, 354.

Woodburn, J. 1968. "An introduction to Hadza ecology," In: *Man the hunter*, (eds.) by R. B. Lee and I. DeVore, pp. 49-55. Chicago: Aldine

Zander, H.A., Hazen S.P., Scott, D.B. 1960. Mineralization of dental calculus. *Proceedings of the Society for Experimental Biology and Medicine*. **103**, 257–60.

Zihlman, A., & Tanner, N. 1978. "Gathering and the hominid adaptation," In: *Female hierarchies*. Eds. L. Tiger and H. Fowler, pp. 163-94. Chicago: Beresford Book Service.

Zipfel B. & Berger L.R. 2010. New Cenozoic fossil bearing site abbreviations for the collections of the University of the Witwatersrand. *Palaeontologia Africana*, **44**, 77-80.

Zipfel B., De Silva J.M., Kidd R.S., Carlson K.J., Churchill S.E. & Berger L.R. 2011. The Foot and Ankle of Australopithecus sediba. *Science*, **333**, 1417-1420.

Zohary, D., & Hopf, M. 2000. *Domestication of plants in the Old World*. Oxford Science Publications. Oxford

APPENDIX A:

The colours of potential calculus deposits are colour-coded to the Munsell Soil Color Charts (1954), wherever possible. The Munsell code is organised first by hue, then value and chroma. A space between the letter representing hue and the number representing number then follows, with finally a forward slash inserted between the two numbers demonstrating value and chroma (Munsell Soil Color Charts 1954).

<u>Descriptions of Probable Calculus on Sterkfontein Hominin Specimens</u>

Descriptions of tooth adherents on StW 53a

RM^1

Probable calculus deposits appear to be adherent to the disto-buccal and occluso-buccal surfaces of RM^1. The bulk of the probable calculus deposit is concentrated in the cervico-disto-buccal and extends to the mid-disto-buccal sections of RM^1. Sub-deposit (a) runs vertically from the cemento-enamel junction to approximately the mid buccal section of the tooth and measures approximately 2.50mm in vertical height and approximately 1.25mm wide at the base of the cervico-enamel junction. The deposit also tapers vertically towards the mid-section of the tooth. The cervico-enamel junction deposit also extends distally for approximately 1.9mm. The deposit presents as a single concentrated concretion. The colour of the deposit is 2.5Y 5/ N4 (dark grey) according to the Munsell Soil Color Charts (1954). The texture is rough, and the shape is formless.

Sub-deposit (b) is located in the mid-occluso-buccal area, within a groove that extends approximately 2.7mm inferiorly from the occluso-buccal margin to the inferior margin of the mid-buccal third (occluso-apically) of RM^1. The vertical measurement of the sub-deposit is 1.95mm with a horizontal measurement of 1.0mm at its maximum, which is approximately 1.8mm from the occlusal edge inferiorly. The texture of this sub-deposit is coarse and presents with a grey (10YR 5/1) and a light grey (10 YR 7/2) colour.

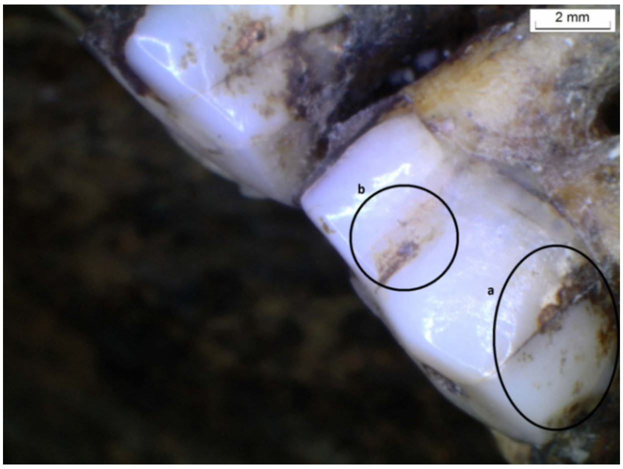

Figure 53: StW 53a RM^1 disto-buccal; occluso-buccal view

RP^4

The probable calculus deposits on this tooth are concentrated predominantly in two locations of RP^4, the disto-buccal area, ranging from the cervico-buccal region to the middle buccal area, and presenting as a broadly diamond shape concretion [sub-deposit (a)] (see Figure 65 and Figure 66) with a vertical measurement of approximately

2.5mm, and a horizontal measurement of approximately 2mm. The cervico-buccal diamond-shaped concretion is composed of a mosaic of colours including, light grey (2.5Y N7); two shades of grey, one bordering on light grey, and a darker shade of grey (2.5Y N6 and 2.5Y N5) in the central, mesial and inferior portions of the deposit; dark grey (2.5Y N4); very dark grey (2.5Y N5) at the most mesial and inferior extent of the deposit; and very dark greyish brown (2.5YR 3/2) superiorly at the apex of the diamond-shaped deposit. The texture is coarse in the mid – to inferior segment and fine in the central diamond-shaped deposit. In the mid-mesial and inferior area of the diamond-shaped deposit are distinctly protuberant elements and the texture of these topographic elevations is thicker than the rest of the adherent material of this sub-deposit. The texture is irregular and uneven. Another relatively large sub-deposit (b) is located chiefly in the middle buccal surface area, measuring approximately 2mm in width and breadth. The colour of the deposit on the middle buccal surface is light grey (2.5Y 7/2); grey (5Y 5/1); light brownish grey (2.5Y 6/2); greyish brown (2.5Y 5/2), and the texture is slightly coarse. There is an additional relatively small, isolated probable calculus deposit adhering to RP^4, measuring approximately 0.75mm vertically and 0.3mm horizontally, and located slightly mesial and occluso-buccal of the mid-buccal deposit. The sub-deposit (c) presents with a range of colours: light-grey (10 YR 7/1); a shade of light grey bordering on grey (10YR 6/1); grey (10YR 5/1). The texture seem to present identically to that of the middle buccal deposit

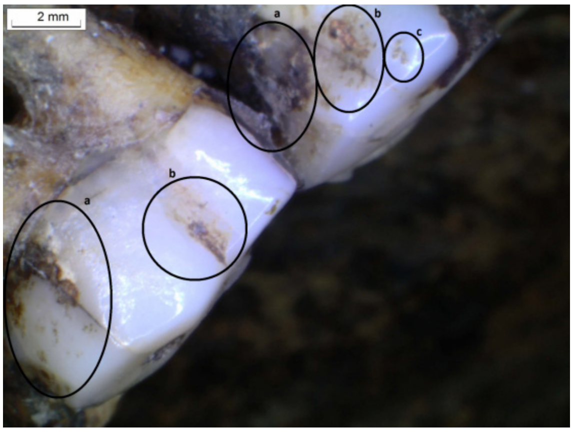

Figure 54: StW 53a RP^4 disto-buccal

RM^2 disto-lingual

A potential calculus deposit is situated disto-lingually on RM^2, and ranges from the superior margin of the cervical third (1.55mm superior to the cervical line) to the inferior margin (1.1mm inferior to the occlusal margin) of the occlusal third (occluso-apically), and for approximately 1.3mm mesially from the proximal margin (mesio-distally) being contained within the disto-lingual third of the tooth. It presents as an irregularly shaped and scattered deposit. The approximate vertical measurement of the deposit is approximately 2mm, and 1mm in width (distal to mesial). The spotted texture of the adherent sub-deposit (a) exhibits a light thickness, and is not very compact exhibiting wide areas of enamel in between the spotted deposit. It presents with a mixture of colours such as brown (7.5YR 5/4); light brown (7.5YR 6/4); light yellowish brown (2.5YR 6/4); light grey (2.5YR 7/2). The disto-lingual surface of RM ^{2} also presents with a smaller darker cluster deposit made up of two dark, isolated and broadly spherical-shaped sub-deposits. The two sub-deposits are located approximately 0.5mm superior to the cervico-enamel margin. Both isolated sub-deposits present with a medium thickness. The disto-lingual surface of RM^2 also exhibits a horizontally clustered deposit which is inferior to the two isolated sub-deposits and located partly on and slightly superior to the junction between the mandible and cervico-lingual area. This cluster is also made up of two sub-deposits. The more distal deposit sub-deposit measures 0.35mm horizontally, and 0.1mm vertically (vertically measured in the middle of the deposit). The more mesial deposit measures 0.35mm horizontally, and 0.25mm vertically are located approximately 0.25mm apart and approximately 0.05mm from the cervical margin. Both sub-deposits of this inferior cluster appear to demonstrate a slight thickness, but less thick than the two superiorly situated isolated spherical sub-deposits. The colouring of the sub-deposits making up this inferior cluster are dark greyish brown (2.5 YR 4/2); very dark grey (5YR 3/1); and a shade of black (5YR 2/2).

Figure 55 StW 53a RM^2 distolingual

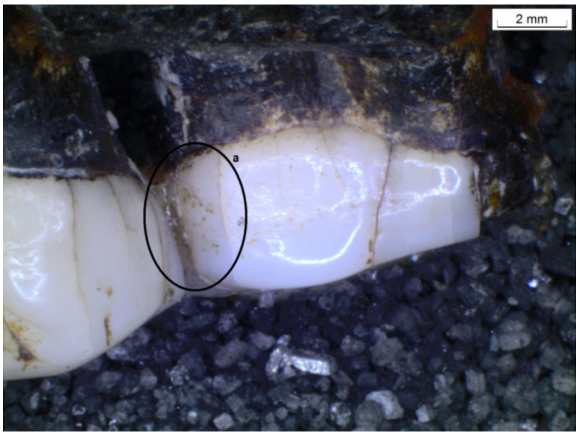

Figure 56: StW 53a RM^2 distolingual

RM^2 linguo-mesial

The predominant deposits on the mesial surface of RM^2 are situated linguo-mesially. The linguo-mesial surface of RM^2 presents with two deposit clusters of probable calculus, one superiorly and the other inferiorly placed (a, and b). There are also two relatively small isolated deposits both located on the occluso-mesial surface, one occluso-lingually and the other occluso-buccally. The more occlusally situated linguo-mesial sub-deposit (a) is made up of four principal constituents: a roundish singular grey deposit sub-deposit (a1) (2.5YR N5), measuring 0.125mm horizontally and 0.25mm vertically. The texture presents as a closely compressed coarse concretion, mainly composed of a single thick protuberance making up the majority of this constituent.

Sub-deposit (a2) which is apical to sub-deposit (a1), has a isolated spherical and topographically protuberant adherence. It is composed of a larger, more or less round deposit measuring approximately 0.25mm horizontally and vertically, measured at its horizontal base, which is at its horizontal maximum. It is grey in colour (2.5YR N5). The texture of this sub-segment is firmly condensed, coarse, grainy and broadly homogeneous, with relatively minor whitely coloured protuberances that are haphazardly situated in this sub-segment, but mainly located in the superior and mid-sections of sub-deposit (a2).

Sub-deposit (a3) which adjoins sub-deposit (a2) is also situated more lingually to sub-deposit (a2). The horizontal measurement is 0.4375mm. It is an amorphously shaped, triple-segmented (a laterally buccal, a mid-section, and an inferior segment), multiple shaded brown and yellow coloured deposit. The bucco-lateral and inferior segments of the sub-deposit consist of a multiple shades of brown chiefly: very pale brown (10YR 7/4); brownish yellow (10YR 6/6); yellowish brown (10YR 5/6) in colour; the middle segment is dark brown (10YR 3/3). The texture of sub-deposit (a3) presents with an uneven globular texture, where the protuberances are not only relatively larger than the grey sub-segment protuberances [sub-deposit (a1) and (a2)], but they have a smoother, and rounder topography.

Sub-deposit (a4) is the most linguo-mesially situated of all the deposits located in sub-deposit (a). It is made up of several colours including a grey (2.5YR N5) coloured spherically shaped central adherence with a light brown deposit extending superiorly, laterally (lingually) and inferiorly outward from it The central grey coloured element of the sub-deposit presents with a compacted, irregular texture. The central roundish adherence presents with a reasonable thickness. The central grey adherence exhibits a series of grey tones: light grey (2.5YR 7/2); and a light brownish grey (2.5YR 6/2).

Inferior to the central spherical element is a sub-segment of the sub-deposit which is thickly protuberant, with a coarse, uneven texture. The sub-deposit exhibits a haphazard in shape. It exhibits a dark greyish brown colour (2.5YR 4/2) in the superior, middle and inferior section, and a light grey shade (2.5YR 7/2) in the buccal region of the sub-segment of sub-deposit (a4). The inferiorly placed sub-segment measures approximately 0.05mm horizontally and measures approximately 0.1mm vertically.

The more apically situated linguo-mesial sub-deposit (b) is located between the cervical and middle third of the mesial surface (cervico-occlusally) of RM^2, and is composed of five major constituents. Although all the constituent elements of sub-deposit (b) are amorphously shaped, all have a different shape configuration. Sub-deposit (b1) is the most supero- buccally located of the constituents of sub-deposit (b). Sub-deposit (b1) appears to taper from the middle area inferiorly, until it reaches a very narrow point at its most inferior point. The texture of sub-deposit (b1) is rough, irregular and dense. The vertical length measures 0.5mm and the horizontal width measures approximately 0.25mm at the superior margin of sub-deposit (b1). The horizontal width at the inferiormost and most narrow point of sub-deposit (b1) is approximately 0.03mm. Sub-deposit (b1) is made up of several colours and shades, predominantly: olive (5Y 5/4); light grey (5Y 7/1); grey bordering on dark grey (5Y 6/1) and grey (5Y 5/1).

Sub-deposit (b2) is located approximately 0.25mm directly inferior to sub-deposit (b1) on the linguo-mesial surface of RM^2, and appears to be a cluster of three different segments. The cluster deposit has no pattern or set shape. The vertical and horizontal extents of the cluster measure approximately 0.25mm from the inferior extent to the superior extent, and bucco-lingually. The texture is mildly coarse and presents a reasonable thickness in the lingual and inferior segments. The buccal (lateral) segment which is relatively much smaller also presents with a much thinner adherent material. The mix of colours in this segment include: greyish brown (10YR 5/2; 10 YR 5/3); light yellowish brown (10 YR 6/4); brownish yellow (10 YR 6/6); pale brown (10 YR 6/3).)

Sub-deposit (b3) is located lingual to sub-deposit (b1 and b2) and presents as the central deposit within the cluster of deposits in sub-deposit (b). Although the deposit is formless, it appears to have a broadly oval shape. The vertical height measures 0.60mm and horizontally measures 0.4mm. The texture is extremely coarse, uneven, granular and compacted. The superior and centro-lingual areas of sub-deposit (b3) present with several amorphous protuberances. The colours displayed by this deposit include: white (2.5Y N6); light grey (2.5Y N7); light grey (bordering on grey) (2.5Y N6); dark greyish brown (2.5Y 4/2); pale yellow (2.5Y 8/4); light olive grey (5Y 6/2); yellow (5Y 8/6).

Sub-deposit (b4) is located supero-lingual to sub-deposit (3), and comprises chiefly of a relatively large central formless segment surrounded by smaller isolated deposits of varying sizes and thicknesses. The central segment is a compacted, rough, uneven textured deposit with a central protuberance. The deposit presents superiorly, laterally (buccally and lingually) with a short extension, and tapers inferiorly from the mid-section, before hooking lingually slightly before the inferior margin of the deposit. The predominant deposit in the centre of this deposit measures both 0.25mm vertically and horizontally (at its maximum), which was measured where the deposit presents with the supero- lateral extensions, near the superior margin of the deposit. The predominant colours include: dark greyish brown (2.5Y 4/2); white (2.5Y N8) light grey (2.5 Y N7); light grey (bordering on grey) (2.5Y N6); pale yellow (2.5Y 8/4); light brownish grey (2.5Y 6/2); light olive brown (2.5 Y 5/4).

Sub-deposit (b5) is located directly inferior to sub-deposit (b4) on the mesio-lingual surface of RM^2, and is the most inferiorly lingual of the constituents in sub-deposit (b5). It presents with a broadly spherical shape and measures approximately 0.53mm vertically, and 0.5mm horizontally. The texture is coarse, uneven and mostly condensed however; there are some areas of enamel visible within this deposit constituent. The adherent material is thick in the supero-lingual and infero-lingual corner of sub-deposit (b5). The colours principally making up this constituent deposit include: yellow (2.5 Y 7/6; 2.5Y 7/8) and olive yellow (2.5Y 6/6; 2.5Y 6/8) in the centro-buccal and infero-buccal regions; yellow (2.5 Y 8/6) in the central deposit; light grey (2.5Y N7) in the infero-lingual and superior area; greyish brown (2.5Y 5/2) in the supero-lingual area.

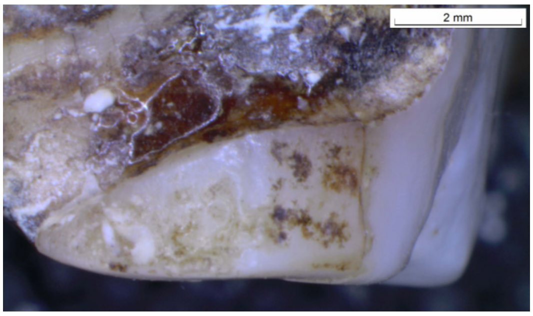

Figure 57 : StW 53a RM^2 occluso-mesial

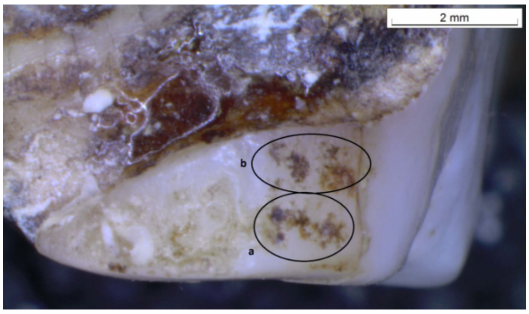

Figure 58: StW 53a RM^2 occluso-mesial; linguo-mesial

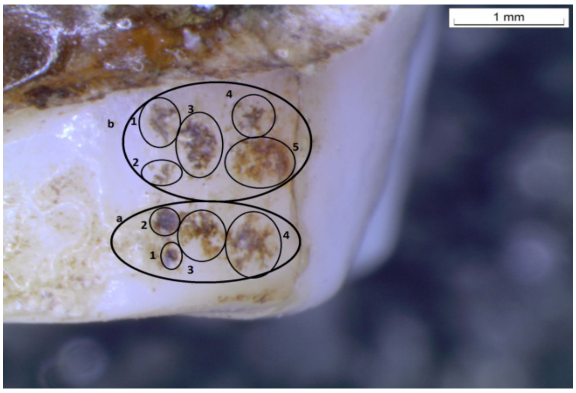

Figure 59: StW 53a RM^2 occluso-mesial

Description of adherent deposits on StW 53a

RM^3

The lingual surface of RM^3 exhibits two predominant deposits, one in the mid occluso-lingual margin and one on the both disto-occluso-lingual margin. The more distal deposit is a broadly triangular shaped adherent mass with the base of the ‘triangle on the occlusal margin. The apex of the ‘triangle’ faces slightly distal. The measurement from the apex of the deposit to the base is approximately 1.24mm and approximately 1.6mm mesio-distally. The texture of Sub-deposit (a) is extremely coarse with concentrated bead-like masses in the mid and inferior sections. The colouring of the base two thirds of the deposit includes: light grey light grey (bordering on grey) (2.5Y

N6) and dark grey (2.5Y N4) very dark grey (2.5Y N3). It is medium dark brown to charcoal. The apical section of the deposit has a series of concavities, is coarse, uneven and presents with ridges. The colouring of the apical third includes: greyish brown (10YR 5/2); pale brown (10YR 6/3); light grey (10YR 7/1; 10YR 7/2).

Sub-deposit (b), the more mesial of the two sub-deposits, is located on the mid-occluso-lingual margin of RM^3. It includes two relatively thin oblique bands, one distal and one mesial. The obliquely and occluso-mesial band has a spherical mass attached to the inferior end, and the obliquely occluso-distal band has more concave-shaped masses at the superior and inferior ends. The enamel area in between the two oblique bands, measures approximately 0.8mm mesio-distally and the enamel area mesial to the obliquely occluso-mesial band and measuring approximately 0.4mm mesio-distally are covered by a very finely film-type textured light brown coloured deposit. The lengths of the oblique bands are grooved into the enamel surface. The ends of both oblique bands appear to be deeper grooved concavely than both the oblique bands themselves. The predominant colours of this sub-deposit include: yellow (10YR 7/8); brownish yellow (10YR 6/6); yellowish brown (10YR 5/6) in the area mesial to the obliquely occluso-mesial; light brownish grey (2.5YR 6/2); white (2.5Y N8); light grey (2.5Y N7) grey (2.5Y N5); light grey/ grey (2.5Y N6); dark grey (2.5Y N4). The colours that are predominant in the obliquely occluso-distal deposit include: greyish brown; light grey / grey (2.5Y N6); grey (2.5Y N5); dark grey (2.5Y N4); very dark grey (2.5Y N3); and pale yellow (2.5Y 7/4).

Sub-deposit (c) is another formless, adherent deposit composed of four different constituent parts found in the mid lingual third (mesio-distally) of the lingual surface RM3 and is situated approximately 0.5mm apical of the inverted 'V'- shaped oblique bands (sub-deposit [b]). This deposit is located supero-distal to the mesial oblique band, and presents an almost arc-shaped continuous deposit, [excepting for the 0.5mm space that separates sub-deposit (b) and (c)]. The arc-shape deposit ranges from the occlusal margin (inferiorly) to the superior (apically) end within sub-deposit (c). The total vertical measurement of the constituent parts making up sub-deposit (c) is 1.8mm and the component parts have horizontal measurements that range from 0.1-0.20mm. The most inferior constituent is characterised by a longitudinal 'tail'. The constituent superior to the most inferior constituent is a solid compacted broadly spherical deposit. The third deposit in the cluster and penultimately superiorly situated in the cluster is a relatively tiny deposit. The fourth and most superior of the constituents of sub-deposit (c) are segmented in three parts. The texture of the first two inferior deposit constituents is coarse and irregular, but thin. The superior two components of the sub-deposit are lightly coarse and uneven. The colours of this sub-deposit include: light grey / grey (2.5YR N6); grey (2.5YR N5); light yellowish brown (2.5Y 6/4); white (2.5Y 8/2); pale yellow (2.5Y 8/4) in the area mesial to the second most inferior constituent of the cluster of sub-deposit (c).

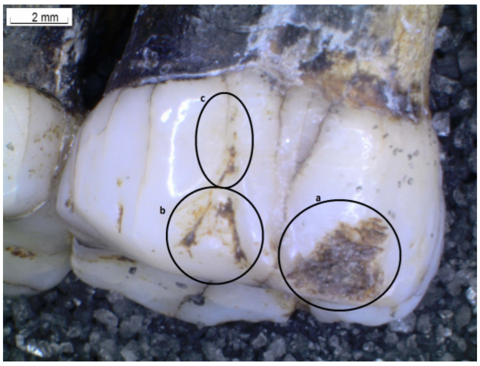

Figure 60: StW 53a RM^3 lingual

RM^3 occluso-buccal

Two probable calculus deposits (sub-deposit [a, and b]) present on the occluso-buccal surface of RM^3. Sub-deposit (a) is located within the mesial third (occluso-apically), and sub-deposit (b) deposit presents within the disto-buccal third (occluso-apically) of RM^3. Sub-deposit (a) appears to be a film-type adherent material. The central area of this deposit exhibits two slightly obliquely mesial elongate-shaped elements, with a 'v'-shaped element placed inferior of the more distal elongate element. The elements of this central cluster present with a relatively substantial thickness compared to the other adherent material in sub-deposit (a), excepting for the most inferiorly adherent material of sub-deposit (a). Supero-mesial to this central cluster is a cluster of amorphous, coarse and bulbous material the texture of which is slightly coarse. A similar textured material appears to present slightly infero-distally to the central deposit cluster. Infero-mesially to the central cluster and on the most inferiormost area within sub-deposit (a) another cluster of medium coarsely adherent material is identified. This inferior element is made up of two constituents, an obliquely distal component and a generally roundish to oval element. Both these inferior elements are coarse, uneven in texture, and exhibit a reasonable thickness, with the more mesial element oval-shaped element also exhibiting a bulbous surface. The predominant colour of sub-deposit (a1) is greyish brown (10YR 5/2), and light brownish grey (10YR 6/2) in sub-deposit (a2); it also has a very dark grey to black colouring (2.5Y N3 – 2.5Y N6) in the infero-distal part of sub-deposit (a2).

Sub-deposit (b) is located approximately 3.8mm distal to sub-deposit (a) on the occluso-buccal surface at the occlusal margin of RM^3. Sub-deposit (b) includes four constituent elements. Sub-deposit (b1) is a relatively small deposit measuring 0.5mm horizontally, with an obliquely mesial superior surface. The texture relatively smooth and lacks thickness.

Sub-deposit (b2) is a shapeless deposit made up of three major parts. The first part is an inferiorly located 'v'-shaped deposit with superiorly located, smaller isolated deposits. The second and supero-distally located part is composed of two broadly longitudinal shaped segments, the more distal part having elements protruding distally from the broadly longitudinal section. The vertical measurement of the mesial longitudinal segment length is 1.1mm and its breadth is approximately 0.2mm at its base. Its width gets wider inferiorly. Its width at its superior margin is approximately 0.10mm. The more distal longitudinal section has a vertical length of 0.9mm and a width of 0.10mm at its inferior base, and 0.20mm where it extends distally. The texture of this portion of the 'v'-shape and longitudinal segments are lightly coarse, irregular and lightly concentrated. The chief colours exhibited in sub-deposit (b2) include: grey (2.5Y N5); dark grey (2.5Y N4); light brownish grey 2.5Y 6/2); greyish brown (2.5Y 5/2).

Sub-deposit (b3) is located distally to deposit (b2), and located 1.1mm apically of the occluso-buccal edge, and on the occlusal surface. This deposit segment exhibits no set pattern or form. The horizontal length of the apical segment deposit at its maximum is 1.8mm. The horizontal width of the occlusal deposit segment of sub-deposit (b3) is 1.98mm. The texture of sub-deposit (b3) is strongly coarse, uneven and firmly concentrated. The major colours of this sub-deposit (b3) include greyish brown (2.5Y 5/2); dark greyish brown (2.5Y 4/2); very dark greyish brown (2.5Y 3/2) and black (2.5Y N7).

Sub-deposit (c) is situated cervico-mesially, and principally characterised by four relatively small concentrated, slightly elevated adherences. Sub-deposit c (1) is located slightly inferiorly of the cervico-mesial margin, with a longitudinal element in the centre of the deposit. The deposit appears to be a thin film-like adherence. Sub-deposit (c2) is placed directly inferior to sub-deposit (c1) and 1.25mm inferior to the cervico-mesial margin within the middle third of the tooth (mesio-distally). This deposit has a rough, irregular and grainy texture. The deposit is not thick. The superior margin of sub-deposit (c2) is 1.1mm from the cervico-mesial margin of RM^3. The predominant colours of sub-deposit (c2) are light grey (2.5Y 7/2); light brownish grey (2.5Y 6/2); greyish brown (2.5Y 5/2). It also exhibits shades of grey (2.5Y N5) and white (2.5Y N8). Sub-deposit (c3) is more mesial than sub-deposit (c2) and is located 1.35mm inferior to the cervico-mesial surface, in the middle third of RM^3 (mesio-distally). It is predominantly characterised by a convex shaped protuberance which presents with a pointed end inferiorly, and extends apically. The vertical length of this protuberant deposit is 0.9mm and horizontally measures 0.20mm at its apical extent. This deposit presents with a smooth texture and is moderately thick, which is exhibited by the convexity of the protuberance. It also exhibits a film-like appearance on either side of the protuberant central deposit. The predominant colours of sub-deposit (c3) include: light grey bordering on grey (2.5Y N6); grey (2.5Y N5); dark greyish brown (2.5Y 4/2); very dark greyish brown (2.5Y 3/2).

Sub-deposit (c4) consists chiefly of a two relatively small isolated deposits located in the inferiormost part of the sub-deposit (c4). The most inferior deposit is relatively larger than the more superior deposit and is situated approximately 2.2mm inferior of the cervico-mesial margin and approximately 2.15mm apical of the occluso-mesial margin; falling into the border of the middle third and the occlusal third of RM^3 (mesio-distally). The inferiormost deposit is moderately thick and has a concentrated and coarse texture. The more superior deposit is a much smaller isolated spherical whitish adherent material, with a homogeneous texture throughout and which exhibits a light coarseness. The principal colours of sub-deposit (c4) include: white (2.5Y N8); grey (2.5Y N5); light grey/ grey (2.5Y N6); light grey (2.5Y 7/2) and pale yellow (2.5Y 7/4).

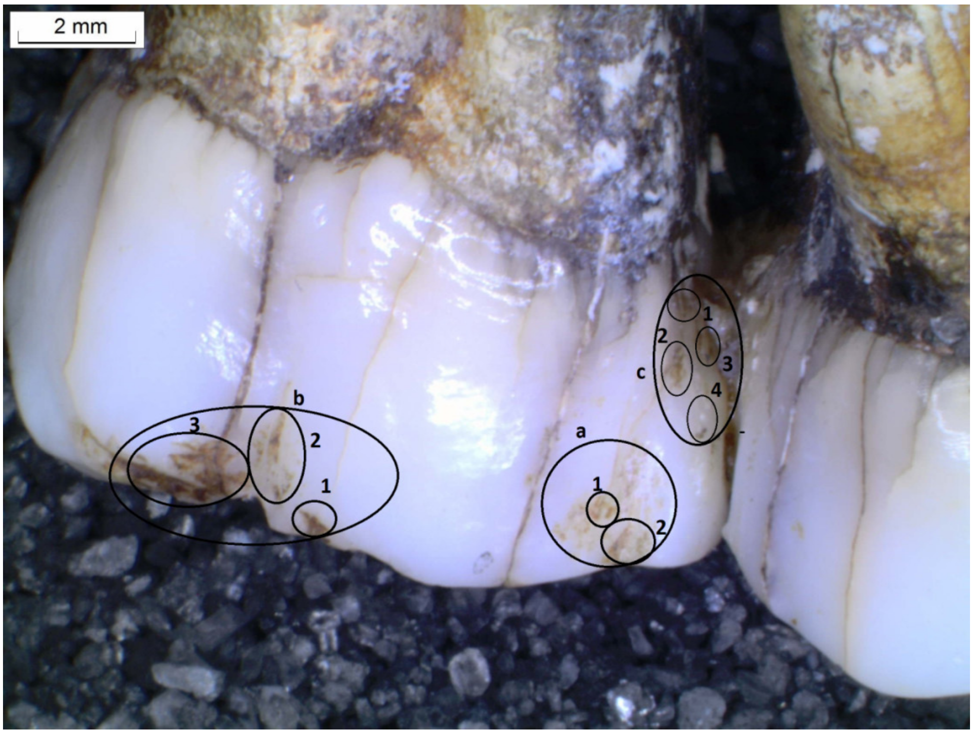

Figure 61: StW 53a RM^3 occluso-buccal; mesio-buccal; a-c: potential adherent deposits and numbers 1-4 represent clusters of different adherent types

RP^4 lingual

The mesio-lingual surface of RP^4 appears to be heavily coated with adherent material beginning from approximately the cervico-lingual margin of RP^4 to the approximate beginning of the margin of the linguo-occlusal third (occluso-apically) (see sub-deposit a). This thick deposit extends mesio-distally from the mesio-lingual margin until the mid-lingual area, and then continues until the distal margin. The adherent deposit appears to get thinner from the mid-lingual surface to the distal margin. The mesial most cervico-mesial deposit starts to narrow vertically from approximately 1.0mm from the mesio-occlusal margin, continuing occlusally up to within 0.8mm of the occlusal surface. This adherent material measures approximately 2mm vertically and 2mm horizontally at its base. The mesio-lingual texture of the sub-deposit (a) presents as extremely coarse, shapeless, irregular, thick, and non-homogeneous and speckled with several vertically shaped protuberances in the mid-lingual area (mesio-buccally and occluso-apically), demonstrating considerable thickness of the adherent material. The disto-lingual texture of the adherent material deposit is less thick, less coarse, formless and homogeneous. The colours of this rough textured adherent material includes: light olive grey (5Y 6/2); grey (5Y 5/1); light grey (5Y 7/2) white shades (2.5Y N8; 5Y 8/1; 5Y 8/2); pale yellow shades (5Y 8/3; 5Y 8/4); dark greyish brown (2.5Y 4/2); the colours of the disto-lingual texture include: greyish brown (2.5Y 5/2) and two shades of light olive brown (2.5Y 5/4; 2.5Y 5/6); dark grey (2.5Y N4); dark yellowish brown (10 YR 3/4); yellowish brown (10YR 5/6); light yellowish brown (10YR 6/4) very dark greyish brown (10YR 3/2).

Sub-deposit (b) is located on the disto-lingual surface, 1.00mm apically from the occlusal surface, and situated within the middle third occluso-(apically) of the tooth. The horizontal breadth is 0.9 mm and the vertical length is 1.3mm. The texture is rough, irregular and thick in the occlusal third (occluso-apical) part of the deposit, approximately 1.3mm from the occlusal margin. The predominant colours of this deposit include: very dark grey (2.5Y N3); light grey (2.5YR N7); very dark greyish brown (2.5YR 3/2) and black (2.5YR N2).

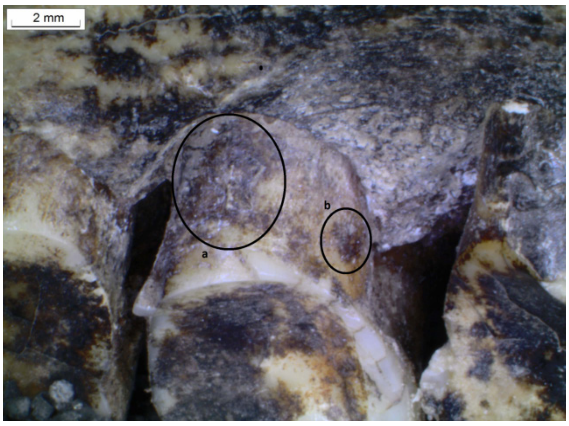

Figure 62: StW 53a RP^4 lingual surface

RP^3 lingual

RP^3 presents with several probable calculus deposits. Sub-deposit (a) is situated on the disto-lingual surface between the occlusal margin and slightly inferior to the cervico-lingual margin. The vertical length of the sub-deposit (a) is 3.3mm and the horizontal breadth is 1.75mm. The deposit is formless. The texture presents as extremely rough, irregular, uneven and compacted. The texture becomes extremely thick as it approaches the interproximal area between RP^3 and RP^4. The colours of sub-deposit (a) chiefly include: dark reddish brown (5YR 3/2; 5YR 2/2); reddish brown (5YR 5/4); white (5YR 8/1); pinkish white (5YR 8/2); pink (5YR 7/3); dark grey (5YR 4/1); pinkish grey (5YR 7/2; 5YR 6/2).

Sub-deposit (b) is located between the mid-cervico-lingual and disto-cervico-lingual surface, and appears to adhere to the cervico-enamel junction in the mid-lingual area, approximately 3.00mm from the mesio-lingual margin of RP^3. At the mesial margin of the sub-deposit its vertical length is extremely narrow, measuring approximately

0.1mm, and increasing as it extends further distally and obliquely, until it reaches a maximum vertical length of 1.1mm from the cervico-enamel junction, thereafter continuing distally for approximately 1.7mm until it terminates adjacently superior to sub-deposit (a). The deposit has an irregular shape, and its texture is uneven, convex mesially and coarse. The predominant colours of sub-deposit (b) include: pinkish white (5YR 8/2); pinkish grey (5YR 6/2); pink (5YR 7/3); light reddish brown (5YR 6/4)

The superior edge of sub-deposit (c) is located on the cervico-enamel junction in the mid-lingual area, with the inferior boundary located within the occlusal third of the tooth (mesio-distally). The deposit measures 1.35mm vertically and 1.85 horizontally. The deposit is formless. The mid-distal area of the sub-deposit exhibits a concave, crater-like element, the outer spherical margin of which, presents with a considerable thickness. The texture is coarse, granular and irregular and bulbous. The colours of sub-deposit (c) include: light grey/grey (5YR 6/1); grey (2.5Y N5); pale yellow (2.5Y 7/4); dark greyish brown (2.5YR 4/2).

The mesio-lingual deposit (sub-deposit d) appears to be distinctly different from the other deposits on RP3. This deposit ranges from the cervical margin of the mesio-lingual surface of the tooth, to the occlusal margin of RP^3 (occluso-apically), and ranges the mesial margin to the middle third of the tooth mesio-distally. The horizontal breadth at the superior margin of sub-deposit (d) measures 1.8mm.The mid- mesio-lingual horizontal measurement measures 1.95mm (measurement taken 1.1mm vertically inferior from the cervico-enamel junction). The supero-distal edge of the deposit runs obliquely distal from the junction with the alveolar bone to the middle third of the tooth (mesio-distally), for approximately 1.1mm occlusal third and thereafter extends directly inferiorly for approximately 1.0 mm, before extending distally for approximately 0.2mm, and then turning obliquely mesially for approximately 1.15mm finishing at the occlusal edge of RP^3. The mid-mesio-lingual area, at approximately 1.0mm inferior of the cervico-enamel border and 1.15mm superior of the occlusal edge presents with a broadly rectangular protuberance, which is approximately 0.1mm thick. The texture of this deposit is very fine and exhibits no adherent width, excepting the protuberance in the mid-mesio-lingual area. The principal colours of this sub-deposit include: very pale brown (10YR 7/3); very dark greyish brown (10YR 3/2); dark reddish brown (5YR 2/2).

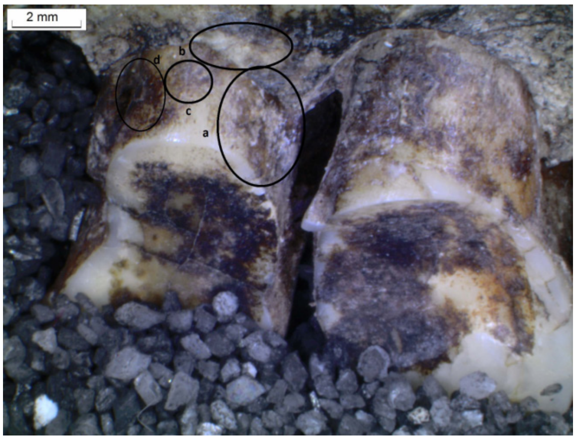

Figure 63: StW 53a RP3 lingual surface (6.3 x)

RP^3 mesial

On the mesio-cervical margin of the mesial surface of RP^3 there are three potential deposits; the first, sub-deposit (a) is situated inferiorly linguo-mesial. The shape of the linguo-mesial deposit presents generally as a four sided deposit, with the inferior angle transversely cut away. The deposit is located obliquely bucco- apical, and it measures 1.7mm at its maximum. The obliquely horizontal diameter at its maximum measures

1.3mm (measured 1.65mm superior of the occluso-lingual angle). The texture is extremely coarse, grainy, and uneven. The main colours of this deposit include: light grey (2.5Y N7); light brownish grey (2.5Y 6/2); greyish brown (2.5Y 5/2); dark greyish brown (2.5Y 4/2); very dark greyish brown (2.5Y 3/2); white (2.5 8/2); grey (2.5Y N5); dark grey (2.5Y N4).

Sub-deposit (b) is located slightly supero-buccal of sub-deposit (a) on the mid-mesial surface of RP^3, and is made up of three major parts. The inferior segment, exhibits the shape of an inferiorly projecting arrow; the middle part appears as a series of amorphously placed more or less round-shaped deposits haphazardly dotted between the inferiorly and superiorly placed deposits; and the superior portion is a broadly flattish superior deposit with a laterally (lingually) inferiorly facing segment. The texture of this sub-deposit is tightly compacted and lightly coarse at the superior and inferior margin (which presents as a 'v'-type deposit). In between the superior and inferior margins, the texture of this deposit presents as an extremely thin film of adherent material. The predominant colours of the superior segment of sub-deposit (b) include: white (2.5Y 8/2); light grey (2.5Y 7/2); light brownish grey (2.5Y 6/2); greyish brown (2.5Y 5/7).

Sub-deposit (c) is located on the cervico-mesial margin between the mesio-buccal margin and the mesio-lingual margin.The bucco-mesial deposit is more or less horizontal tracing out the mesio-cervical margin, excepting in the mid cervico-mesial margin area where it extends apically for approximately 0.75mm, before reversing and resuming its extension lingually until it the linguo-mesial margin. The texture is rough, uneven, and concentrated. The principal colours of sub-deposit (c) include: greyish brown (2.5Y 5/2) light grey (2.5Y 7/2); light brownish grey (2.5Y 6/2); light grey (2.5Y N7); light grey / grey (2.5Y N6); grey (2.5Y N5); white (2.5Y N8) and very dark greyish brown (10YR 3/2).

Figure 64: StW 53a RP^3 mesial surface (6.3 x)

Description of tooth adherents on StW 53h

Isolated LM$_3$ distal

The distal surface of LM$_3$ exhibits several potential calculus deposits, generally spread from the lingual to the buccal margins. The sub-deposit (e) is a formless deposit and located apical slightly apical of the occlusal margin (approximately 0.20mm) in the occlusal third of the distal surface of LM$_3$ approximately 3.85mm from the lingual margin (bucco-lingually). The texture presents as coarse, highly compacted, with several thick protuberant elements, notable one on the buccal end and one on the lingual end of the deposit. The approximate horizontal width is 1.3mm bucco-lingually (measured in the midline of the deposit – equidistant (approximately 0.65mm) from the superior and the inferior ends of the deposit. This deposit is surrounded linguo-distally, bucco-distally, and occluso-distally by an irregular cluster very finely spotted potential deposits. The spotted amorphous spotted deposits lack any adherent thickness. Colour of sub-deposit (e) is a dark grey (7.5YR N3) and brown (7.5 YR 5/2).

Sub-deposit (b) is located approximate 2.1mm inferior to the occlusal edge, in the middle third of the distal surface between the occlusal and the cervical thirds of LM_3. The shape is irregular and measures about 2.0mm horizontal width (bucco-lingually) and vertical height (superior segment) is approximately 0.8mm (occluso-cervically). There is a longitudinal segment which adjoins the superior segment at broadly right angles. The vertical length of the longitudinal segment is 1.2mm from the superior extent of sub deposit (b) The texture of the superior segment is coarse, uneven and condensed; the texture of the lingual segment of the sub-deposit (longitudinal section) is less coarse and dense The colouring is light brown (7.5YR 6/4).

Sub-deposit (a) is located 2.1mm apically from the occlusal surface and situated disto-lingually (approximately 2.25mm from the lingual margin), within the middle third of the tooth (ocluso-apically). The deposit is broadly spherical shaped, with a coarse and compact texture. Approximately 1.0mm bucco-distally of sub-deposit (a) is an isolated spherical deposit sub-deposit (f) very similar in shape to sub-deposit (a).

Sub-deposit (f) is located in the middle third of the distal surface of the tooth (occluso-apical). It is thickly attached to the enamel and protrudes from it. Surrounding this relatively small, spherical protruding deposit are several small deposits superiorly and disto-buccally with no apparent thickness and appear more like staining than adherent deposits. Colours are shades of browns (7.5 YR 5/2; 3/2)

Sub-deposit (g) is located in the middle third of distal surface of LM_3 (ocluso-apical). It is a cluster of amorphous, relatively small adherent deposits that are concentrated and coarse. Interspersed within this cluster deposit may have the same type of probable staining exhibited surrounding the spherical deposit in sub-deposit (f).

Sub-deposit (c) is located almost at the bucco-distal margin ranging between the occlusal third and the apical third (ocluso-apically). Sub-deposit (c) commences approximately 1.8mm inferior of the occlusal margin. The vertical length of the deposit measures 4.9mm; the horizontal width (measured in the midline of the deposit) is 2.2mm. This deposit consists of several disparate adherent deposits. The superior portion of the deposit is made up of grainy, relatively thick and closely situated cluster-type deposits. The middle part of the deposit consists of larger isolated and roundish deposits, which are thickly adherent. The inferior part of the deposit is grainy, concentrated and coarse but presents with a generally homogeneous texture. The inferior bucco-distal end of sub-deposit (c) is less grainy, and more irregular than the inferior linguo-distal end. Colour is coded to grey brown (7.5YR N3)

Sub-deposit (d) is located between the mid-cervico-distal surface and the disto-lingual margin, within the cervical third of LM_3. The horizontal breadth of the deposit measures 4.35mm; and the vertical length measures 2.35mm (occluso-apically-measured from the midpoint of the deposit horizontally, approximately 2.17mm from the disto-buccal end of sub-deposit [d]). The texture is extremely coarse, bulbous in the superior mid-section, irregular, thickly adherent, and has no form. Colour is coded as grey / brown hues (7.5YR N3 and 7.5YR 6/4)

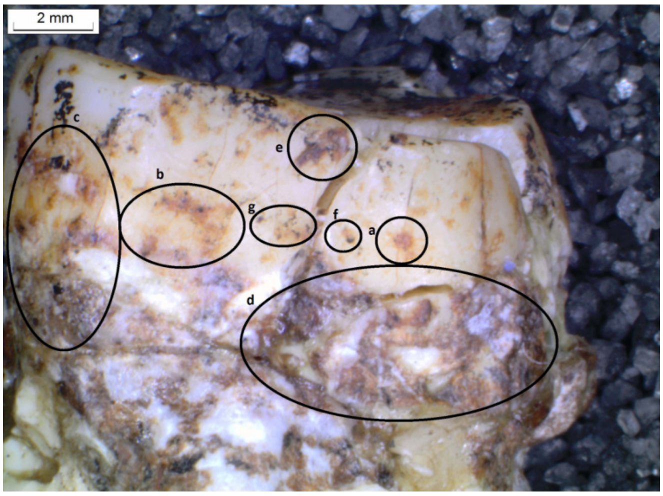

Figure 65: Stw 53h Isolated LM$_3$ distal surface (6.3 x mag)

Description of tooth adherents of StW 53f

Isolated LM$_3$ mesial

Several probable calculus deposits present on the linguo-mesial and bucco-mesial surfaces of LM$_3$. Sub-deposit (a) is located on the linguo-mesial surface approximately 1.8mm occlusally of the cervical margin. This sub-deposit cluster consists of a variety of elements. The central and slightly infero-lingual areas each presents with an isolated, relatively small, spherical and protuberant deposit, demonstrating some thickness (a1 and a2). Sub-deposit (a3) exhibits as an isolated, broadly roundish and relatively larger than deposit (a1) and (a2). Sub-deposit (4) presents as a longitudinal deposit, the vertical length is 1.75mm and the width measures 0.1mm at the superior edge. Sub-deposit (5) is very light textured, and amorphous shaped. Colours for sub-deposit a is grey, brown (7.5YR N3; 7.5YR 6/4)

Sub-deposit (b) is located on the liguo-mesial surface approximately 0.1mm slightly apical of the occlusal edge of LM_3. The horizontal width and vertical length both measure approximately 1.15mm. It appears to exhibit potential calculus deposits, however they present as very thin and slight. On both locations on the mesial surface they are irregularly laid out and present as a speckled deposits, and light brown in colour. There are two locations on the occusal margin, the linguo-mesial and bucco-mesial which exhibit a slightly rougher texture than the rest of the mesial surface deposits. There colouring is darker brown tending to charcoal. The middle section of the mesial surface between the lingual and buccal thirds has very slight, light brown deposits, amorphously situated, and the texture is almost flush with the enamel surface, that it tends to look like possible staining only.

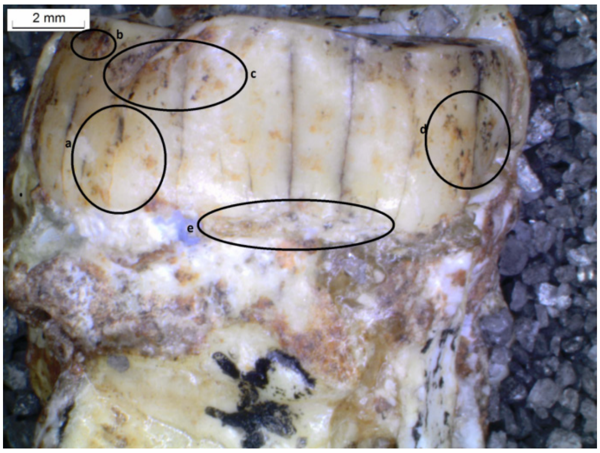

Figure 66: Stw 53f Isolated LM_3 mesial (6.3 x mag)

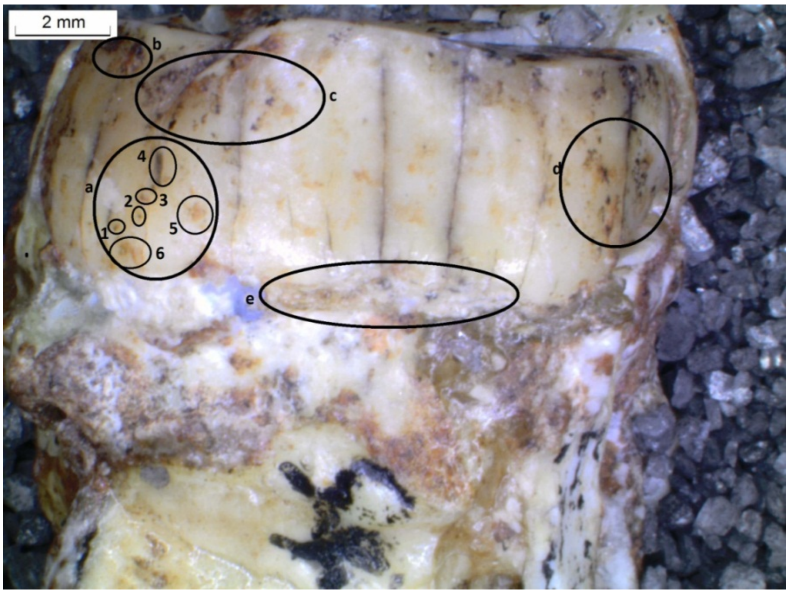

Figure 67: Stw 53f Isolated LM_3 mesial 6.3x mag

Description of adherents on StW 53f

Isolated LM_3

Probable calculus deposits present predominantly on the disto-lingual, mid-lingual, occluso-lingual and mesio-lingual areas of LM_3. The disto-lingual cluster represented by sub-deposit (a) is composed of three specific cluster deposits; one in the mid-distal portion of sub-deposit (a);one in the mid-mesial area, which extends inferiorly ; and a infero-distal cluster, directly below the mid-distal cluster. The mid-distal and the mid-mesial cluster is separated by a narrow longitudinal convex deposit which is adherent to the enamel, and extends apically for approximately 2.4mm and commences approximately 1.0mm apically from the occluso-lingual margin. The mid-mesial deposit has a vertical length of 1.2mm and measures 1.0mm horizontally (measured at its superior surface). The mid-mesial cluster appears to taper inferiorly and mesially.

The deposit clusters making up sub-deposit (a) appear to be composed of two distinct types of material deposits: a darker more variegated material which is a rough, granular textured deposit, and a lighter coloured, less coarse, slightly protuberant material. The cluster deposits of sub-deposit (a) are formless. Colour coding for sub-deposit a is a mix between browns and greys (7.5YR N3; 7.5YR 6/4; 7.5 YR 5/4)

Sub-deposit (b) is located on the mid-lingual surface of LM_3. The deposit ranges from the occlusal margin to the middle third of the tooth, and measures 1.8mm in vertical length from the occlusal edge to the apical extent of the deposit. The horizontal width of the deposit is approximately 2.1mm. This deposit is made up of various different elements, a lightly coarse deposit at the occlusal edge, which exhibits a slight thickness; thickly adherent material interspersed with a lightly coloured and lightly coarse deposit in the mid-section. The mid-section of sub-deposit (b) also contains a cluster of darkly coloured, speckled, irregularly shaped, and tightly condensed adherent material, which does not exhibit a considerable thickness. Colours are close to greys, light to dark browns (7.5YR N3; 7.5YR 6/4; 7.5 YR 5/; 7.5YR N5).

The mesio-lingual cluster deposits (sub-deposits [c and d]), present with a series of probable calculus deposits located on the occluso-lingual margin, the middle third, the cervical third, and the cervico-enamel junction of the lingual surface of LM_3. Sub-deposit (c) is located on and slightly apical of the occluso-mesial margin, and presents with two deposits. The more distal deposit ranges from the occlusal margin inferiorly and measures 1.15mm in length vertically. It measures 0.75mm in width (measured at the superior margin of the deposit). This segment of sub-deposit (c) tapers inferiorly, curving slightly mesially at its inferior extent. Its inferior width at this point measures approximately 0.05mm. The texture of the superior segment presents as smooth, with the inferior part of the sub-deposit has a smooth and a coarse texture. The coarse, uneven texture is associated with the darker part of the deposit. The more mesial deposit is composed of two isolated segments. One is relatively small, the other larger. The smaller isolated, spherical-type deposit is darker. The larger deposit is amorphous, appears to have a dark central protuberance. The area around the protuberance appears to be smoother than the central area, which appears coarser. Colour coding for sub-deposit (c) is brown and gray hues (7.5YR N3; 7.5YR 6/4)

Sub-deposit (d) is located between the middle third and the cervico-enamel margin. It begins 2.0mm apical of the occluso-mesial margin and extends 4.0mm inferiorly. It is made up of various different elements. Slightly superior to the middle deposit is an extremely thick, generally elongate, coarse protuberance. Adjoining this protuberance infero-mesially, is another coarse amorphous, granular and thickly adherent deposit (see sub-deposit [d1]). Directly inferior to these protuberant elements are several isolated, small variegated deposits, exhibiting some thickness. Inferior to the cluster of small variegated deposits, is a group of four fairly thickly adherent deposits (sub-deposit d2). The texture of (d2) is smooth and exhibits a slight thickness. Colours are coded to greys, light to dark browns (7.5YR N3; 7.5YR 6/4; 7.5 YR 5/; 7.5YR N5).

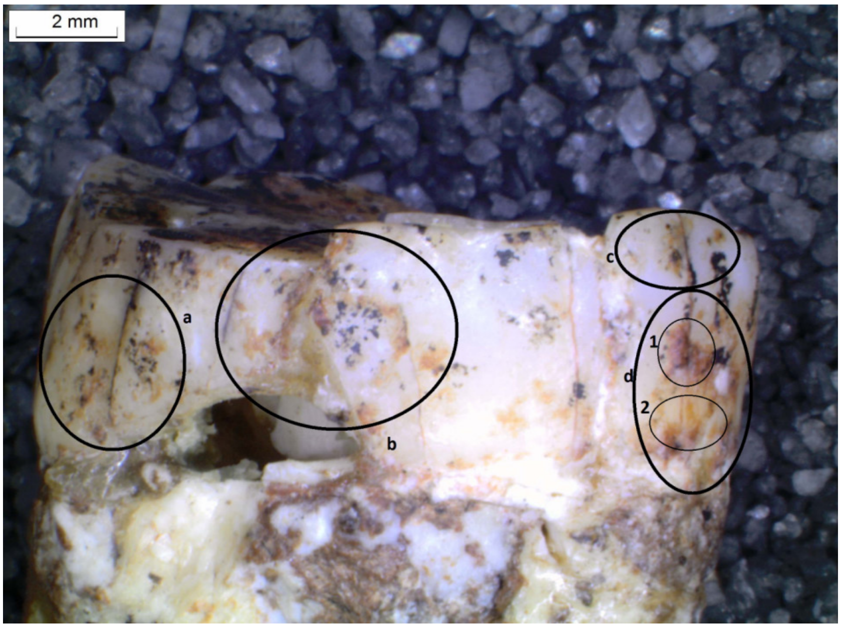

Figure 68: Stw 53f Isolated LM_3 lingual (6.3 x mag)

Description of adherents on StW 53a

LP^4

The distal surface of LP4 presents with five deposits, four of which are located on the cementum and one on the disto-buccal surface of the tooth enamel. One of the deposits is situated on the mid-cemento-enamel junction [sub-deposit (d)], with one deposit adjoining it lingually (sub-deposit [e]); one adjoins sub-deposit (d) apico-buccally [sub-deposit (c)]; and one deposit [sub-deposit (a)] lies buccal to sub-deposit (c); sub-deposit (b) lies inferior to subdeposit (a) on the disto-buccal surface.

Sub-deposit (a) is located on the buccal side of the root which begins at the cemento-enamel junction and extends apically for approximately 5.3mm. The horizontal width at the cemento-enamel junction is 1.6mm. The horizontal width at the base of the root area of the deposit is 0.9mm. The width at the superior margin of the deposit on the buccal side of the root is 0.20mm. This sub-deposit (a) is a formless, compact, adherent mass which has an irregular and protuberant nature. The texture has a medium thickness. The colour of this attachment deposit is light brown (7.5YR 6/4)

Sub-deposit (b) is located on the disto-buccal surface of LP^4 and lies between the disto-cemento-enamel junction and the occlusal third. It extends 1.9mm occlusally (vertically) from the cemento- enamel junction and concludes 1.95mm apical of the occlusal surface. The texture of the deposit is rough, 'crater-like', irregular and thickly adherent. It is not homogeneous and is amorphous in form. Sub-deposit (b) also presents with a thin deposit that begins in the central area of the deposit and extends 2.0mm lingually. The texture of this thin band is light and slightly coarse. Colour brown/ grey (7.5YR 6/4; 7.5 YR N3)

Sub-deposit (c) is located lingual of sub-deposit (a) on the situated on cementum on the tooth, 1.85mm apical of the cemento-enamel junction. It measures 1.0mm horizontally and vertically 0.65mm. The texture of this deposit is bulbous, uneven and coarse, consisting largely of two relatively large, broadly circular protuberant masses on the buccal side of the deposit. The protuberant masses present as moderately thick. Colour is brown/ grey (7.5YR 6/4; 7.5 YR N3).

Sub-deposit (d) is located in the mid-distal area of the tooth and is situated on and extends 2.1mm apically from the cemento-enamel junction. The horizontal width of the deposit is 3.6mm (measured at the CEJ). The lingual edge of the deposit slopes obliquely lingually until it reaches the CEJ, where the horizontal width measures 1.7mm. The texture of the deposit is uneven, extremely coarse and granular. The deposit is moderately thick. Colour is greyish (7.5 YR N3).

Sub-deposit (e) is located lingually to sub-deposit (d) and directly occlusal to the bifurcation of the tooth. The deposit lies on the cemento-enamel junction and measures 1.8mm horizontally and 1.0mm vertically. The texture appears moderately uneven and coarse, but does not present with considerable thickness. Colour characterised by dark brown hues (7.5 YR 6/4; 7.5 YR 3/2)

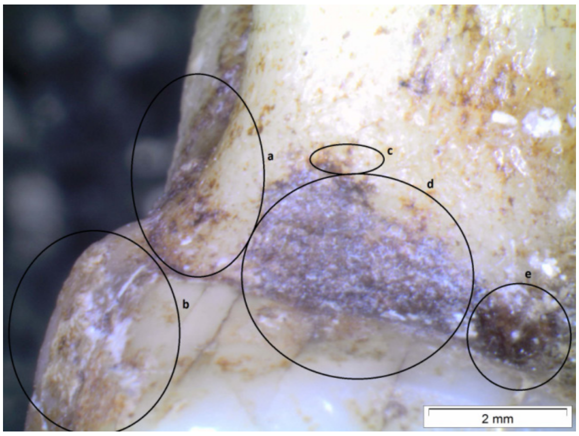

Figure 69: Stw 53a LP^4 distal view (12.5 mag)

Description of adherents on Stw 53f

LM^2

The buccal surface exhibits three locations of probable calculus deposits. Two distinct deposits are situated mesio-bucally, sub-deposits (a, and b) and one is located disto-bucally, sub-deposit (c). Sub-deposit (a) is located obliquely distal, within the cervico-buccal third where the cervico-buccal margin is the apical limit of the deposit. The vertical measurement of this deposit, which begins from the cervico-enamel junction and ranges occlusally to the inferior most point of this deposit, is approximately 2.1mm. The texture of the inferior part of the sub-deposit is grainy, condensed, irregular and lightly coarse, while the superior part of the deposit is, medium coarse, uneven, not tightly compacted. There is some adherent material, which is lying horizontally on the cemento-enamel junction. This deposit has a moderately thick texture, is not compacted, and has a narrow width (approximately 0.10mm). Colour is brown (7.5YR 5/4; 7.5YR 5/2).

The first and more mesially situated of the two occluso-buccal cluster deposits (sub-deposit b) is made up of three irregular shapes. The most mesial deposit has an oblique shape, barely distinguishable on the enamel surface, very fine in texture and light brown on colour. The second and more distal of the deposits is more or less rectangular, slightly more rough in texture and measures 0.9mm vertically (occluso-apically) and mesio-distally (horizontally) 0.25mm. The third deposit which is the most distal of the occluso-buccal deposit, is substantially larger than the latter two occluso-buccal deposits and has a slightly mesially concave shaped longitudinal section, measuring approximately 2.1mm from the inferior (occlusal) base to the superior edge of the deposit; and is joined by a separate relatively square section divided into two rectangles, one superior and one inferior situated on the superior end of the longitudinal section. The width of the longitudinal deposit is approximately 0.4mm at its base and approximately 0.35mm at its apical end. The inferior edge lies on the occluso-buccal margin. The sub-deposit has an amorphous configuration. The texture of the most mesial sub-deposit of the mesio-buccal cluster deposit is extremely coarse, and has a dark brown colour (7.5 YR 6/4; 7.5 YR 5/4)

The second and more distally located of the two occluso-buccal cluster deposits (sub-deposit c) is located between the middle third and the occlusal third of the tooth. It is an irregular shaped deposit, with its component parts positioned in no obvious pattern. There is a superior sub-cluster and an inferior sub-cluster within this sub-deposit, separated with a small portion of adherent-free enamel. The inferior edge of this occluso-buccal deposit measures approximately 0.5mm from the occluso-buccal junction. The superior edge of the deposit measures approximately 2mm from the cervico-buccal junction. The texture of this subdeposit has a compact component mesially and a small compact component inferiorly, and is coarse and uneven throughout, excepting for the highly compacted areas. It exhibits a moderate adherent thickness.

LM^3 buccal

Four probable calculus deposits are exhibited on the buccal surface of LM^3. The first deposit is situated mesiobuccally, with its inferior limit more or less on the occluso-buccal edge (sub-deposit a). The configuration of the deposit appears to be unstructured, with the most occlusal (inferior) extremities exhibiting a coarse texture and a dark brown colour. The superior portion of this deposit is less coarse and has a light brown colour. The deposit measures approximately 2mm vertically (occluso-apically) and horizontally (mesio-distally) approximately 2mm. The width of the deposit at its apex is approximately 0.12mm.

The second deposit, the centro-buccal deposit (sub-deposit b) exhibits a possible calculus deposit with its inferior extremity on the occluso-buccal margin. The deposit is characterised by a square base which appears dark brown to charcoal, with a rough texture tapering superiorly until the margin of the middle third of the buccal surface. At this point the deposit has transformed from dark brown and partly charcoal to a light brown colour. Thereafter the deposit breaks up into isolated parts and ends at approximately the proximal margin of the cervical third.

The third and cervico-buccal deposit (sub-deposit c) is characterised by two parts, joined at more or less right angles to each other. The first component comprises a vertical-type deposit which begins at the cervico-buccal margin and ends approximately at the inferior end of the cervical third. The deposit is coarse and light brown in colour. It appears to be placed in a buccal development groove emanating from the cervical margin. The measurement of the vertical deposit from its cervical base to its distal limit is approximately 2.2mm. The horizontal width of the vertical deposit at its maximum is approximately 0.5mm, and at its minimum, which is at its most distal point is approximately 0.1mm. The measurement of the horizontal base (cervical margin) is approximately 2.5mm, with a very narrow width of at least 0.05mm. It has a fine texture, and is light brown in colour. At the inferior base of the junction where the longitudinal section of the deposit meets the horizontal section, there is a generally circular shape moderately thick protuberance This deposit then extends distally along the cervico-buccal margin, forming the base of 'right-angle' shaped deposit. The horizontal deposit appears as an extremely thin band across the cervico-buccal margin. This thin band extends into and joins sub-deposit (d).

The fourth potential calculus deposit is located cervico-buccally (sub-deposit d), and extends from the cemento-enamel junction to slightly apical of the occluso-buccal margin (approximately 0.55mm). The shape of the cervico-buccal deposit is irregularly shaped, substantially thick and coarse in texture, uneven and extremely compacted and protuberant. The colouring is a light brown in the deeper parts of the deposit and dark brown on thickest parts of adherent surface material. The base width of the supero-mesial deposit measures 2.2mm and the height measures approximately 2.0mm. This deposit extends to the middle third of the disto-buccal surface where the texture changes from extremely concentrated and thick, to a thinner, banded and unstructured longitudinal lines situated vertically(occluso-cervical). The most mesial of the longitudinal lines of deposit material is the widest measuring approximately 0.5mm at its widest and 0.25mm at its narrowest, which is at the base where the deposit tapers to its narrowest point. The narrowest point intersects with the occluso-buccal edge. The colouring of this deposit is dark brown to charcoal grey inferiorly, and light brown more superiorly. There are four more vertical longitudinal line deposits lying distal to the widest longitudinal (mesial) deposit, with some intersecting with the occlusal edge of the distobuccal surface of LM^3. All these longitudinal deposits have the same thick texture. The second vertical deposit is extremely narrow and measures approximately 0.2mm in width at its widest, and has the shortest vertical measurement (0.8mm) with the most occlusal point measuring approximately 0.1mm. All the other vertical deposits range from the occlusal margin to the cervical margin of the buccal surface of LM^3. The third and middle deposit of the five longitudinal deposits on the disto-buccal surface is the second widest and measures approximately 0.25mm in width at its widest and also tapers to a point on the occlusal edge. Its cervico-buccal extremity widens considerably as it reaches the cervical edge and the colour of the deposit at the cervical edge is extremely dark brown approaching black. The texture is extremely thick and coarse at the cervical edge. The fourth longitudinal deposit and penultimately distal of the longitudinal deposits is extremely short vertically and measures approximately 1.0mm vertically. It texture is finer than the other vertical deposits and its colour is light brown. Its superior extremity is dark brown and is capped by an obliquely running inferiorly distal. The fifth and most distal of the vertical deposits located on the buccal surface deposit is the most narrow and the longest vertically. Its superior extremity touches the cervico-buccal edge and its most inferior end meets the occluso-buccal edge. Its most inferior extremity has a circular end, and the deposit is very fine in texture its colour is light brown. The vertical measurement of the most distal deposit measures 1.8mm and the horizontal measurement (width) is approximately 0.03mm at its widest.

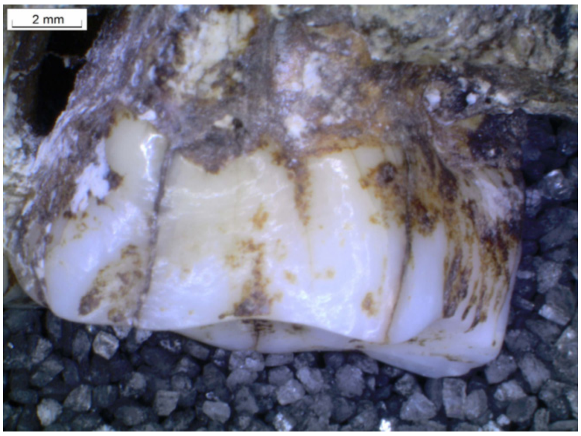

Figure 70: StW 53f LM3 buccal

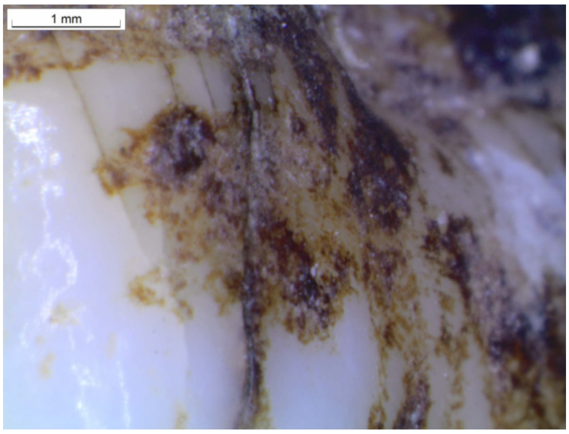

Figure 71: StW 53f LM3 buccal 6.3 x mag

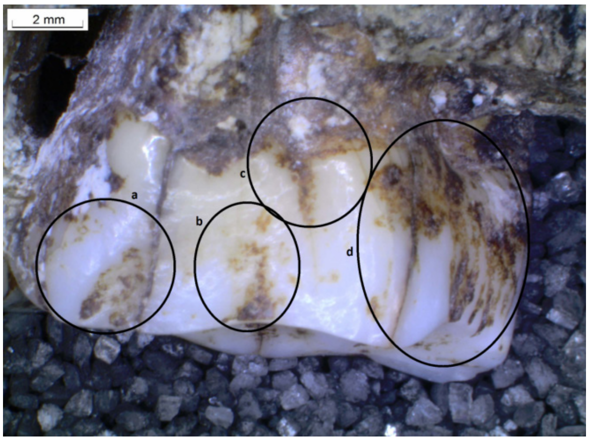

Figure 72: StW 53f LM^3 buccal 20x mag

Stw 53f LM^3 lingual (cervico-lingual and occluso-lingual)

The lingual surface of LM^3 exhibits six potential calculus deposits. A mesio-lingual deposit (sub-deposit f), a mid-occluso-lingual deposit (sub-deposit b), a disto-lingual deposit (sub-deposit a), a mid-centro-lingual (sub-deposit d) and two cervico-lingual deposits, one mid-cervical (sub-deposit c) and one mesio-cervical (sub-deposit e).

The mesio-lingual deposit (sub-deposit f) is made up of four disparately shaped elements, two in the occlusal margin, and two in the occlusal third of the tooth. The most mesial deposit within sub-deposit (f) looks like a hooked cane-shaped and is located approximately 0.75mm from the occlusal margin, and 0.55mm from the mesial margin of the tooth. Slightly distal (approximately 0.10mm) to this deposit is a narrow longitudinal deposit, which begins at the cemento- enamel junction and ends 0.75mm from the disto-occlusal surface. The texture is lightly coarse and uneven. Approximately 0.30mm distal to the longitudinal deposit is a narrow longitudinal deposit that curves distally and meets the occlusal edge. The superior (apical) edge of the deposit starts 1.95mm apical of the occlusal edge, and as it approaches the occlusal edge it curves distally. The texture of this deposit is coarse, uneven, condensed, and has no set configuration. The colours of all these mesio-lingual deposits are a range of light browns to dark browns (7.5 YR 6/4; 7.5 YR 5/4; 7.5 YR 5/2; 7.5 YR N2; 7.5 YR 3/2).

The mid-occluso-lingual deposit (sub-deposit b) is located within the middle third (mesio-lingually) of the tooth with the inferior margin (occlusal) on the occlusal edge. The sub-deposit ranges apically by 1.85mm from the occlusal edge. It is divided into two irregular and haphazard shapes with no set design one part tending obliquely distal, measuring 1mm horizontally at the superior end, 2,25mm horizontally measured at the occlusal base, and measures 2,2mm vertically. The distal segment curves distally and continues horizontally along the occlusal edge, while the mesial segment is situated obliquely mesial and measures 2.3mm vertically and apically from the occlusal margin. The horizontal width of the mesial deposit is 1.35mm measured at its occlusal base. It is an extremely tightly compacted deposit, roughly textured, amorphous and irregular with a mixture of light and dark brown colours (7.5 YR 6/4; 7.5 YR 5/4; 7.5 YR 5/2).

The disto-lingual deposit (sub-deposit a) is characterised by three isolated irregularly shaped sub-deposits. The most inferior deposit segment of sub-deposit (a) is located within the inferior margin of occlusal third and 1.9mm apical of the occlusal surface. It measures approximately 1.8mm horizontally at it maximum and approximately 1.2mm vertically at its maximum. It is an amorphous deposit with no set configuration. The texture in the distal portion is coarse and uneven. The mesial texture is more compacted, and grainy, but more homogeneous. The middle segment of sub-deposit (a) is located in the disto-lingual area of the tooth (the tooth has preserved without the complete distal end). It measures 0.45mm in diameter mesio-distally, and 0.25mm vertically. The superior deposit segment consists of three adjoining deposits; the most superior segment consists of two horizontally adjacent protuberances, each with a bulbous surface. Directly and obliquely below these two adjacent protuberant deposits is another two adjoining deposit segments. The superior deposit segments are all situated on an obliquely, narrowly longitudinal and inferiorly mesially oriented deposit. The oblique longitudinal deposit appears to originate from the inferior end of the superior deposit segment and eventually links the supero-mesial margin of the inferior deposit segment of sub-deposit (a). The predominant colours of sub-deposit (a) are browns (7.5 YR 5/2; 3/2; 4/2)

The cervico-lingual surface is characterised by two major deposits: infero-mesio-cervical (sub-deposit (e) and disto-, mid-, and mesio-cervical (sub-deposit [g]). Sub-deposit (g) is situated at the most distal cemento-enamel surface of the tooth, and extends through the mid-cervico-lingual area to the mesio-cervico-lingual surface. The disto-cervico-lingual presents with an irregular shaped darkish protuberance, located

1.00mm inferior to the mandibular margin. The mid-cervico-lingual surface presents with a large lightish coloured protuberance 1.25mm inferior to the mandibular margin. The mesio-cervico-lingual area presents with a spherical protuberant deposit which appears attached to a protuberant area approximately 0.9mm inferior to the mandibular margin. The cemento-enamel junction in the mid lingual area presents with a bulbous and smooth hemi-spherical-type deposit, approximately 1.1mm from where the root joins the mandible. The deposit that is adherent to the distal cervico-lingual areas of the root presents as granular, coarse, concentrated, and irregular. The texture of the mesial cervico-lingual area presents as concentrated, homogeneous and coarse, and less irregular. Colours are dark to light brown (7.5 YR N2; 7.5 YR 5/2; 7.5 YR 3/2).

The cervico-mesial deposit (sub-deposit [e]) appears to be a continuation of sub-deposit (g) however; this deposit appears to be attached to the cemento-enamel junction. The texture of this deposit appears homogeneously distributed over the deposit, concentrated, coarse, and the adherent material is not thick. Colour is dark brown (7.5 YR 3/2; 7.5 YR 5/2)

Sub-deposit (d) is located in the central, mid-lingual area, of the tooth. It measures 1.9mm horizontally in width, and 0.9mm in vertical height. The deposit has no set design or pattern and its texture presents with some thickness, the thickest of which presents with two vertical ridges and is located in the central area of the sub-deposit. This deposit is not fully condensed with adherent deposit material, showing enamel visible in several places between protuberant elements of deposit material. Colouring same as deposit (e)

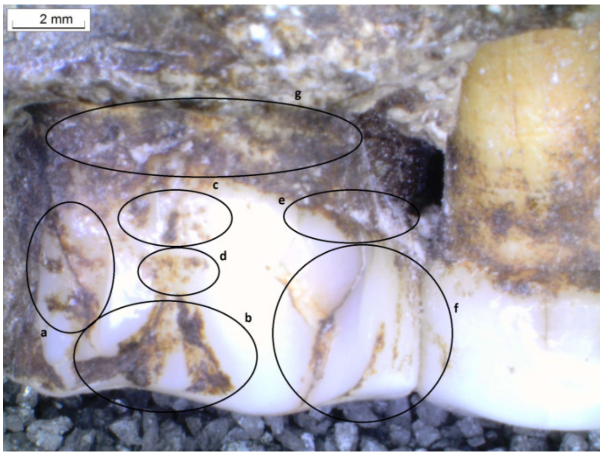

Figure 73: StW 53f LM3 cervico-lingual and occluso-lingual

Description of the adherents on Stw 532

LM_3 lingual

The lingual surface appears to be composed of several different types of deposits which could potentially be calculus. Sub-deposit (c) is located on the mesio-lingual surface and exhibits three major cluster deposits. The most inferior cluster, sub-deposit (c1) is composed of smooth and coarse deposits. The superior section of (c1) presents with two irregular, slightly coarse deposits, exhibiting a moderate thickness lying approximately 1.85mm and 3.0mm (c1iii and c1 ii) respectively distal from the mesio-lingual margin. Approximately 0.55mm distal to (c1ii) is a relatively small coarse and granular deposit (c1i). Sub-deposit (c1iv) lies 1.45mm distal of the mesio-lingual margin. It is a coarse and granular and uneven deposit. Sub-deposit (c1v) is made up of several different elements, for example, a rough spherical type deposit at the most distal part of the deposit with a narrow longitudinal deposit running through it; this longitudinal deposit extends superiorly into (c1ii) and inferiorly curves distally into sub-deposit (e). All sub-deposits (c1i-v) are located in the middle third of the tooth (mesio-lingually). Colours are seen as different hues of brown (7.5 YR 5/2; 3/2; 4/2)

Sub-deposit (c2) is composed of: a distal dark coloured deposit which appears to be associated with sub-deposit (c1iv). Mesial to the darkish deposit is a longitudinally narrow deposit. Its superior end is 1.15 apical to the occlusal edge. The longitudinal deposit measures 1.15mm vertically and horizontally measures 0.05mm wide. Sub-deposit (c2) presents with a smooth protuberance in the inferior part of (c2). Mesial to the smooth spherical-type deposit is a broadly rectangular deposit that is darkish superiorly and has a rough granular and moderately thick texture inferiorly. Colours

Subdeposit (c3) is composed of predominantly two deposit clusters located on the occlusal margin of the mesio-lingual surface of LM3, with the most mesial (c3i) and (c3ii) being 1.75mm more distally placed. Sub-deposit (c3i) can be further broken down into two elements, a broadly long element with a narrow width and superiorly exhibiting two 'horns' in mesial and distal superior corners, and an isolated more supero-mesial element. This deposit element appears lightly coarse and tightly compacted. Mesial and adjacent to this element is a thicker adherent deposit which is uneven and appears less coarse. Within sub-deposit (c3i) is an isolated relatively small deposit, approximately 0.10mm mesial of the larger distal element. This isolated element is lightly coarse, uneven, has a slight adherent thickness, is not compacted and not homogeneous in texture. Sub-deposit (c3ii) is located approximately 2.1mm distal from the mesio-lingual margin (measurement taken from the superior surface of [c3ii]). It measures approximately 1.15mm horizontally (at it maximum), and 1.8mm vertically. Deposit (c3ii) comprises a haphazard grouping of thickly adherent material with no apparent pattern. The texture of the material in the mid-distal area is coarse, granular and presents with several spherical protuberances, and the overall texture of deposit (c3ii) is coarse, uneven and heterogeneous. Colours are browns (7.5 YR 5/2; 3/2; 4/2)

Sub-deposit (a) comprises a cluster of different deposits and is situated on the distal cervico-lingual surface of LM_3. All deposits in this cluster are located within the distal third of the tooth (occluso-apically). Deposit (a1) is located 1.75mm from the distal margin of the tooth, and is made up of several irregularly shaped deposits, which appear to be stains and have no adherent depth. Sub-deposit (a2) is situated on the cemento-enamel junction, and extends 1.35mm occlusally from the CEJ. It is 1.9mm wide horizontally, and is 1.0mm mesial of the disto-lingual margin. Deposit (a2) also presents with a globular spherical element, located slightly mesially of the centre of the cemento-enamel boundary of (c2). The texture of deposit (a2) is coarse, granular and homogeneous. Sub-deposit (a3) is located slightly mesial deposit (a2) on the cemento-enamel junction and appears to be a continuation of (a2), and consists of a roundish protuberance, which is surrounded with a smooth material with no granular texture. Mesial of the protuberance is smooth material with no adherent depth. The deposit has no set pattern or design. Sub-deposit (a4) appears to begin inferiorly at the cemento-enamel junction (slightly out of the demonstrated circle of [a4]), and is characterised by a bifurcation with the two divisions of the bifurcation indicating infero-distally and infero-mesially. It appears to be composed of a thinly adherent material, with some thickness. It measures 2.05mm vertically and 1.75mm at it widest, which is in the superior area of the deposit.

Sub-deposit (d) is located on the cemento-enamel junction, which is composed of three separate and moderately thick adherent deposits. The texture is uneven, and moderately coarse. This deposit also presents with a sharply-edged, relatively small double protuberance (d2) directly below the middle element of the deposit (d1) on the CEJ. The texture of (d2) appears highly concentrated, and moderately coarse. Colour (7.5 YR 5/2; 3/2; 4/2).

Sub-deposit (b) is located in the distal occluso-lingual and mid-occluso-lingual surface of the tooth. Deposit (b1) consists of two different types of material; a lightly adherent distal element with minimum adherent depth and thickness, and a slightly supero-mesial element which is coarse and granular and contains a roundish protuberance in the supero-distal corner of (b1). Deposit (b2) is made up predominantly of two deposits, one on the occluso-lingual margin in the middle third of the tooth (occluso-apoically), and the other directly inferior to the first. The deposit located on the occlusal margin is has an approximate horizontal width of 1.9mm, and a vertical length of 1.75mm from the occlusal margin. The texture of the deposit situated on the occlusal margin is coarse, uneven, and exhibits a considerable thickness in the central portion of the deposit. This central deposit also presents with a dark colour. The texture on either sides of the dark central deposit exhibits a slightly less coarse texture, and the colour of the deposits located on either side of the central deposit are several tones lighter. Sub-deposit (b3) is located in the mid-occluso-lingual area, with the superior portion of deposit (b3) located on the occlusal margin, measuring 1.35mm horizontally, and 0.25mm in vertical width (at its maximum). Both ends of the superior part of the deposit taper narrowly and horizontally, with the distal end coming to a point, and the mesial end measuring 0.05mm in vertical width. The inferior portion of the sub-deposit (b3) may be divided into two elements. The infero-mesial element is situated 0.75mm apically from the occlusal margin, and the infero-distal segment is located 0.25mm apically from the occlusal margin. The distal segment of the inferior deposit of (b3) has a coarse, uneven, thick adherent material. The texture of the inferior most part of the inferior segment of (b3) is compact, grainy and even. The texture of the middle section of the inferior segment of the deposit (b3) is coarse, uneven and not condensed or grainy. Colours are described as brown and grey (7.5 N3; 5/2; 3/2).

Sub-deposit (e) is located on the mesio-lingual cemento-enamel junction, 1.35mm distal of the mesio-lingual margin. The vertical length of the deposit is 2.05mm, with the horizontal width measuring 1.975mm. The texture on the inferior portion of (a3) is coarse, haphazardly moderately thickly adherent and uneven. The supero-distal texture is compact, and heterogenous; the supero-mesial texture is granular, coarse and uneven. Colour (7.5 YR 5/2; 3/2) is brown.

Sub deposit (f) is located at the occluso-disto-lingual margin of LM_3. The occluso-horizontal width measures 1.45mm and the vertical length from the occlusal margin measures 1.50mm. The texture is rough, grainy, and uneven, with many adherently thick, relatively small haphazardly placed protruding elements, exhibiting an irregular surface. The general shape is amorphous. Colour is a mix of browns (7.5 YR 5/2; 3/2; 4/2).

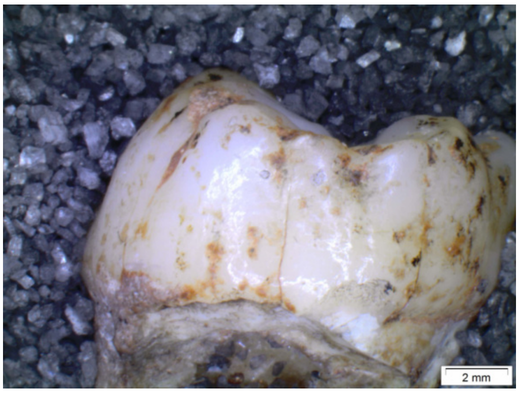

Figure 74: Stw 532 LM$_3$ lingual

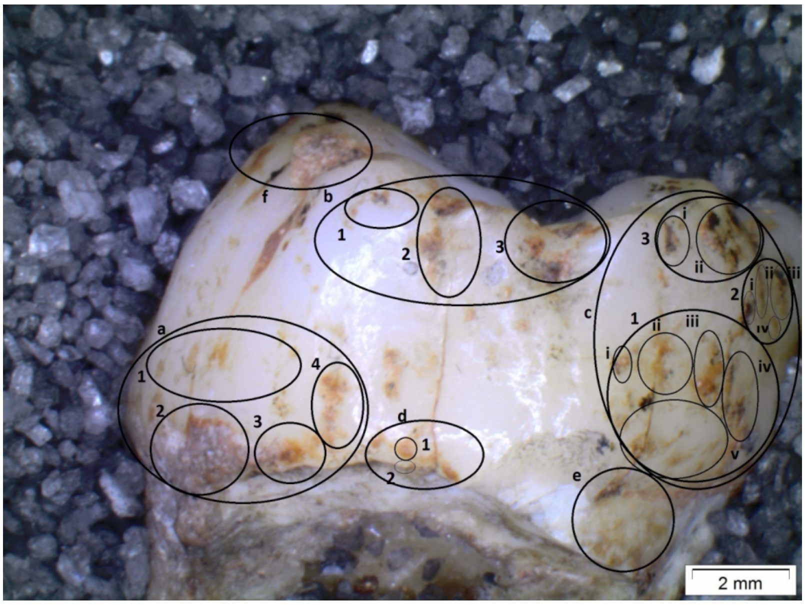

Fig. 23 Stw 532 LM$_3$ lingual

Descriptions of adherents on Stw 498*d*

LM$_1$ disto-lingual

The disto-lingual surface of LM1 presents with an extremely coarse deposit (sub-deposit [a]) of probable calculus, that begins at the disto-occlusal margin on the lingual surface of the tooth, and extends apically (inferiorly) through the middle third into the cervical third of the tooth. The deposit then extends mesially from the disto-lingual area to the start of the middle third of the lingual surface (mesio-lingually). As the deposit extends mesially, the deposit presents with several isolated small sub-deposits by the time it reaches the middle lingual third. The distal material presents as extremely thick and 'crater-like' in appearance and considerably coarse and irregular, and the distal part of the deposit is (colour) reddish dark brown tending to a grey-brown colour as it extends mesially. The supero-, mid-distal, and infero-distal, and the distal cervico-lingual surfaces of sub-deposit (a) are extremely coarse, highly irregular and amorphous, and present with no apparent organised pattern. The coarseness of sub-deposit (a) tends to become relatively less coarse and more homogeneous as the deposit extends mesially. The horizontal width of the superior edge of occluso-disto-lingual deposit is approximately 3.2mm and the horizontal width of the inferior portion of the disto-lingual deposit is 4mm wide. Sub-deposit (a) measures approximately 4mm vertically.

The middle-cervical and mesio-cervical areas (see sub-deposit [b]) appear to exhibit a thick, irregular and coarse deposit. Sub-deposit (b) measures 6.35mm horizontally, and ranges from the middle cervico-lingual third to the mesio-lingual margin. The vertical length is 2.1mm. The deposit in the central portion of the cervico-lingual margin appears to extend into the cementum of the tooth (b1). The mesio-cervical deposits are a pinkish grey (7.5YR 6/2). The distal and middle parts as well as the mesial part of the occluso-lingual junction appears to have a series of isolated light brown stains, but seems to have an absence of extractible material. There is no topographical depth to this series of deposits.

Sub–deposit (c) is composed of a very light film-like deposit; however it is smooth and exhibits no thickness. It appears as if there is no extractible material from this film-like material. This deposit also presents with several distinctly isolated, thicker, coarser and uneven deposits, one of which is located on the mid-occluso-lingual surface. It is longitudinal in shape (c1) and extends apically by1.05mm from the occlusal surface. Two other isolated coarse, smaller deposits (c2) are located approximately 0.75mm apical of the occlusal deposit situated in the middle third of the tooth. Sub-deposit (c) also presents with an extremely narrow longitudinal deposit 1.1mm mesial of (c1), and it appears as if this deposit formed in a crack at the mid-occluso-lingual margin. This deposit begins at the mid-occluso-lingual margin and extends apically 1.35mm from the mid-occluso-lingual margin. The colour of the sub-cervical enamel junction deposit is also a pinkish grey (7.5YR 6/2).

Sub-deposit (d) is a broadly longitudinal deposit located 0.75mm from the mesial edge of supero-mesio-lingual margin of this deposit. It ranges approximately 4.0mm apically from the occluso-mesio-lingual edge to the lower approximate margin of the middle third of the tooth. The texture of this deposit is coarse, irregular and presents with a moderate thickness, however the texture exhibits a larger thickness especially 1.15mm apical of the occluso-mesial margin, where this deposit appears to exhibit a roundish protuberance, which is adherently extremely thick, and coarse. This deposit does not present with a set pattern, other than being formed in a crack, which appears to give it a longitudinal form. Colours present with dark browns and greys (7.5 YR N3; 5/2; 3/2; 4/2).

Figure 75: StW 498d LM1 disto-lingual

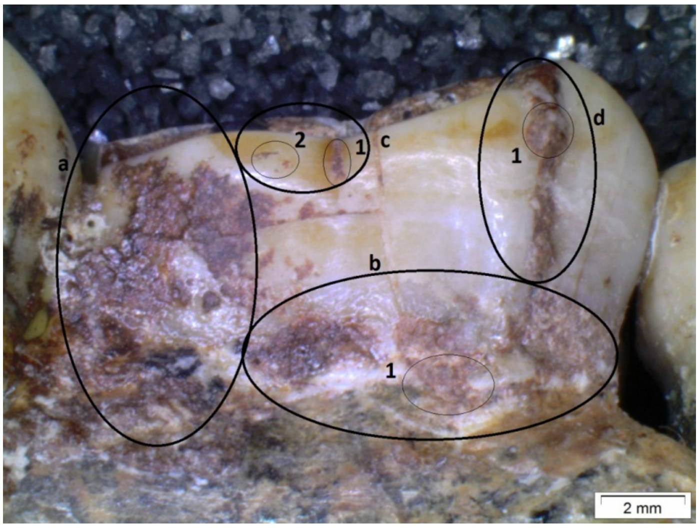

Figure 76: StW 498d LM1 disto lingual 6.5 x mag

Stw 498d

LM_1 distobuccal

Several potential calculus deposits appear to be located on the buccal surface of LM_1. Sub-deposit (a) presents with three sub-segments, which are located on the middle disto-buccal margin (ai), disto-cervico-buccal surface (aii), and in the infero-cervico-distal inter-proximal space between LM_1 and LM_2, deposit (aiii).

Sub-deposit (ai) is made up of two sub-segments, one of which is situated on the middle disto-buccal margin. The other sub-segment is located 0.20mm mesial of deposit (ai), and is a relatively small, isolated deposit presenting with several protuberances and exhibiting a moderately thick texture Sub-segments (ai and aii) appear to be a conjoined deposit and (aiii) presents as a separate, isolated deposit. Sub-deposit (a) and its sub-segments exhibit as an irregularly shaped deposit. The disto-buccal deposit [sub-segments (ai) and part of (aii), presents with an oblique mesial margin, and extends supero-distally from the cervical margin (which falls into sub-segment [aii]) to the beginning of the inferior margin of the occlusal third (approximately 1.35mm from the occlusal margin). Sub-segment (aii), appears to extend from the disto-cervico-buccal area apically (inferiorly) onto the mandibular bone and lies inferior and partly mesial to the interproximal deposit. Its texture is coarse, granular and uneven. Sub-segment (aiii) is located infero-distal of sub-segment (ai) and distal of sub-segment (aii). Although the surface texture of the sub-segment (aiii) presents as rough and uneven, it appears as if the surface of this deposit is covered with a glazed glue-type covering. The colouring of the disto-buccal, the sub-cervico-buccal, and the interproximal space between LM_1 and LM_2 is brown (7.5YR 5/2). In the centre of this deposit there is an inner circular shaped form which has a dark brown colour (7.5YR N2/0). The circular inferior part of this deposit has a lighter brown colour (7.5YR 6/4). The mesial side of this circular deposit is brown (7.5YR 5/2). The extreme distal part of the interproximal deposit has circular adherence exhibiting a pink colour (7.5YR 8/4). The most inferiorly distal part of the deposit is characterised by a longitudinal form which is attached to the inferiorly mesial part of LM_2. The inferior horizontal measurement of the interproximal deposit on the cervico-buccal margin is

2.1mm, and the vertical measurement from the cervical boundary to the superior extent of the interproximal deposit is 1.7mm.

Sub-deposit (b) is located on the distal portion of the occluso-buccal surface, within the distal third of the tooth (mesio-distally). It begins at the distal margin and ranges for 3.00mm mesially from the distal margin. The texture is smooth and appears to have no thickness. It presents as a probable staining as it demonstrates no removable material. Colour mix is browns and greys (7.5 YR N3; 3/2; 4/4; 4/2).

Sub-deposit (c) is another potential deposit which is located in the mid-buccal cemento-enamel area, within the middle third of the tooth (mesio-distally). The deposit measures 2.25mm horizontally and measures 0.20mm wide at its mesial end. The deposit appears broadly as a generally rectangular deposit, with the superior edge curving inferiorly distally at approximately 1.1mm from its mesial end. The texture of this deposit is coarse, grainy and uneven. Colour (7.5 YR N) is grey.

A mesial deposit is located in the middle third of the tooth mesio-distally at the cervico-enamel junction. The deposit is coarse and exhibits a similar brown colour to the disto-buccal and subcervico-buccal deposits (7.5YR 5/2). This deposit has a more or less horizontally longitudinal form and dips slightly inferiorly distal. It measures 2.4mm horizontally and has a vertical width of 0.85mm at its maximum.

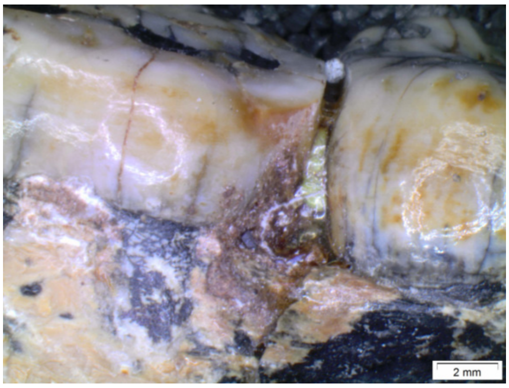

Figure 77: StW 498d LM1 distobuccal

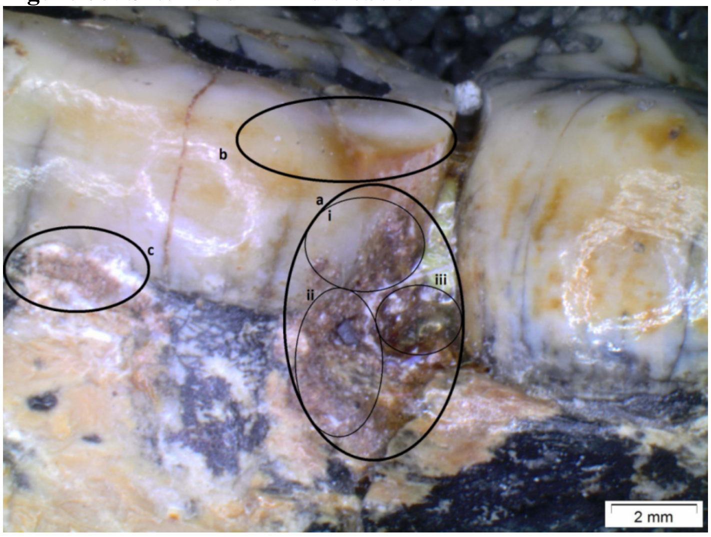

Figure 78: StW 498d LM1 distobuccal

Stw 498d

LM$_2$

On the buccal surface especially on the mid cervico-buccal section there appears to be a layer of potential calculus. The deposit seems to be extending slightly obliquely inferiorly into the adjoining mandibular bone and also appears as if this deposit lies distinctly between the enamel and the adjoining bone. The deposit is thinner at its mesial part and gradually gets wider distally. The mesial portion curves superiorly ending in a point. The mesial section of the superior surface exhibits a small upward pointing hook form. The distal end of this deposit appears to end in a circular shape.

The horizontal measurement of this portion of the deposit is 3.1mm with a vertical width of 0.9mm at its minimum and 1.2mm at it's widest. This deposit is composed of two colours. The mesial and mid-section of the deposit is grey (7.5 YR N5), while the distal circular section exhibits a black colour (7.5 N2). The circular black section potentially exhibits a courser material than the rest of the grey deposit. This deposit continues to extend cervico-buccally and until slightly before the disto-buccal margin where it extends supero-distally until the distobuccal margin is reached.

In the more distal mid-cervico-buccal surface the deposit appears to change colour. This section of the deposit exhibits a white colour (7.5YR N8). The texture appears coarse and irregular in form. The horizontal white section of the deposit meausures approximately 3.15mm, and measures 1.7mm vertically. The deposit continues to extend distally changing colour again, the next section of the deposit approaching in parts, the dark black colour (7.5 N2) of the circular section in the mid-section of the buccal service. The final section of the distal cervico-buccal deposit is characterised by two sections differentiated by colour. The mesial section is a light grey (7.5YR N7) colour, while the distal section is a pinkish grey (7.5YR 7/2). The texture appears slightly coarser than the most mesial deposit's texture. The mesial section has width vertically of 1.6mm and tapers distally to a minimum width of 1.5mm, whereas it measures 1.9mm horizontally. The centre of this section of the deposit has a grey colour (7.5YR N5). The second part and distal section of this deposit is situated slightly supero-distal to the mesial section and has a minimum width of 0.8mm at the mesial end of the deposit which tapers distally to a maximum width of 1.8mm where the tooth surface ends, and it appears as if there is a missing fragment before mesial surface of

LM_3 begins. Slightly mesial to the surface of the adjoining LM_3 there appears to be a further thin longitudinal potential calculus deposit attached to the mesial LM3 buccal surface. The horizontal width at the base of the deposit is 1.2mm and the vertical height is 1.65mm.

Disto-buccal

The disto-buccal surface of LM_2 presents with a potential calculus deposit that comprises a superior and an inferior segment, which is divided by an area of relatively clear enamel [sub-deposit (a)]. The sub-deposit begins 1.15mm sub-occlusally and ranges apically for 3.8mm until it reaches the beginning of a disto-buccal cavity, located adjacent distally to LM_3 and which continues inferiorly to the mandibular bone. The superior segment of sub-deposit (a) is an irregular, coarse and uneven deposit that exhibits a moderate thickness tending to become thicker as it extends distally towards the interproximal area between LM2 and LM3. The texture of the inferior segment is rough, uneven, concentrated and extremely coarse, and presents generally with a light colour, although the lateral sides of the inferior segment of sub-deposit (a) exhibit a variety of different colours. The inferior base of this sub-deposit, which is also the superior margin of the distal cervical space, appears to have a crumbly texture. The maximum horizontal measurement is approximately 2.25mm, and reaches a maximum of 3.9mm vertically. The colour of the superior portion to the middle section of the mesial part of the sub-deposit is dark grey (7.5YR N 4). The colour of the mesial portion from the middle section to the base inferiorly is borderline light grey and grey (7.5 YR N6), and the distal portion is pinkish white (7.5YR 8/2). This particular subdeposit is characterised by two predominant colours split vertically down the middle superiorly until the centre of the deposit, where an isolated portion of the mesial deposit extends into the distal half. The colouring of the mesial portion inferior to the middle then extends obliquely into the distal section resulting in the distal colouring becoming narrower inferiorly until the base where the colour of mesial part of this deposit dominates.

Distobuccal (occlusal third; middle third)

There appear to be two probable calculus deposits located between the occlusal third and the proximal area of the middle third of the distobuccal surface. Another cluster deposit is located with one subdeposit on the middle margin dividing the buccal surface relatively in half; and two associated subdeposits, one located slightly infero-mesial to the subdeposit on the middle-marginal deposit and one located inferiorly to the distally situated middle-marginal deposit.

The most inferiorly mesial deposit is attached to the occlusal third of LM_2 and is characterised by an irregular shape, has a light cream colour, and appears the deposit is composed of a coarse material, but much finer than the texture of the deposit on the most disto-buccal surface. It is made up of a superior mesial deposit and a more distal longitudinal deposit which appear to be joined superiorly. The maximum horizontal width measures approximately 1.8mm, and the length of the longitudinal section is 2.1mm.

Slightly mesial to this creamy deposit, there is a relatively large, dark reddish grey (10YR 3/1) deposit located superiorly on a distally located occluso-buccal development groove, which extends between the occlusal surface margin and the middle third of the disto-buccal surface. The texture of this deposit is extremely well compacted and coarse. The deposit measures 4.1mm vertically (measured to the occlusal surface), and 1.8mm at its maximum which is slightly superior to the midline (mesio-distally) of LM2. The minimum width is found at the inferior base of this deposit, and measures 0.9mm.

A cluster deposit consisting of a series of unstructured, irregular formed deposits, the first of which is located on the midline (mesio-distally) of the LM2 appears to be mostly dark brown (7.5YR 3/2), tending to become light brown (7.5 YR 6/4) at the edges of most isolated sub-eposits of this part of the cluster deposit. The texture appears very tightly compacted and reasonably coarse although still finer than the mid-cervico-buccal deposits. The direction of the deposit lies mesio-distally, and measures 2.1mm horizontally and 1.15mm vertically.

The deposit lying infero-mesially to the deposit on the midline of the tooth is a small deposit which appears to be compactly structured with a textured surface that is fine to slightly coarse in structure. It can be characterised as having a spherical head and base with a short wavy vertically longitudinal element joining the two spherical head-type forms proximally and distally. It measures 1.05mm vertically with a width of 0.65mm. The colour is grey (7.5 YR N5).

Another potential sub-deposit lies directly inferior to the middle marginal deposit which appears to be situated on the margin that divides the buccal surface in half, and forms part of the inferior placed disto-buccal cluster. The deposit has a shape which is wider at the superior end than the inferior end. Its mesial corner has a dark corner fragment, with the rest of the deposit appearing rough with a comparable texture to the most distobuccal deposit. The colour of this inferior deposit is gray (10YR 5/1) with the darker supero-mesial corner fragment a very dark grayish brown (10YR 3/2). The horizontal measurement of the superior and wider end is 1.85mm and the base width is 1.00mm. This deposit measures 2.2mm vertically.

Figure 79: StW 498d LM$_2$ mid cervico-buccal; disto-cervicobuccal

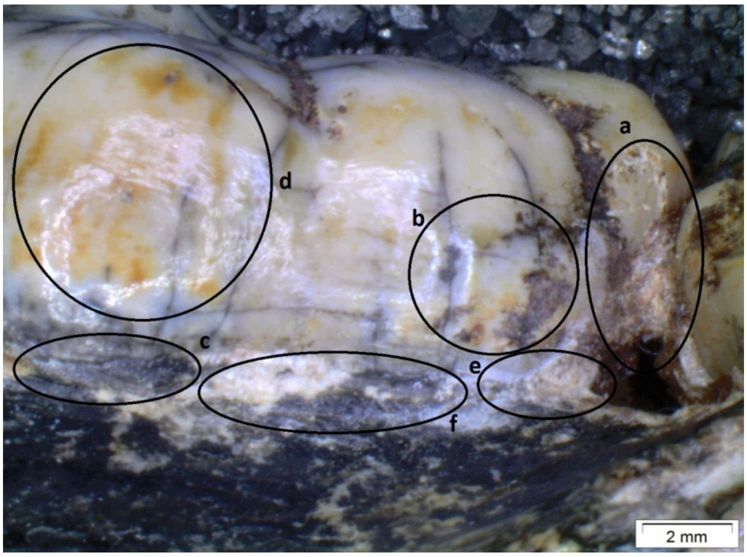

Figure 80: StW 498d LM$_2$ disto-buccal; occluso-buccal

Stw 498d LM_2

Mesiolingual; cervicolingual

There appears to be two major areas of probable dental calculus, the mesiolingual side of LM_2 between the cervicolingual and middle third of the tooth designated by the larger of the superior circular figures (Figure 83), and the cervicolingual area, which extends for most of the mesiodistal length of the tooth demarcated by the lower four circled areas (Figure 83). There is also several much smaller potential calculus depositions clustered in an amorphous manner in the central cervicolingual area, designated by the second largest circular figure located above the four lower circular figures and distal to the largest circular figure (Figure 83).

Mesiolingual

The deposit situated on the mesiolingual side of the tooth extends mesiodistally from approximately the central lingual area to the more or less the mesiolingual border, between the cervico-lingual third and the superior margin of the middle third of the tooth. The superomesial part of deposit is characterised by a very dark colouring in two shades of dark reddish brown which extends inferiorly mesial to the cervico-lingual border. The more mesial part of the deposit is a dark reddish brown (5YR 3/4) and the more distal part of the deposit is a shade lighter (5YR 3/3). The texture of the material of this deposit appears to be finely compacted and is devoid of any pattern. As the mesiolingual deposit extends more distally, more particularly the portion of the deposit that lies toward the centre of the tooth lingually and superiorly to the cervico-lingual deposits, the colouring changes to dark grey (5YR 4/1). This part of the deposit appears slightly coarser than the rest of the mesiolingual deposit. The horizontal mesiolingual deposit measures approximately 7.9mm in diameter, while the vertical height measures 3.3mm at its maximum.

Cervico-lingual

The cervico-lingual deposit which is indicated by the lower four circular figures (Figure 83) appear to extend across most of the tooth mesiodistally and is adherent to the cervico-enamel border. The texture is thicker and coarser throughout this deposit than the mesiolingual deposit, and is composed of a different colouring than the mesiodistal deposit. The colouring of this deposit is a weak red (2.5YR 5/2) and appears to be homogeneously distributed throughout.

Disto-lingual cluster

Slightly superior to the distal cervico-lingual deposit and more or less in the central lingual area is a potential calculus cluster deposit, made up of amorphously placed small circular-formed spotted deposits. This calculus deposit adheres to the enamel directly. The texture is compact and coarse and similar in coarseness and colour to the cervico-lingual deposit, being a weak red (2.5YR 5/2). The extent of the horizontal diameter measures approximately 3.2mm and the approximate vertical width of the cluster is 1.2mm.

Figure 81: StW 498d LM2 mesio-lingual

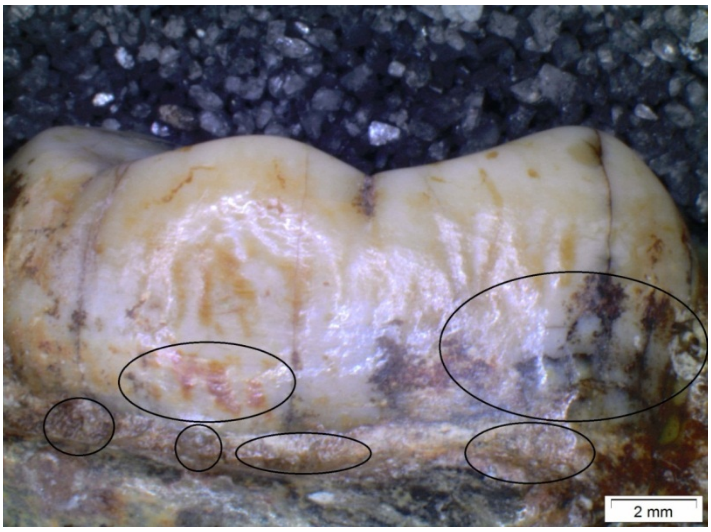

Figure 82: StW 498d LM2 mesio-lingual enlarged with potential deposits

Stw 498d LM_3

Distobuccal

The buccal side of LM_3 appears to have two predominant areas of probable calculus. The two predominant deposits and other minor deposits are situated distobuccally and are irregular in form. The more mesial of the two distal deposits extends superiorly buccal, from the cervical third until the middle third mesiodistally. This deposit is situated at the vortex of two fractures on the buccal surface and extends to approximately the middle of the 'V' shaped fracture, thereafter it decreases in thickness and tapers obliquely mesially and distally as the 'v' fracture widens. The portion of the mid-buccal deposit located on the more mesial oblique fracture line is much wider than the deposit on the distal oblique fracture line. The second and more distal deposit intersects inferiorly at the base of the more mesial deposit and extends distally along the cervical border of the buccal surface until the distobuccal angle is reached. There is a further smaller and finer textured deposit in the superior portion of the 'v' shaped fracture. This subdeposit is much darker in colour than all the other buccal deposits of LM_3.

The texture of all the deposits appears to have a similar coarse texture, and is resolutely attached to the buccal enamel surface. The cervico-buccal deposits seem slightly coarser than the deposits more superiorly placed on the mid-buccal surface.

The cervicobuccal base of most inferiorly mesial of the buccal deposits of LM_3 has a very dark grey colour (5YR 3/1). The more superior deposit on the mesial oblique 'V' shape fracture is dark grey (5YR 4/1). The smaller finer deposit that is superiorly placed between the 'v' shape fracture appears mostly black (5YR 2/1). The colour of the two more distally placed cervicobuccal deposits is (5YR 4/1) with the more mesial of the two having a yellowish red base (5YR 4/8). The most superior edge of the yellowish red base of the cervicobuccal deposit is darker and has a more dark reddish brown colouring (5YR 3/4). There is a patch of yellowish red on the superior edge of the most distally cervicobuccal deposit.

The more mesial of the distobuccal deposits has a vertical measurement of 3.7mm at its maximum, which is measured from the cervicobuccal base to the maximum extent of the deposit at the obliquely mesial and distal extremities of the 'V' fracture. The horizontal measurement of this portion of the cervicobuccal deposit is 2.5mm at its widest, which is at the cervicobuccal base. The vertical width of the cervicobuccal base deposit (occluso-apically) is 1.0mm. The middle cervico-buccal deposit measures 1mm horizontally and 0.5mm vertically. The most distally cervico-buccal deposit measures 1.5mm horizontally and 1.5mm at its vertical maximum.

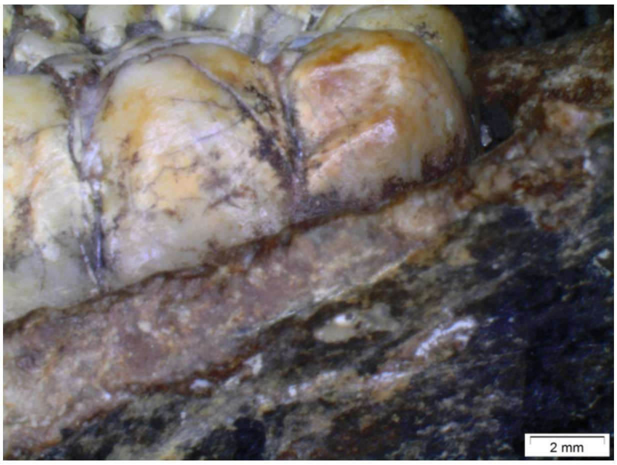

Figure 83: StW 498d LM3 disto-buccal

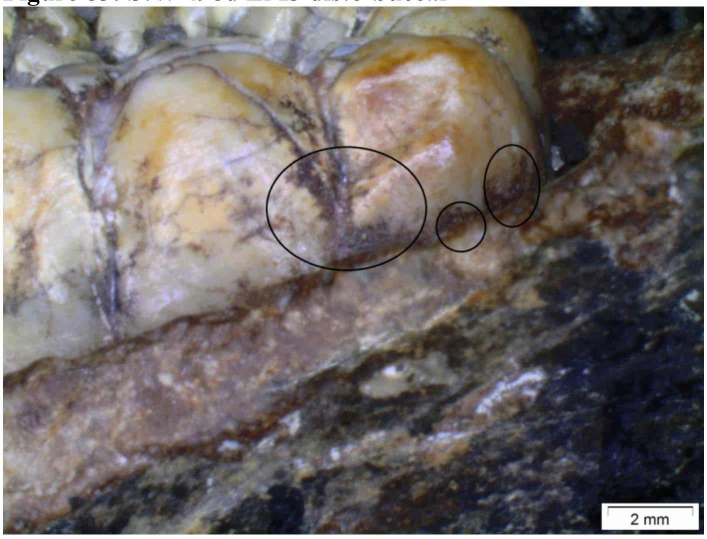

Figure 84: StW 498d LM3 distobuccal enlarged

Stw 498d LM_3

Distolingual; cervicolingual

The major locations of probable calculus deposits on the lingual view of LM_3 are found on the distolingual and cervicolingual areas and are enclosed distinctly in five circular figures and one rectangular one (see Figure 87).

The most distolingually located deposits are demonstrated by the three most distally circular figures making up this particular cluster of potential calculus deposits. The most superior subdeposit in the cluster appears to be a very finely textured, slightly coarse material, and is formless. The colour of this subdeposit is grey 7.5YR N6. It has an approximate vertical measurement of 1.9mm and measures approximately 1.7mm horizontally. The second part making up the deposit cluster is a subdeposit which lies slightly infero-distal to the first subdeposit, and is similar in coarseness, general texture and it is a similar grey colour to the more superior subdeposit (7.5YR N6). The second subdeposit measures approximately 1.9mm vertically and approximately 1.9mm horizontally. The third subdeposit making up this cluster lies inferior to the second subdeposit and exhibits a similar haphazard formless pattern; however this subdeposit has a coarser texture and a different colour than the latter two subdeposits. The horizontal width of this deposit measures approximately 1.8mm and the vertical height measures 1.8mm. The colour of this deposit is a slightly darker shade of grey (7.5YR N5).

The fourth probable deposit is demonstrated by a larger singular circular figure which lies slightly mesial to the three latter distal deposits. The fourth deposit lies beneath a fracture line which runs vertically from the occlusal surface of the tooth to approximately where the superior area of the deposit begins. This deposit appears to be composed of a different texture and colouring to the first and second subdeposits but is somewhat similar to the third and inferior of the latter deposits. The texture of this deposit is coarser when compared to the very fine texture of the first two subdeposits of the first cluster. It exhibits a creamy coloured material which is intermittently interspersed within the darker parts of the deposit. The deposit is much thicker than the latter three distal subdeposits, and the distal part of this fourth deposit appears to have an adherent thickness that is at least greater than the thicknesses of the latter finely textured distal subdeposits. The horizontal width of this deposit measures approximately 3.1mm, and has a vertical height of approximately 3.55mm. The colour of this deposit is dark grey (7.5YR N4).

The fifth subdeposit lies mesial to the fourth deposit and it exhibits similar qualities. For instance, it appears to be composed of the same material texture and thickness and the same intermittent creamy deposit meshes its way into the dark areas of the deposit. Its thickness and adherent qualities seem to be identical to the fourth deposit. The colour of this deposit appears as pinkish grey (7.5YR 6/2).

The sixth deposit lies on the cervico-enamel junction of LM_3 and the junction with the mandible. It is illustrated inside a rectangular box. It is the most inferior of the potential deposits on the lingual side of the tooth. It has a linear structure and ranging mesially until the most mesial extent is positioned directly inferiorly to the most mesial extent of the fourth deposit. The texture of this deposit is lightly coarse distally, extremely coarse in the central part, and then tapers off into a light coarse texture mesially. The central part of this inferior deposit appears to spread obliquely mesially and inferiorly onto the mandible. The approximate horizontal deposit measures 5.95mm, and the vertical width measures approximately 0.9mm. The colour in the central part of this deposit is pinkish grey (7.5YR 6/2). The distal and mesial ends are light grey (7.5YR N7)

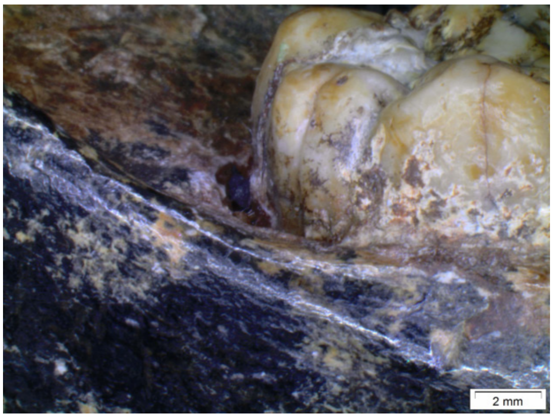

Figure 85: StW 498d LM3 distolingual

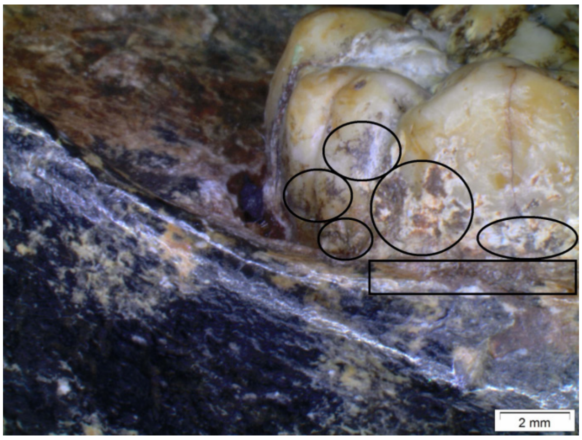

Figure 86: StW 498d LM3 distolingual with potential deposits

Description of adherents on Stw 559

RM^3

Mesial

Cervico-mesial

Subdeposit (a) contains a probable calculus deposit which appears to be adherent to the cervico-mesial surface of RM^3. This deposit is located mostly between the cervical and middle thirds of the mesial surface of the tooth. It extends apically adhering to the *cementum* and occlusally adhering to the enamel of the mid-mesial and bucco-mesial surfaces. The deposit also extends into the occlusal third, between the bucco-mesial and mid-mesial thirds, but it does not the reach the occlusal margin. The texture horizontally (bucco-distally) along the mesial surface is very coarse and granular. The cervico-mesial deposit appears to begin at the buccal edge and extends toward the mid-cervico-mesial area. This deposit extends occlusally into the cervico-mesial third. This deposit also extends apically from the cervico-mesial margin within the buccal third onto the cementum apical to the CEJ (cemento-enamel junction). As the deposit extends occlusally the texture appears to get generally thinner and finer on this surface of the tooth, however there are three distinctly thick globular areas to this deposit. The first globule (see figure 88 [1]) is located slightly occlusal to the *cemento*-enamel junction within the bucco-mesial third. The second globule (see Figure 88 [2]) is located slightly infero-buccal to globule (1), and the third globule (see Figure 88 [3]) is directly inferior to the globule (2). The horizontal measurement of the cervico-buccal portion of the subdeposit (a) is 3.95mm, and the maximum cervico-buccal vertical width is 1.8mm. The horizontal measurement of the portion lying apically from the cervico-buccal margin is 3.05mm, and the vertical width of this portion is 3.05mm. The total maximum vertical width of subdeposit (a) is approximately 4.85mm. The thickeness of the subdeposit (a) appears to be at least 0.5mm thick at the bucco-mesial border and more or less horizontally (bucco-lingually) across the cervico-mesial area.

Subdeposit (a) is made up of mainly of one colour of yellowish brown with two distinct shades. One of which is a shade of yellowish brown (10YR 5/4), and appears in the most bucco-mesial area, at the bucco-mesial margin where the deposit extends over into the *cementum*; the other is a slightly different shade of yellowish brown (10YR

5/6), and is the predominant shade of this sub-deposit (a), occurring in the most bucco-mesial area, and extending horizontally across the horizontal cemento-enamel margin for approximately half the area of the tooth, ending midway into the midmesial third of the tooth bucco-lingually.

Sub-deposit (b) is mostly attached to the *cementum*, slightly apical to the mid-bucco-mesial margin of RM^3. A small portion of this sub-deposit also adheres to the mid-cervico-mesial margin in the middle third and close to the beginning of the lingual third of RM^3. It is a smaller deposit than sub-deposit (a). Horizontal measurement of this sub-deposit is approximately 1.1mm and its vertical measurement is approximately 1.1mm. It has an amorphous shape. The texture of this deposit is generally coarse and it appears that the thickest part presents with a very thick, darker globule in the supero-lingual aspect of sub-deposit which is located adjacent to the lingual third of RM^3, lying slightly apical to the cemento-enamel junction (CEJ). The small sub-deposit (b) presents as a shade of brownish yellow (10 YR 6/8).

Sub-deposit (c) shows that the extension of the sub-deposit (a) and globular deposits (1-4) which began on the *cementum* and cemento-enamel junction as a very thick, coarse and granular deposit, has culminated into a very thinly adherent deposit [see sub-deposit (c) in Figure 88] and it has diminished to a slight and much finer deposit of small spotty speck-like material. The colours in this sub-deposit are shades of yellowish brown (10YR 5/4) and (10YR 5/6).

Figure 87: StW 559 RM^3 mesial

Description of adherents on Stw 483

LM^3

Buccal

Deposit (a) is a singular deposit and located on the distobuccal surface, slightly apical to the occlusal margin of LM^3 and mostly in the occlusal third (mesiodistally), with the supero-distal corner extending into the middle third of LM^3. The horizontal measurement is 1.45mm, and the vertical measurement is 2.2mm. The texture of this deposit is extremely coarse and granular and is amorphous. The texture varies in thickness, and in some places appears to reach approximately 0.5mm. Deposit (a) is made up of 3 different colour groups, a1, a2, and a3. Deposit (a1) located supero-distally, comprises 3 different colour groups: a supero-buccal segment within sub-deposit (a1) which is dark red (2.5YR 4/4); a distal segment which is black (2.5YR N2); and an inferior segment which is very dusky red (2.5YR 2/2) (see fig.37). Deposit (a2) which is located bucco-distally, is dominated by a dark reddish brown colour (5YR 3/2). Deposit (a3), which is located bucco-inferiorly, is dominated by two colours, light grey and very dark greyish brown (10YR 7/2 and 10YR 3/2).

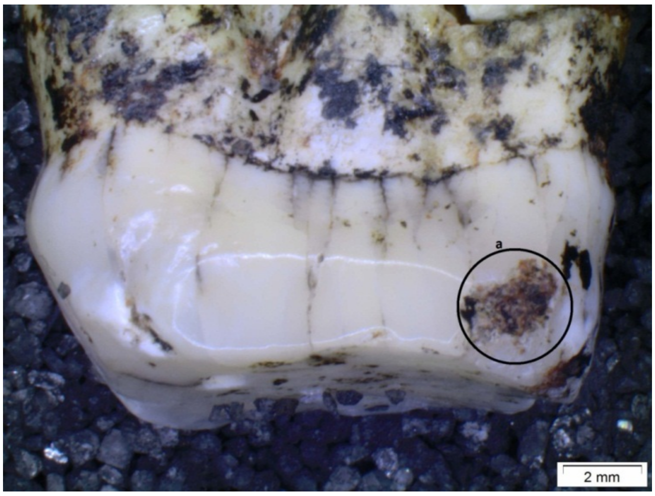

Figure 88: StW 483 LM^3 buccal

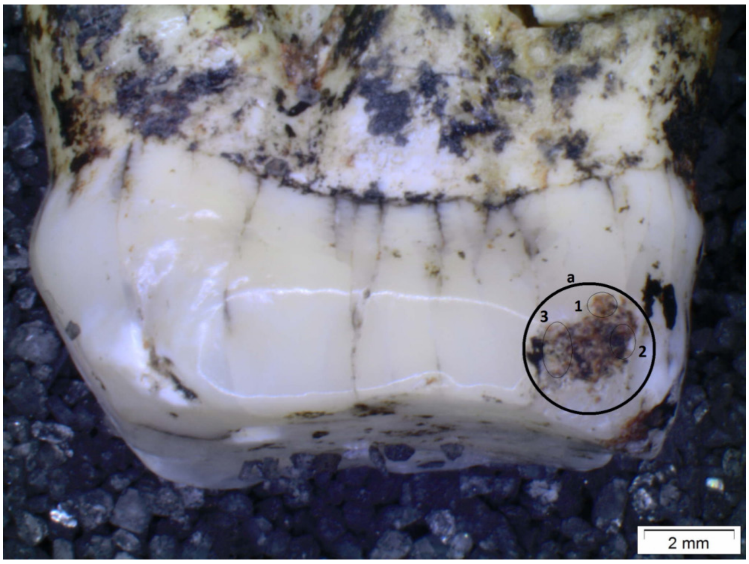

Figure 89: StW 483 LM^3 buccal. Note areas of different colouring, coarseness, and deposit thickness.

Stw 483 LM^3

Occluso-distal; cervico-distal

Three probable calculus sub-deposits are discernible on the distal surface of LM^3. Sub-deposit (b) is located on the occlusal margin and sub-deposit (a) is located on the cervico-distal surface of LM^3 (see Figure 90).

Sub-deposit (a) is located on the cervico-distal margin and extends apically into the *cementum* for most of the sub-deposit. The horizontal measurement is 2.20mm and the vertical width measures 3.3mm. The texture of sub-deposit (a) is less coarse and granular than the occluso-distal sub-deposit (b), and appears more homogenous throughout. The colour of this sub-deposit is generally homogenous exhibiting a dark grey colour (2.5YR N4), the supero-lingual corner exhibits a dark yellowish brown colour (10YR 3/4).

Sub-deposit (b) is located on the occluso-distal edge of the tooth within bucco-distal third (bucco-lingually), extending slightly apically along the occlusal third. It is coarse, grainy and amorphous in shape. The horizontal measurement is 2.25mm and the vertical measurement is 1.95mm. The thickness of the adherent material appears approximately 0.5mm. This deposit appears to have a concave shape, and appears more homogenous throughout. The colour of this sub-deposit is twofold. The superior portion is black (5YR 2/2) and the inferior section of the sub-deposit is mainly an olive colour (5YR 5/3). The majority of the bucco- and mid-inferior section including the concavity is a shade of olive (5YR 5/3).

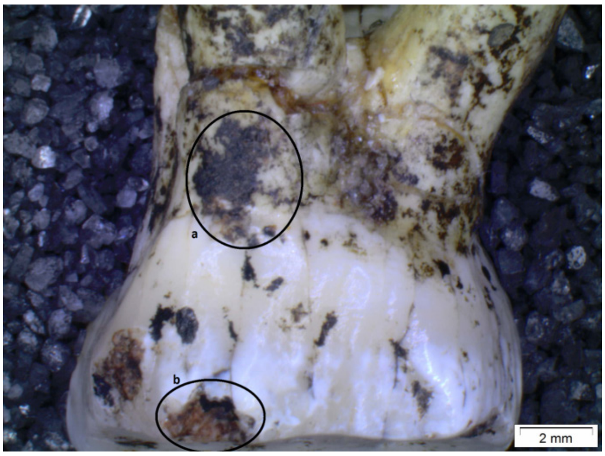

Figure 90: StW 483 LM^3 occluso-distal; cervico-distal

Description of the adherents on Stw 246

LM^1

Buccal

Sub-deposit (a) is located on the cervico-buccal surface and extends from the mesio-buccal third to the disto-buccal margin of LM^1. Sub-deposit (a) measures 7.05mm horizontally and 3.9mm vertically. The texture presents as particularly coarse, granular and globular, and has no set shape pattern. It is amorphous, and there are areas that are coarser and grainier than others. In the most mesial areas of sub-deposit (a), it is less coarse than the mid-buccal area, which is pockmarked in places. In the disto-buccal area, the texture is grainy with rough 'crater-like' convexities. The overall surface is uneven and has a range of variation of topographies throughout sub-deposit (a). Sub-deposit (a) comprises several colours: light brownish grey (2.5YR 6/4), in the mesio-buccal segment, and superior area of sub-deposit (a1); lighter shade of grey (2.5YR 7/2) in the mid distal segment of sub-deposit (a1), light yellowish brown in the central area of sub-deposit (a1); light grey (2.5YR N7), grey (2.5YR N5) and white (2.5YR N8) in the mesio-buccal location and inferior segment of sub-deposit (a1); very dark grey (2.5YR N3) in the mesio-buccal area and in the centre of sub-deposit (a1). Sub-deposit (a2) comprises very dark grey, in the superior and inferior segments (2.5YR N3); light grey (2.5YR N7) and grey (2.5YR N6)

Although sub-deposit (b) is located on the bucco-distal surface of LM^1 (see Figure 93), it can also be seen from the buccal view (see sub-deposits [b] in both Figure 92 and 93). Sub-deposit (b) is discussed under the distal view.

Sub-deposit (c) is located on the mid-occluso-buccal surface. The deposit ranges from the occlusal margin through the occlusal third of the mid-buccal surface of LM^1. Sub-deposit (c) has a horizontal measurement of 2.6mm and 2.00mm vertically. The texture is smooth except for the mid-section which is coarse and uneven. The colouring exhibited by sub-deposit (c1) is pink (7.5YR 8/4) in the mesial area of the sub-deposit; light (7.5YR N7) and dark grey (7.5 YR N3) in the superior and central portions of the sub-deposit (c1). The colours exhibited by the inferior part of the sub-deposit (c2), located slightly distal from the occlusal surface is reddish yellow (7.5YR 7/8) and a strong brown (7.5YR 5/8).

Sub-deposit (d) lies on the disto-buccal surface slightly apical of the occlusal margin of LM^1. It measures 1.15mm horizontally and 0.8mm vertically. The texture is course in the midsection and coarser and granular in the inferior segment of sub-deposit (d). Sub-deposit (d) comprises several colours: dark brown (7.5YR 3/2) and dark grey (2.5YR N4), and black (2.5YR N7) in the central part of the sub-deposit; very pale brown (10YR 8/3; 10YR 7/3) in the mesial parts of the sub-deposit. The inferiorly distal part of the sub-deposit presents with a shade of light grey (2.5YR 7/2). Sub-deposit (e1) (see fig. 42) has been highlighted for its colour variation. It exhibits an olive yellow (2.5YR 6/8) in the superior segment, of the disto-buccal view of sub-deposit (e1) of LM^1. Sub-deposit (e2) presents with a very dark greyish brown (2.5 Y 3/2) on its mesial border and a dark grey (2.5Y N4) central area.

Distal

Sub-deposit (a) is located on the linguo-distal surface of LM^1, and is situated on the cemento-enamel junction, extending 0.5 mm inferiorly onto the cervical third and apically into the *cementum* by approximately 0.25mm. The horizontal width of subdeposit (a) is 0.7mm and the vertical width measures 0.75mm. The texture of the deposit is coarse, grainy, uneven and protuberant in places. The colour of sub-deposit (a) is chiefly pinkish grey (7.5YR 6/2). It also contains grey (7.5YR N6) and dark grey (7.5YR N4) in the central parts, and light grey (7.5YR N7) and white (7.5YR N8) in the central and superior parts of sub-deposit (a).

The sub-deposit (b) is made up of a coarse, granular deposit which is located mid-distally and has a large protuberant mass located bucco-distally, extending superiorly (see sub-deposit (ba) in fig.42). The sub-deposit (b) has a horizontal measurement 5.15mm and 4.45mm vertically. The protuberant segment of the deposit is longitudinal. It begins in the centro-distal area of LM^1 and extends apically into *cementum* of the tooth. The width of the inferior base of the protuberance is 1.8mm, and the most superior width of the protuberance is 1.7mm. The protuberance measures 5.1mm vertically. The topographic character of the protuberance is evident from the buccal view (see fig. 41). The centre of the protuberance evidences the thickest portion of the sub-deposit (b) where it reaches 0.85mm. Thereafter it tapers off slightly until it reaches the cemento-enamel junction where the height of the deposit measures 0.60mm thick. The sub-deposit (b1) is made up of several colours: two shades of dark reddish grey; (10R 4/1; 10R 5/1); and a shade of white (10 YR 8/2). Sub-deposit (b2) is made up of very pale brown (10YR 7/4). Sub-deposit (b3) is composed of reddish grey (10YR 5/1), reddish yellow (7.5YR 6/8); pink (7.5YR 7/4); strong brown (7.5YR 5/8), and dark brown (7.5 YR 3/2), in the most bucco-distal segment of (b3). Sub-deposit (b4) is made up of chiefly light brown (7.5YR 6/4) and brown (7.5 YR 5.4). Sub-deposit (b5) contains a predominance of light brown (7.5YR 6/4); very dark grey in the central area of (b5) (7.5YR N5); and dark brown in the most bucco-distal area of (b5) (7.5 YR 3/2).

Subdeposit (ba) is located bucco-distally and forms part of the longitudinal protuberant deposit of subdeposit (b). The predominant colour of the central and superior areas of sub-deposit (ba1) is light brown (7.5YR 6/4). In the central area of the subdeposit (ba1) there is a reddish yellow segment (7.5YR 7/8); bucco-distally the deposit presents with a borderline brown/dark brown colour (7.5YR 4/4). The colouring of the sub-deposit (ba) situated slightly outside of (ba1), and bucco-distally exhibits ranges of light grey (7.5YR N7), grey (7.5YR N6) and dark grey (7.5YR N4) as well as very dark grey (7.5YR N5).

Sub-deposit (c) is located on the *cementum* apically to sub-deposits (a, and b). The central area of this sub-deposit is coarse and has a slight topographical elevation. Light grey (7.5YR N7), grey (7.5YR N6) and dark grey (7.5YR N4) are the principal colours. Horizontal measurement is 1.2mm and vertically measures 0.9mm.

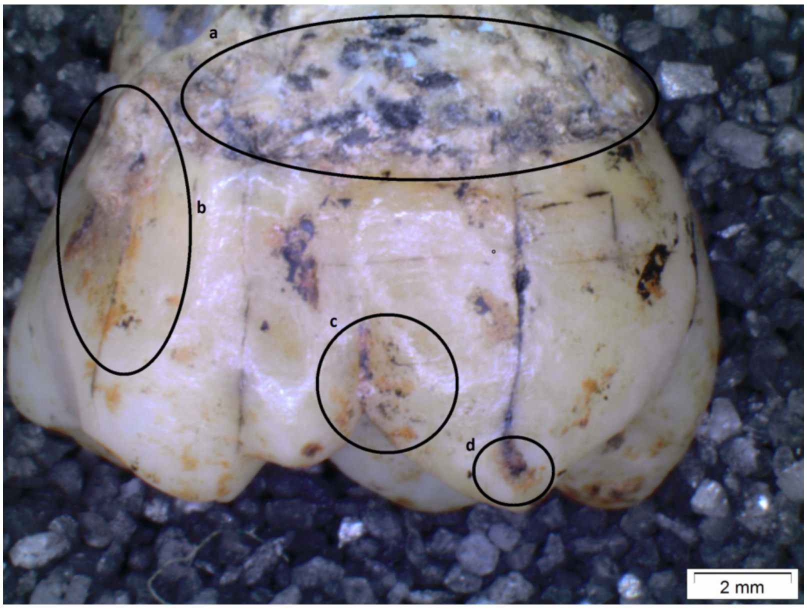

Figure 91: StW 246 LM¹ buccal

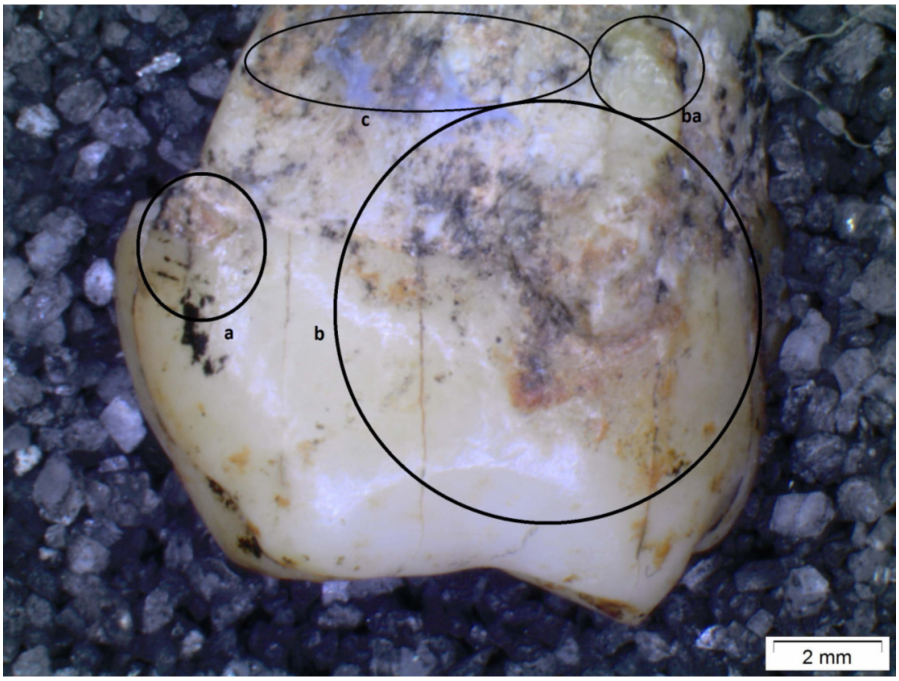

Figure 92: StW 246 LM¹ distal

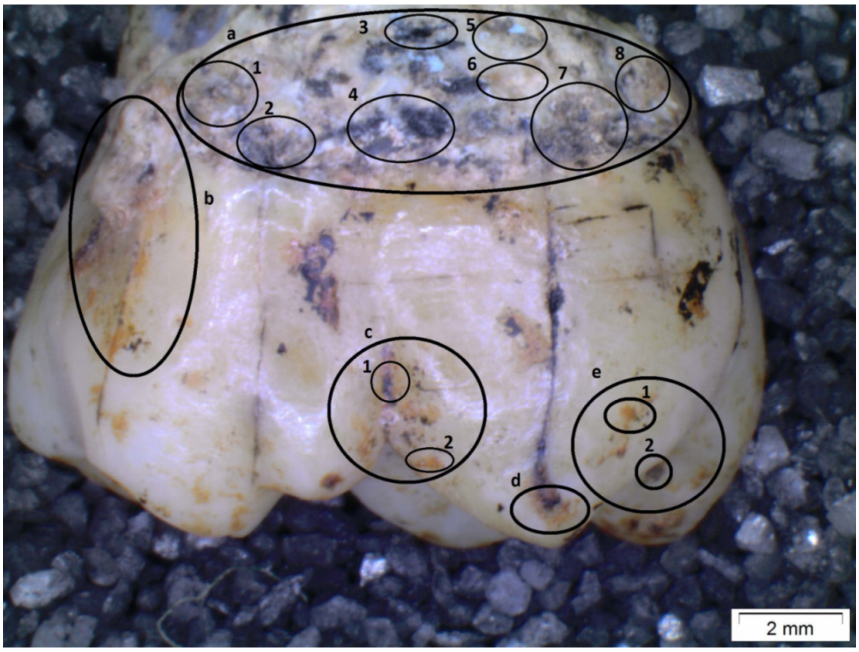

Figure 93: StW 246 LM^1, buccal showing differential colours in subdeposits (a-e)

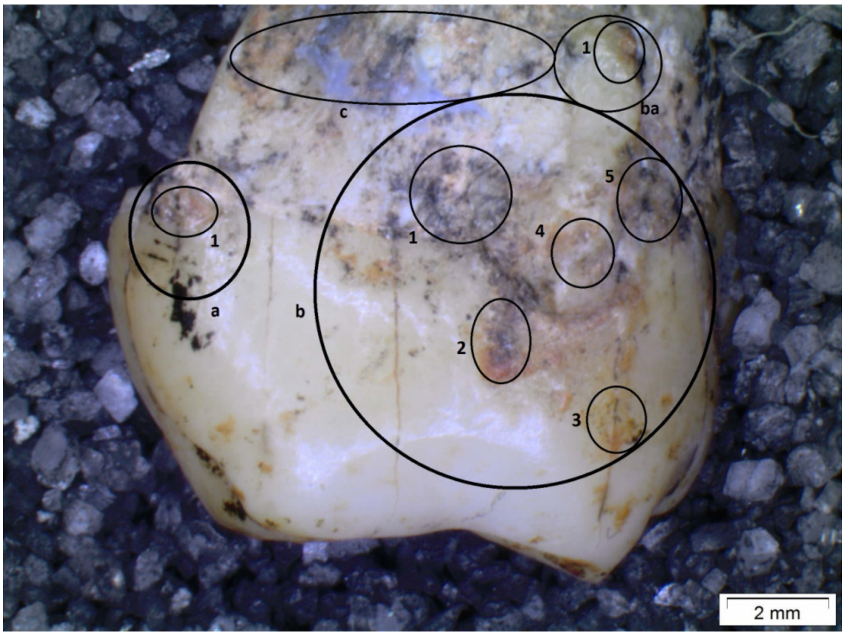

Figure 94: StW 246 LM^1, distal, showing different colours in sub-deposits (a-c; ba)

Description of adherents on Stw 183

LM^1

Mesio-buccal; mid-buccal

Sub-deposit (a) is situated on the most mesio-buccal enamel surface of LM^1, and approximately 0.10 mm inferior to the cemento-enamel junction. Sub-deposit (a) has a vertical height measurement of 1.15 mm, and measures 0.65mm horizontally. The texture is coarse and the adherent material, although the deposit is small it protrudes visibly from the enamel surface. It has a rough uneven and ridged surface. There is a very dark grey (5YR 3/1) spherical protuberant constituent located in the superior segment of the sub-deposit and slightly inferior to the cement-enamel margin. Superiorly placed but more distal is a portion of the sub-deposit which exhibits a combination of two shades of light reddish brown (5YR 6/4; 5YR 5/4) and a shade of dark reddish brown (5YR 3/2). The inferior portion of the subdeposit presents with a pink colouring (5YR 7/3).

Sub-deposit (b) is located superiorly and distally to sub-deposit (a), and extends approximately 0.9mm apically and obliquely from the cemento-enamel margin into the *cementum* zone. The colour of section of the sub-deposit is a shade of white (5Y 8/1) and light grey (5Y 7/1) There are several isolated, amorphously shaped and unevenly spaced nodules, making up this sub-deposit which range distally across the cemento-enamel junction within the mesio-buccal surface of LM^1. The colour of these protuberances is a mixture of a shade of white (5Y 8/2) and very dark grey (5Y 4/1); a shade olive grey (5Y 4/2); light olive grey (5Y 6/2). The texture of these protuberances along the cemento-enamel junction is coarse and uneven, against the relatively smooth cementum surface on which it is located. Two isolated rounded nodules are found on the *cementum* located above the mesio-buccal surface approximately 1.10 mm apical to the cemento-enamel junction. Their texture is slightly coarse and their colouring is a mixture of a white shade (5Y 8/1) interspersed with light grey (5Y 7/2). At the most distal point within the demarcated sub-deposit (b) and lying more or less in the mid-buccal area of LM^1, there is a roundish protrusion adhering to the cemento-enamel junction measuring approximately 0.1mm in diameter, and which appears to have a small convexity in the centre of its outer surface. The texture of this protuberant deposit is rough, uneven and granular. The colour of this portion of the sub-deposit material is pale yellow (5Y 7/4) and pale olive (5Y 6/4) in the most distal section of the protuberance; a shade of white (5Y 8/1) and light grey (5Y 7/1) in the more mesial and central portion and a shade of white (5Y 8/2) and pale yellow (5Y 8/3) in the most mesial portion of the protuberance.

Sub-deposit (c) is located distal to sub-deposit (a), infero-distal to sub-deposit (b) and close to the mid-buccal surface of LM1. The mesio-buccal and mid-buccal surfaces of the sub-deposit contain four relatively large, distinct deposits, as well as several smaller ones too. The three superiorly located bucco-mesial and mid-buccal superior deposits c (*i-iii*) appear to have a coarse and more compacted texture than the larger distally placed deposit c (*iv*). The distal deposit appears to be as coarse as the mesial deposits of sub-deposit (c), but less compacted. The smaller sub-deposits making up the total sub-deposit (c) are all amorphous forms with no set pattern or shape. Sub-deposit c (*i*) has a horizontal width of 0.625mm, and a vertical height of 1.0mm. Sub-deposit c (*ii*) has a horizontal measurement of 0.95mm and vertically 1.15mm. Sub-deposit c (*iii*) is

0.7mm wide (mesio-distally) and 0.75 mm (occluso-apically). Sub-deposit c (*iv*) has a horizontal width of 1.65mm and a vertical height of 1.85 mm. Sub-deposit c (*iv*) lies mesial to a less coarse and compacted sub-deposit c (*v*), and which forms part of the larger sub-deposit (f) running obliquely and infero-distally to sub-deposit (d). The texture of sub-deposit (f) of which c (*v*) also falls into, is slightly coarse, with the exception of c (*v*) which is coarse. Sub-deposit c (*iv*) appears to be closely associated with c (*v*), hence the intersection with sub-deposit (f). The superior portion of c (*i)* exhibits a reddish grey colour (5YR 5/2). The mid-mesial part of the deposit c (*i*) exhibits a combination of a shade of white (5YR 6/1); a shade of grey (5YR 6/1, bordering light grey and grey) and dark grey (5YR 4/1). The colouring of c(*ii*) is similar to c (*i* and *iii*). The dominant colour of deposit c (*iv*) are two shades of reddish yellow (5YR 7/6; 5YR 7/8). Deposit c (*v*) is similar to c (*iv*).

Sub-deposit (d) lies distal to sub-deposit (b) and is situated slightly apical to the cemento-enamel junction. It presents as a thick coarse deposit adhering to the *cementum* of the tooth. The texture exhibits an uneven surface, containing several spherical and amorphous shaped nodules. The deposit measures 0.7mm horizontally and 2mm vertically at its diagonal maximum. The infero-mesial area is predominantly is light reddish brown (2.5YR 6/4) and light red (2.5YR 6/6). The superior portion is composed of two shades of dark reddish brown (2.5YR 3/4; 2.5YR 2/4). The mid-distal area presents with a grey colour (2.5YR N6).

Subdeposit (e) is located on the mid-buccal surface of the tooth and slightly infero-distal to sub-deposit (d), supero-distal to sub-deposit (c). This deposit is thick and although it is relatively small, its protrusion is quite noticeable from the enamel surface of which it adheres. The texture is coarse, uneven and grainy and measures 1.45mm wide and 1.2mm vertically. The central area of the sub-deposit is composed mainly of two colours, pink (5YR 7/3) and light reddish brown (5YR 6/4). The inferior portion of the deposit is a shade of white (5YR 8/1) and reddish yellow (5YR 7/6), and mesial to the shade of white is a grey (2.5YR N5) which extends infero-distally into subdeposit (f).

Sub-deposit (f) is located on the mid-buccal surface of the tooth and infero-distal to sub-deposit (e). The subdeposit is composed of various disparate elements, such as a small longitudinal isolated nodule (c [v]), situated in the intersection of sub-deposit (c) and sub-deposit (f), a flat compacted dark deposit slightly infero-distal of sub-deposit (e), and a relatively large thick and obliquely longitudinal element which ranges from the infero-mesial area of sub-deposit (f) to the supero-distal area of the sub-deposit. It presents as the majority element of this sub-deposit. The middle, superior and supero-distal portions of sub-deposit (f) mainly exhibits a shade of light grey (2.5 YR 7/2). The supero-mesial portion of the sub-deposit presents with a distinct grey (2.5YR N5).

Figure 95: StW 183 LM^1, bucco-mesial

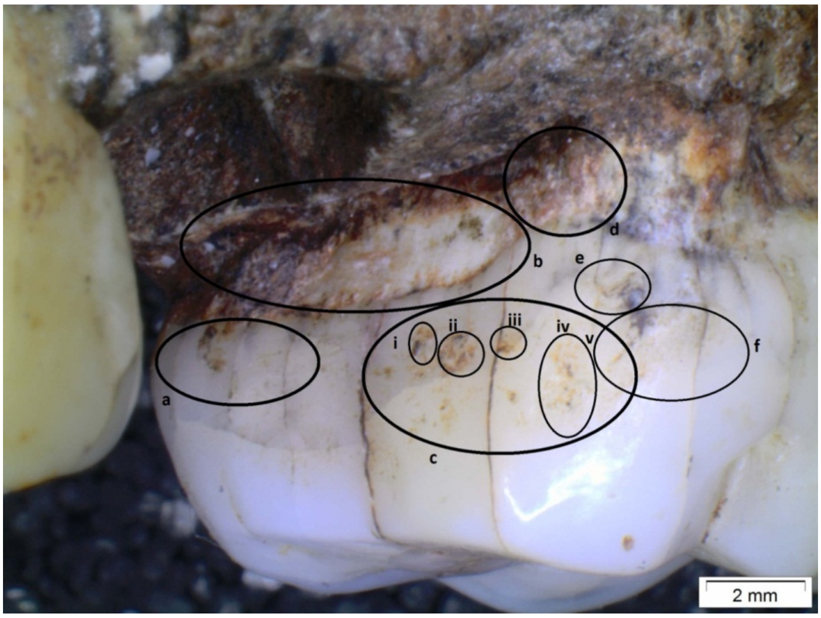

Figure 96: StW 183 LM^1, bucco-mesial and mid-mesial with differentiated sub-deposits (a-f)

Description of adherents on Stw 151

Ldm^1

Distal interproximal

Sub-deposit (a) is located on the occluso-distal (interproximal), cervico-distal, and on the *cementum* surfaces, which are apical to the buccal and distal surfaces of Ldm^1. The deposit is mostly located on the cementum, amorphously distributed and lacks form. The texture is rough and the deposit is not very compacted except on the supero-distal area of the *cementum* where there is a compacted area shaped like an inverted ‘V’ (^) where the superior portion presents as bifurcated. The two inferior segments extend obliquely buccal distal from the centre of the bifurcation respectively. The vertical height of this segment is 0.8mm, and the the buccal and distal oblique measurements are 0.9mm. The thickest parts of the deposit present on the distal interproximal surface, at the intersection of the bifurcation and the two obliques (‘three pointed deposit’). The

two longitudinal and parallel deposits adjacent to the three pointed deposit also present with the same thickness (see fig. 46 [a1]). The colour range of sub-deposit (a1) is a spectrum of light grey/grey/dark grey (5YR 7/1; 5YR 6/1; 5YR 4/1); as well as white spotted area (5YR 8/1) in the most interproximally distal area of the cementum of the tooth. The colour shades presented in the area more or less superior to sub-deposit 2(i), characterised by four isolated small deposits, are a spectrum of two shades of pink (5YR 8/4; 5YR 7/4), light reddish brown (5 YR 6/4) and reddish brown (5YR 5/4).
Sub-deposit 2(*i*) and 2(*ii*) presents on the cervico-enamel margin of the interproximal distal surface, and is relatively thicker than the disto-buccal portion, located laterally buccal of the interproximal segment. The vertical width of the interproximal distal deposit (fig. 46 2[*ii*]) is 0.65mm at its maximum and its horizontal width is 1.6mm. The horizontal width of 2 (*i*) is 1.25mm and the vertical width of the deposit at (2*i*) is 0.425mm. Sub-deposit 2 (i) exhibits shades of light grey bordering on grey (5YR 7/1 bordering 5YR 6/1); a shade of pink (5YR 7/4) and a shade of light reddish brown (5YR 6/4). Sub-deposit 2(ii) exhibits a shade of white (5YR 8/1); a shade of light grey (5YR 7/1); a shade of yellowish red (5YR 5/6); a light grey bordering on a shade of grey (5YR 6/1); and another slightly darker shade of grey (5YR 5/1).

Sub-deposit 3(a) presents with two inferiorly situated and isolated occluso-distal adherences, slightly apical of the occlusal margin, on the interproximal distal enamel surface. They present as closely clustered associated deposit. The more buccal of the two has a relatively longitudinal shape and is located infero-distal to the other. They both measure 0.10mm horizontally. The more infero-distal (buccal) of the two adherences has a vertical width of approximately 0.05mm, and the more occluso-distal measures 0.10mm vertically. The infero-buccal portion of sub-deposit 3a exhibits shades of light reddish brown 5YR 6/4) and reddish brown (5YR 5/3) and the more distal of the two portions making up sub-deposit 3a, is chiefly a shade of dark reddish brown (5YR 3/4). It also exhibits a shade of reddish yellow (5YR 6/6); and a shade of yellowish red (5YR 5/6).

Figure 97: StW 151 Ldm[1], buccal view, distal interproximal

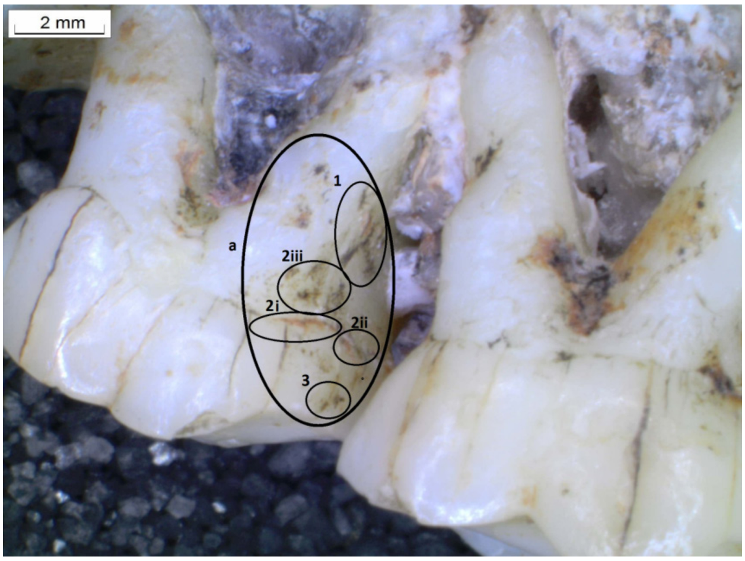

Figure 98: Stw 151 Ldm1, buccal view, distal interproximal with deposits demarcated

Stw 151, left maxilla,

Ldm^2

Cervico-buccal; cervico-mesial and interproximally mesial; mesio-buccal

The three areas of potential calculus on Ldm^2 are illustrated in fig. 48(a-c). Sub-deposit (a) is located, cervico-buccally (a3), cervico-mesially (a1) and interproximally mesial (a2). The cervico-buccal portion is both situated in the mesial third of the tooth at approximately the supero-mesio-buccal corner, and also lies directly on the cemento-enamel junction. It extends apically by 0.8mm into the *cementum* and occlusally by approximately 1.98mm into the enamel of the tooth from the cemento-enamel margin. Mesial to the inferior end of the mesio-buccal enamel adherence is an isolated thick dark roundish deposit (a1). Inferior to the mesio-buccal and the more mesially placed isolated roundish adherence are two parallel adherences, which are different in colour and texture to both the superiorly located mesio-buccal portion or to any other part of the subdeposit (a). The most distal part (a4) of the centrally located adherence of sub-deposit (a) which lies on the cemento-enamel junction in the centre of the mesial third of Ldm^2 appears to extend into two dark parallel amorphous segments (a4), one superior and one inferior the cemento-enamel junction.

The measurements of sub-deposit (a): (a1) measures 0.4mm horizontally and vertically 0.7mm. Both longitudinal deposits of (a2) measure 0.7mm vertically in height; the horizontal width of the more mesial measures 0.1mm and the more distal measures 0.2mm. (a3) is 0.8mm vertically and 0.9mm horizontally. (a4) the horizontal measurements of the more inferior of the two distal deposit segments is 0.8mm; the vertical measurement is 0.20mm. The superior segment is 0.20mm horizontally and its vertical width is 0.7mm. The texture of deposits (a1), (a3) and (a4) are concentrated and coarse, whereas (a2) is mostly a fine, not a concentrated adherence. It does however present on the distal side with isolated material that is coarse and similar to that of (a3).

Shades of yellowish red (5YR 4/8) and dark reddish brown (5YR 3/4) make up the colouring of the major central area of sub-deposit (a1). The area located mesially and distally to the central area presents with shades of white (7.5YR N8), light grey (7.5YR N7) and grey (7.5YR N6). Sub-deposit (a2) presents with shades of pink 7.5YR 7/4), reddish yellow (7.5YR 7/6) and light brown (7.5YR 6/4) superiorly. Distally sub-deposit (a2) presents with a shade of white (7.5YR N8) and light grey (7.5YR N7). Sub-deposit (a3) presents predominantly with a shade of white (7.5YR N8), light grey (7.5YR N7), a darker shade of grey (7.5YR N5) and dark grey (7.5YR N4). Sub-deposit (a4) presents with a dark shade of grey (7.5YR N5) supero-mesially, pink (7.5YR 8/4) superiorly, reddish brown (2.5YR 4/4); and grey (2.5YR N6), dark grey (2.5YR N5) and very dark grey (2.5YR N3) inferiorly. Sub-deposit (a4) presents superiorly with very pale brown (10YR 7/4); dark grey(7.5YR N4); a shade of white (2.5YR N8); a shade of light grey (10YR 7/1) centro-distally; and reddish brown (5YR 5/3) infero-distally.

Sub-deposit (b) is located on the cementum situated mesially to the bifurcation. It presents with three major components; a superiorly apical section, a relatively large superior and mid-mesial section, and an inferiorly mesial section. The superiorly apical section is made up of two sections, a smaller mesial component and a larger distal section. The smaller mesial section is shaped like a 'chopper'; the distal section has no form. They both have no formal shape pattern. The texture of this portion of the sub-deposit is compacted and coarse, but not thick, and appears homogenous throughout. The superior and mid-mesial section of the sub-deposit is characterised principally by a staining on the *cementum* and in two places a lighter material is attached to the *cementum*. The texture of the superior mesial section of this subdeposit is rough and bulbous, with a smooth central core. The texture of the slightly infero-mesial deposit is rough and granular throughout. The texture of the inferiorly mesial part of the sub-deposit is coarse, thick, granular and uneven. The texture is irregularly compacted.

Sub-deposit (b1) is predominantly composed of light grey (2.5YR N6) and darker shades of grey (2.5YR N4). Sub-deposit (b2) presents with a pinkish grey (5YR 6/2) on the mesial and distal sides of the smooth central area; light reddish brown (5YR 5/4) superiorly; and grey in the supero-mesial area (5YR 5/1). Sub-deposit (b3) comprises several colours: grey (2.5YR N5) centro-mesial; dark grey (5YR 4/1) slightly infero-distal; reddish yellow (5YR 7/6) light reddish brown (5YR 6/4) infero-mesial and infero-central.

Sub-deposit (c) lies on the cemento- enamel junction and is distal to subdeposit (a). Sub-deposits (c) [1-4] exhibit all have no pattern or form. There appears to be several small isolated deposits dotted along the cervico-enamel margin. The first and most mesially situated element presents as a formless, concentrated and homogenous texture. Sub-deposit (c2), is a longitudinal element and slightly distal to the sub-deposit (c1), and extends 0.85mm infero-distally from its superior horizontal angle at the cemento-enamel junction where the deposit begins. The deposit is located inside of a crack, which begins at the cemento-enamel margin and continues inferiorly buccal until the occusal margin. This element of the deposit extends 1.1mm from the cemento-enamel deposit inferiorly onto the enamel.

Sub-deposit (c3) is located mostly on the *cementum*, and begins on the cemento-enamel margin. It extends 0.33mm apically into the *cementum* from the cemento-enamel junction. The texture of this element is the same as the other elements in this sub-deposit. Sub-deposit (c4) extends 0.9mm inferiorly into the enamel segment from the cemento-enamel junction. Its texture is similar to the other isolated deposit elements of sub-deposit (c). Sub-deposits (c) [1-4] predominantly exhibit a shade of light grey bordering on grey (2.5YR N6); and light brownish grey (2.5YR 6/2) on the superior, mid-mesial and infero-mesial areas of sub-deposit (c4).

Sub-deposit (d) is the most distally located of the sub-deposits on Ldm^2. It presents similarly to sub-deposit (b). It is composed of four chief components, a supero-mesial (d1) and supero-distal (d3), a mid-mesial (2i), a mid-distal (d4) and an infero-mesial section (2ii). The supero-mesial (d1) and mid-mesial (d2i) deposit are mostly stained and contain two obliquely longitudinal elements supero-mesially. The oblique horizontal measurement of the more superiorly distal of the two is 0.85mm. The width at its maximum is approximately 0.10mm and 0.05mm at its minimum. The more infero-mesially oblique deposit has a horizontal measurement of 0.4mm and a width of 0.10mm at its maximum and 0.05mm at its minimum. The two obliquely longitudinal deposits are separated by a relatively small cluster of roundish and irregular protuberant deposits. The texture of the longitudinal deposits is closely compacted. The supero-distal (d3) and supero-mid-distal areas (d4) are covered by a general staining that is similar to sub-deposit (b2).

Supero-distally (d3) it has a round darkish isolated deposit, and appears as if the texture is rough, compacted, and homogeneous. Inferior to the isolated spherical deposit (d3), is a stained rough patch. The texture of this section is rough and uneven, and has a topographic elevation to it, giving it an irregular thickness in places, especially slightly infero-mesial to the dark roundish small deposit (d3). Directly inferior to this stained patch is another small isolated dark deposit (d4), which presents with a similar texture to the superiorly located spherical isolated dark deposit (d3).

Infero-mesially the adherent deposit extends from the lower margin of the infero-mid section to the most infero-mesial part of the sub-deposit (d2ii). The infero-mesial deposit is made up of a small obliquely longitudinal section with a thick inferior spherical protuberance (2i), the horizontal oblique section measuring 0.5mm and a width of 0.1mm at its maximum and 0.05mm at its minimum. Directly inferior to the protuberance is a relatively thick, coarse and uneven oblique deposit that extends distally to the most inferior mid-section of sub-deposit (d2ii). The inferiorly oblique deposit measures 1.7mm in length and 0.8mm at its maximum and 0.66 at its minimum. The superior extent of sub-deposit (d2ii) has a portion which attains a maximum width of 0.9mm. The adherent deposit has an amorphous form. Distal to the infero-mesial deposit is another area of staining, and adherent to the staining is an isolated cluster of relatively small spherical bulbous elements (d5). Sub-deposit (d1) is mostly made up of different shades of grey. A dark shade of grayish brown supero-mesially (2.5YR 4/2); a light grey to light brownish grey in the central, mid-distal, infero-mesial and infero-distal areas of sub-deposit (d1). Sub-deposit (d2i) exhibits shades of white (2.5YR N8); light grey (2.5YR N7), and a shade bordering on light grey/ grey (2.5YR 2.5YR N6). Sub-deposit (d2ii) exhibits supro-mesially a shade of very dark grey (2.5YR N3), and black (2.5YR N2); light grey and a darker shade of grey (2.5YR N5) superiorly and supero-inferiorly; and light brownish grey (2.5YR 6/2) infero-distally. Sub-deposit (d3) is predominantly made up of the spherical deposit which comprises of different shades of three principal colours, dark greyish brown (2.5YR 4/2), very dark greyish brown (2.5YR N3) , and very dark grey (2.5YR N5). Sub-deposit d4 has a combination of a shade of light grey (2.5YR 7/2) bordering on pale yellow (2.5YR 7/4), superiorly, supero- mesially and infero-mesially; and light grey bordering grey (2.5YR N6), and grey (2.5YR N5) infero-distally. Sub-deposit (d5) is composed of a white shade (2.5YR N8); and light grey (2.5YR N7) superiorly, and two pale yellow shades (2.5YR 8/4; 2.5YR 7/2) with a mix of light yellowish brown (2.5YR 6/4) mid-mesially, infero-mesially, supero-distally, mid-distally, and infero-distally.

Figure 99: StW 151, left maxilla Ldm^2, cervico-mesial

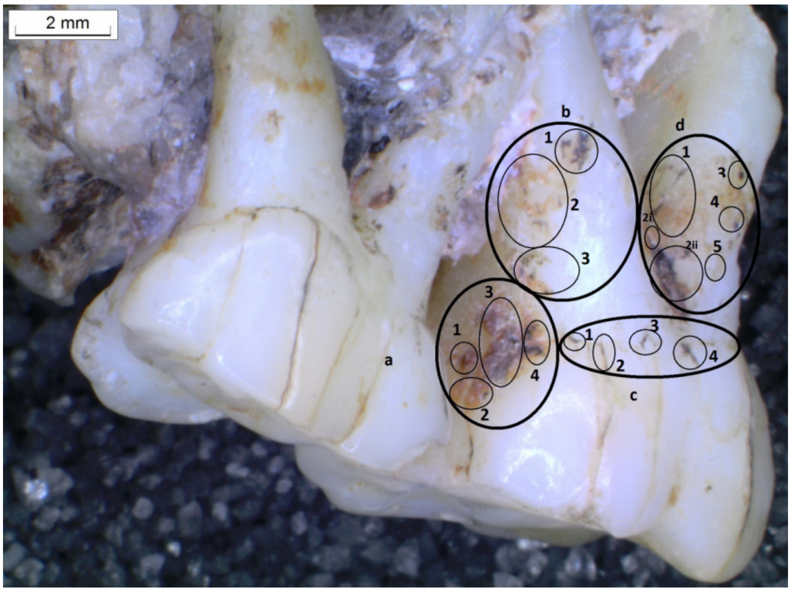

Figure 100: StW 151, left maxilla Ldm2 with sub-deposits (a-d)

Description of adherents on Stw 131

RM$_1$

Mesial

Sub-deposit (a) is located more or less at the margin where the inferior margin of the occlusal third joins the middle third (bucco-lingually), on the bucco-mesial surface of RM_1. It is made up of two irregular amorphous deposits (a1-a2). Sub-deposit (a1) is situated more mesially than sub-deposit (a). The vertical height of deposit (a1) measures approximately 0.65mm, and measures 0.9mm horizontally. The texture of (a1) is slightly coarse and presents with relatively small, isolated spherical protuberances, supero-mesially, supero-distally, infero-distally and centrally. The protuberances present as the thickest area of this deposit, and appear to be approximately 0.05mm in thickness centrally. Subdeposit (a1) chiefly comprises colour shades centro-mesially and supero-linguo-mesial of light brownish grey (10YR 6/2); a shade of white (10YR 8/2) supero-linguo-mesial and centro-lingio-mesial; light grey / grey border (2.5YR N6) centro-linguo-mesial; two shades of pale yellow (2.5YR 8/4; 2.5YR 7/4) infero-centro-mesial, and two shades of white (2.5YR N8; 2.5YR 8/2) infero-mesial.

Sub-deposit (a2) is situated slightly supero-laterally to sub-deposit (a1). It measures approximately 0.65mm vertically and approximately 0.25mm horizontally. The texture is slightly rough, and the majority of the surface of (a2) is made up of several bulbous protuberances. The protuberances present as the thickest parts of the deposit, the maximum of which could reach up to between 0.05-0.1mm. The enamel surface that is situated linguo-mesially and infero-mesially to sub-deposit (a) and bucco-mesial to sub-deposts (b-c) presents with a scatter of relatively much smaller amorphously placed deposits. Sub-deposit (a2) comprises a darker shade of grey (2.5YR N5) mid-bucco-mesial, inferiorly and infero-linguo-mesial; a light grey bordering on grey (2.5YR N6) centrally, superiorly and bucco-mesial; greyish brown (2.5YR 5/2) mid-bucco-mesial and light brownish grey (2.5YR 6/2) supero-bucco-mesial.

Sub-deposit (b) is located 1.2mm infero-linguo-mesial to sub-deposit (a). It is a singular deposit. It measures approximately 0.75mm horizontally and approximately 0.65mm vertically. The texture is coarse irregular and uneven, and includes a cluster of small protuberances, situated more or less in the central area of the deposit. Sub-deposit (b) is chiefly composed of light grey (2.5YR N7) centro-bucco-mesially; infero-mesially and centro-linguo-mesially; dark grey (2.5YR N4) centro-bucco-mesially; very dark grey (2.5YR N3) centro-mesially; a shade of white (2.5YR 8/2) infero-mesially.

Sub-deposit (c) is located infero-linguo-mesially to subdeposit (b), and appears to be located in the cervical third on the bucco-mesial surface of RM_1, approximately 0.85mm inferior to sub-deposit (b). The deposit may be partially obscured to some degree by the way RP4 has preserved, which is mesially placed in front of RM_1. This thickly adherent deposit presents as coarse, bulbous and uneven. The horizontal base measures 1.35mm and the vertical width 1.75mm. The deposit presents as a rectangular shape. The supero-bucco-mesial corner presents as the thickest part of the deposit. The colouring is mostly different shades of brown (7.5 YR 5/2; 5/4; 4/2; 4/4)

Sub-deposit (d) is located in the middle third of the tooth bucco-lingually. The deposit presents as a rectangular mosaic of different sub-deposits with a thickly prominent material which is adherent to the enamel in the middle section of the deposit. It ranges horizontally, for 3.75mm from the intersection of approximately the bucco-mesial and mid-mesial margin to approximately two-thirds of the mid-mesial third, before dipping inferiorly obliquely, forming another subdeposit, which is shaped like a downward pointing arrowhead.

The bucco-mesial section of the sub-deposit has a higher vertical height than the rest of the deposit which measures 1.4mm, and presents as a relatively ‘square-shaped’ deposit, whereas the maximum vertical height of the rest of the deposit measures 0.9mm. The linguo-mesial edge of the horizontal deposit proceeds obliquely inferiorly and exhibits a downward pointing ‘v’ shape sub-deposit. The horizontal measurement of the downward-pointing ‘v’ shaped deposit is 1.1mm measured from the beginning of the inferiorly sloping oblique sub-deposit or the beginning of the ‘v’ shape. The vertical depth of the ‘v’ shaped deposit from the horizontal to the inferior point of the ‘v’ is 0.9mm. The horizontal superior margin dips inferiorly in the middle of the’v’-shaped sub-deposit

Superiorly placed to the ‘v’-shaped linguo-mesial sub-deposit is another sub-deposit which is sub-divided further into a larger superior closely compacted deposit with smaller isolated and tightly compacted deposits on either side of it, and an inferiorly placed sub-deposit cluster of relatively smaller isolated ‘mini-deposits’. The horizontal measurement of the superior cluster of the occluso-mesial sub-deposit (d) is 0.9mm; with a vertical measurement of 1.0mm.The horizontal width of the inferior cluster of isolated mini-spherical deposits is 0.8mm. The texture of the larger and smaller isolated mini-deposits is coarse, uneven and thick, and the larger superior deposit is bulbous and protrudes noticeably from the enamel surface. The thickness of the smaller isolated deposits appears to be at least 0.5mm thick, and in the larger superior compacted deposit appears to be at least 0.10mm thick.

The inferior centro-mesial horizontally longitudinal section of the deposit appears to be very tightly compacted, and continues to be so extending into the ‘v’ shaped infero-linguo-mesial deposit. The superiorly linguo-mesial deposit which is located directly above the tightly compacted horizontal deposit, is composed of isolated relatively smaller amorphous deposits, and is not as thickly compacted as the inferior deposit. Most of the isolated smaller deposits of this section of the sub-deposit are located linguo-mesially, with less adherent material on the more mesial section located directly superior to the horizontally longitudinal segment of the sub-deposit. The most superior segment of the sub-deposit is made up of an isolated, relatively larger deposit, which is tightly compacted and has a coarse texture. It presents as the thickest part of the sub-deposit measuring approximately 0.1mm. The colouring is mostly shades of brown and grey (7.5YR 5/4; 5/2; 4/4; 4/2; N3).

Sub-deposit (e) is located superiorly and linguo-mesially to sub-deposit (d), and the superior margin of the deposit is situated on the occluso-mesial margin of RM_1. Both sub-deposits (d and e) appear to be continuous with each other, and are joined at the supero-linguo-mesial margin of sub-deposit (d) with the inferior mesial, middle and infero-lingual margin of sub-deposit (e). The texture of sub-deposit (e) is extremely coarse and uneven. It is firmly compacted, and does not present with a homogeneous pattern. There are two isolated deposits superiorly located more or less on the occluso-mesial margin, with the relatively smaller isolated deposit on the occluso-mesial margin, and a relatively larger one situated slightly inferior to it. The colour is a greyish brown.

Sub-deposit (f) is composed of four subsections (1-3, and 3a) and is located linguo-mesially between the occluso-mesial and mid-mesial thirds of RM_1. Sub-deposit (f1) is a deposit fragment situated slightly inferior to the occluso-mesial margin and on the linguo-mesial surface. It presents with a generally coarsely concave and uneven texture, and with three relatively small bulbous protuberances, one superiorly, one infero-mesio-buccally, and one infero-linguo-mesially placed. It exhibits a triangular shape with its apex pointing occluso-lingually. Horizontally and vertically they both measure 1.0mm at its respective maximums. The slightly oblique longitudinal base exhibits a tubular-like convexity. Colours are browns and greys (7.5 YR N3; 5/4; 5/2; 4/4; 4/2)

Sub-deposit (f2) is a larger deposit than, and lies infero-mesial to sub-deposit (f1). The bucco-mesial segment of (f2) measures 2.15mm at its maximum, and measures 0.85mm horizontally at its most superior occluso-mesial edge. Sub-deposit (f2) has a rough, uneven texture. The inferior area of sub-deposit (f2) is adherent and protrudes mesially. The texture of the superior portion of the subdeposit (f2) presents as less thick and less compacted than the inferior segment of the sub-deposit. The colour is greyish brown.

Sub-deposit (f3) lies further linguo-mesially to sub-deposits (f1and f2). Sub-deposit (f3) presents as two narrow longitudinal deposits that range from the occluso-mesial junction to the margin of the mid-linguo-mesial third, in the case of the more bucco-mesial deposit, and to the centre of the mid-linguo-mesial third, with regard to the more linguo-mesial deposit. The more bucco-mesial of the two longitudinal deposits (f3) Subdeposits appear to be located in a natural development groove. The thickest area of the sub-deposit appears to be in the mid- linguo-mesial third approximately 3.2mm inferior to the occluso-mesial junction, exhibiting a thickness of approximately of 0.5mm. The vertical measurement of the more linguo-mesial longitudinal deposit is 5.2mm and is measured from the occluso-mesial junction (f3) to the beginning of the cervico-mesial third sub-deposit (f3a); and the horizontal width generally measures 0.3mm at its minimum and measures 0.75mm at its widest which occurs simultaneously in the mid-linguo-mesial third at area of thickest adherence. Linguo-mesial to the more bucco-linguo-mesial deposit and running more or less parallel to it is another longitudinal deposit ranging from almost the occluso-mesial margin to the beginning of the linguo-mesial third of the tooth. The vertical longitudinal length measures 5.9mm. The horizontal width measures approximately 0.1mm in the occluso-mesial third. The width of the deposit from the mid-linguo-mesial area inferiorly to the cervico-mesio-lingual area is approximately 0.5mm. The more bucco-mesial longitudinal deposit presents with a less thick texture than that of the more linguo-mesial deposit, of approximately 0.25mm.

The sub-deposit (f3a) is the continuation of deposit (f3).The deposit (f3a) curves slightly obliquely infero-mesio-buccally from the mid-mesial area for 0.9mm until it reaches a thickly textured longitudinal area whereafter it then proceeds inferiorly (f3) for approximately 0.7mm. The central area of deposit (f3a) is the thickest area of this continuation deposit and appears similar in thickness (approximately 0.5mm) to the mid-linguo-mesial thickness of sub-deposit (f3). Colouring greyish brown (7.5 YR N3; 5/4; 5/2; 4/2; 4/4).

Sub-deposit (g) lies slightly inferiorly buccal to sub-deposit (f) on the cervico-mesial surface, and is situated within the linguo-mesial third (bucco-lingually) of the tooth. It measures 2.25mm horizontally and vertically measures 0.97mm at its maximum. The texture is smooth, uneven and irregular. Sub-deposit (g) presents as being inferiorly attached to the cervico-mesial segment of a material other than enamel, which has interposed itself between the linguo-mid-mesial and the most linguo-mesial third. This relatively large and interposed material is thick, longitudinal, convex mesially, and measures 7.425mm vertically, and measures 2.0mm horizontally. It ranges from the occluso-mesial junction to the cervico-mesial junction, and at a vertical depth of 5.85mm makesadjoins sub-deposit (g), and is convex mesially. The colour of sub-deposit (g) is cream to white (7.5 YR N8; 8/2; 8/4; 8/6).

Sub-deposit (h) is located at the base of the most linguo-mesial third at the cervico-mesial margin where the inferior portion of the visible enamel coincides with the adjoining bone material. The horizontal width of the deposit measures 0.7mm and vertically measures 0.9mm at its maximum. The texture is coarse, uneven, and presents with a central and superiorly placed spherical-shaped bulbous protuberance which exhibits a thickness of approximately 0.5mm. Colour is brown and grey (7.5 YR N3; 5/2; 5/4; 4/2; 4/4)

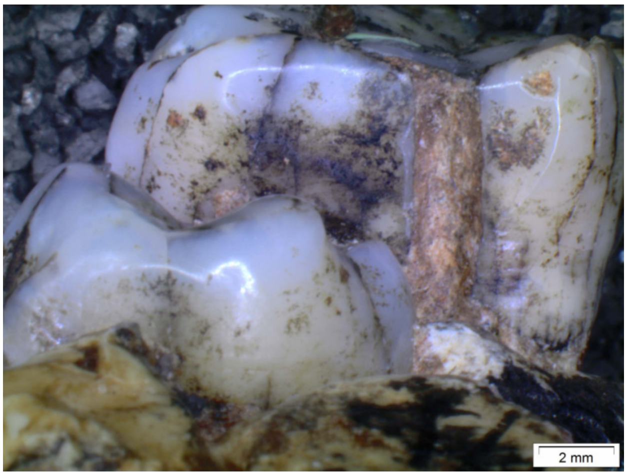

Figure 101: StW 131 RM$_1$ mesial

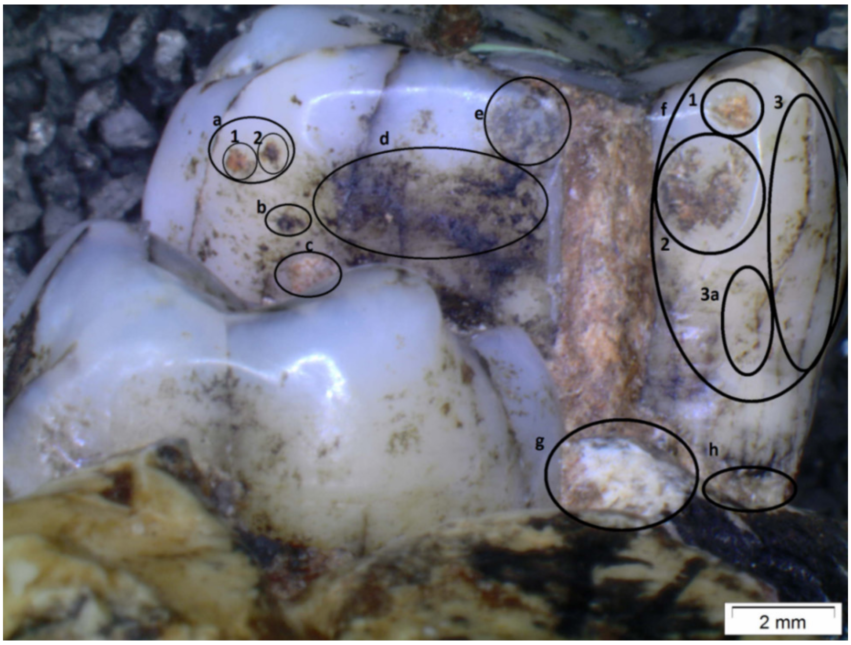

Figure 102: StW 131 RM$_1$ mesial with deposits

Description of adherents on StW 127

LC^2

Mesial

Sub-deposit (a) is situated in the mid-mesial third of LC2. It texture presents as compact, medium coarse and homogeneous, but formless. The superior edge of the deposit horizontally measures 4.15mm and vertically measures 4.95 mm at its bucco-mesial margin. The vertical measurement at its linguo-mesial edge is 1.8mm. The superior and inferior margins follow an arc-like shape (bucco-lingually). Sub-deposit (a) exhibits a thickness of approximately 0.025mm. Approximately 1.0mm from the superior margin midpoint of the sub-deposit (bucco-lingually), and supero-mesio-lingually to the larger inferior deposit (a) is an isolated smaller amorphous, but thicker deposit, with a depth of approximately 0.05mm. The isolated deposit (a2) has a horizontal measurement of 1.25mm vertically measures 1.0mm at is maximum midpoint; measuring 0.9mm at both its bucco-mesial and linguo-mesial margins. Colours are several hues of brown.

Sub-deposit (b) is located supero-lingually to sub-deposit (a). The deposit is situated at the most linguo-mesial cervico-enamel margin. The texture is very coarse, grainy, and bumpy and with many relatively small multi-spherically protuberant components, and also exhibits a pockmarked-type textured surface. The bucco-mesial surface of the cervico-enamel junction of sub-deposit (c) presents with a very similar textured surface. Colour is composed of various shades of browns.

Sub-deposit (d) is located inferiorly to sub-deposit (b) and presents as an isolated separate deposit. It measures 1.0mm vertically and 0.85mm horizontally. The texture is slightly coarse and uneven, but presents as smoother and not as tightly compacted, grainy or bumpy as the other sub-deposits on LC^2. Colour of sub-deposit (d) is brown.

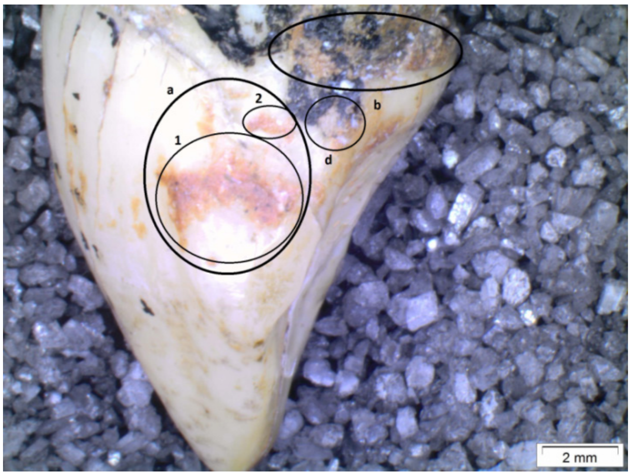

Figure 103: StW 127 LC^2; mesial

Description of adherents on StW 109

RM_2

Mesio-buccal

Sub-deposit (a) is one of three sub-deposits identified on the mesio-buccal surface of RM_2. It is found on the mesio-buccal surface, slightly above a concavely longitudinal area slightly above the cervico-enamel junction. The texture is medium coarse, bulbous and irregular. It is divided into two parts; the distal part exhibits a thicker centre than the slightly infero-mesial segment of the sub-deposit. A similar adherent material is exhibited on the ramus of the mandible and inferiorly to the cervico-enamel line extending inferiorly from the mid-buccal to the mesio-buccal area. The obliquely mesial horizontal width of sub-deposit (a) is 2.2mm, vertically 0.75mm at its widest, 0.10mm vertically at it mesio-buccal margin, and 0.65mm at the mesio-distal margin. Colour is grey and cream (7.5 YR N3; 8/2; 8/4).

Sub-deposit (b) is located slightly supero-mesial to sub-deposit (a) on the buccal surface of RM_2. It presents as four separately isolated deposits that cluster vertically and longitudinally and can be viewed as one deposit. It begins in the mid-buccal third and extends to the cervico-buccal third. The texture of sub-deposit (b) (the longitudinal cluster deposit), is lightly coarse and amorphous and uneven. It shares a margin distally with an adjacent dark, coarse, amorphous and thinly, but extremely condensed adherent deposit. The texture of the adjacent (dark) deposit presents as coarse, granular, uneven, and homogeneous. The total vertical measurement of the sub-deposit (b) cluster is 2.15mm. The horizontal width of the superiormost margin of the superior segment is 0.20mm, with a vertical measurement of 0.60mm. The second or next inferior to the superior segment measures 0.1mm wide and vertically 0.25mm; the third segment or penultimately inferiorly situated segment in the sub-deposit (b) has a horizontal measurement of 0.10mm at its maximum and 0.6mm vertically. The horizontal width of the most inferior segment of the sub-deposit cluster is 0.05mm, with a vertical measurement of 0.20mm. The colour is dark brown to black (7.5 YR N2; 2/2; 2/4).

Sub-deposit (c) is located slightly supero-distal to sub-deposit (b) and mesiobuccally within the occluso-buccal third of the tooth. The deposit presents as a very thin film-like deposit overlying the deeper and coarser adherent material which appears to be similar to a dark manganese-type material. It appears to be very thin and film-like in its texture bucco-distally, and thicker and darker in the centre, and infero-mesially approaching the bucco-mesial margin. Sub-deposit (c) presents more as a stain-like biofilm overlaying the darker adherent material. The texture is smooth, stain-like, and has no depth to it, as it appears to adhere flush with the enamel of the tooth, or over the darker compacted manganese-type deposit. The deposit material is amorphous. The stain-like film extends disto-buccally and infero-buccally outside of sub-deposit (c). The stain-like deposit appears to continue supero-distally into the occluso-buccal third on the mesio-buccal surface. The stain-type deposit seems to get gradually less compact as it approaches the occlusal margin, whereupon it presents as a group of relatively tiny spherical dotted deposits, which are haphazardly spread out approximately 0.125mm inferior from the occlusal edge within the mesiobuccal third and 0.75mm mesial to the margin of the mid-mesial third. Colour is very dark brown to black (7.5YR 7.5 YR N2; 2/2; 2/4).

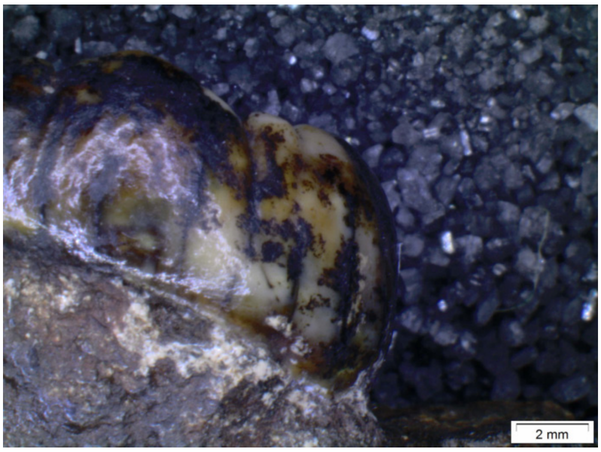

Figure 104: StW 109 RM^2 mesio-buccal

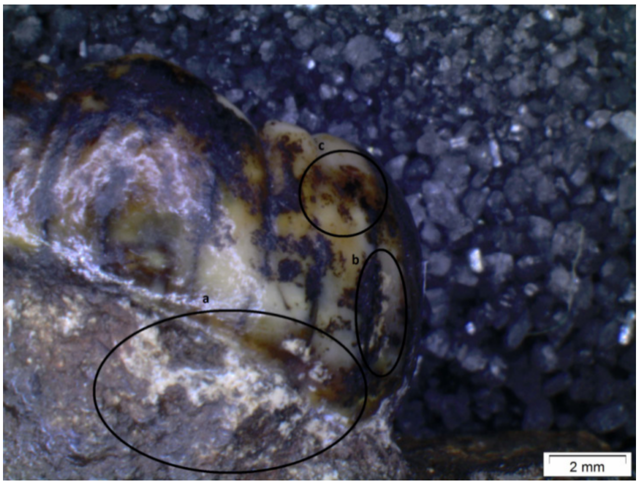

Figure 105: StW 109, RM^2

Description of adherents on StW 131,

RP$_4$ *buccal*; RM$_1$ *buccal*

Sub-deposit (a) is located on the disto-buccal surface within the occluso-buccal and mid-buccal thirds of RP$_4$. The mid-buccal area presents with a spherical-like deposit extending outwardly in a loose fan-like pattern until it ends slightly inferiorly to the occlusal edge of the bucco-distal and mid-buccal area. The sub-deposit has a loose inverted 'triangle' shape with the spherical part of the deposit being at the apex of the 'triangle' facing inferiorly. The texture of the spherical-type deposit on the mid-buccal surface is coarse and tightly compacted, whereas the deposit fans superiorly it remains coarse but the deposit is less compacted with more enamel becoming visible as the deposit extends superiorly. The spherical element of the sub-deposit exhibits a thickness of approximately 0.05mm. The rest of the deposit appears not to be more than 0.25mm at any point in this sub-deposit. Colour is grey and dark brown (7.5 YR N3; 5/2; 5/4; 4/2; 4/4).

Sub-deposit (b) is located mesial to sub-deposit (a) and lies on the mesio-buccal surface, which begins in the occluso-buccal third and ranges to the mid-buccal third of the tooth. The deposit begins at the occlusal margin, where it is extremely thin and longitudinal and extends inferiorly along a protuberant ridge for approximately 0.8mm until the start of the mid-buccal margin. Thereafter the protuberant vertical ridge separates into a gradually widening groove in the mid-buccal area where the deposit becomes wider and profoundly compacted. Distal to the grooved deposit is another substantially compacted and coarse deposit separated by an enamel area. This deposit is joined to the mesially located grooved deposit by a thin piece of material in its mid-section. Mesial to the grooved deposit segment is a less compacted area of material characterised by an oblique deposit (mesio-distally) made up of six elongate sections of adherent material, with no set shape pattern, except for the the most infero-distal of which exhibits a spherical shape. The obliquely elongate sections appear to be at least 0.05mm thick. The obliquely horizontal measurement of this sub-segment is 2.65mm, and 0.10mm at its maximum. The slightly coarse deposits infero-distal and mesial on either side of the grooved sub-segment exhibit a slight staining on the enamel. The infero-mid section exhibits an obliquely disto-mesial, thin and longitudinal segment, which ends in a bifurcation, with the mesial segment shorter than the distal one. Colour is a mixture of greys and browns, and is the same as sub-deposit (a).

Sub-deposit (c) lies directly inferior to sub-deposit (a). This sub-deposit is located infero-disto-buccally between the cervical third and the middle third, mesiobuccally, and also appears to lie on the infero-disto-buccal junction with the mandible. It presents with a very lightly adherent, non-compacted and lightly coarse material. It is brown in colour.

Sub-deposit (d) lies mesial to sub-deposit (c) and slightly infero-mesial to sub-deposit (b). It is located infero-mesio-buccally on RP_4. The deposit is very lightly adherent and slightly coarse. The deposit presents with no tightly compacted material. The material generally has a slight thickness, excepting for three isolated relatively small, but thick protuberant sections, two of which are located mesio-buccally, with one directly superior to the other, and are located 0.5mm from the junction of the most infero-mesio-buccal surface and the mandible. The other is located more distally to the other two mesial sections, and is in the same plane as the superiorly more mesially placed protuberance. Colour is a mixture of greys and browns and is the same as sub-deposit (a) and (b).

Sub-deposit (e) is located infero-distal to sub-deposit (a), and is located on the most distal extent of the disto-buccal surface, in the middle third of the tooth, where RP_4 joins the mandible. The deposit is a long narrow cluster of disparately shaped adherent material which collectively has an amorphous shape. The texture of this sub-deposit is coarse and appears at least 0.025mm thick. Colour is a mix of grey and dark browns [same as sub-deposit (a), (b) and (c)].

StW 131, RM_1

Buccal; mesiobuccal; interproximal mesial

Sub-deposit (f) is located on the mesio-buccal and interproximo-mesial surfaces of RM_1. An isolated deposit is situated on the mesiobuccal surface, and is distal to a longitudinal crack in the enamel in the middle mesiobuccal third of the tooth. The vertical width is 0.55mm and its length is 0.15mm in the middle of the deposit. The inferior end of this deposit comes to a point. The superior edge has a horizontal width of 0.1mm. Slightly supero-mesial to mesio-buccal deposit and mesial to the vertical crack in the enamel that is evident in sub-deposit (f), is a larger and thicker isolated deposit. This isolated deposit is located in the interproximal mesial surface is noticeably protuberant, and displays a thickness of at least 0.10mm, from the enamel surface. Both isolated deposits are amorphous and are formless. Surrounding and inferior to both isolated deposits on the interproximal mesial surface of RM_1, are relatively tiny multiple dotted adherent deposits. More or less infero-mesial to the relatively large protuberant deposit on the interproximal mesial surface of RM1 (sub-deposit [f]), is a darkish coloured isolated deposit. The oblique length of which is approximately 0.20mm, with a width of 0.10mm in the middle of the deposit, and a base width of 0.25mm. Inferior to this segment of the deposit is a slightly diagonally longitudinal deposit measuring 1.1mm in vertical diagonal length and approximately 0.8mm in width at its inferior base; it is approximately 0.15mm wide at its superior end. Distal to the longitudinal deposit is an amorphous cluster-type deposit made up of five relatively small parts, the most inferior of which being the largest, and the most superior is an upwardly pointing segment. The middle segments are relatively the smallest in this sub-cluster deposit. The colour of this deposit is brown.

Sub-deposit (f1) is situated infero-distally to sub-deposit (f1). It appears to be an extension of sub-deposit (f). The deposit is an irregularly placed group of relatively small spotty, light textured, formless, and widely spread out components. It lacks compacted texture of sub-deposit (a, and b).

Sub-deposit (g) is located more distal of sub-deposit (f and f1). Sub-deposit (g) is located on mesio-buccal surface within the cervico-buccal third. The deposit is amorphous, and extends superiorly from the cervical border with the mandible until the beginning of the mid-buccal margin. The texture is thin and extends 2.1mm vertically from the cervical line superiorly. The horizontal width of (g3) is 1.65mm at its widest, and has a vertical maximum height of 2.25mm. Sub-deposit (g3) tapers inferiorly until the cervico-buccal border.

Sub-deposit (g2), made up of three smaller components, and is located slightly supero-mesially of the mid-point of the horizontal superior horizontal surface margin of the mid-deposit has a vertical height of 0.5mm. Supero-distally of sub-deposit (g2) is sub-deposit (g1). It is characterised as a series of relatively smaller, amorphously placed deposits and is laid out on three levels; an inferior level, containing a horizontal shaped segment; a middle level containing four horizontally placed component deposits; and a superior level containing two relatively larger component deposits, one on the distal end of the superior level and one on the mesial end of the sub-deposit (g1). Slightly infero-distal to the superior level of deposits of sub-deposit (g1), and in between the middle and superior level of sub-deposit (g1), is an obtusely angled segment which joins the distal end of both the superior and middle level component deposits of (g1). Colours are greys and shades of light to dark brown (7.5 YR N3; 5/4; 5/2; 4/4; 4/2).

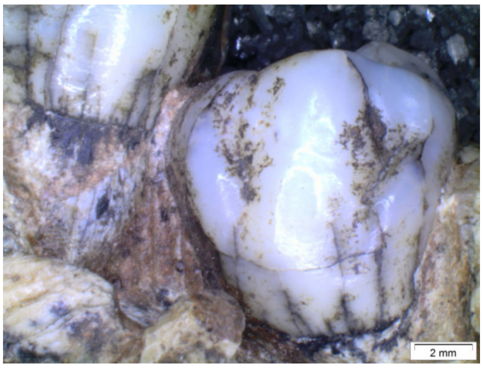

Figure 106: StW 131 RP_4, buccal, RM_1 buccal

Figure 107: StW 131 RP_4 buccal; RM_1 buccal

Description of adherents on StW 61

RM_2

Disto-cervical; disto-occlusal

Sub-deposit (a) presents broadly with four sides, and is located disto-cervically and is situated between the linguo-distal and mid-distal thirds of RM_2 (bucco-lingually). The disto-lingual margin measures 3.1mm vertically; the horizontal superior edge of the deposit (occluso-distal) measures 3.9mm. The disto-buccal margin measures 0.9mm; and the inferior margin measures 3.35mm. The superior margin of the sub-deposit (a) appears to taper obliquely and inferiorly buccally; the inferior horizontal also tapers obliquely and superiorly buccally. The vertical disto-lingual edge presents as concave for approximately two thirds of the vertical margin, thereafter it spreads obliquely buccally until it reaches the linguo-occlusal angle of the sub-deposit. Sub-deposit (a) ranges from the linguo-distal to mid-distal third and inferiorly to the cervico-distal margin, excepting in the linguo-distal area, where the deposit extends apically by 0.8mm onto the *cementum*. The texture presents as extremely coarse, irregular, granular, and contains several closely compacted bulbous protuberances, especially on the lingual margin inferiorly, where it adheres to the *cementum* and also in the centre of deposit (a). The colours of this deposit are different hues of brown.

Sub-deposit (b) is a longitudinal deposit within a groove which is located in the middle-distal third of the tooth, and extends from the occluso-distal surface to the disto-cervical line. The width measurement of this deposit is 0.6mm (at the occluso-distal margin); 0.5mm in the central mid-distal area at a point slightly superior to a slight widening (lingually) in diameter of the longitudinal deposit. The texture is homogenous and slightly coarse, excepting for some bulbous material in the superior part of the deposit. The colour is brown (7.5 YR 5/4; 5/2; 4/2; 4/4).

Sub-deposit (c) is located centrally on the lingual surface, in the middle third (bucco-lingually), and slightly mesial of the buccal groove of RM_2. This deposit cluster is principally made up of two distinct parts, one superior, and the other directly inferior to it. The superior segment is relatively larger than the inferior segment. The superior segment is divided further into three components: a relatively small supero-distal segment; a relatively much larger mid-mesial segment; and an inferior segment that is relatively larger than the supero-distal segment, but smaller than the mid-mesial segment. The supero-distal segment is broadly "L" shaped, and is slightly coarse and has a slight thickness that protrudes form the enamel. The mid-mesial and largest segment of sub-deposit (c) has a thick protuberant texture; the thickness is approximately 0.05mm from the enamel surface on which it is attached. The inferior segment is shaped like the letter ‘w’ and attached to the point of origin, approximately 1.75m superior to the cervical line where the buccal groove starts divide inferiorly. This inter-buccal division widens until it reaches the bucco- cervical margin. The width of the division at the junction with the ‘w’ shaped deposit is 0.20mm, and the width at the base of the division and adjoining the bucco-cervical junction is 0.75mm. The vertical height of the inter-buccal division is 2.0mm. The texture of the inferior segment is slightly coarse with the more distal half of the sub-segment (left side of the ‘w’) of the deposit thicker than the more mesial half sub-segment. Colour is brown (7.5 YR 5/4; 5/2).

Figure 108: StW 61, RM_2; disto-cervical; disto-occlusal

Figure 109: StW 61, RM_2; disto-cervical; disto-occlusal

Descriptions of adherents on StW 9b,

RM^1

Occluso-mesial

The adherent deposit (a) is situated on the occluso-mesial surface of RM^1 and close to the bucco-mesial junction, and presents as a 'corner remnant'. The deposit is amorphous and presents with two types of adherent material; a darker 'manganese-type' smooth material, and a more charcoal coloured, rough and coarser material. The superior surface margin exhibits a broadly convex shape, with the inferior edge buccally horizontal for approximately 0.75mm, then rising sharply and exhibiting a broadly vertical edge, thereafter flattening out generally horizontally for 0.75mm. The buccal edge of the deposit is broadly obliquely mesio-lingual and measures approximately 1.25mm; the lingual edge of the deposit exhibits a general concavity and measures approximately 0.6mm. The general shape of the deposit however, is amorphous, and the margins are not continuous. The thickness of texture is absent from the darker material, and the grey/charcoal material appears to be more concave and 'crater-like' rather than present with a prominent thickness. Colour is dark brown (7.5 YR 3/2).

RM^1

Disto-lingual

Sub-deposit (a) is situated on the distolingual surface within the middle third of RM^1. It is made up of five distinctly disparate components. The most mesial of which sub-deposit (a1) presents as broadly rectangular. The longer sides of the rectangular figure are mesio-distally situated, with the shorter sides situated occluso-apically. It measures 0.6mm vertically (supero-inferior); the inferior horizontal width is 0.5mm and measured at its inferior horizontal base, and 0.4mm wide at the superior horizontal margin of the deposit. The texture is coarse, irregular, exhibiting some areas of enamel in the discontinuously adherent deposit. The thickness of sub-deposit (a1) is approximately 0.1mm. Colour is light and dark brown (7.5 YR 5/4; 5/2; 3/2).

The deposit situated adjacent and distal to (a1) is (a2). Sub-deposit (a2) is formless, exhibits a 'y' shape, is lightly coarse, and firmly compacted. It measures 0.4mm vertically and 3.5mm at its maximum which is at its superior margin. The horizontal width of its inferior base is 0.2mm. The thickness of this deposit appears to be at least 0.1mm. Colour is very dark brown (7.5 YR 3/2).

Sub-deposit (a3) lies distal of sub-deposit (a2). It appears to be broadly spherical in shape, and appears to present with a similar material to sub-deposit (a2). The texture is formless, compacted, and appears mildly coarse, excepting for a roundish area in the centre of the deposit that lacks any material and through which the enamel surface is visible. The supero-mesial and the supero-distal sections of the sub-depost (a2) are wider in diameter to the infero-mesial. The horizontal width measures 0.45mm and the vertical diameter measures 0.4mm. The thickness of the deposit measures approximately 0.05mm. Colour is a very dark brown (7.5YR 3/2).

Sub-deposit (a4) lies directly inferior to sub-deposit (a2). The vertical height measures 0.35mm and the base of this deposit ends in a narrow rounded point, and measures 0.20mm in width at its base. The maximum horizontal measurement is at its superior margin and measures 0.25mm. Sub-deposit (a4) is formless, exhibits a light coarse and compacted texture, which appears similar to the texture of sub-deposits (a2, a3 and a5). The thickness of this sub-deposit is approximately 0.05mm. Colour is very dark brown (7.5 YR 3/2).

Sub-deposit (a5) is situated infero-distal to sub-deposit (a4) and slightly infero-distal to sub-deposit (a3). The deposit is formless, but exhibits a ‘p’ shape. It measures 0.33mm vertically; 0.25mm at its superior horizontal margin; and 0.05mm at its inferior margin. The texture is slightly coarse, and compact, with a thickness of approximately 0.05mm. The colour of this deposit is extremely dark brown bordering on black (7.5 YR 3/2; N2).

Sub-deposit (b) is located mesial of sub-deposit (a1). It appears almost identical in its inferior aspect to sub-deposit (a1). The inferior edge appears to be obliquely horizontal (mesio-distally) with the distal corner almost at right angles to the horizontal edge. The corner remnant presents with a triangle of dark material. The horizontal base of sub-deposit (b) measures 0.4mm, and the vertical height measures 0.45mm. The texture of sub-deposit (b) is lightly coarse, irregular and granular, but coarser on the inferior, mid-distal, and superior edges of the sub-deposit. The thickness of the adherent material of sub-deposit (b) is approximately is approximately 0.05mm. Colour is light to medium brown (7.5 YR 5/4; 5/2; 4/4; 4/2).

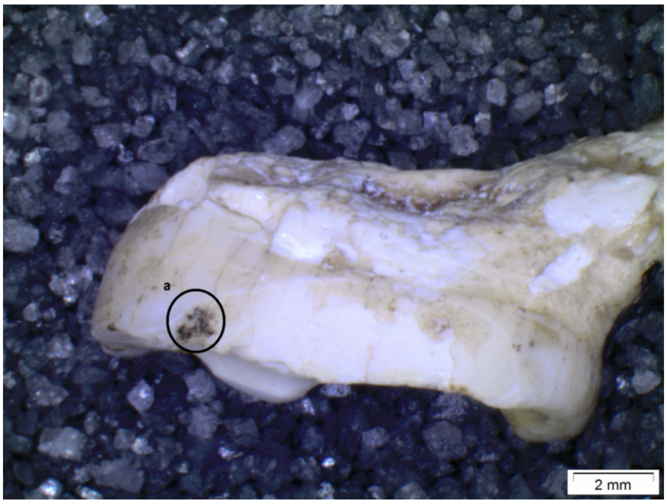

Figure 110: StW 9b, RM^1, occluso-mesial

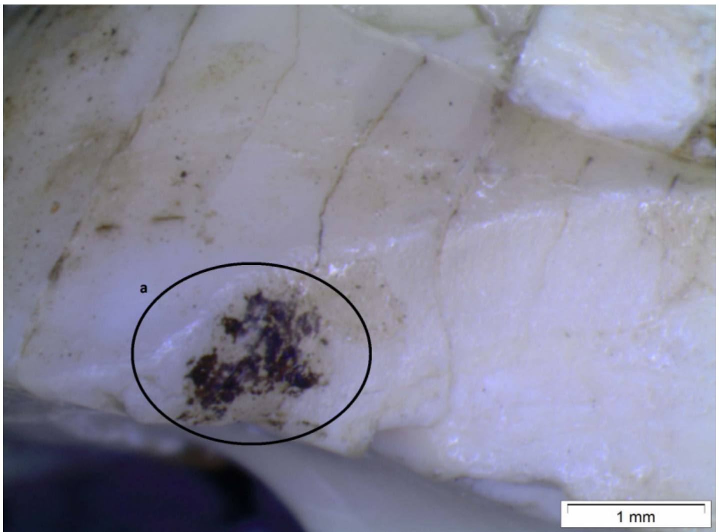

Figure 111: StW 9b, RM^1, occluso-mesial 20 x mag

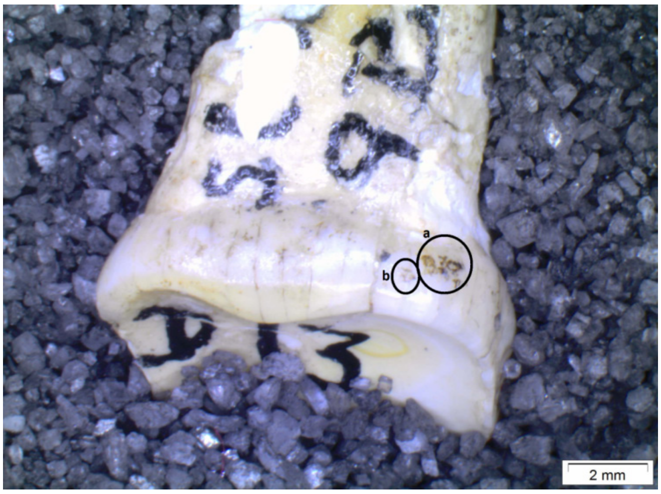

Figure 112: StW 9b, RM¹ disto-lingual

Figure 113 : StW 9b; RM¹ disto-lingual 20 x mag

Figure 114: StW 9b; RM[1] with sub-deposits (a1-5)

Description of adherents on StW 12

LM^3

Disto-lingual; occluso-distal

Sub-deposit (a) is located on the disto-lingual surface within the middle third of the LM^3 (occluso-apically). The sub-deposit measures 3.35mm horizontally; 1.65mm vertically, and is located 2.00mm superiorly from the occlusal margin. Sub-deposit (a) presents with a minimum of 10 individual pits, the two largest are located in the most distal part of sub-deposit (a), and range supero-inferiorly. The more mesial of the two generally longitudinal and concave deposits, is darker superiorly and lighter inferiorly. Slightly mesial of the two longitudinal-type pit-deposits, the sub-deposit presents with a cluster of spherical-type pitting. The superiorly located pits are filled with a deposit material, but presents with little material surrounding the pits. The inferior group of pits are not only filled with deposit material, but the adherent material presents on the enamel surrounding the pitting. The pitted areas are filled with a darker material than the material surrounding them and attached to the enamel. The inferior segment of the sub-deposit appears to have more surrounding adherent material, than on the more superior segment of sub-deposit (a). There are two relatively small, isolated deposits located mesially of the demarcated sub-deposit (a) and don't appear to be associated with any pitting or with the distally located cluster of pits in sub-deposit (a). Colour

Sub-deposit (b) is located distally to sub-deposit (a) on the disto-lingual surface, and ranges occluso-apically from approximately the cervical third (estimated as the apical portion is missing) to the occlusal margin of LM^3. The deposit is concavely shaped. The sub-deposit is made up of three isolated distal deposits and two mesial deposits. the superior of the three distal isolated deposits appear to be a spherical-shaped pit containing a dark coloured deposit. It measures approximately 0.20mm vertically and approximately 0.1mm horizontally. Infero-distally (to the superior pit-deposit) is a flat roundish deposit measuring 0.2mm wide and 0.5mm vertically. The superior portion of the deposit is characterised by a darker colour than the rest of the deposit. The superior texture appears coarse, and the inferior portion is smooth. The most inferior of the three distal and isolated deposits making up sub-deposit (b) presents as a broadly rectangular deposit with the more distal part of the deposit appearing smooth in texture and a lighter colour than e more mesial half of the deposit, which is also darker and coarser. It measures 0.7mm horizontally and 0.50mm vertically at the distal margin and 0.4mm vertically at the mesial margin. The more mesial, (and situated centrally in sub-deposit [b]) of the two mesial deposits is supero-mesially and obliquely longitudinal. At approximately 2.00mm inferiorly from the superior margin the deposit widens for approximately 0.7mm and then narrows until the inferiormost margin is reached. The measurement from the inferior most point of the widening until the inferior margin, which is coincident with the disto-occlusal margin is 1.95mm. The texture of this deposit is mildly coarse. The most mesial of the deposits in sub-deposit (b) is more of less longitudinal shaped but smaller than the deposit distal to it. The approximate vertical height is 3.0 mm and composed of a narrow superior longitudinal section which is approximately 0.1mm wide, and extends inferiorly and vertically for approximately 1.00 mm where it joins a relatively small roundish concavity; thereafter the deposit widens vertically for 1.3 mm; the horizontal width of the widened section being 0.6mm. The deposit thereafter continues inferiorly by another 0.6mm until it reaches its inferior limit, which is marked by a roundish constituent which presents as darker than the rest of the deposit. The colour is light brown (7.5 YR 6/4; 6/2).

Sub-deposit (c) is located in the occlusal third (mesio-lingually) of the mid-lingual surface of LM^3. It presents with three component parts. A supero-distal dark coloured element which is broadly spherical in shape, with a coarse texture, surrounded by a smoother texture with a lighter colour. The horizontal and vertical measurement both are approximately 0.1mm. The thickness of this deposit appears to be at least 0.1mm. Approximately 0.2mm directly inferior to the distal component is another component, which is rectangular and concave and extends 1.2mm from the superior edge of the deposit to the occlusal edge. It measures 0.9mm vertically, and measures 0.20mm horizontally at the mid-point of the deposit. The most inferior edge of the deposit measures 0.05mm horizontally, and has the narrowest width of the whole component. Supero-mesial to the inferior deposit constituent and mesial to the distal component deposit is a dark spherical-type depression with the infero-mesial section being a lighter colour. The distal vertical edge of this constituent is 0.15mm in length, and the horizontal diameter at its centre is 0.15mm wide. The texture appears smooth, and the thickness of this component is unknown. The colour is dark brown (7.5 YR 3/2).

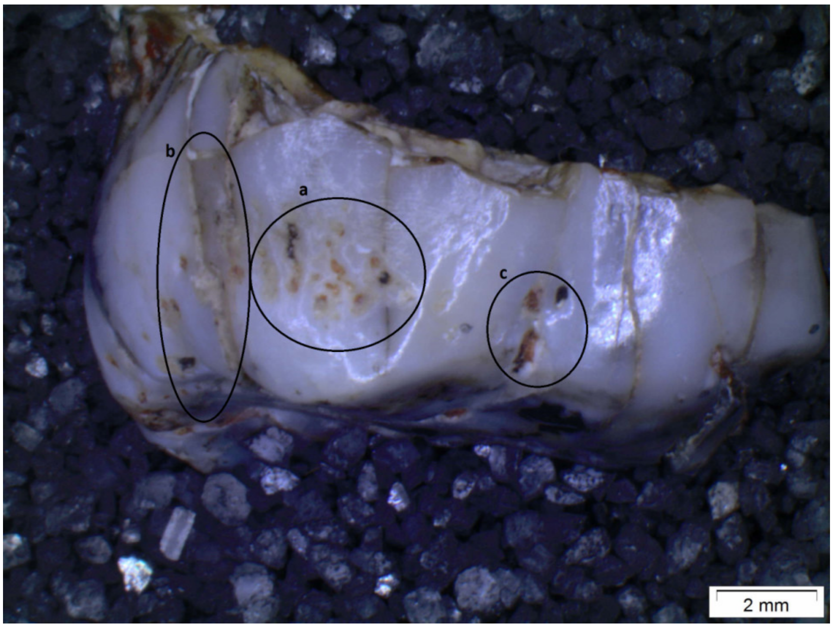

Figure 115: StW 12 LM^3, disto-lingual; occluso-lingual (illustrating sub-deposit b)

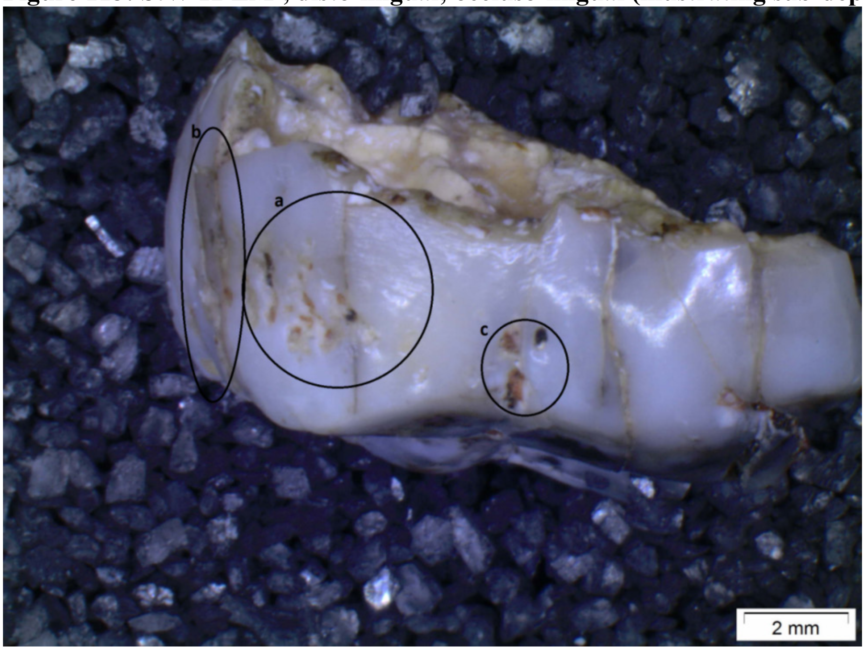

Figure 116: StW 12 LM^3 disto-lingual; occluso-lingual (illustrating deposit a)

StW 12 LM^3

Buccal

The components of Sub-deposit (a) are located between the occlusal margin and the superior margin of the middle third (occluso-apically); and the mid-buccal third (mesio-distally) of LM^3. Sub-deposit (a) comprises four components, a superior component, two in the middle, and an inferior one. The superior component is made up of two sub-components, mesial and distal. The mesial one is very lightly adherent, with a lightly coarse texture, and not much thickness. The colour is cream and brown. The distal component is made up of a mesial, a distal and an inferior element, all three distinct and isolated. The distal component appears to have a coarser texture than the mesial component. The inferior sub-component presents with the thickest texture of the three, and protrudes considerably from the enamel surface, reaching an apex. The colour is light brown. The middle component is composed of a cluster of two relatively large elements, one directly superior to the other and a third relatively small isolated mesial element. The superiorly located component is more or less rectangular with a portion that extends superiorly from the mesial corner, and a portion that spreads inferiorly from the middle area of the deposit. The superior element is 1.5mm in width horizontally; 1.2mm at its maximum. The texture of the superior element is coarse, granular and irregular. The mesial segment of the superior deposit has portions that are thicker in places than the distal segment, which is less thick in general. The inferior element of the middle component is located 0.5mm below the superior element, and measures 0.5mm vertically and 0.65mm horizontally, presents with a smoother texture than the superior element. The mesial margin presents with the same thickness as the mesial margin of the superior element. The inferior element of sub-deposit (a) is shaped like a four sided figure with each side having different dimensions. It is located on the occlusal margin and extends superiorly from the occlusal margin by 0.9mm. It is 1.9mm horizontally wide and 1.00mm vertical at its maximum. The superior edge of the inferior element rises obliquely from mesial to distal; the distal vertical edge descends obliquely mesial to distal. The texture of the inferior element is smooth mesially and distally, however it is coarse in the mid-section. The Colour is light brown and cream (7.5 YR 6/4; 6/2; 8/4; 8/2).

Sub-deposit (b) is located distal to sub-deposit (a) on the mid-buccal surface and extends from the cervico-buccal margin to 0.55mm superior to the occlusal margin, where it joins the inferior component of the deposit. It is principally made up of two principal components; a longitudinal and a four sided component, which is located inferior to the longitudinal deposit, but adjoins it. The horizontal width at the cervico-buccal margin is 0.3mm. The horizontal width of the longitudinal deposit in the mid-buccal area is 0.45mm at its maximum. At the inferior margin to the cervical third on the buccal surface of the longitudinal deposit, which is approximately 2.00mm inferior to the cervico-enamel margin, there is an element that protrudes mesially and obliquely superiorly by approximately 0.625mm. The texture of the longitudinal section is coarse, uneven and grainy, and the deposit is shaped concavely for approximately 1.4mm inferior of the cervico-enamel, thereafter the deposit follows a convex shape for approximately 2.1mm. The deposit then stops, and the longitudinal groove continues for approximately 1.4mm without any deposit filling. The final 1.0mm of the groove is filled with a thinner deposit material, than was the case with the superior part of the deposit, excluding where there was no filling. The inferior edge of the longitudinal deposit merges with the superior edge of the inferior four irregular-sided element which is located on the occlusal margin and extends superiorly by 0.9mm from the occlusal margin. The texture of the inferior four-sided deposit is smooth and presents with a generally thinner texture than in the occlusal and middle thirds of the longitudinal deposit (which ranges from approximately 1.4mm from the cervico-enamel junction and extends inferiorly by 1.9mm) which presents with a thicker texture. The colour is light brown and cream (7.5 YR 6/2; 6/4; 8/4; 8/2).

Sub-deposit (c) is located supero-distal to sub-deposit (b). It is located approximately 0.65mm inferior to the cervico-enamel junction on the disto-buccal surface of LM^3 and presents as a coarse deposit with some thickness which is hard to estimate and presents with a different colour to the rest of the deposits on this tooth. The colour is dark brown (7.5 YR 5/4; 5/2).

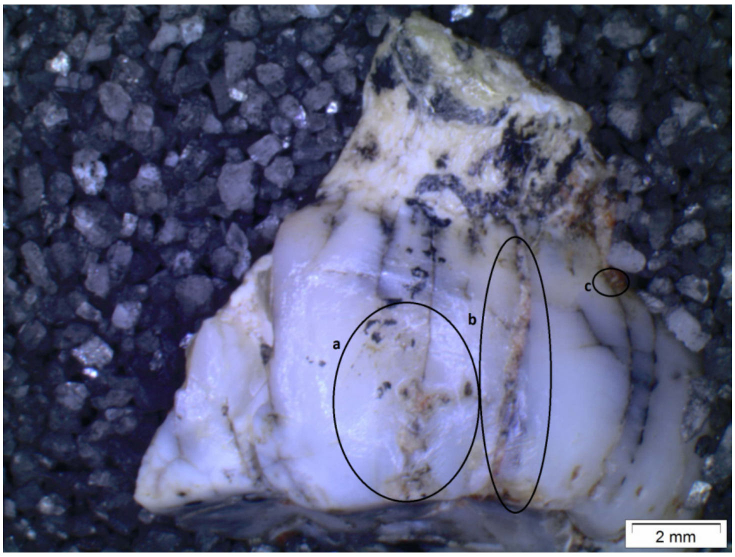

Figure 117: StW 12 LM^3; buccal